DISTRIBUTION OF GOLD MINERALIZATION AT THE NEW BRITANNIA MINE IN SNOW LAKE, MANITOBA: IMPLICATIONS FOR EXPLORATION AND PROCESSING

By

PAMELA J. FULTON

A thesis submitted to the Faculty of Graduate Studies in Partial Fulfillment of the Requirements for the Degree of

MASTER OF SCIENCE

Department of Geological Sciences
University of Manitoba
Winnipeg, Manitoba

THE UNIVERSITY OF MANITOBA

FACULTY OF GRADUATE STUDIES

*****

COPYRIGHT PERMISSION PAGE

DISTRIBUTION OF GOLD MINERALIZATION AT THE NEW BRITANNIA MINE IN SNOW LAKE, MANITOBA: IMPLICATIONS FOR EXPLORATION AND PROCESSING

BY

PAMELA J. FULTON

A Thesis/Practicum submitted to the Faculty of Graduate Studies of The University of Manitoba in partial fulfillment of the requirements of the degree of

Master of Science

ABSTRACT

Gold is distributed in three ways in the New Britannia Mine, as free gold, as gold in the form of inclusions in sulphide minerals and as "invisible" gold within sulphide minerals. Invisible and inclusion gold are interpreted as being deposited before free gold, along with the sulphide minerals pyrite and arsenopyrite. Free gold was found overgrowing pyrite and arsenopyrite and is interpreted as being deposited after pyrite and arsenopyrite crystallization.

Free gold grains have a composition of 40-99% gold with 1-60% silver and trace amounts of copper and mercury. Free gold in association with sulphide minerals ranges in size from 15 to 75 microns, free gold in association with only silicates and calcite ranges in size from 15 to 190 microns. Inclusion gold ranges in size from 3 to 16 microns and is found within arsenopyrite and pyrite.

Where gold occurs as "invisible" gold within sulphide minerals, arsenopyrite usually contains higher concentrations than pyrite. Ion imaging shows this gold can be zoned within arsenopyrite and to have a heterogeneous distribution in pyrite. The zoning in arsenopyrite and the heterogeneous distribution found in pyrite are interpreted as growth features. With lower concentration gold fluids depositing blebs of gold in pyrite and the higher concentration gold fluids depositing the continuous zones in arsenopyrite.

Of the Zones analyzed in this study, the Dick and the Ruttan Zones of the New Britannia Mine and the No. 3 Zone produced favorable results that would indicate good recoveries in the mill. The Birch zone produced results that would indicate low recoveries in the mill, and in the Boundary Zone results indicate good recoveries from H1, 5 & 6, but relatively poor recoveries in H2, 3 & 4, as these horizons contain higher concentrations of invisible gold in the sulphide minerals.

Results suggest that gold amenable to conventional milling techniques is to be found in proximity to faults with associated arsenopyrite, where the invisible gold in arsenopyrite has been remobilized to produce free gold.

I hereby declare that I am the sole author of this thesis. I authorize the University of Manitoba to lend this thesis to other institutions or individuals for the sole purpose of scholarly research.

Pamela J. Fulton

I further authorize the University of Manitoba to reproduce this thesis by photocopying or by other means, in total or in part, at the request of other institutions or individuals for the purpose of scholarly research.

Pamela J. Fulton

The University of Manitoba requires the signatures of all persons using or photocopying this thesis. Please sign below, and give address and date.

ACKNOWLEDGMENTS

I would like to thank all the staff at the New Britannia Mine, Management, Geology and Mining for all their help both above ground and under. I especially thank Richard Kilpatrick, Bill Lewis, Bob Tandy, Janet Wishart, Tom Fleming, Ernie Guiboche, Martin Dupuis, Craig Mihalicz, Peter Snajdr, Gerald Trembath, and finally John Danko for providing the funding and the goad to do the work, for his courage to step back and let me get on with the work, and for listening.

I would like to thank Louis Cabri, Greg McMahon, and Vic Chartrand at CANMET, for the use of and their careful guidance in SIMS, Ian Campbell and Bill Teesdale for the use of PIXE, short though it was, and I would also like to thank George Gale, from Manitoba Energy and Mines, for his extensive knowledge and expertise in the Snow Lake area.

I would also like to thank everyone in the Department of Geological Sciences at the University of Manitoba for their teaching, help, guidance and open ears, especially my immediate lecturers Lorne Ayres, Adrienne Larocque and George Clark and my teachers and mentors for the Electron Microprobe and Image Analysis, Ron Chapman and Sergio Mejia. Most especially I am indebted to Norman Halden, my supervisor, for his support, enthusiasm, trust and knowledgeable guidance, but most of all for keeping me going when I couldn't see the way out.

CONTENTS

LIST OF FIGURES

LIST OF PLATES

LIST OF TABLES

LIST OF GRAPHS

CHAPTER 1 - INTRODUCTION

Snow Lake is situated in west central Manitoba on the eastern side of the Flin Flon - Snow Lake greenstone belt (Fig. 1). Gold mineralization in the Snow Lake area occurs in a sequence of metavolcanic rocks of Proterozoic age.

The Snow Lake region has a long history of gold mining and more recently base metal exploration. First staked in 1925 by C.R. Parres, many of the areas being mined, or further explored today, were found in the 1930's. One such mineralized zone is the New Britannia Mine, currently owned by TVX Gold Inc. and High River Gold, and operated by TVX Gold Inc. Other mineralized zones associated with the New Britannia Mine include the No. 3 Zone (mined out to 300' depth), the Birch Zone, and the Boundary Zone.

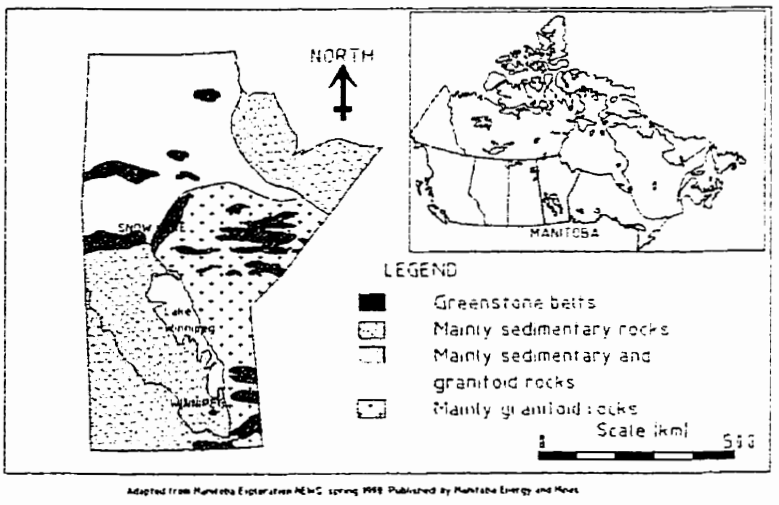

Figure 1- Snow Lake location and general geology map (Manitoba Energy and Mines, 1998).

Statement of the problem

With an estimated 6% of Canada's 1870 tons of gold reserves lying in tailing ponds (Robertson, 1989) it is important that we know why this gold is not liberated during processing. According to Harris (1990) there are six mineralogical factors that can contribute to poorer recoveries, these are;

1. The nature of the "gold-containing" minerals.
2. Gold grain size.
3. The nature of the gangue minerals.
4. The associated sulphide minerals.
5. Coatings on gold.
6. "Invisible" gold.

In and around the New Britannia Mine, gold is found primarily in association with arsenopyrite and pyrite, and more specifically high assays have been found in areas containing both fine and coarse grained acicular arsenopyrite. Exploration has consequently concentrated on ore containing acicular arsenopyrite, ore which can contain high proportions of unrecoverable gold.

Gold found in association with sulphide minerals at the New Britannia Mine occurs either as microscopic inclusions enclosed in sulphide minerals, as inclusions fully or partially enclosed in sulphide minerals, or as free gold grains. With proper grinding and direct cyanidation or by selective flotation and treatment of the concentrates, good recoveries can be achieved with ore containing free gold. However, if the gold occurs as submicroscopic inclusions or as chemically bound gold in sulphide minerals the ore is

considered refractory, collectively this gold is known as invisible gold. The invisible gold falls below the limit of the field of direct cyanidation, and will not be recovered, unless roasting of the ore is employed (Harris, 1990). Invisible gold is thought to occur in any one of the following ways ;

a. As dispersed minute particles of colloidal sized gold (Fleet et al., 1993).

b. Associated with arsenopyrite. Arsenic in arsenian pyrite can be present as a metastable solid solution of the type $Fe(S, As)_2$. Gold could then be incorporated by attachment of either monoatomic ions or ionized clusters of gold atoms at sites of As-rich growth. Alternatively, gold (Au^{3+}) can substitute for As^{3+} in arsenopyrite (Fleet et al., 1993).

c. A physical mixture of pyrite, arsenopyrite and sulphosalt phase rather than atomic substitution (Griffin et al., 1991).

Objectives

With regard to the gold mineralization at the New Britannia Mine and surrounding deposits, the aims of this study are to;

1. Determine the degree to which the gold mineralization is associated with arsenopyrite.
2. Determine what other minerals may be associated with the gold mineralization.
3. Determine if there is an association between the size and shape of the sulphide grains and high gold assays.
4. To assess the proportion of gold occurring as invisible gold .

5. To determine the range in gold grain sizes.

6. Assess which ore, from the various locations, contains the most free or recoverable gold, in contrast to ore which has a high concentration of gold within the sulphide minerals, i.e. gold which will not be recovered by conventional milling techniques.

To assess the associations, distribution and size of the gold, instrumental techniques such as Secondary Ion Mass Spectrometry (SIMS), Electron Microprobe Analysis (EMPA), and Image Analysis (IA) have been used.

CHAPTER 2 - REGIONAL GEOLOGY

General

The town of Snow Lake, Manitoba, is situated in the early Proterozoic Flin Flon - Snow Lake volcanic sedimentary greenstone belt and is part of the southern Reindeer Terrane in the Trans Hudson Orogen of the Canadian Shield. This greenstone belt extends 30 km to the east of Snow Lake and 50 km to the west of Flin Flon, it has dimensions of 250 km east-west by 50 km north-south, and is bounded to the North by the Kisseynew Domain and overlain to the south by Paleozoic limestones (Richardson & Ostry, 1996)(Fig. 2). It has been recognized by Syme et al., (1998) that this greenstone belt along with the Glennie Domain is in effect sandwiched between metaplutonic rocks of the 'Sask craton' and marine turbidites and alliuvial-fluvial sandstones of the Burntwood and Missi Groups in the Kisseynew Domain.

Historically the Flin Flon - Snow Lake greenstone belt has been described as an assemblage of subaqueous and subaerial volcanic rocks, synvolcanic intrusions and associated sedimentary rocks, the Amisk Group. The Amisk Group is now recognized as a collage of distinct tectonostratigraphic assemblages that was assembled prior to the emplacement of voluminous granitoid plutons and regional deformation related to the ca. 1.8 Ga Hudsonian Orogeny, and hence is now referred to as the Amisk Collage (Syme et al., 1998). The Amisk Collage is disconformably overlain by a sequence of terrestrial sedimentary and minor subaerial volcanic flows and associated high level intrusions, the Missi Group. Both rock groups are intruded by a number of

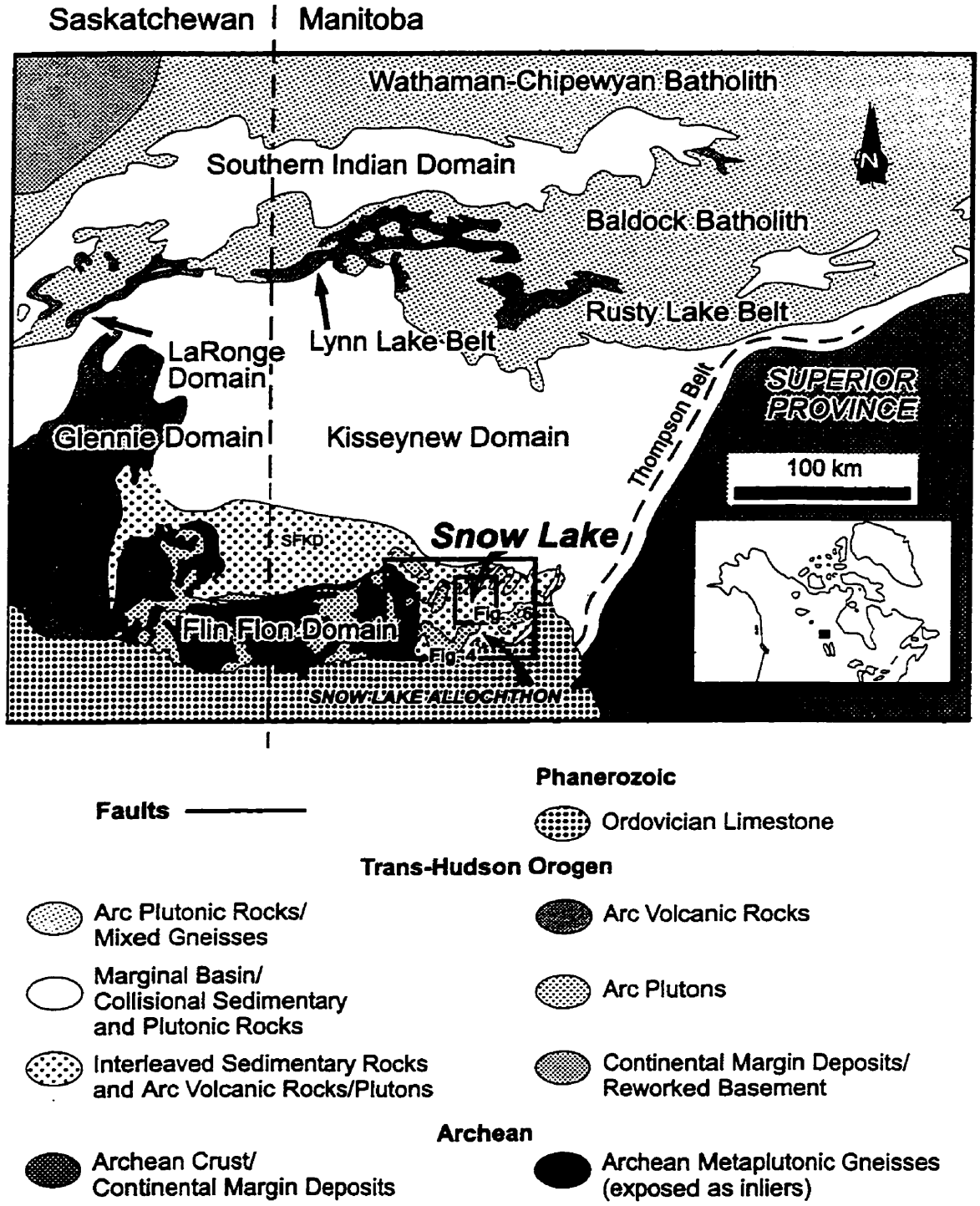

Figure 2 -Reindeer Terrane geological map showing the lithotectonic Kisseynew Domain, the Flin Flon and the Snow Lake Allochthon. (SFKD; the Southern Flank of the Kisseynew Domain) (Kraus and Menard, 1997).

intermediate to felsic, syn to late kinematic intrusions (Galley et al., 1990; Froese & Gasparrini, 1975)(Fig. 3).

In Flin Flon, the Amisk Collage is dominated by subaqueous mafic volcanic rocks with rare intercalated rhyolite flows. These rocks were deposited in a shallow to moderately deep marine environment with some pyroclastics erupted subaerially and deposited under water (Galley et al., 1990; Byers & Dahlstrom, 1954).

In the Snow Lake area, the Amisk Collage is comprised of both arc and back-arc volcanic assemblages. The assemblage includes bimodal mafic and felsic volcanic flows with associated volcaniclastic rocks that host synvolcanic granitoids and gabbros. Chemically, the Amisk Collage volcanic rocks exhibit both tholeiitic and calc-alkaline affinities (Stauffer et al., 1975; Fox, 1976). The prevalence of pillowed lavas, mafic to felsic volcanism, submarine volcaniclastics and turbidite deposits and the tholeiitic chemical affinity displayed by the least altered mafic volcanic rocks suggest deposition in an island-arc tectonic-environment (Stauffer et al., 1975; Fox, 1976; Syme et al., 1982; Richardson & Ostry, 1996). The overlying Missi Group is composed of a metaturbidite sequence (Harrison, 1949; Froese & Moore, 1980; Bailes, 1980; Walford & Franklin, 1982; Kraus & Williams, 1993; Kraus & Williams, 1998).

Most recently, the Flin Flon - Snow Lake greenstone belt has been described as composed of lithotectonic domains of the Trans-Hudson Orogen, the Flin Flon Domain and the Snow Lake Allochthon. The Snow Lake Allochthon structurally overlies the Flin Flon Domain, which structurally underlies magmatitic paragneisses

Figure 3 - General geology of the Flin Flon - Snow Lake greenstone belt showing locations of gold deposits (modified from Galley et al., 1990).

and granitoids of the Kisseynew Domain to the north and east, and continues as the Clearwater Domain southward underneath the Phanerozoic cover (Kraus & Williams, 1998).

Within the Snow Lake Allochthon there are three distinct tectonostratigraphic assemblages, the Burntwood Suite, the Missi Suite and the Snow Lake Assemblage (Fig. 4). The Burntwood Suite is composed of Fe-rich, Al-poor distal metaturbidites, which were deposited on oceanic crust in the marginal Kisseynew basin at 1.86-1.84 Ga, probably during rifting. The Missi Group is a fluvial deltaic sequence, the sandstone of which was deposited on top of the Snow Lake Assemblage. The Snow Lake Assemblage, comprising ca.1.9 Ga island arc rocks and synvolcanic intrusions, are coeval with the amalgamated island arc and oceanic assemblages of the Amisk Collage to the west, although the Snow Lake Assemblage and the Amisk Collage are chemically and structurally distinct (Kraus & Menard, 1997).

The area between the McLeod Road and Birch Lake Faults, north of the Snow Lake Assemblage is interpreted to be thrust repetitions or imbricates of the adjacent Snow Lake Arc Assemblage (Bailes & Schledewitz, 1998).

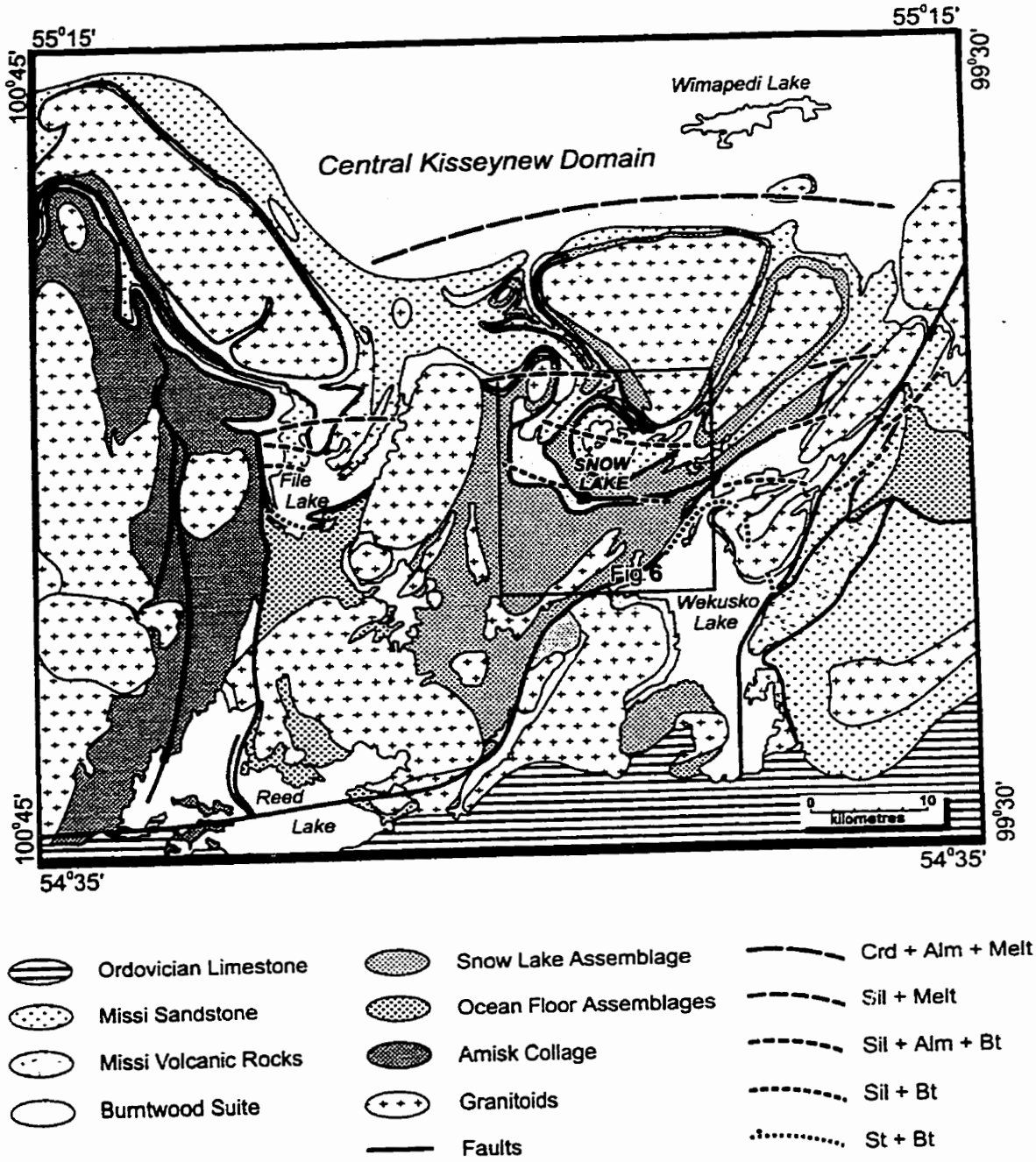

Figure 4 - Snow Lake - File Lake - Wekusko Lake geological map showing the Missi Group, the Burntwood Group, the Snow Lake Assemblage and the Amisk Collage (modified from Kraus and Menard, 1997).

Metamorphism

The volcanic and sedimentary rocks of the Snow Lake area have undergone several metamorphic and deformational events. The metamorphic grade increases towards the north, with the deposits of Snow Lake occurring between the biotite - sillimanite and the biotite-sillimanite-almandine isograds (Froese & Gasparrini, 1975)(Fig. 6).

In Snow Lake, metamorphism began during the waning stages of Missi Magmatism, at 1.832 Ga, continuing to 1800 Ma (Richardson & Ostry, 1996). The D1 deformational phase produced a chlorite grade schistosity, D2 was associated with an increase in pressure of 1-2 kbars, up to approximately 5 kbars and a temperature increase of 10-50 ^{o}C up to 550 ^{o}C, and folding (F2). The peak metamorphic mineral assemblage associated with this metamorphic phase includes staurolite + garnet + biotite, and kyanite + chlorite. Sulphide removal from schists near massive sulphide lenses and consequent sulphide deposition occurred during F2 (Menard & Gordon, 1996). The third phase of metamorphism and deformation produced a crenulation fabric along with minor chloritization at 400-450 °C. An overview of this can be seen in Figure 5 (Kraus and Williams, 1998).

The biotite-sillimanite isograd to the south of Snow Lake, but north of Anderson Lake, marks the lower boundary of the biotite-staurolite-sillimanite zone, and occurs near the kyanite-sillimanite transition. Staurolite becomes unstable according to the reaction;

Staurolite + muscovite +quartz <=> biotite + sillimanite + almandine + H_2O.

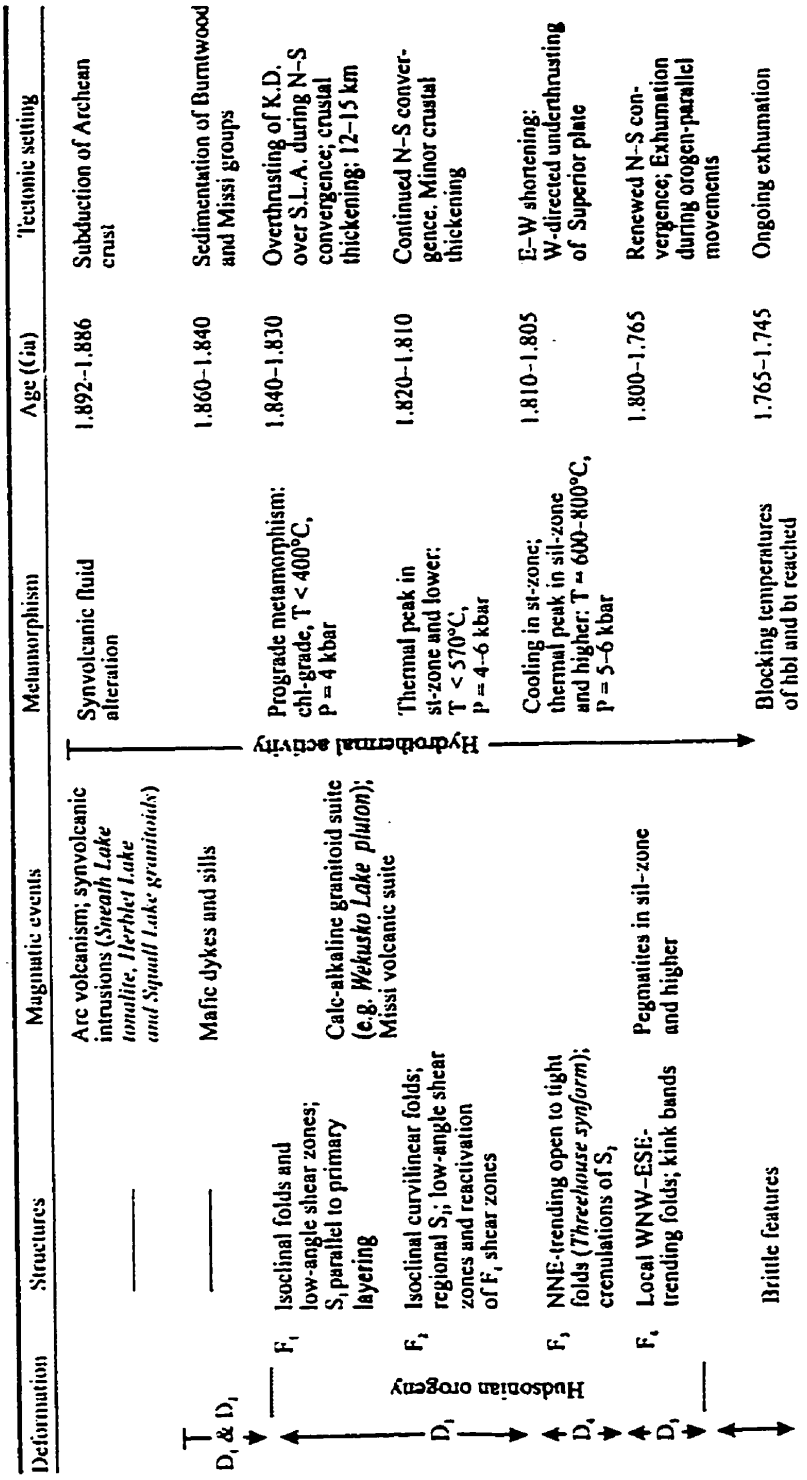

Figure 5 - Summary of the tectonometamorphic history of the Snow Lake Allochthon, Kraus & Williams (1998) in press (K.D. Kissewnew Domain; S.L.A. Snow Lake Assemblage).

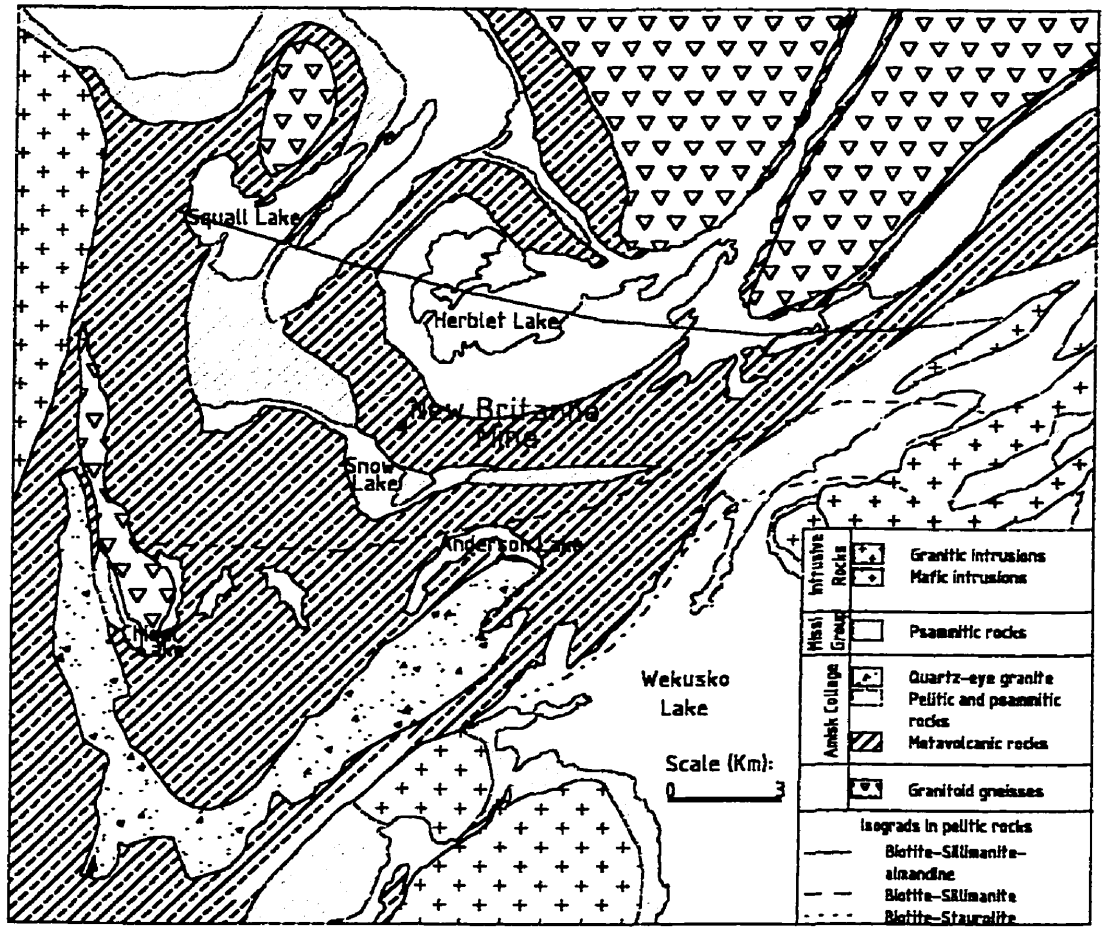

Adapted from Froese & Gasparrini, 1975.

Figure 6 - Regional Geological Map of the Snow Lake Allochthon showing the location of the New Britannia Mine and metamorphic isograds (modified from Froese and Gasparrini, 1975).

This reaction defines the biotite-sillimanite-almandine isograd and marks the lower boundary of the biotite-sillimanite-almandine zone. All reactions result in the production of significant amounts of biotite as well as quartz and a fluid phase. Gold has been found in association with coarse grain size - recrystallized biotite as well as silicified areas, the later possibly being the result of silicic acid being carried in a hydrous fluid phase.

Structure

During the D1 to D3 deformational phases, the geological history of the Snow Lake area can be interpreted as a single, long lived deformational event resulting from a large scale NW-SE crustal shortening. This is accompanied by regional prograde changes in the orientation of fabrics during docking of the various tectonic units along major structures such as the McLeod Road Thrust Fault and associated brittle structures. This thin-skinned brittle deformation is also responsible for the crack and seal veins found within the mineralized areas. Further movement along the McLeod Road Thrust resulted in "locking-up" of its northerly section and hence the movement was accommodated by the North Canada Fault and by folding which resulted in the McLeod Lake Synform which folds the McLeod Road Thrust (Kraus & Williams, 1998).

Later work by Fieldhouse (1999) has shown that the D1, D2 and D3 phases of deformation were due to compressional stresses in two different orientations. The D1 and D2 resulted from NE to SW compression, producing NE trending lineations. The

D3 was due to ESE to WNW compression, which resulted in the formation of the Threehouse Synform, folding of the McLeod Road Thrust, and thrusting of the Snow Lake Assemblage over the Burntwood Suite in a WNW transport direction. Further, this ramping produced imbricate structures and tension fractures between rock types, producing favourable locations for gold deposition, such as the New Britannia Mine and the No. 3 Zone (personal communication, Fieldhouse, 1998).

Local geology

The New Britannia Mine is situated in a block of the Snow Lake Assemblage bounded on the west and south by the McLeod Road Thrust and to the northwest by the Birch Lake Fault (Richardson & Ostry, 1996). The Snow Lake Assemblage is comprised of island arc rocks and synvolcanic intrusions, composed of both mafic and felsic rocks.

The mafic rocks can be divided into 2 main groups; volcaniclastic and pillowed basalts (Galley, Ames & Franklin, 1988). The basalt flows and pillows are principally aphyric (no phenocrysts), with minor plagioclase porphyritic flows, but generally fine to medium grained with their massive portions locally subophitic. The volcaniclastic rocks are composed of one third mafic tuff, displaying graded bedding, cross bedding, and slump features, and the rest is composed of interlayered lapilli tuff and tuff breccia which form a series of coarsely-graded debris flow deposits (Galley, Ames & Franklin, 1988).

The felsic volcanic rocks in the area are largely fragmental. In general, the

felsic tuff is massive with few observed outcrop scale primary structures. The tuff is primarily feldspar-quartz phyric, and consists of a very fine-grained matrix of feldspar, quartz and biotite, with millimetre scale bands rich in biotite and garnet (Galley, Ames & Franklin, 1988).

Altered rocks and mineralization

The alteration rock types found in association with the gold mineralization are (Figs. 11-17);

1. Quartz and calcite veins - which usually occur along or in the faults, quartz can also be found in tension gashes in proximity to the faults.

2. Quartz dominated unit - this unit is composed primarily of quartz, with up to 90% polygonal quartz in sample DB29, from Level 2210. Other minerals include 5-10% calcite, 0-20% biotite, +/- tremolite, +/- feldspar, +/- epidote, +/- hornblende, 0.5-3% arsenopyrite, 0.5-2.5% pyrrhotite, +/-pyrite, +/- chalcopyrite, +/-gold. Gold has been found in this rock type on Level 2210, in samples DB7, 28, and 30. All these rock types contain quartz, calcite, feldspars, arsenopyrite and pyrrhotite. This unit usually occurs next to faults, the majority of the quartz occurring as secondary quartz, introduced as a consequence of fluid movement through the rock.

3. Banded biotite schist - this unit is composed of quartz, biotite, +/- tremolite, calcite, feldspar, +/- hornblende, tourmaline, epidote, +/- scheelite. The majority of the sulphide minerals is as arsenopyrite, then pyrrhotite and lastly as pyrite. This unit usually occurs next to, or in proximity to faults, where there has been movement of

fluids.

4. Fine grained schist - this unit is composed primarily of quartz, sillimanite, biotite, tourmaline, plagioclase, orthoclase, epidote, and +/- scheelite. The sulphide minerals present are mainly pyrrhotite and small amounts of arsenopyrite. The quartz and feldspar are the main rock forming minerals, and the sillimanite, biotite, tourmaline, and epidote appear to be the main alteration assemblage. This unit usually occurs in proximity to, but not adjacent to faults, where there has been some fluid movement but not enough to produce coarse grained biotite.

5. Black amphibolite - This unit is composed primarily of hornblende, feldspar (plagioclase and orthoclase), plus biotite, quartz, tourmaline, and calcite. This unit contains little sulphide minerals, the majority of which is pyrrhotite with some arsenopyrite. This unit usually occurs well away from the faults, and is a result of the regional metamorphism and not the local fault associated mineralization.

For each degree of mineralization in the Snow Lake area there is a representative suite of minerals, these are as follows; hornblende represents the unaltered metamorphic rocks, the amphibolites. Actinolite/ tremolite and epidote represent the weakly altered rocks. Biotite, dolomite and albite represent the moderately altered rocks, the biotite schists. Arsenopyrite represents the strongly altered rocks containing gold, the biotite schists and the quartz dominated units adjacent to faults.

According to Galley et al. (1990) there is a well defined alteration halo, which includes the following mineral changes with increased proximity to the mineralized

zone:

Titanomagnetite → titanite → ilmenite → rutile*.

Andesine → andesine/oligoclase → oligoclase → albite*.

Hornblende → actinolite → biotite → chlorite → sericite*.

Calcite → ferroan dolomite → ankerite*.

Pyrrhotite → arsenopyrite-pyrrhotite → arsenopyrite-pyrite*.

* minerals present within the breccia veins (Fig. 7).

The alteration assemblages are interpreted to be chemical fronts, characterized by an increase in potassium, sodium, sulphur, carbon dioxide (CO_2), water (H_2O), boron, tungsten, silver and gold. There is a progressive drop in anomalous element concentrations away from the ore zone.

Gold occurrences

Gold mineralization is known in the File Lake - Snow Lake area; on the east shore of Wekusko Lake (The Herb Lake Camp) and north of the town of Snow Lake (the Bounter Zone, Thorne Zones, Caper Zone, New Britannia Mine, Birch Zone, No. 3 Zone, Sherry Zone, Hill Zone and the Boundary Zone).

In the Herb Lake Camp, gold mineralization occurs in sedimentary and volcanic rocks of the Missi Group and is aligned along the north limb of the Herb Lake Syncline near the contact between the sedimentary and volcanic rocks of the Missi Group, and sub-parallel to the axial trace of the Herb Lake Syncline. Along the north limb of the Herb Lake Syncline mineralization occurs in quartz veins and lenses that

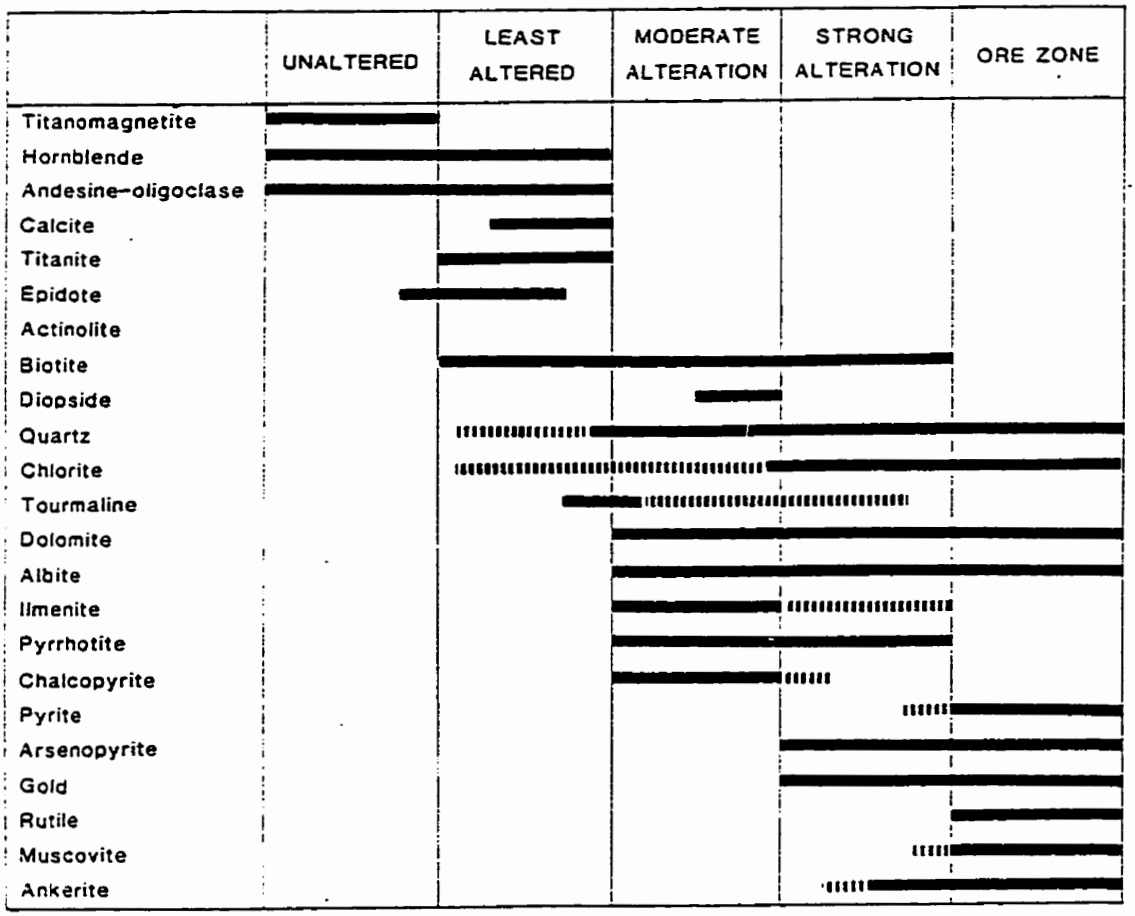

Figure 7 - The associated alteration assemblage zonation to gold mineralization at the New Britannia Mine (modified from Galley et al., 1990).

strike N– NE, parallel to both the regional stratigraphy and a major fault that occurs along the east shore of the lake (Galley et al., 1986).

Most gold occurrences are contained within, or show a spatial association to quartz feldspar phyric units. Within the felsic porphyritic rocks, mineralization is associated with distinct quartz veins. In the sedimentary rocks and mafic dykes, mineralization is associated with irregular quartz lenses and stringers in shear zones. Sericite and / or carbonate alteration is associated with this mineralization. Galley et al. (1986), interpreted these alteration events to have overprinted the regional metamorphism. Mineralization aligned sub-parallel, and in proximity, to the axial trace of the Herb Lake Syncline consists of gold and pyrite in quartz lenses and stringers hosted by mafic volcanic rocks, now altered to biotite schist.

North-east of the McLeod Road Thrust Fault, the gold deposits of Snow Lake occur in volcanic rocks characterized by felsic and mafic fragmental units. All deposits exhibit a spatial association to faults. Gold is hosted in structures that occurred before closure of the McLeod Road Thrust Fault at the boundaries between mafic and felsic volcaniclastics in the New Britannia Mine and the No.3 Zone (Fieldhouse, 1999)(Fig. 8). The mineralization consists of gold, pyrite and arsenopyrite in association with quartz and calcite veins and stringers, hosted by mafic volcanic rocks and basalts commonly altered to biotite schist.

Study area

The area under study deals with four main zones; the New Britannia Mine, the

Birch Zone, No. 3 Zone and the Boundary Zone (Fig. 8). Fieldwork conducted during the summers of 1996 and 1997, entailed mapping of the Birch Pit, the surface outcrop at the No. 3 Zone and seven Levels of the New Britannia Mine. Sampling with the aid of geological maps, drill core, and gold assay data has been completed in the Birch Zone, the Boundary Zone, the Kim Zone, the Thorne Zones and the Sherry Zone. Due to time constraints on analyzes the Kim, Thorne and Sherry Zones were not analyzed.

Mineralization

Gold mineralization is hosted within the Amisk Group volcanic sequence, with the major deposits and occurrences situated within 500 m of the surface expression of the McLeod Road Thrust Fault (Galley, Ames & Franklin, 1988). All deposits exhibit a spatial association to faults that are sub-parallel to, merge with, and terminate on the McLeod Road Thrust (Galley et al., 1986). The gold zones plunge moderately to the northeast along fault planes parallel to the plunge of the regional D2 L-S fabric (Galley et al., 1990). It can also be noted that at the New Britannia Mine and the No. 3 Zone the gold mineralization occurs at the boundary between felsic and mafic volcaniclastics. This may have significance if a chemical mechanism for the precipitation of the gold is employed.

As a consequence of mapping and assay results from the New Britannia Mine, the No. 3 Zone and the Birch Zone, the majority of the gold is in portions of the sulphide rich biotite schist and quartz dominated units, which are adjacent to faults. Deviations from this are possibly due to remobilization of gold by fluids, or to original

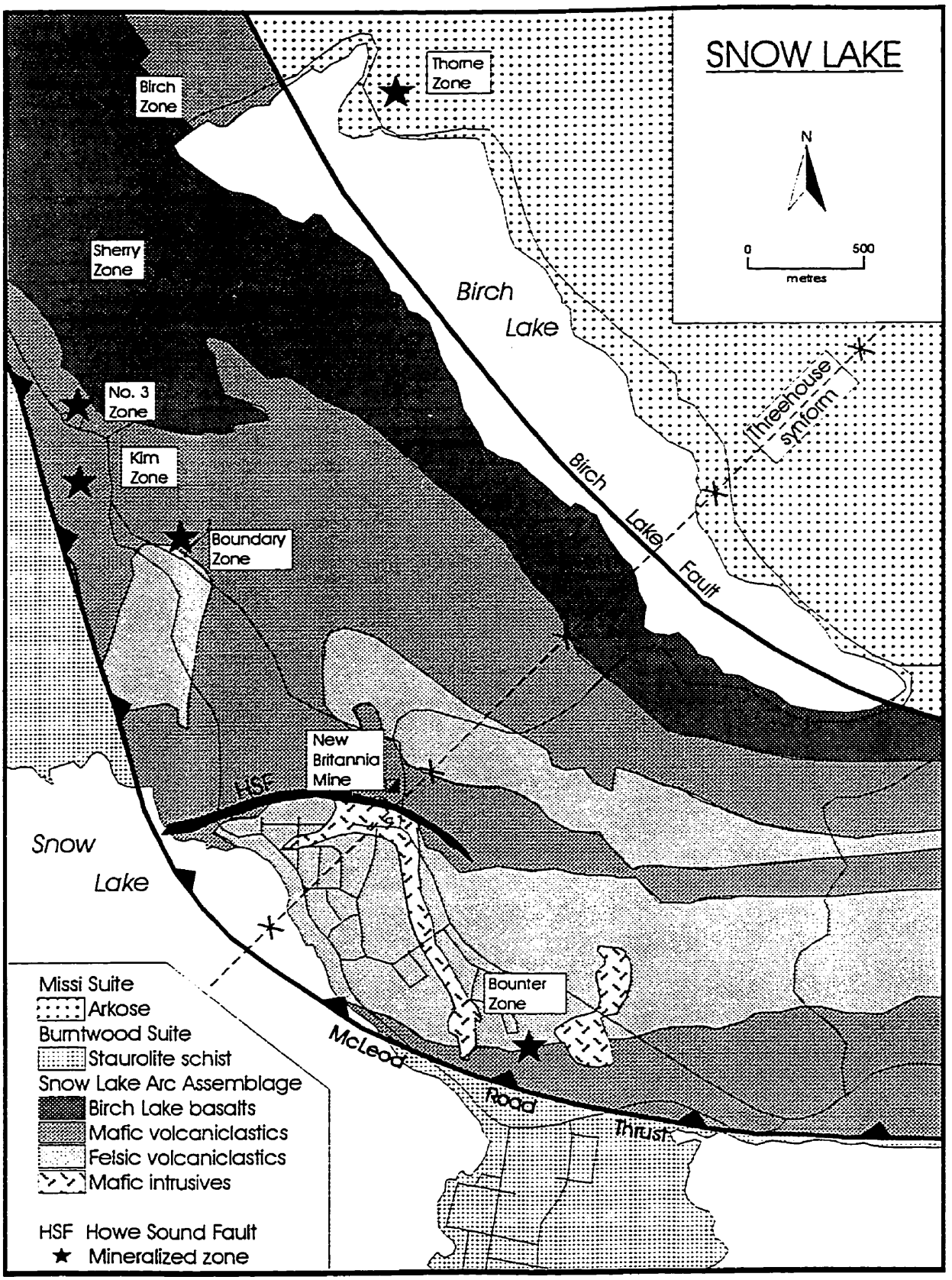

Figure 8 - Geological Map of the mineralized zones, the Birch Zone, the Boundary Zone, the No. 3 Zone, the Bounter Zone, the Thorne Zone, the Kim Zone, the Sherry Zone and the New Britannia Mine (Fieldhouse, 1999).

gold deposition fluid pathways other than along the major faults seen today.

According to Bailes et al., (1987) common features of the mineralization include: auriferous veins and stringers characterized by quartz-carbonate plagioclase breccia with incorporated altered wall rock; intense wall rock alteration characterized by biotite, chlorite, carbonate and tourmaline; associated quartz-carbonate-tourmaline veins in both the hanging wall and the footwall; and associated sulphide minerals that include arsenopyrite, minor pyrite, pyrrhotite, sphalerite and galena (Richardson & Ostry, 1996).

Underground mapping at the New Britannia Mine, Snow Lake and examination of alteration lithologies by optical microscopy of Levels 2006 (the Ruttan Zone) and 2210 (the Dick Zone) would suggest a sequence of alteration as follows;

1. Production of chalcopyrite, pyrrhotite, and then an Fe/Ti sulphide within the volcanic pile before or during early metamorphism.

2. Regional metamorphism of the mafic volcanic rocks to amphibolite, during which fluids containing As, Fe, S and Au caused the precipitation of gold and arsenopyrite followed by the precipitation of gold and pyrite, in between which there was the precipitation of a Ti Fe sulphide in the Ruttan Zone. Further metamorphism and fluid movement caused the alteration of the amphibolite to biotite actinolite schist in areas adjacent to NE - SW and NW - SE orientated faults.

3. Silicification /carbonization within the faults and within certain portions of the biotite schist and the quartz dominated units, causing gold to be further

deposited or remobilized from areas containing invisible gold in pyrite and arsenopyrite.

4. The presence of small amounts of gold mineralization in shallow angle faults, parallel to the strike of the McLeod Road Thrust, indicates closure of this thrust during gold remobilization, or, the deposition or remobilization of the gold at a later time, not documented here.

5. Deposition of pyrrhotite in both the Dick and Ruttan Zones followed by deposition of euhedral chalcopyrite, then by pyrrhotite in the Ruttan Zone.

The Birch Zone

The Birch Zone is a mineralized area to the northwest of the New Britannia Mine. Seven Horizons, denoted as H1 (shallowest), H2, ...to H6 (deepest)(see Appendix 1), of mineralization have been identified at depth from Drill Hole B96001. This mineralization is set in a sequence of felsic and mafic volcanic rocks, now dominantly amphibolite. A test pit was developed on the Birch Zone during 1997. This surface mineralized zone, the Birch Pit, has been mined out to a depth of 60'. The Birch Pit is primarily composed of a layered biotite, feldspar, quartz, ferroactinolite schist. This schist containing up to 15% acicular arsenopyrite, minor amounts of pyrite and chalcopyrite, accessory tourmaline, and staurolite. The sequence of sulphide mineralization is: chalcopyrite (earliest), Ti Fe sulphide, arsenopyrite, pyrite (latest). This zone dips to the north at ~30°, plunges towards the northeast, and strikes east-west (Fig. 9).

The New Britannia Mine

Mineralization in the New Britannia Mine is divided into three main zones the Toots Zone, the Dick Zone and the Ruttan Zone (Fig. 10). This mineralization is hosted within a sequence of quartz dominated rocks and mafic amphibolites.

Mapping of Level 780 shows that the mineralization in the Toots Zone is associated with quartz veining and a quartz dominated unit (Fig. 11). Mapping of Levels 2006, 2030, 2150, 2186, 2210 and 2260 indicates an association of the mineralization with northerly dipping NE – SW striking faults in the Dick Zone and NNW - SSE to NW - SE to WNW - ESE striking faults in the Ruttan Zone (Figs.12-17).

Rock types found to contain gold in the Dick Zone are of two types. First, is a quartz dominated rock with variable amounts of hornblende, calcite, feldspar and 2-4% sulphide minerals (arsenopyrite and pyrrhotite); samples DB28 and DB30. The second is a feldspar (orthoclase) rich lithology, with variable amounts of biotite, tremolite, epidote, calcite and 5-7% sulphide minerals, made up of equal proportions of arsenopyrite and pyrrhotite with minor amounts of chalcopyrite; samples DB7 and DB16b. The sequence of sulphide mineralization is chalcopyrite (earliest), pyrrhotite, Ti Fe sulphide, arsenopyrite and pyrrhotite (latest).

Samples found to contain gold in the Ruttan Zone, samples; RA1, RA4 and RC2, are typically quartz flooded areas containing variable amounts of feldspar, tremolite, hornblende, calcite, epidote, +/- tourmaline. From most abundant to least abundant sulphide minerals are ordered: arsenopyrite, pyrrhotite, and pyrite. The sequence of

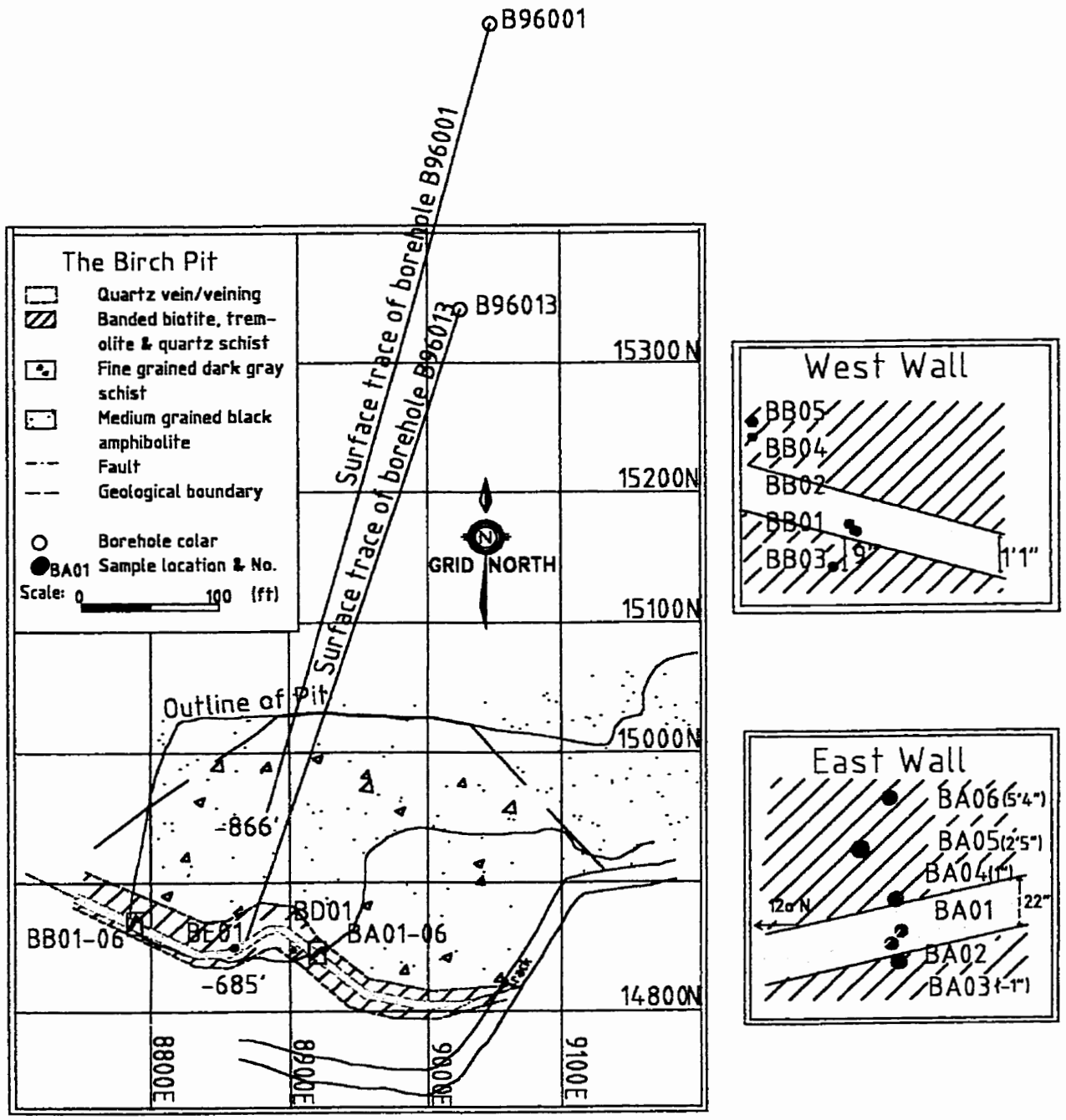

Figure 9 - Geological map of the Birch Pit, showing locations of drill holes and samples. The Birch Pit is dominated by an E - W fault, which has associated gold plus arsenopyrite mineralization.

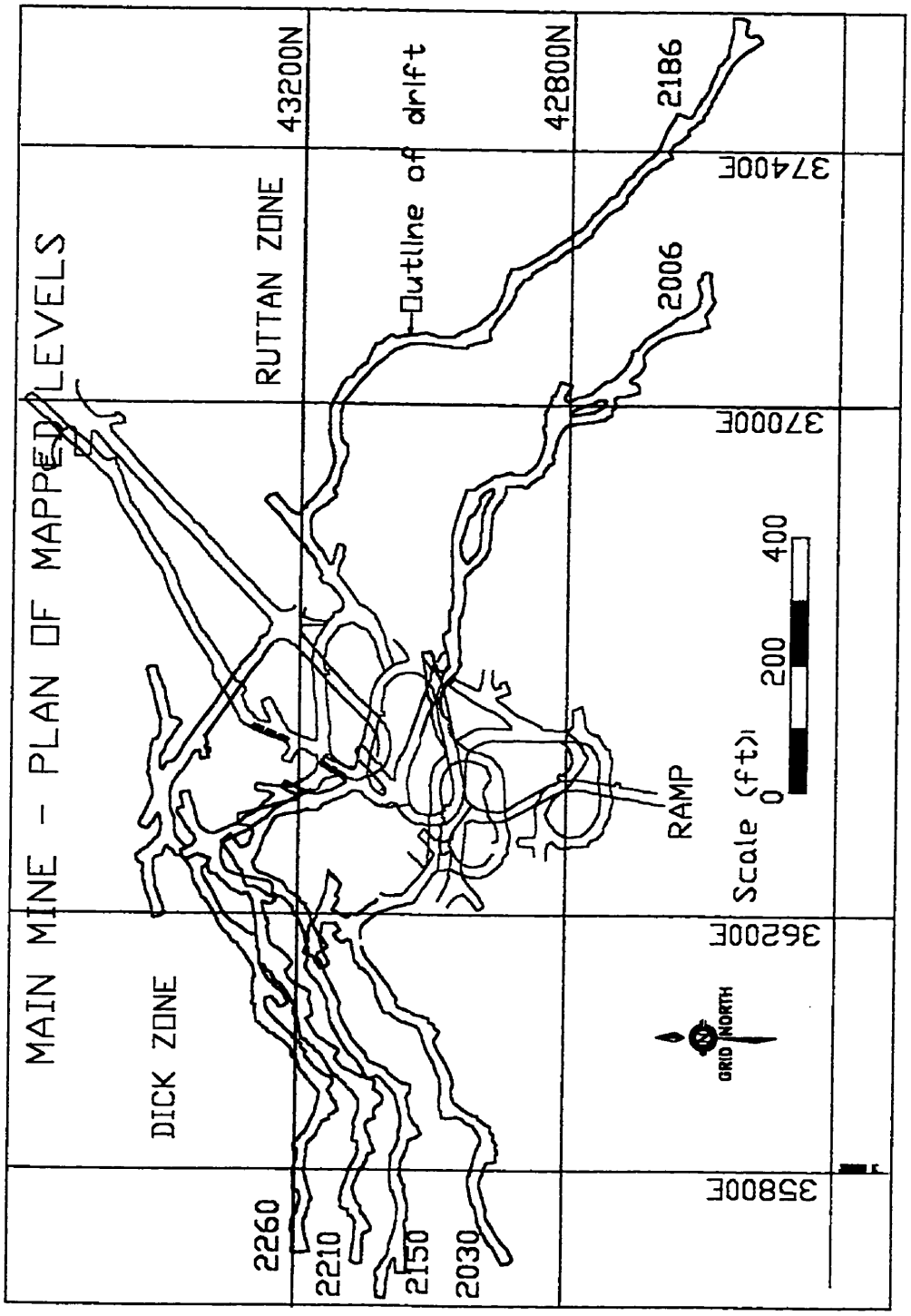

Figure 10 - Plan of the mapped drifts in the New Britannia Mine , showing strike and dip of the ore, and the locations of the different zones. Numbers beside each drift indicate depth in feet.

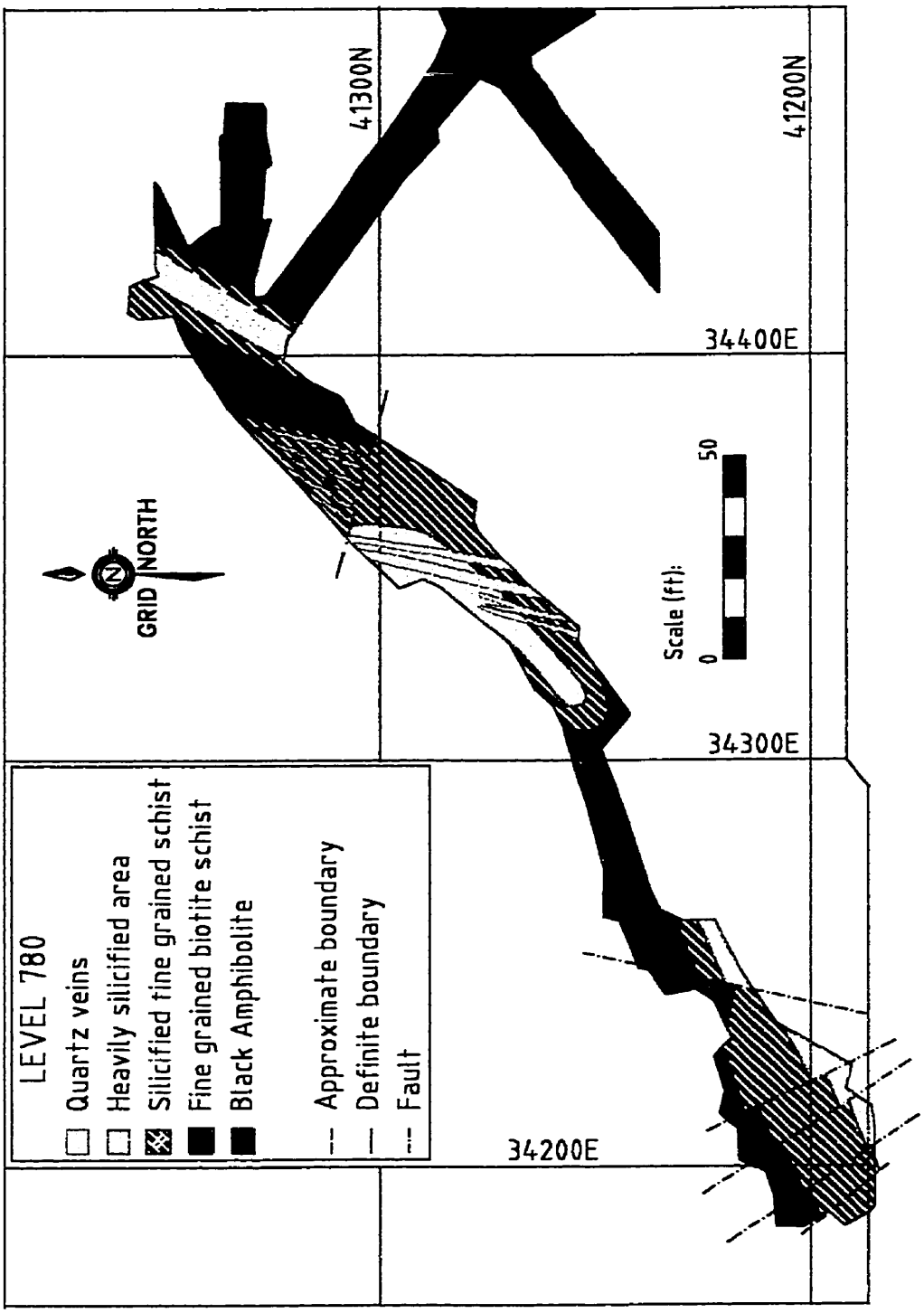

Figure 11 - Geological map of Level 780 in the Toots Zone, showing 2 phases of silicification, the first of which altered the surrounding rock. Both stages have been cut by faults.

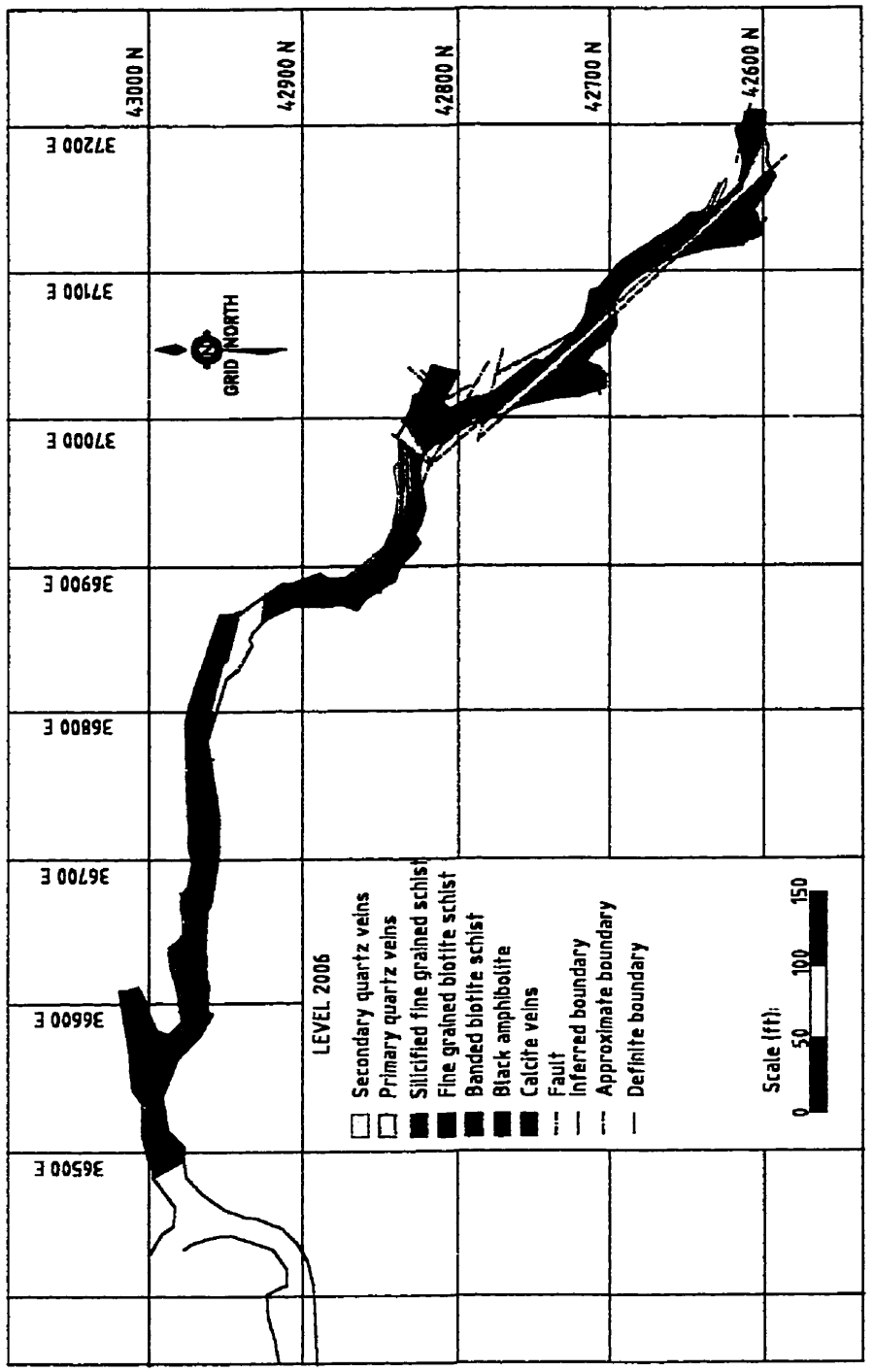

Figure 12 - Geological map of Level 2006 in the Ruttan Zone, showing multiple phases of faulting, the latest of which is in a E-W becoming WNW - ESE orientation towards the east. This cuts the ore which is associated with faults in a NW to SE orientation.

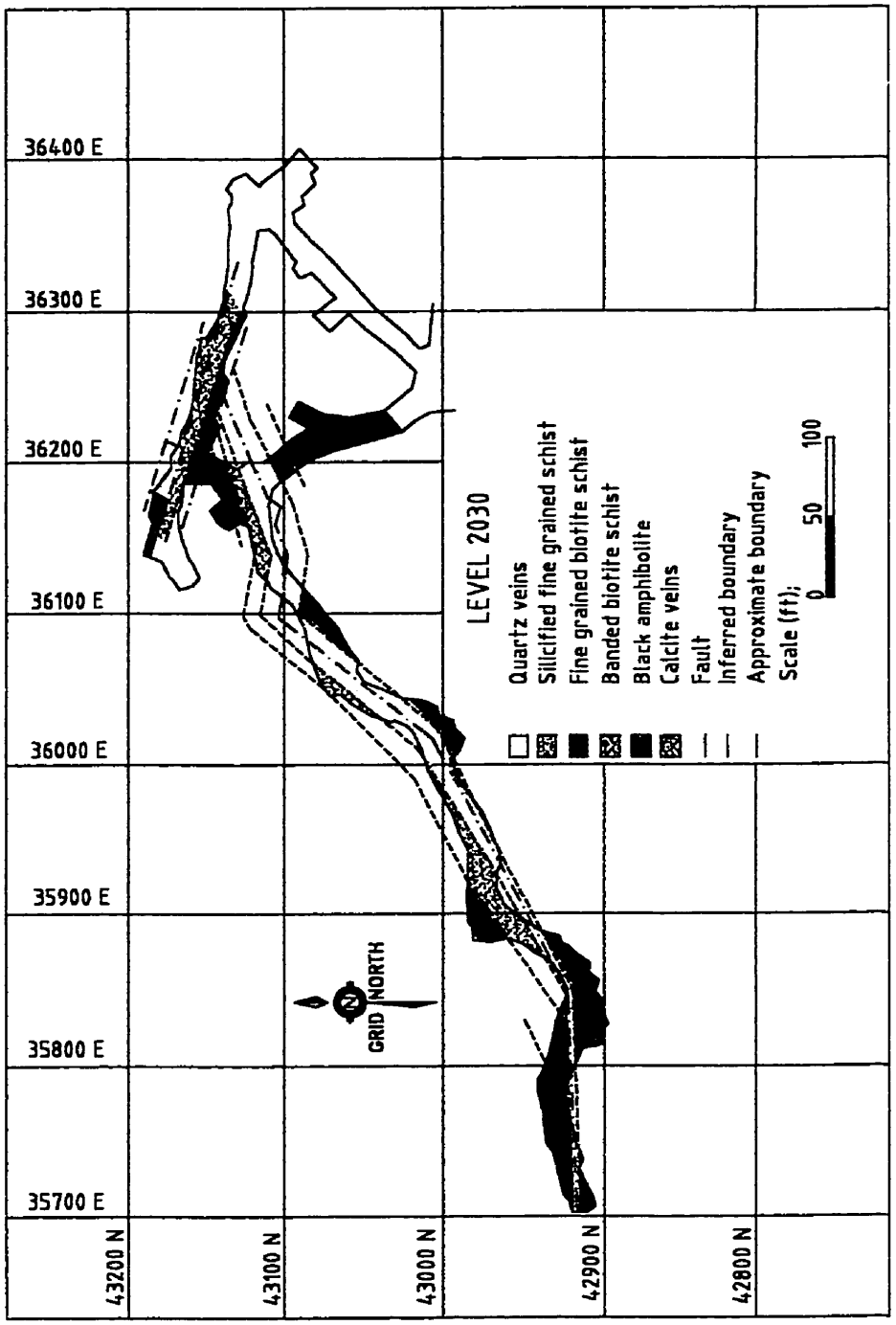

Figure 13- Geological map of Level 2030 in the Dick Zone, showing the ore primarily associated with a fault orientated in a NE - SW direction, terminated by a second ore bearing fault orientated in a WNW - ESE direction.

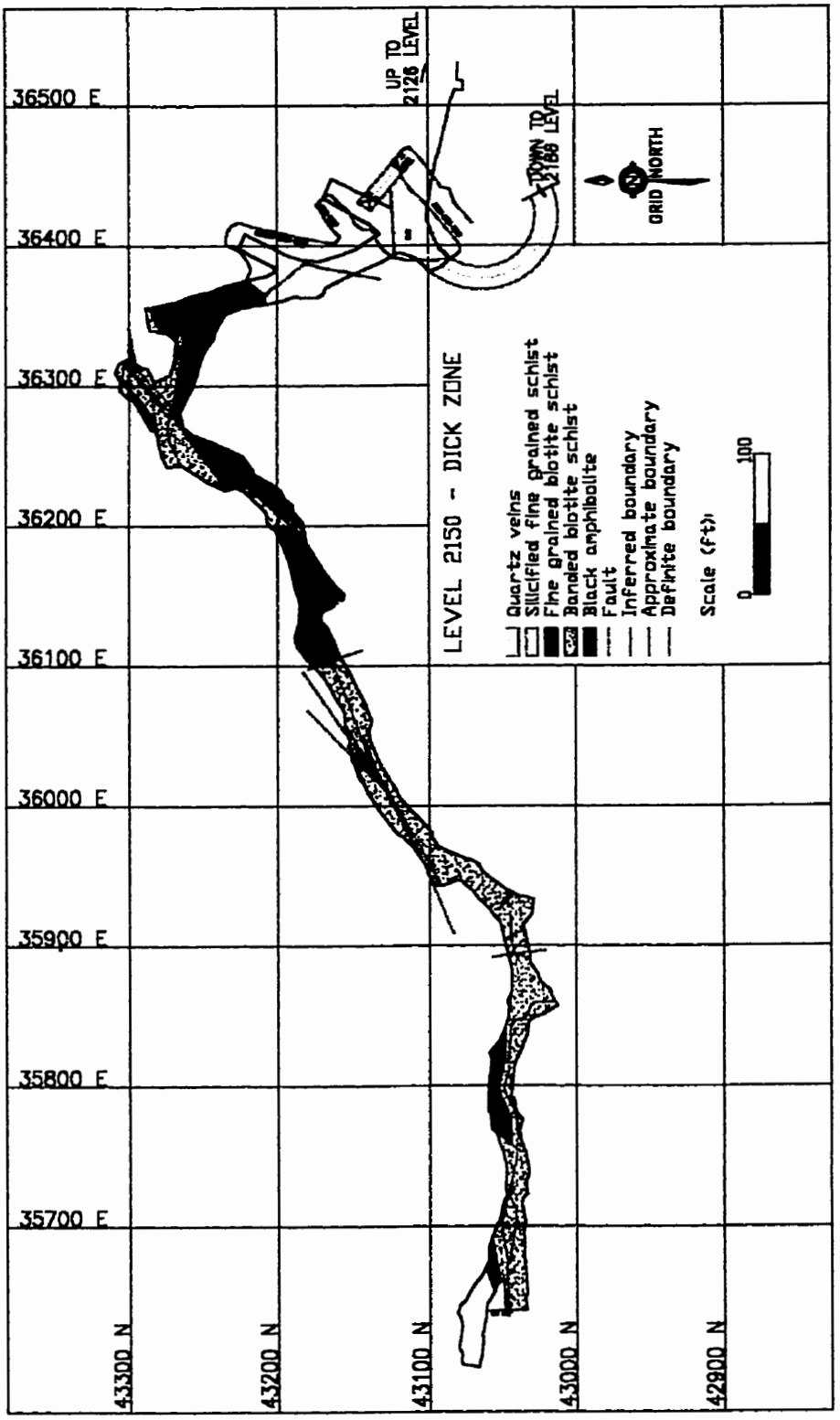

Figure 14-Geological map of Level 2150 in the Dick Zone, showing the ore associated with faults in a NE - SW orientation, becoming E - W towards the west. These faults are terminated by faults in a NNW - SSE orientation.

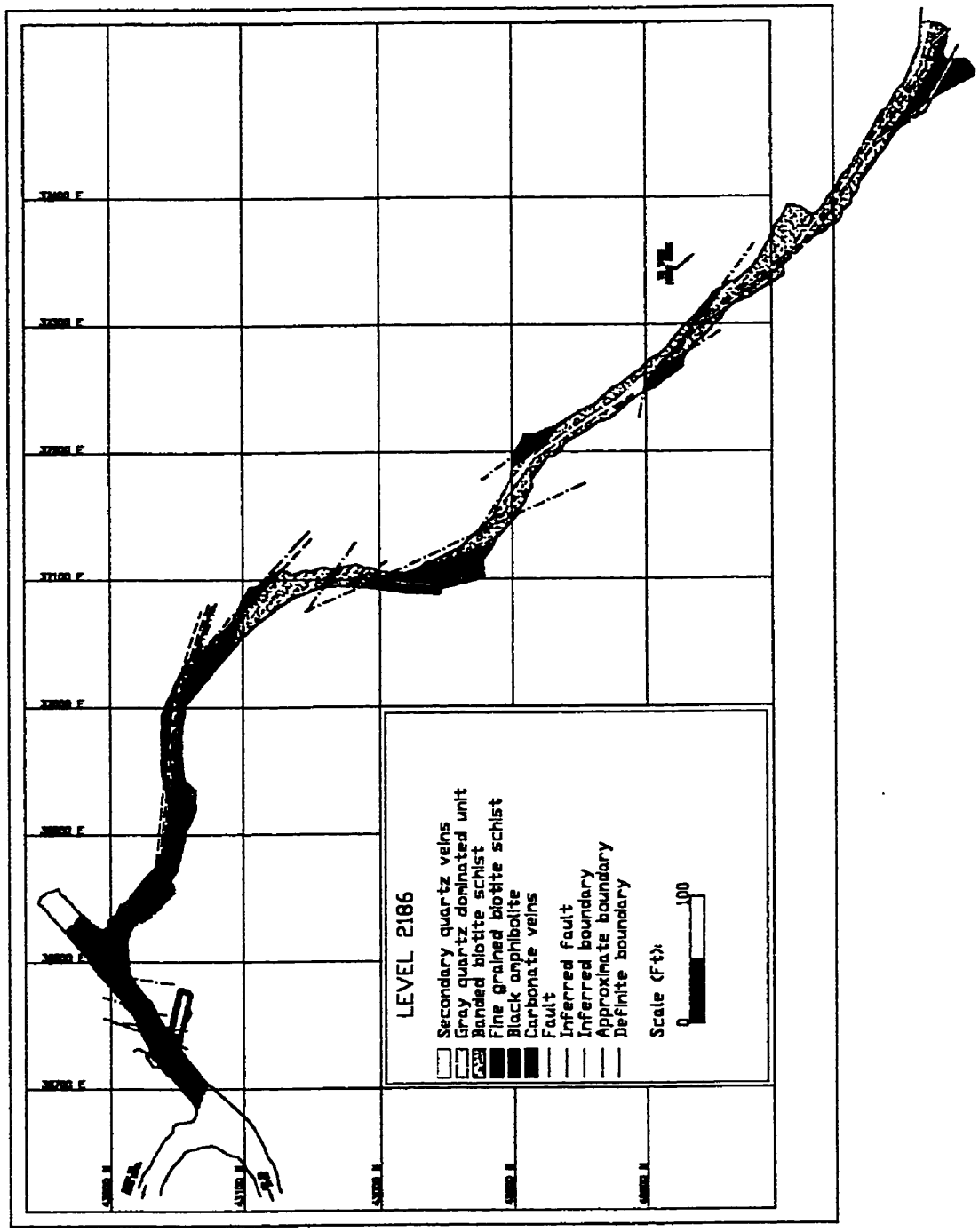

Figure 15 - Geological map of Level 2186 in the Ruttan Zone, showing the ore associated with faults in an NW - SE becoming an WNW - ESE orientation towards the east. These faults are terminated by faults in a WNW-ESE, which are further terminated by faults in a NNW - SSE orientation.

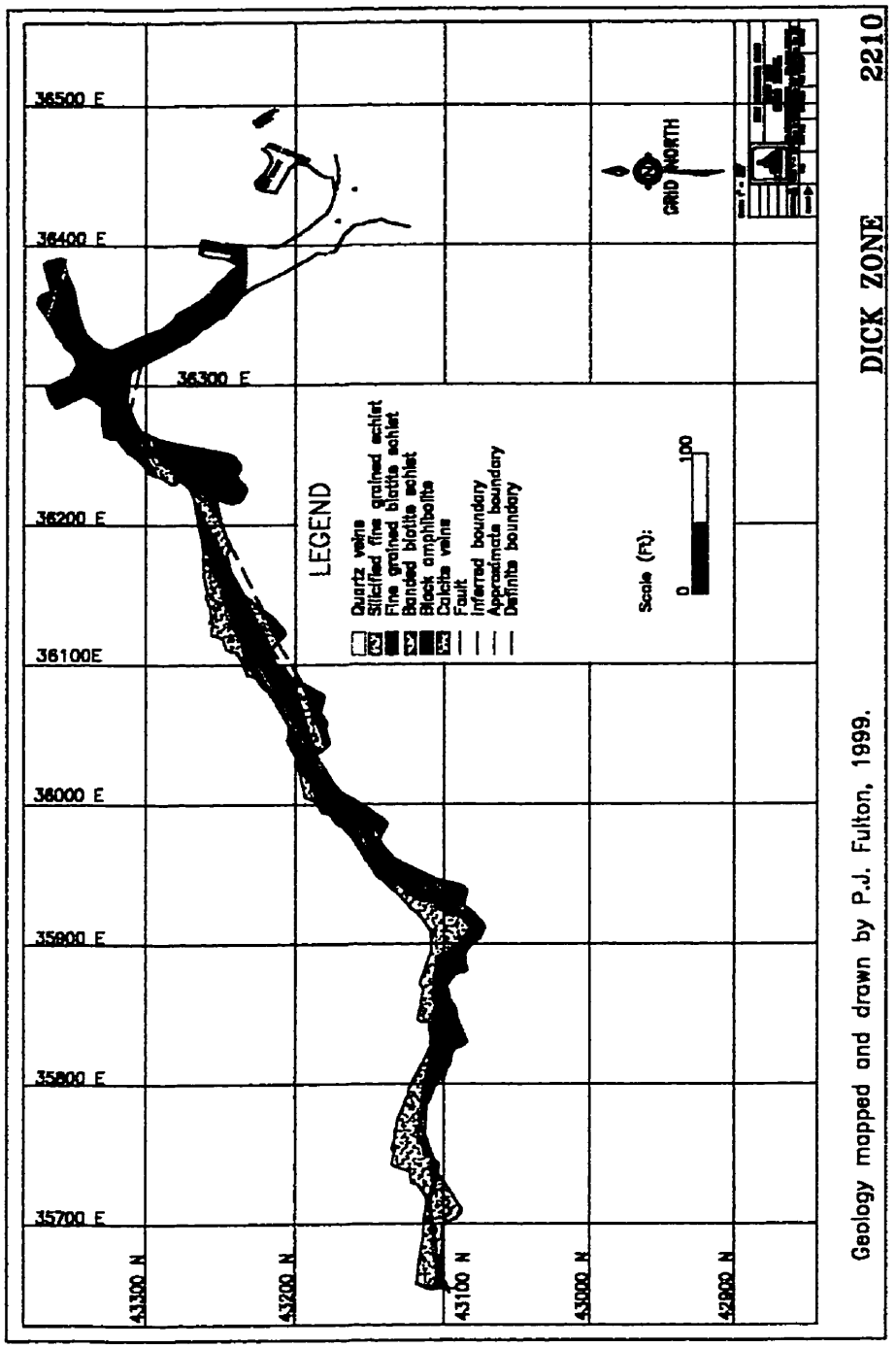

Figure 16 - Geological map of Level 2210 in the Dick Zone, showing the ore associated with faults in an primarily NE - SW orientation becoming E-W towards the west, which are cut by a shallow angle fault in a E -W orientation.

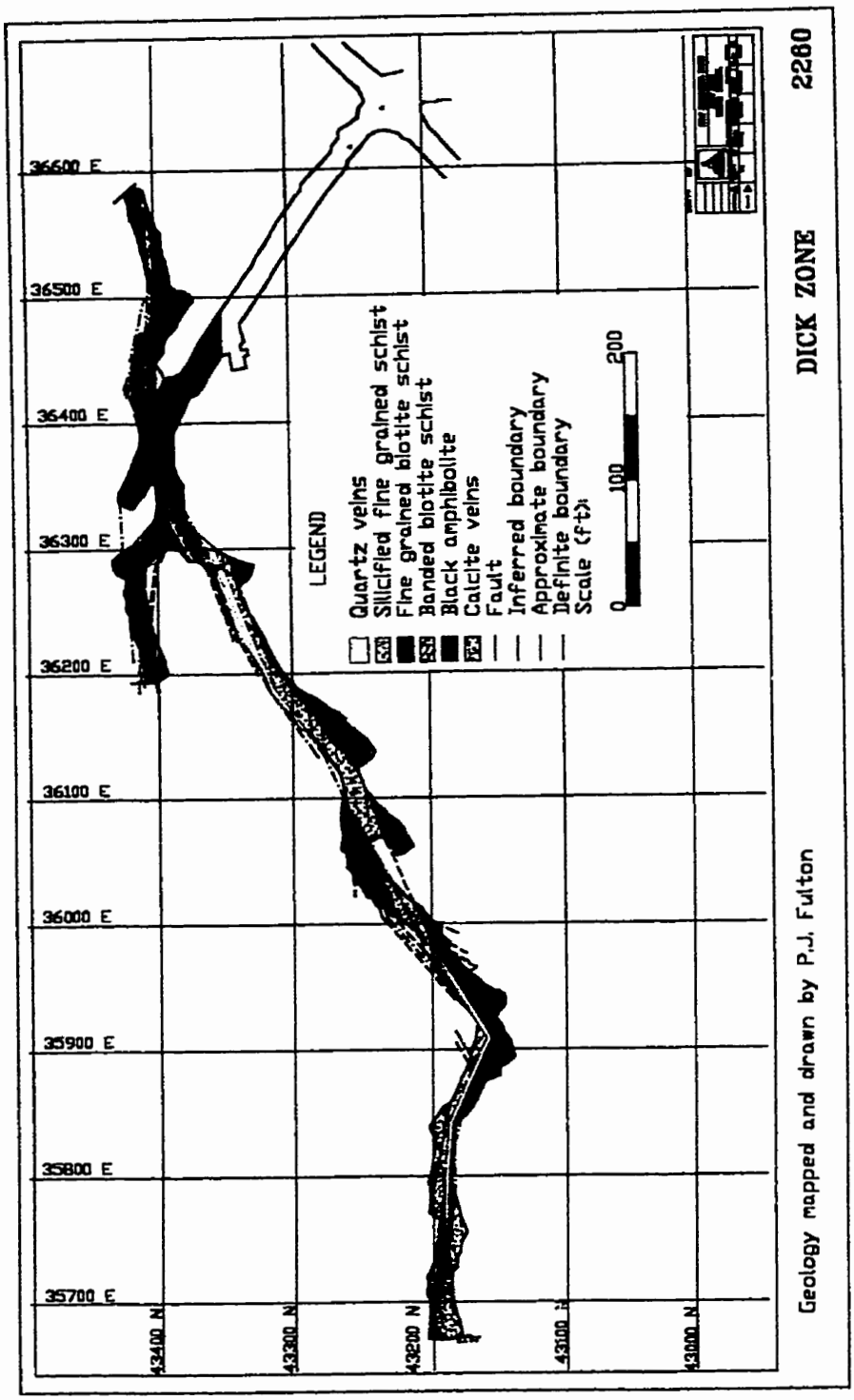

Figure 17 - Geological map of Level 2260 in the Dick Zone, showing the gold mineralization associated with a NE-SW orientated fault terminating on an E - W mineralized fault towards the west .

sulphide mineralization is chalcopyrite (earliest), Ti Fe sulphide, arsenopyrite, Ti Fe sulphide, pyrite, pyrrhotite, chalcopyrite, pyrrhotite (latest).

No. 3 Zone

The No. 3 zone has been mined out to 300', with drilling confirming the existence of mineralization at depth. Mapping has been conducted of the surface outcrop of this zone (Fig. 18). This outcrop displays a series of quartz veins in a variety of different orientations, revealing a sequence of quartz vein emplacement. A north-north-east to south-south-west set of quartz veins (earliest) are terminated by an east west iron stained vein, which is further cut by large north-east to south-west quartz veins (latest). The gold bearing ore is a biotite quartz schist which has been influenced by quartz veins and contains between 5 - 10% sulphide, the majority of which is arsenopyrite. A sequence of sulphide mineralization is seen; pyrrhotite (earliest), Ti Fe sulphide, arsenopyrite, pyrite, pyrrhotite (latest). The highest % free gold is found in sample N3-4, which contains ca. 5% sulphide minerals and a high proportion of plagioclase and orthoclase in the country rock. Invisible gold has been found in pyrite and arsenopyrite, free gold has been found adjacent to the primary quartz veins, overgrowing arsenopyrite, and also in the wall rock to the latest phases of quartz veining, and associated with calcite at the boundaries of biotite grains. This zone is different from the other zones under study as it shows a higher than normal percentage of gold in association with quartz and silicates.

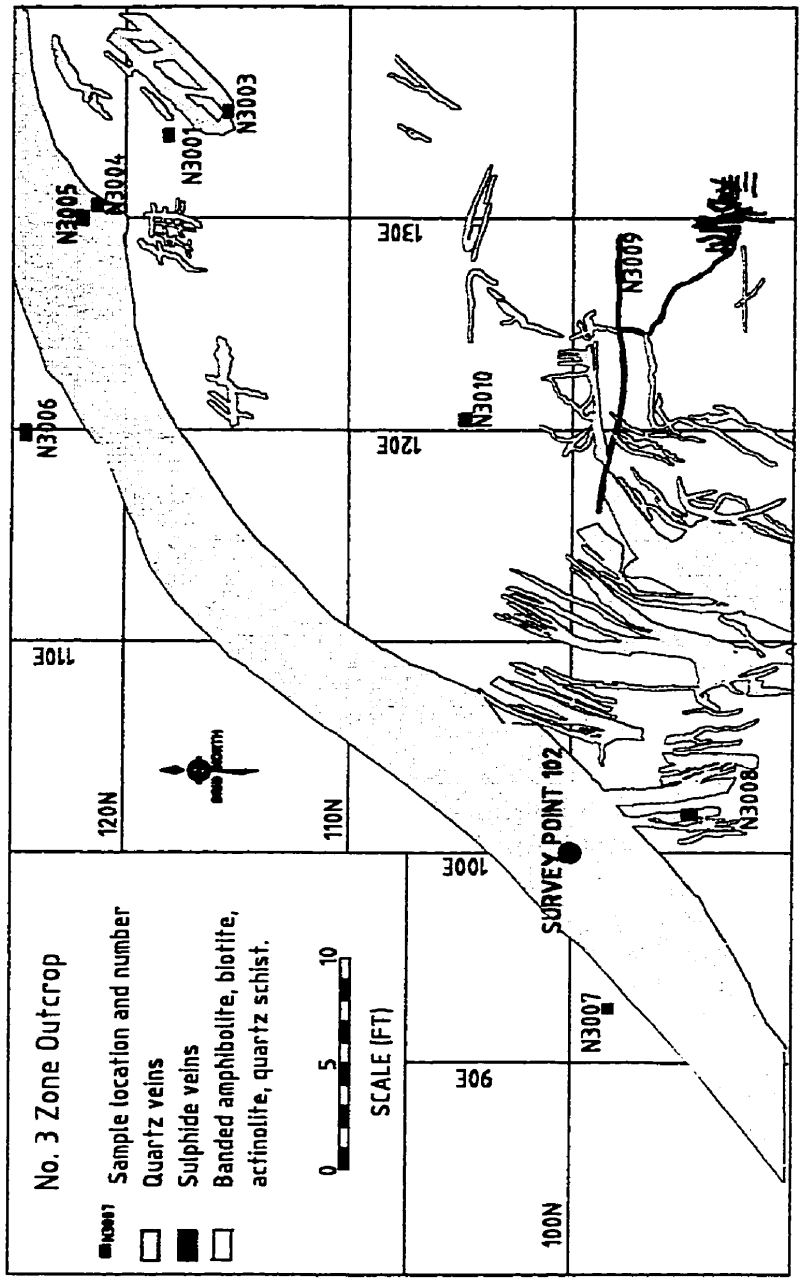

Figure 18 - No. 3 Zone outcrop geology map, showing 3 vein orientations. The first is a set of thin quartz veins orientated in a NNE - SSW direction terminated by an iron stained vein orientated E-W and N-S. The primary quartz veins are also terminated by a larger quartz vein orientated NE-SW.

CHAPTER 3 - METHODS

Sampling Techniques

In this study, sampling was conducted from surface outcrop, underground drifts, and boreholes. Mapping was done on surface at the No. 3 Zone (Fig. 17) and the Birch Zone (Fig. 8) and underground at the New Britannia Mine on Levels 780, 2006, 2030, 2150, 2186, 2210, and 2260 (Figs. 7-14 & Appendix for sample locations) to aid sample collection. Sampling of boreholes was conducted with the aid of borehole logs and gold assays, where assays greater than 0.1 oz/ton gold were obtained. The boreholes sampled were, Birch Zone; B96001, B96004, B96013; New Britannia Mine; 1780-410, 1280-424, Boundary Zone; BNDY 83-02, Sherry Zone; DO-82-N1, Thorne Zones; TZ-83-1, and Kim Zone; KZ-83-03. Samples taken are representative of rock types containing gold, intersected in diamond drilling of the Zones.

Instrumental techniques

Optical Microscopy was used to examine the ore and associated minerals under reflected and transmitted light. The major rock forming minerals were identified and semi-quantitative assessment was made of the mineral percentages, textures and relative timing of crystallization events. Powder X-Ray Diffraction was used to determine the mineralogy of the very fine grained components of the rock.

Image Analysis is a technique used for automated characterization and classification of minerals in terms of size and shape, with the ultimate product being numerical values for each feature of the minerals. Features which can be measured include

length, width, boundary irregularities, roundness, sphericity, size distributions, distances between features, number of features that have specific properties, as well as textural relationships between features. Two types of measurement can be made, individual measurements for each feature in the image (feature specific), and global measurements for all the features in the image (field specific). Performing Image Analysis involves obtaining the image, image enhancement, segmentation, mineral identification, measurement, data manipulation and interpretation of results.

Combination of Electron Microprobe Analysis (EMPA), with computerized Image Analysis, adds the ability to include mineral composition discrimination. This is done using Back Scattered Electron (BSE) image procurement, from the Electron Microprobe using the Image Analyzer (IA). The IA records this image and measures the differences in brightness across the image, these levels of brightness are split into categories called dark levels. Each dark level corresponds to the atomic number of the elements within the mineral, and discriminates mineralogy on the basis that each mineral has its own dark level.

Definitions

Gold may be in contact with a number of minerals in the New Britannia Mine. The relative proportion of the gold in contact with these minerals is of interest because it gives us information on the gold associations. Association can be used as a form of classification describing the degree to which gold is in contact with minerals such as; quartz, silicates (including biotite, chlorite, calcite, amphiboles and quartz), pyrite (including pyyrhotite), arsenopyrite and chalcopyrite. The association of the grain of interest with these phases

can be calculated with respect to the percentage perimeter of the gold grain in contact with these different phases. Therefore a grain which is found in 100% association is defined as being locked in that mineral phase (as an inclusion). A grain is referred to as being free if it occurs along the grain boundaries between adjoining grains, as is commonly the case when the gold is found in association with silicates.

Expanding on this theme can provide for varying degrees of association. This is a slight modification of the terminology used for ore processing where these terms were originally applied to crushing ore (Petruk, 1989). The following terms are of use; *Locked/exclusively associated,* refers to where a mineral encloses a gold grain, i.e. 100% of the perimeter of the gold grain is in contact with a single mineral phase such as, i.e. pyrite. *Highly associated,* refers to a gold grain where greater than 75% of its perimeter is in contact with another single phase. *Moderately associated,* refers to a gold grain where approximately 25 - 75% of its perimeter is in contact with a single phase. *Associated* refers, to a gold grain where 0.01 - 25% of its perimeter is in contact with a single mineral phase. *Spatially associated,* refers to a gold grain where its perimeter is not in contact with the mineral in question but is within the image analysis field of analysis, an area 40 x 60μm. A locked grain of gold smaller than the size ground to in the mill, will not be recovered, whereas a free or spatially to highly associated grain of gold that occurs on grain boundaries will be recovered in the milling process.

BSE images from the Electron Microprobe (EMP) were used primarily for dark level differentiation of gold grains. This was done by importing the BSE images from the EMP to the Image Analysis System (IAS). Gold, because of its high atomic number, appears bright and may be discriminated from the other rock forming minerals, which

appear darker. These darker minerals can also be discriminated from each other using differences in dark levels, the darkest mineral being quartz, followed by other silicates, pyrite, arsenopyrite and gold, the brightest.

In general, the area used for analysis was kept constant at 19,000 x 12,000 μm^2, which is approximately half the area of a mineral thin section and the area of a polished mount. The mapping and locating of gold grains was done automatically. To accomplish this the EMP acts as a slave to the IAS which conducts a motorized search, using a meander movement to move between successive fields of 40 x 60 microns, within an area defined by the four corners a, b, c and d (Fig. 19). In this way the gold search is done systematically without operator bias.

Once the gold is found, a screening program is run at magnification 400 x. This allows the grains found in the gold search to be analyzed to determine if they are gold. These grains of interest are then centered in the analysis field. Using Wavelength Dispersive Spectrometry (WDS) or Energy Dispersive Spectrometry (EDS) analysis, each gold grain is analyzed. The complete screening and classification program presents relative values of Au, Ag, Hg and Cu. This is an inaccurate technique, which does not use a known standard, but the relative values obtained can be used to gauge relative proportions. Mineral modal analysis is then done on each field containing a centered gold grain producing modal percentages of the respective minerals in the different fields.

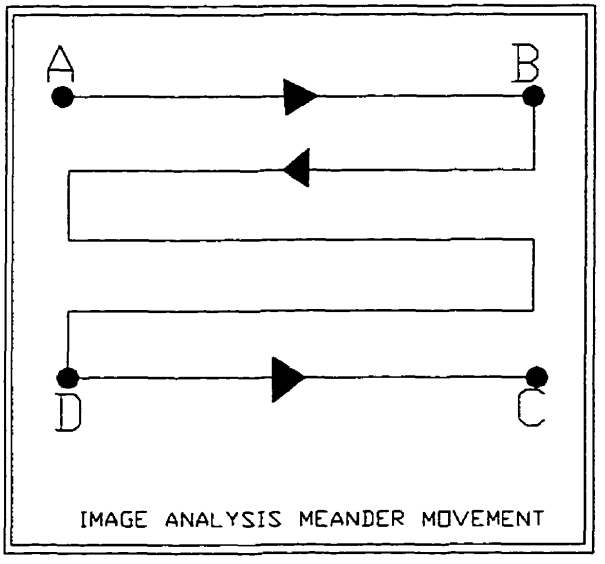

Figure 19 -Diagram describing the movement the Electron Microprobe beam takes when conducting the Gold Search with the Image Analysis System. This Meander Movement allows for a consistent and non-biased search of each sample.

Electron Microprobe Analysis (EMPA)

Chemical analysis by EMPA was conducted to obtain the compositions of the sulphide minerals: arsenopyrite, pyrite, pyrrrhotite, chalcopyrite, galena and sphalerite, and of the gold found during Gold Search. This was performed on the Cameca SX 50 Electron Microprobe using Wavelength-Dispersion Analysis at 20 KV and 20 nA, with a beam diameter of 1- 2μm. Counting time was 10 seconds for AsL$\propto$ (cobaltite), FeK$\propto$ (pyrite), SK$\propto$ (pyrite), CuK$\propto$ (chalcopyrite), TeL$\propto$ (PbTe), ZnK$\propto$ (sphalerite), NiK$\propto$ (pentlandite), AgL$\propto$ (Au60Ag40), AuM$\propto$ (pure gold), and PbMβ (PbTe). Data reduction was performed using the PAP procedure of Pouchou and Pichoir (1985).

This element list allowed the discrimination between the different sulphide phases, and of variations within these phases which provide evidence of fluid evolution. Due to

interferences with the Au Lα Lines and the As kα Lines on the mass spectrum and poor sensitivities in the parts per million (ppm) to parts per billion (ppb) range for the spectrometers, an alternative technique was needed to determine if any gold was present in the sulphide minerals, and hence refractory to normal cyanidization recovery techniques.

Secondary Ion Mass Spectrometry (SIMS)

The two main choices for analyzing gold are Proton Induced X-Ray Emission (PIXE) and Secondary Ion Mass Spectrometry (SIMS). SIMS was chosen over PIXE, as in Micro-PIXE there is a low yield on the Au Lα Line (at 9.7 KeV) coupled with spectral overlap on this line from the arsenic (As) kα Line (at 10.54 KeV). This overlap is present even with the use of a Gallium (Ga) Critical Filter, which is interposed to decrease the ratio of As kα X-Rays to Au Lα X-Rays. Without the Ga Filter the Minimum Detection Limit (MDL) for Au in the presence of As is significantly higher, requiring higher concentrations of gold within sulphide minerals to detect the gold (Halden, Campbell & Teesdale, 1995).

SIMS was used to determine the gold (Au) concentration in the sulphide minerals associated with the gold mineralization. The sensitivity of the SIMS technique is similar to that of bulk analysis methods such as Neutron Activation or Atomic Absorption, but the microbeam nature of SIMS with its accompanying spatial resolution allows for the practical analysis of individual grains with dimensions as small as 40-50 μm. SIMS is better suited to this type of analysis as it can determine the average gold content of a sufficiently small volume of sulphide and because of its lower practical MDL for gold, approximately 400 parts per billion by weight (ppbw) (Cabri et al., 1991). Potential

problems with SIMS exist in the form of the use of RSF's (Relative Sensitivity Factors), where due to matrix effects, different mineral compositions with the same concentration of certain elements may produce different intensities on a Secondary Ion Image (Pratt et al., 1997). Nonetheless, the use of the SIMS RSF technique has produced some surprising but extremely interesting results, not the least of which is that gold concentrations within the sulphide phases vary as a consequence of mineralogy and location.

Relationship between Assays and Optical Estimates

A gold assay is a method by which an assessment of the total amount of gold within a given sample is obtained. An optical estimate is a method by which the total amount of free gold in a given area and the invisible gold within sulphide minerals is measured and connected to assays through mass balance calculations. The optical estimate uses Image Analysis, to measure the amount of free gold in a sample and the percentage sulphide. SIMS is used to measure the amount of gold within representative grains for each sulphide mineral. The average concentration of gold within each type of sulphide is then used to determine the proportion of gold occurring as invisible gold. The total amount of gold is partitioned into the percentage invisible and the percentage free. This division is extremely useful in providing information on how each ore should be treated in the milling process and whether or not the ore is economical to mine.

CHAPTER 4 - ANALYSIS RESULTS

Rocks associated with the gold mineralization at Snow Lake fall broadly into two categories. Felsic rocks which have been affected by carbonatization and silicification and are typically fine grained, and rocks which have been metamorphosed to coarse grained biotite schist +/- staurolite, sillimanite and tourmaline. These rocks occur in structurally controlled areas on or adjacent to faults. Within the rocks, gold was found to occur in four main ways:

1. As free gold in association with sulphide minerals.
2. As free gold showing no association with sulphide minerals.
3. As inclusions within sulphide minerals.
4. As invisible gold within sulphide minerals.

Gold morphology

Gold grains in association with sulphide minerals are typically anhedral in shape (Plate 1), occurring at grain boundaries preferentially with other sulphide minerals, but can also exhibit a subeuhedral appearance (Plate 2) . Free gold grains in association with sulphide minerals range in size from 15 to 75 microns.

Free gold showing no association with sulphide minerals is also typically anhedral in shape (Plate 3). It occurs at the grain boundaries between silicates, and it too can exhibit a subeuhedral appearance. This character is probably influenced by the crystal faces of surrounding minerals (Plates 4 & 5). Such gold grains range in size from 15 to 190

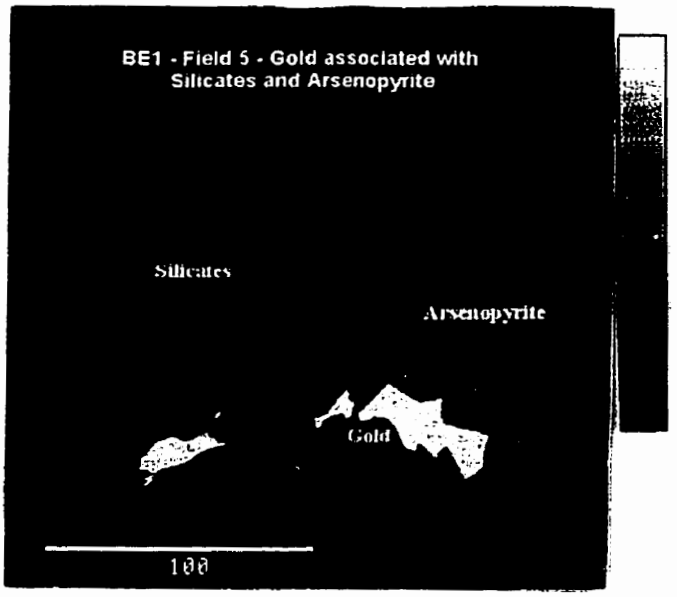

GRAY LEVEL DISCRIMINATION DIAGRAM

GOLD

ARSENOPYRITE
PYRITE & PYRRHOTITE

SILICATES
QUARTZ

Plate 1 - BSE image of sample BE1, showing gold moderately to highly associated with silicates and moderately associated with arsenopyrite. Accompanying diagram shows the relationship of image brightness with mineralogy.

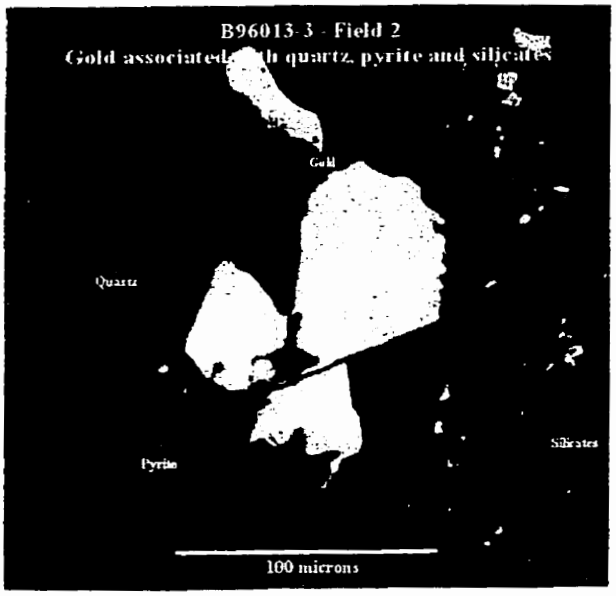

GRAY LEVEL DISCRIMINATION DIAGRAM

GOLD

ARSENOPYRITE
PYRITE & PYRRHOTITE

SILICATES
QUARTZ

Plate 2 - BSE image of sample B9613-3 showing gold coating pyrite, which is also highly associated with quartz and silicates. Accompanying diagram shows the relationship of image brightness with mineralogy.

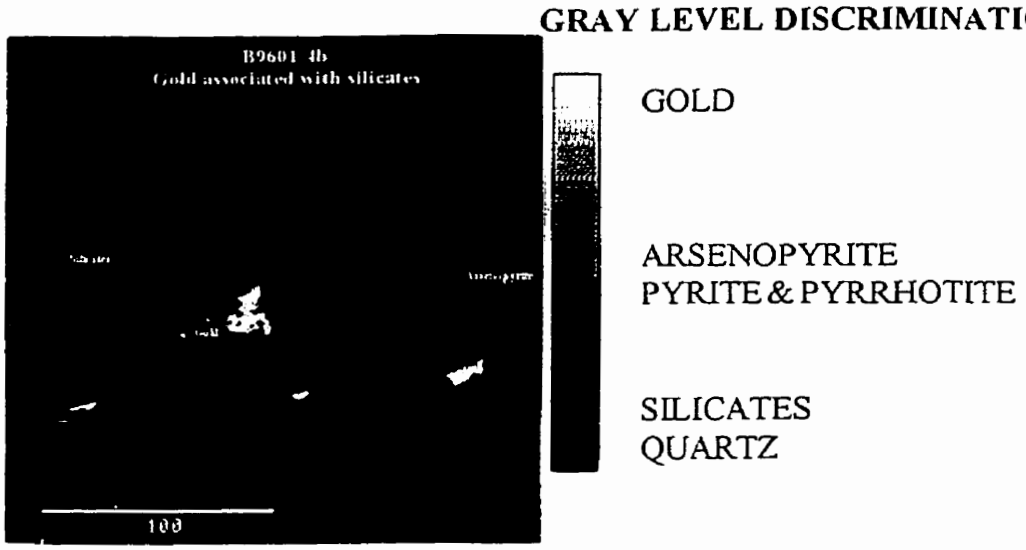

Plate 3 - BSE image of sample B9601-4b showing gold exclusively associated with silicates. Accompanying diagram shows the relationship of image brightness with mineralogy.

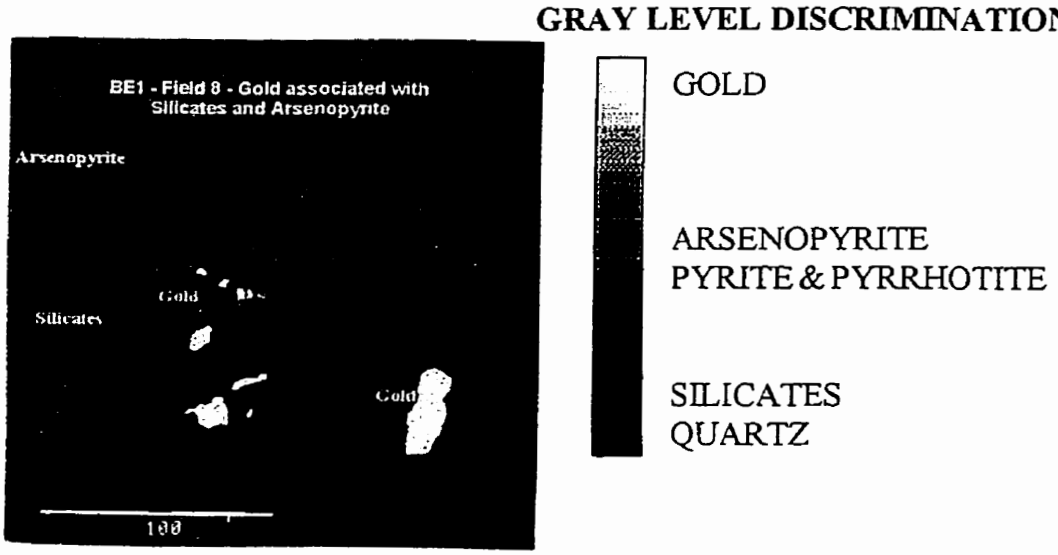

Plate 4 - BSE image of sample BE1 showing gold associated with arsenopyrite and highly associated with silicates. Accompanying diagram shows the relationship of image brightness with mineralogy.

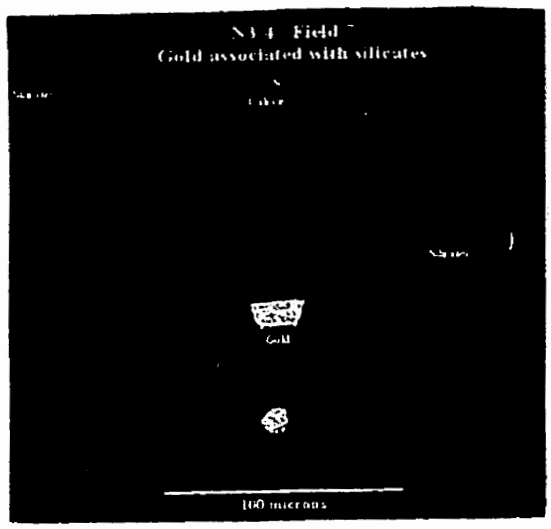

GRAY LEVEL DISCRIMINATION DIAGRAM

GOLD

ARSENOPYRITE
PYRITE & PYRRHOTITE

SILICATES
QUARTZ

Plate 5 - BSE image of sample N3-4 showing gold exclusively associated with silicates. Accompanying diagram shows the relationship of image brightness with mineralogy.

GRAY LEVEL DISCRIMINATION DIAGRAM

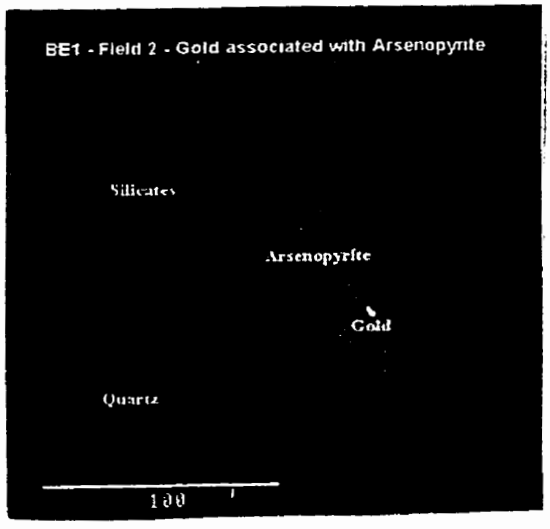

GOLD

ARSENOPYRITE
PYRITE & PYRRHOTITE

SILICATES
QUARTZ

Plate 6 - BSE image of sample BE1 showing gold locked within arsenopyrite. Accompanying diagram shows the relationship of image brightness with mineralogy.

microns (longest dimension) in the anhedral grains, to 23 to 42 microns in subeuhedral grains. Inclusion gold within sulphide minerals has only been found to be anhedral in shape (Plate 6); it varies in size from 3 to 16 microns (longest dimension).

Invisible gold within sulphide minerals is thought to occur as either minute dispersed particles of colloidal gold or structurally bound gold (Laroque et al., 1995). In general at the New Britannia Mine invisible gold is typically present in larger concentrations within arsenopyrite than in pyrite. Using ion imaging, the gold distribution can be seen to vary with sulphide mineralogy. For example, arsenopyrite from the Birch Pit and Birch Horizon 4 (H4) has distinct growth bands with elevated concentration gold (Plate 7), whereas gold in pyrite has an inhomogeneous or patchy distribution throughout the grain (Plate 8).

Similar gold distributions within the pyrite and arsenopyrite are also seen in the Boundary and the No. 3 Zones. In the No. 3 Zone however, the growth banding in arsenopyrite appears to have been disrupted, such that invisible gold has been removed from zones rich in gold (see Appendix 5, gold images N3-1-D & N3-1-E in comparison to oxygen Ion Images for the same grains but at greater depth in the grains).

Gold has also been seen as a coating on the outside of pyrite and arsenopyrite (Plates 2 & 9), or infilling the space between contacting grains of pyrite, arsenopyrite or both (Plate 10).

Sulphide morphology

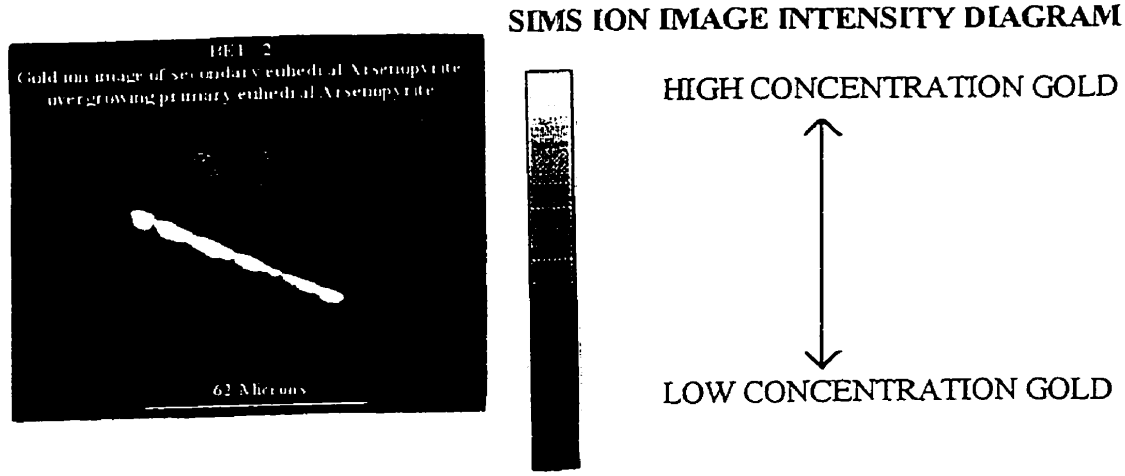

Plate 7 - SIMS gold ion image of euhedral arsenopyrite from sample BE1 from the Birch Pit, with diagram explaining gold concentration in relation to image brightness.

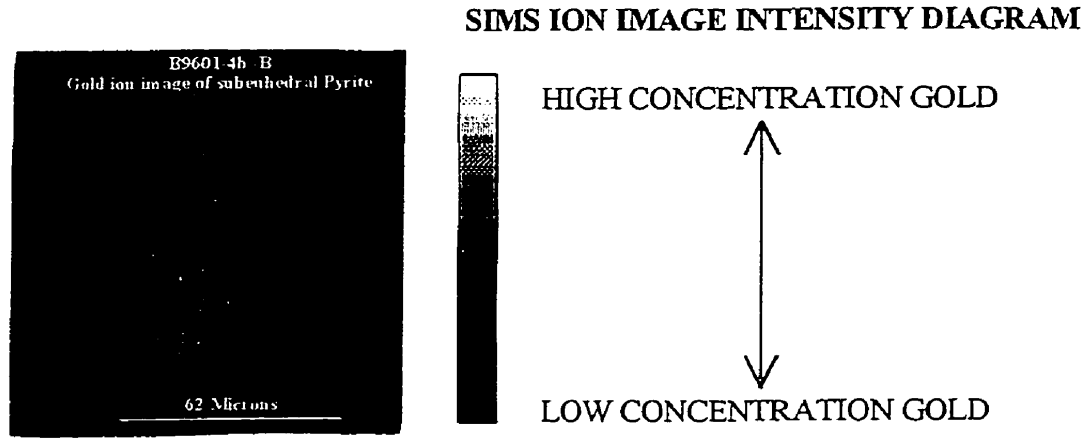

Plate 8 -SIMS gold ion image of pyrite from sample B9601-4b, from Horizon 4 in Borehole B96001, with diagram explaining gold concentration in relation to image brightness.

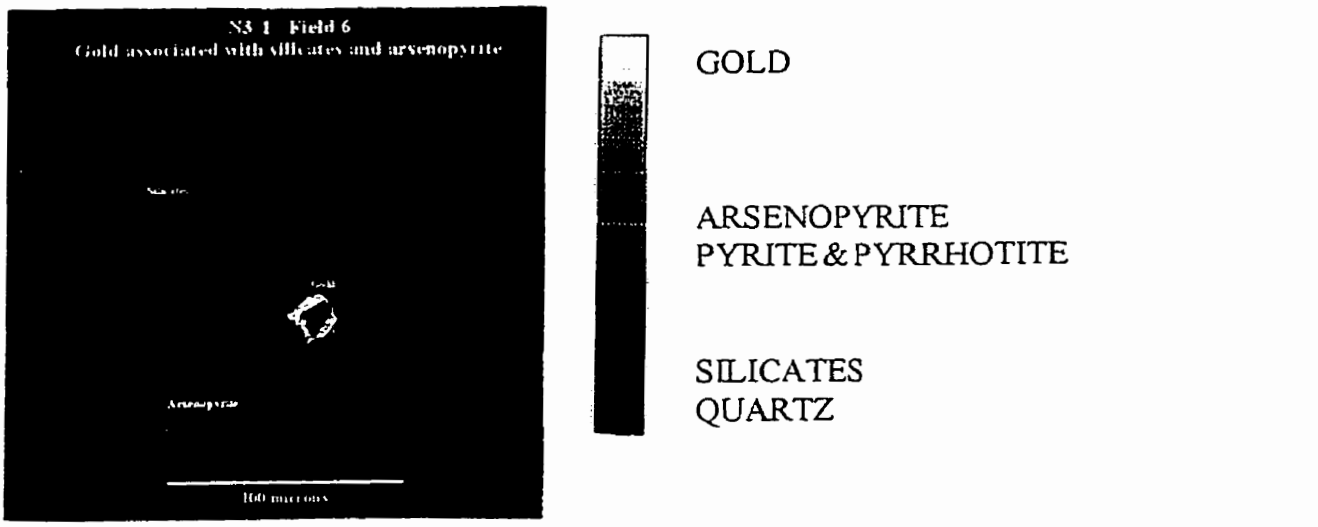

Plate 9 -BSE image of sample N3-1, from the No. 3 Zone showing gold coating arsenopyrite and moderately associated with silicates. Accompanying diagram shows the relationship of image brightness with mineralogy.

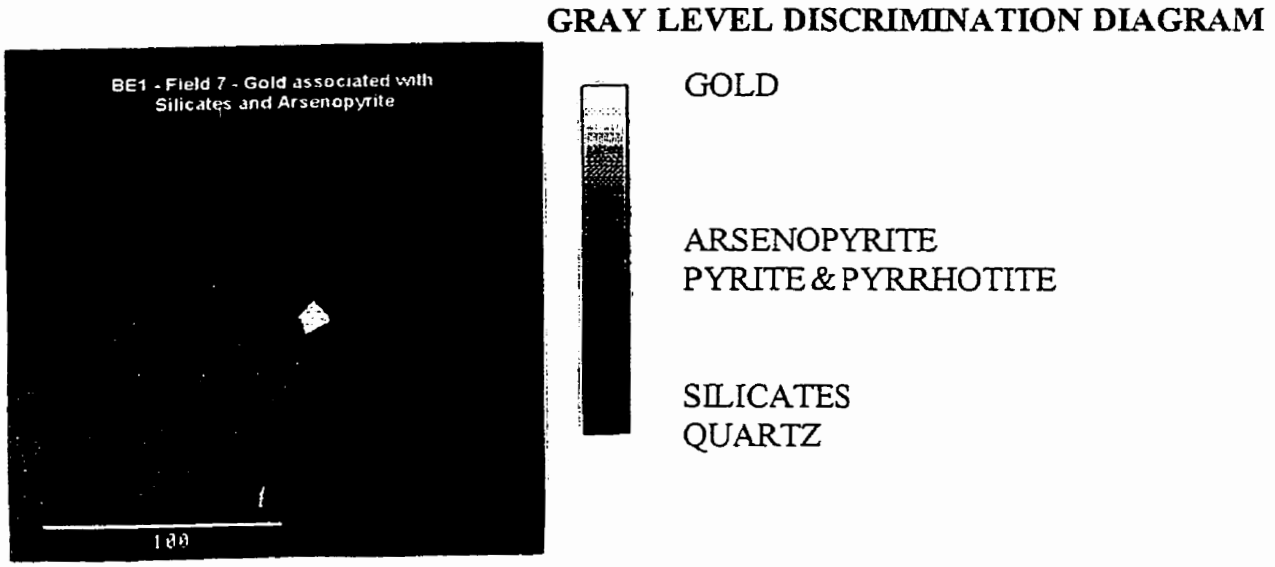

Plate 10 - BSE image of sample BE1 from the Birch Pit showing gold moderately associated with arsenopyrite and associated with silicates. Accompanying diagram shows the relationship of image brightness with mineralogy.

Attention has also been given to the shape and the size of the sulphide minerals. Using SIMS, sulphide grains of different sulphide composition, size and shape were analyzed for ppm gold. From these results no correlation between the gold concentration within arsenopyrite and shape or size has been found (Appendix 5 - table of results). In the Birch Pit, the Dick Zone of the New Britannia Mine, and the No. 3 Zone the highest gold concentrations are found in sulphide grains greater than 100 microns in size. At depth in the Birch zone, H1 and H4 of borehole B96001, and borehole B96013, the highest gold concentrations are found in sulphide grains 10-50 microns in size (Graph 1). Arsenopyrite and pyrite grain shape show no correlation with gold concentration. Irrespective of grain shape, arsenopyrite contains greater concentrations of invisible gold than pyrite, except at borehole B96001 at 705-710' depth (H6). The Birch Pit and borehole B96001 at 389-392' depth (H1)contain the highest concentrations of invisible gold (Graph 2).

Gold Perimeter & Modal Associations

In general, free gold found during the gold search has perimeter associations firstly with silicate minerals and quartz, then with arsenopyrite and lastly with pyrite (Graph 3)(Appendix 2). In samples with the most free gold, i.e. N3-4, BE1 and B9613-3 gold grains have perimeter associations with silicates and quartz (85-88%), then pyrite (between 10-11%) and lastly arsenopyrite (between 2-4%). This would suggest that the development of such grains is related to silicification. In samples with high average gold concentrations within sulphide minerals, >100 ppmw, the free gold grains found have perimeter associations of

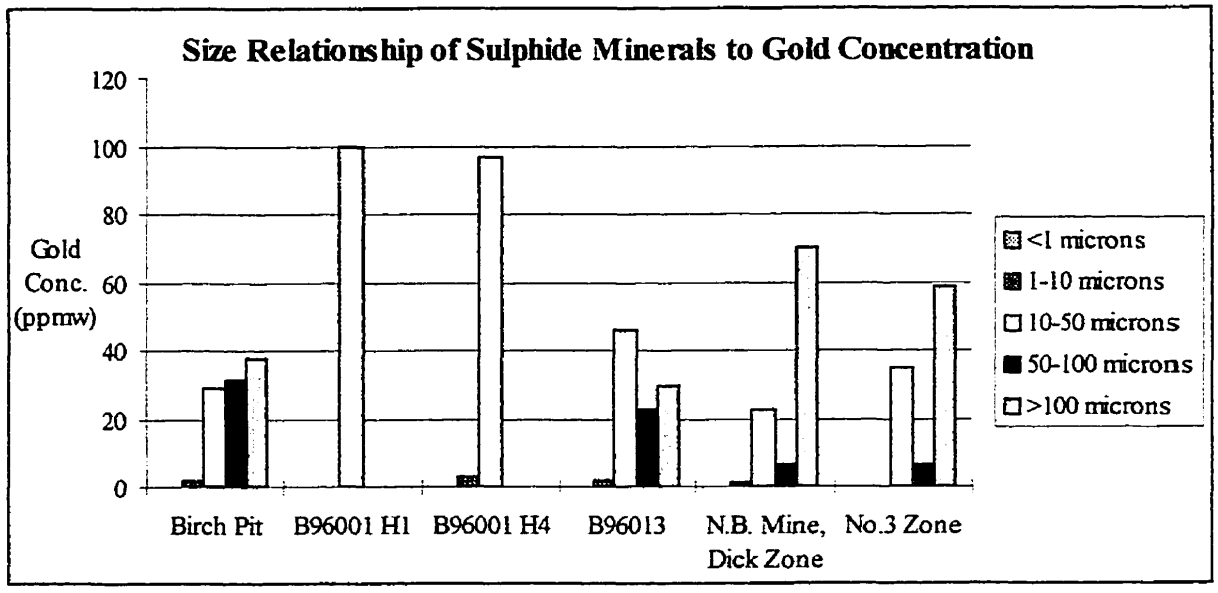

Graph 1 - Gold concentration (in ppmw) in sulphide minerals versus sulphide grain size. In the Birch Pit, the Dick Zone, and the No. 3 Zone the highest gold concentrations are found in sulphide grains greater than 100 microns in size. In H1 and H4 of borehole B96001, and borehole B96013, the highest gold concentrations are found in sulphide grains 10-50 microns in size (grain size is in microns, 10^{-6}m).

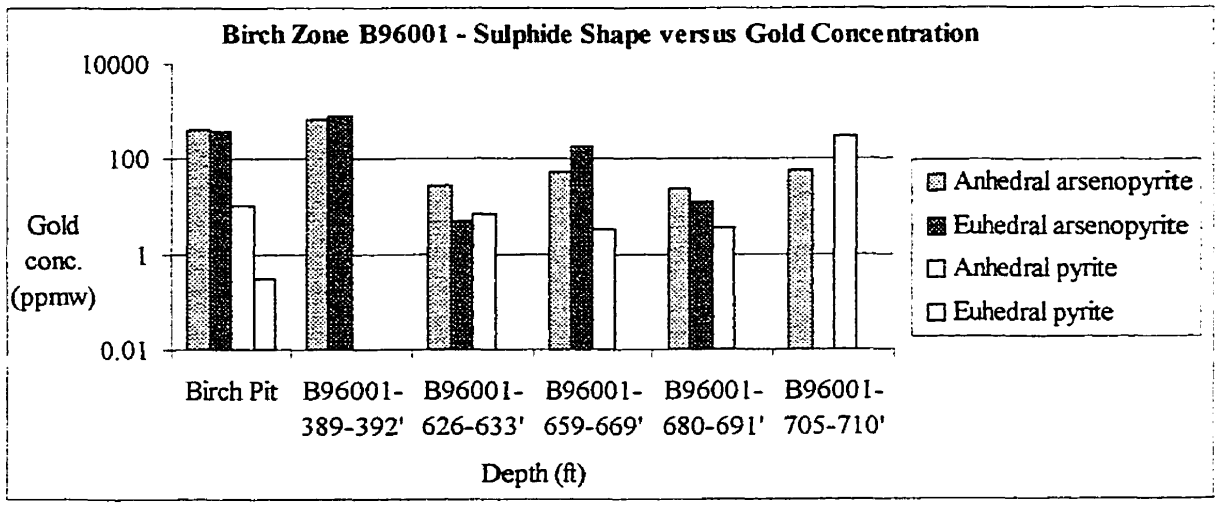

Graph 2 -Gold concentration (in ppmw) versus the shape of the sulphide minerals for the Birch Pit and borehole B96001 in the Birch Zone. Irrespective of grain shape, arsenopyrite contains greater concentrations of invisible gold than pyrite, except at borehole B96001 at 705-710' depth (H6). The Birch Pit and borehole B96001 at 389-392' depth (H1)contain the most invisible gold.

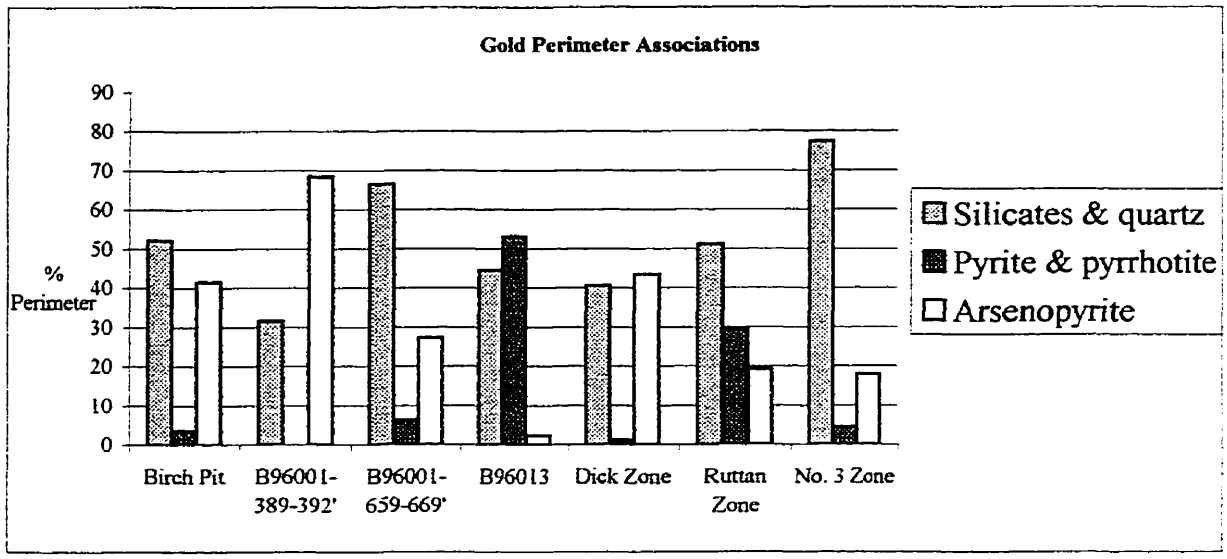

Graph 3 - Graph showing the average percentage perimeter, gold grains from each zone have with silicates and quartz, pyrite and pyrrhotite, and arsenopyrite. In the Birch Pit, borehole B96001- 659-669' (H4), the Ruttan Zone and the No.3 Zone the gold has a relationship mostly with quartz and silicates. In borehole B96001 389-392' (H1), and the Dick Zone the relationship is mostly with arsenopyrite, and in borehole B96013, of the Birch Zone, the relationship is mostly with pyrite and pyrrhotite.

between 48-51% with arsenopyrite, 47-58 % with quartz and silicates, and 0.2-10.5 % with pyrite (Graph 3), indicating, in these cases, a much stronger relationship of the free gold to the sulphide mineralization.

Overall, in samples containing larger modal proportions of gold (i.e. B9613-3 from borehole B96013) it can be seen that the gold has an association mainly with quartz and silicates, secondarily with pyrite and lastly with arsenopyrite. This is in comparison to samples with a high gold concentration within the sulphide minerals, in which free gold is found in association primarily with arsenopyrite, quartz and silicates, and lastly with pyrite.

These changing gold associations between and within Zones are documented below.

The Birch Zone

In comparison to the whole slide in general, modal analyzes of fields found to contain gold indicate an increased percentage of arsenopyrite and a reduction in the percentage silicates and quartz, in samples from the Birch Pit (Table 1).

In borehole B96001, in the Birch Zone, fields containing gold were found to have higher concentrations of quartz and silicates, except in sample B9601-35b, in comparison to the whole slide modal analysis (Table 2). The perimeter associations indicate a strong association of gold with quartz and silicates, and arsenopyrite.

The New Britannia Mine

On Level 2006 of the Ruttan Zone in the New Britannia Mine, fields containing gold in contrast to the whole sample analyzed were found to contain less quartz, and greater amounts of silicates and arsenopyrite. The perimeter associations indicate a variable association of gold with silicates, quartz, pyrite and arsenopyrite (Table 3).

On Level 2210 of the Dick Zone in the New Britannia Mine, fields containing gold were found to have lower percentages of quartz, higher percentages of silicates except in DB37, and consistently higher percentages of arsenopyrite and lower percentages of quartz and silicates together, in all samples analyzed (Table 4). Perimeter associations indicate an association principally with silicates and secondarily with arsenopyrite, except in sample RC2, which has an association primarily with pyrite and then with arsenopyrite.

Sample No.	Type	% Silicates & quartz	% Pyrite & pyrrhotite	% Arseno-pyrite	% Gold
BA05	Perimeter Association	40.65	7.48	51.87	-
	Gold field Modal Analysis	85.24	0.39	14.23	0.13
	Whole Slide Modal analysis	95.65	0.31	3.70	8.50 E-5
BD01	Perimeter Association	62.36	0.74	36.89	-
	Gold field Modal Analysis	92.60	0.04	7.20	0.11
	Whole Slide Modal analysis	98.65	0.14	1.2	1.32E-4
BE01	Perimeter Association	58.52	2.74	38.74	-
	Gold field Modal Analysis	77.97	1.11	20.52	0.40
	Whole Slide Modal analysis	88.26	0.51	10.80	1.12 E-3

Table 1 - Birch Pit gold Perimeter Associations, Gold Field Modal Analysis and Whole Slide Modal Analysis results.

Sample No.	Type	% Silicates & quartz	% Pyrite & pyrrhotite	%Arseno-pyrite	% Gold
B9601-35b	Perimeter Association	31.58	0.00	68.42	-
	Gold field Modal Analysis	98.84	0.01	1.12	0.04
	Whole Slide Modal Analysis	99.19	0.06	0.75	6.49E-6
B9601-4b	Perimeter Association	85.07	1.9	13.04	-
	Gold field Modal Analysis	91.28	7.43	0.54	0.436
	Whole Slide Modal Analysis	90.91	4.35	4.75	6.79E-4
B9601-6a	Perimeter Association	47.92	10.42	41.67	-
	Gold field Modal Analysis	95.37	1.38	3.15	0.099
	Whole Slide Modal Analysis	92.99	2.54	4.47	2.7E-8

Table 2 - Birch Zone bore hole B96001, Perimeter Associations, Gold Field Modal Analysis and Whole Slide Modal Analysis results.

Sample No.	Type	% Quartz	% Silicates	% Pyrite & pyrrhotite	% Arseno-pyrite	% Gold
DB7	Perimeter Association	-	42.19	3.13	54.19	-
	Gold field Modal Analysis	-	85.46	0.72	5.81	0.26
	Whole Slide Modal analysis	49.10	48.02	0.45	2.43	1.46E-4
DB21b	Perimeter Association	12.50	87.50	0.00	0.00	-
	Gold field Modal Analysis	78.79	12.82	0.04	7.97	0.30
	Whole Slide Modal analysis	90.51	7.81	0.24	1.44	5.61E-4
DB30	Perimeter Association	35.81	10.14	0.00	54.05	-
	Gold field Modal Analysis	97.88	1.83	0.00	0.14	0.16
	Whole Slide Modal analysis	99.37	0.23	0.02	0.38	7.18E-4
DB37	Perimeter Association	0.00	0.00	1.97	98.03	-
	Gold field Modal Analysis	0.01	0.58	0.43	98.00	0.88
	Whole Slide Modal analysis	53.08	45.92	0.18	0.83	1.75E-3

Table 3 - New Britannia Mine, Ruttan Zone Level 2006, Perimeter Associations, Gold Field Modal Analysis and Whole Slide Modal Analysis results.

Sample No.	Analysis type	% Quartz	% Silicates	% Pyrite & pyrrhotite	% Arse-nopyrite	% Gold
RA1	Perimeter Association	0	100	0	0	-
	Gold field Modal Analysis	0.07	98.09	0.11	1.65	0.08
	Whole slide Modal Analysis	0.18	98.14	0.19	1.26	1.74E-5
RA4	Perimeter Association	0	53.33	0	46.67	-
	Gold field Modal Analysis	0	77.21	0.03	22.70	0.07
	Whole slide Modal Analysis	0.17	98.19	0.025	1.46	1.46 E-5
RC2	Perimeter Association	0.27	0	88.59	11.14	-
	Gold field Modal Analysis	0.033	0.12	98.88	0.19	0.78
	Whole slide Modal Analysis	0.17	97.58	0.02	2.2	4.66E-4

Table 4 - New Britannia Mine, Dick Zone Level 2210, Perimeter Associations, Gold Field Modal Analysis and Whole Slide Modal Analysis results.

The No. 3 Zone

In the No. 3 Zone outcrop, fields containing gold contain lower percentages of silicates and quartz, but higher percentages of arsenopyrite than in each sample on average. Perimeter Associations indicate an association principally with quartz and silicates, secondarily with arsenopyrite and lastly with pyrite (Table 5).

Comparison of the zones

In Graph 4, it can be seen that a high percentage of sulphide in the rock correlates with a high average gold concentration within the sulphide minerals, except in Horizon 1 of the Birch Zone. Overall, there is a negative correlation between the percentage sulphide in the fields containing gold and the average gold concentration in the sulphide minerals. No correlation is observed between the percent free gold and the percentage of sulphide in the ore or average gold concentration in the sulphide minerals. From all the Horizons in the Birch Zone analyzed, it can be seen that there is approximately the same percentage of sulphide in fields containing gold as in the whole slide. This is in contrast to the No. 3 Zone and the Dick Zone of the New Britannia Mine, where there are greater percentages of sulphide in fields containing gold than in the whole slide in general.

Sample No.	Type	% Silicates & quartz	% Pyrite & pyrrhotite	% Arseno-pyrite	% Gold
N3-1	Perimeter Association	49.00	0.20	50.8	-
	Gold field Modal Analysis	84.6	2.20	12.5	0.3
	Whole Slide Modal analysis	94.54	0.46	2.71	3.96 E-4
N3-3	Perimeter Association	100	0.00	0.00	-
	Gold field Modal Analysis	93.70	0.01	3.10	0.05
	Whole Slide Modal analysis	97.40	0.23	0.52	2.26 E-5
N3-4	Perimeter Association	83.44	13.23	3.01	-
	Gold field Modal Analysis	94.30	0.60	0.60	4.06
	Whole Slide Modal analysis	100.00	0.00	0.00	8.85 E-4

Table 5 - No. 3 Zone outcrop, Perimeter Associations, Gold Field Modal Analysis and Whole Slide Modal Analysis results.

Gold mineralogy

Chemical analysis of the gold shows high Au/Ag ratios for all of the gold grains analyzed in the Birch Zone, except for samples taken from bore hole B96013 which lies to the NNE of the Birch Pit, east of bore hole B96001 (Graph 5).

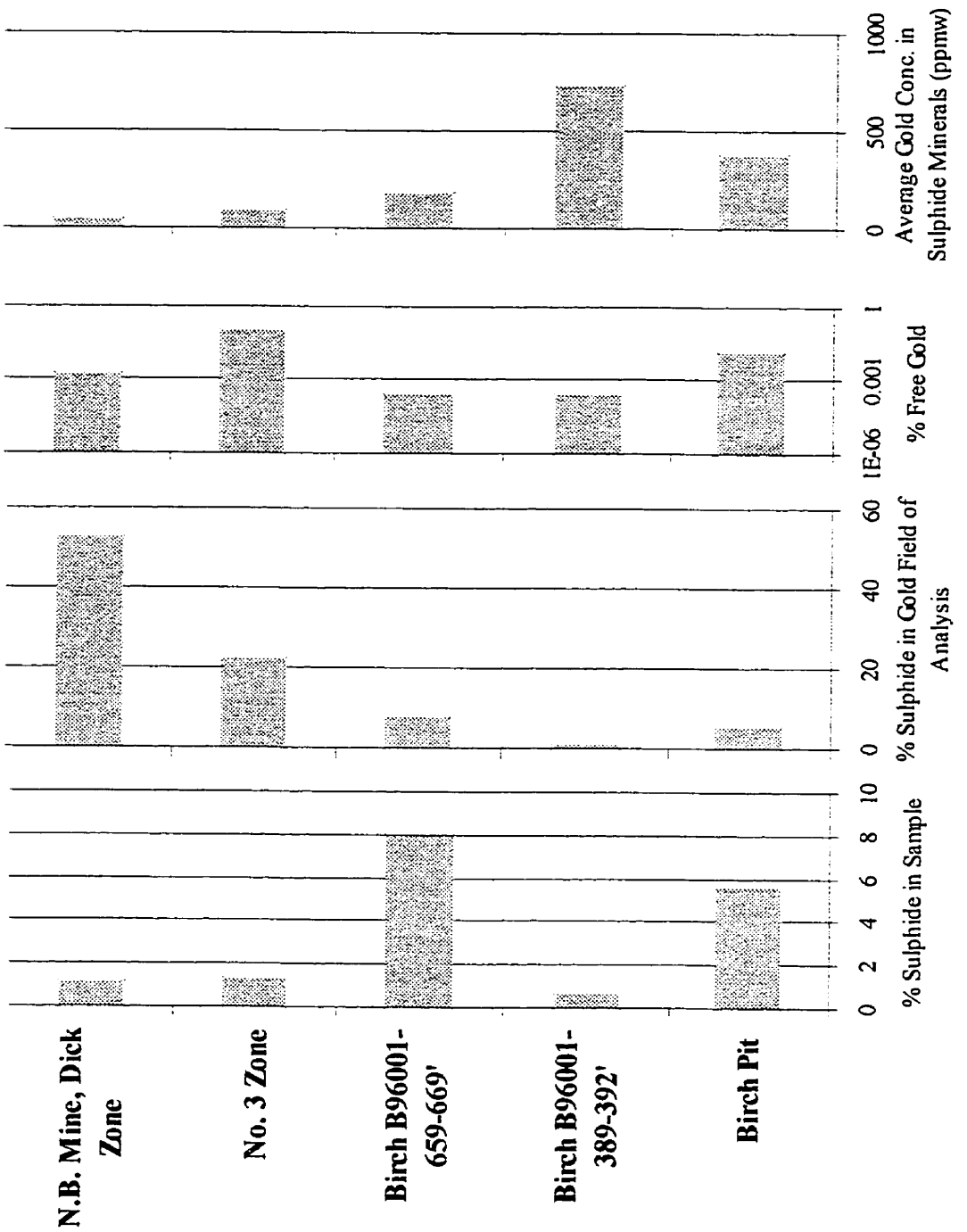

Graph 4 - Graphs showing the % Sulphide versus % Free Gold versus Average Gold Concentration (in parts per million by weight) in sulphide minerals, for the Dick and Ruttan Zones of the New Britannia Mine, the No. 3 Zone and the Birch Zone.

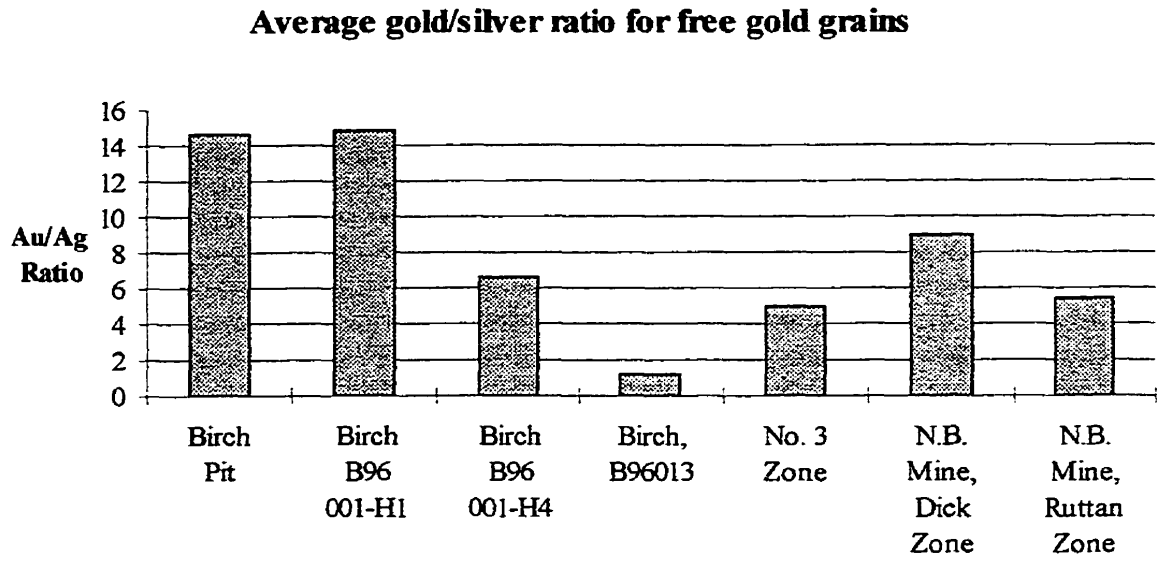

Graph 5 - Au/Ag ratio of free gold from all the zones analyzed. This shows that the free gold, gold concentration varies between zones.

Sulphide Mineralogy

Quantities and modal proportions of pyrrhotite, pyrite and arsenopyrite vary between zones. Composition, which is relatively static in pyrrhotite, varies in pyrite and arsenopyrite, as shown by EMPA. In the Birch Zone, there are variations in arsenopyrite elemental proportions from 44-49 Wt% arsenic, at iron 36-40 Wt% and sulphur 15-18 Wt%. Pyrite has a variable composition from 52-55 Wt% iron, 45-48 Wt% sulphur, and 0-2 Wt% arsenic. Pyrrhotite varies in composition from 62-68 Wt% iron, and 32-38 Wt% sulphur (Graph 6)(Appendix 4).

In the New Britannia Mine, Level 2006 in the Ruttan Zone, displays static pyrite and pyrrhotite values, but a trend in arsenopyrite values from 43 -54 Wt% arsenic (Graph 7). Level 2210, in the Dick Zone, shows the same evolution in arsenopyrite, 43-52 Wt%

arsenic, with another shallower trend of increasing arsenic with decreasing iron and increasing sulphur. There are two main compositions of pyrite, the first at 52 Wt% iron (48 Wt% sulphur) and no arsenic, the second at 53-54 Wt% iron and 0-2 Wt% arsenic. Pyrrhotite displays a variation in composition along the S-Fe axis from 61 Wt% iron/ 39 Wt% sulphur to 70 Wt% iron / 30 Wt% sulphur (Graph 8).

In the No.3 Zone, there is an evolution in arsenopyrite values from 43 -52 Wt% arsenic, and in pyrite a variation in iron from 50-54 Wt%. Pyrrhotite varies in composition from 66-67 Wt% iron (Graph 9).

In the Boundary Zone, there is a variation in arsenic values in arsenopyrite from 42-47 Wt%, and in pyrite, at 55 Wt% iron, from 0-7 Wt% arsenic. Pyrrhotite composition varies from 67-68 Wt% iron (Graph 10).

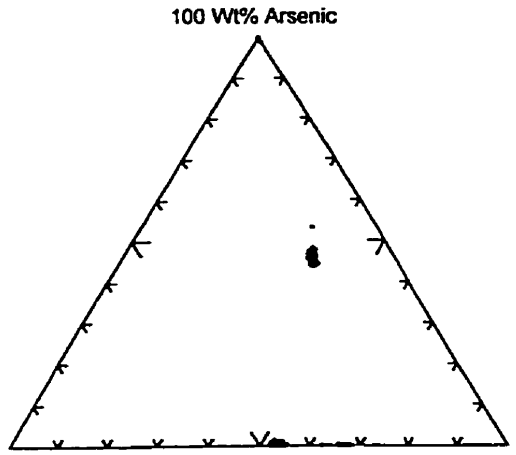

Graph 6

Birch Zone S-As-Fe plot of all the sulphide minerals analyzed by EMPA.

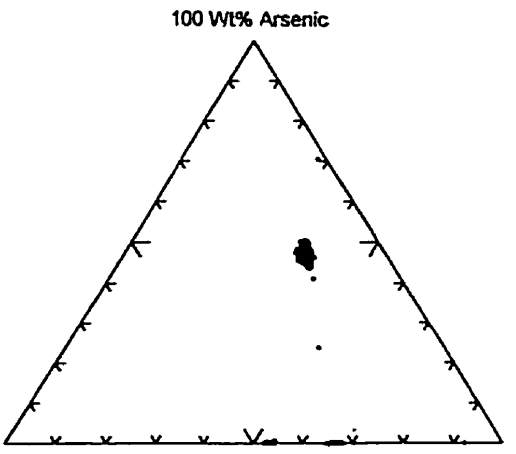

Graph 7

New Britannia Mine, Ruttan Zone S-As-Fe plot of all the sulphide minerals analyzed by EMPA.

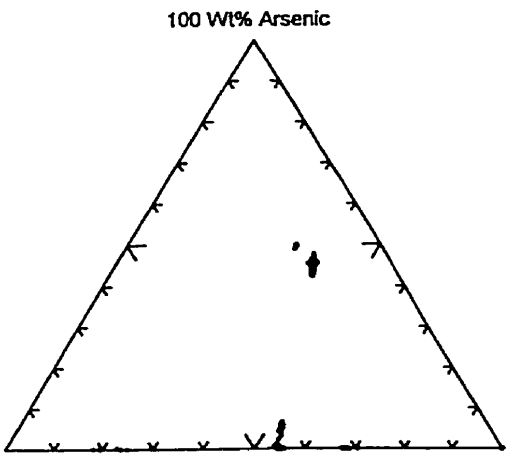

Graph 8

New Britannia Mine, Dick Zone S-As-Fe plot of all the sulphide minerals analyzed by EMPA.

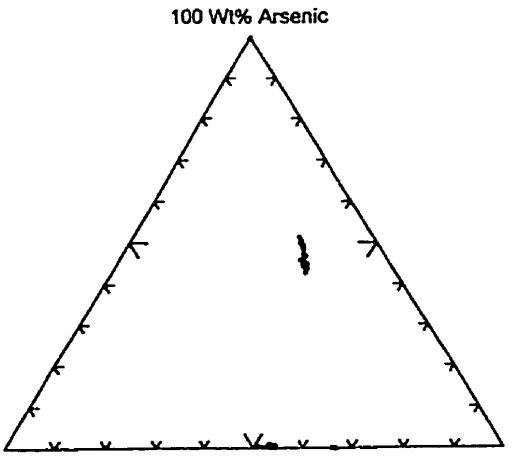

Graph 9

No. 3 Zone S-As-Fe plot of all the sulphide minerals analyzed by EMPA.

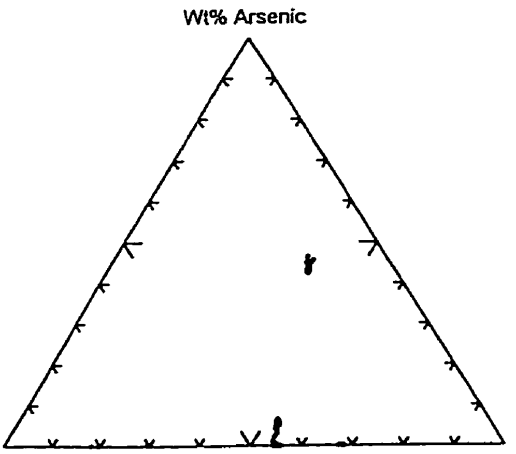

Graph 10

Boundary Zone S-As-Fe plot of all the sulphide minerals analyzed by EMPA.

CHAPTER 5 - DISCUSSION

Gold is found in a variety of settings in and around the New Britannia Mine. There is a considerable proportion of free gold, however there is also a measurable amount of gold occurring as "invisible gold" that is currently inaccessible to cyanidization. Both of these types of gold are associated with faults in the Dick, Ruttan and Birch Zones and with quartz filled tension gashes and veins at the No. 3 Zone.

Summary of ore characteristics

In the Abitibi, Wabigoon, Wawa, and Uchi greenstone Belts of the Canadian Shield, carbonization is the most common gold-related alteration on both regional and mine scales. Mineral assemblages indicative of sulphidation, silicification, oxidation and potassic metasomatism are also characteristic, but tend to be more locally associated with the gold (Colvine et al., 1988).

Mapping and thin section work has shown that high assays are commonly found associated with areas rich in biotite, quartz, +/- chlorite, +/-actinolite and calcite, or the higher grade equivalent containing fibrolite. Such associations are typical of the Birch Zone, the No.3 Zone, the Boundary Zone and the New Britannia Mine. The biotite and actinolite are usually found at the margins of quartz or calcite veins as a wall rock alteration product, and the fibrolite usually occurs in discrete patches. This would suggest that the late free gold, which is found associated with the silicates biotite, quartz, and actinolite, and the sulphide minerals pyrite and arsenopyrite (and in the No.3 Zone with

calcite), is carried in silicic or carbonaceous fluids.

Sulphide minerals are found throughout the rocks in proximity to faults and not just around quartz and carbonate veins. Typically, there is a sequence of sulphide crystallization seen in all the zones studied. The sequence is from chalcopyrite (earliest), pyrrhotite , Fe Ti sulphide, arsenopyrite, Fe Ti sulphide, pyrite, pyrrhotite, euhedral chalocopyrite, to pyrrhotite (latest). Gold is found within pyrite and arsenopyrite (invisible and inclusion gold), as well as overgrowing pyrite (in sample B9613-3, from bore hole B96013) and arsenopyrite (in sample N3-1) as free gold. This suggests that gold has been mobile more than once and that the free gold occurred after arsenopyrite crystallization.

Mineralogical associations of gold bearing rocks

In general at Snow Lake, gold is found as free grains within silicate host rocks, as inclusion gold contained within sulphide minerals and as invisible gold in sulphide minerals. No association between sulphide mineral shape or size and sulphide gold concentration has been found. Free gold is found in association with arsenopyrite or pyrite, overgrowing biotite or along grain boundaries between silicate minerals. Inclusion gold is found within arsenopyrite and pyrite. No gold has been found within chalcopyrite or pyrrhotite. A similar situation has been described by Mumin et al., (1994) who found that gold was most commonly associated with arsenopyrite and/or arsenian pyrite, or occurring as free grains in the quartz-albite-ankerite gangue along wall rock partings in the Bogosu-Prestea mining district of the Ashanti Gold Belt, Ghana. Occasionally, gold is enclosed within or at and near the margins of chalcopyrite and sphalerite grains, 90% of

the microscopic gold is directly associated with pyrite and arsenopyrite, 89% of which is associated with arsenian pyrite, mostly in voids and fractures. Also spongy core areas, due to conversion and alteration of earlier sulphide minerals, of arsenopyrite grains were found to accumulate gold grains and hence to act as traps for gold (Mumin et al., 1994).

In general, of the deposits examined in the Snow Lake area, free gold has a composition of 80-95% gold to 20-5% silver(Appendix 2). In the Birch Zone bore hole B96013, however, the free gold has a composition of up to 60% silver and inclusion gold was not found. Laboratory experiments have shown that silver bearing ore is easily attached by sulphide ions, and hence gold grains high in silver are more likely to be found in association with, as free gold, or within, as invisible gold, sulphide minerals. Pure gold is inert, and less likely to be found in association with or within sulphide minerals (Harris, 1990). This would suggest that inclusion and invisible gold has a higher silver content than free gold. However, inclusion gold in the Birch Zone, where large enough to get an electron beam onto for analysis, showed a similar composition to free gold. In areas where the silver content of the gold was higher, such as in bore hole B96013, free gold showed a greater preference for silicates and quartz than for sulphide minerals. The lack of sulphide minerals in this particular rock however, may have been a major factor in the free gold having an association mainly with silicates and quartz, as one of the few sulphide grains in proximity to the free gold is barley visible beneath its coating of gold in sample B9613-3-field 2 (Plate 2).

Birch Zone

Based on modal analyzes, assays and SIMS analyzes(Appendices 2 & 5), high proportions of sulphide minerals in the ore (ca.8%) are associated with low concentrations of invisible gold within the sulphide minerals (an average of 99 ppmw for arsenopyrite and 3 ppmw for pyrite in Birch Horizon 4, 659 to 669' depth in bore hole B96001). Conversely, where there is a low proportion of sulphide minerals in the ore (ca.1%), there is a high concentration of invisible gold within the sulphide minerals (average arsenopyrite is 731 ppmw in Horizon 1 of the Birch Zone, 389 to 392' depth in borehole B96001) (Graph 4). This indicates that the percent sulphide in the ore is irrelevant in areas containing invisible gold, as the overall amount of gold held within the sulphide minerals will be the same regardless of quantities of the sulphide minerals.

In the Birch Zone, comparison of the Pit and H 1 (389 to 392' depth in B96001), H2 (580 to 584' depth in B96001) & 3, and H 4, 5(676 to 691' depth in B96001) & 6, suggests that the gold concentrations in the sulphide minerals differ for the different horizons, they also have different proportions of sulphide minerals and different assay proportions of gold. In the Birch Pit and H 1, 2 and 3, there is 1 to 60% sulphide minerals in the ore, with high gold concentrations in arsenopyrite but low in pyrite. In H 4, 5 and 6 of the Birch Zone, there is 3 to 10% sulphide in the ore , low gold concentrations in the arsenopyrite, but high gold concentrations in the pyrite. This suggests that there are at least two distinct mineralogical zones in the Birch Zone gold deposits. These differences may be due to the degree of metamorphism, or lithological differences expressed as garnet and fibrolite in H1, 2, & 3, that are not present in H4, 5 & 6. Such mineralogical differences may result from locally higher temperatures connected to fluids. These fluids

could have remobilized the gold. Alternatively, the difference could signify the different timing of gold mineralization between these zones, the gold being precipitated along with pyrite in H4, 5 and 6, earlier than the gold associated with arsenopyrite in the Pit, and H 1, 2, and 3. There may be a late stage major fault between H3 and 4, which may have been responsible for interdigitizing the packages after gold mineralization.

In the lower zone of mineralization, H 4, 5 & 6 of the Birch Zone, H5 has a low concentration of gold within arsenopyrite, an average of 20 ppmw. This is in comparison to H4 & 6 which have average arsenopyrite values of 150 ppmw and 59 ppmw respectively. This is a distinguishing feature suggesting that H5 may not have seen the same amount of gold rich fluids during the arsenopyrite phase of deposition, or that fluid flow along faults has caused remobilization of the gold from the arsenopyrite. This later theory however does not make sense when we consider that a fractured arsenopyrite grain in H5 contains the most invisible gold, unless the area where the fractured grain was found was a local area of gold deposition and not leaching. Further suggesting that gold deposition was a consequence local chemistry or pressure differences.

The Boundary Zone

In the Boundary Zone, SIMS analysis was performed on samples BY1 to BY6. It was found that arsenopyrite gold concentration increases with depth, and pyrite gold concentration increases to BY2 then decreases from BY2 to BY4. Of the 11 samples, one from each area of high assays at depth in borehole BNDY83-02, analyzed by Image Analysis and Electron Microprobe, none were found to contain free gold. This lack of free

gold would suggest that either the sampling was not adequate, this zone may have discrete areas containing large quantities of free gold - the nugget effect or that the Boundary Zone never received the late gold rich fluids to precipitate the free gold, unlike the New Britannia Mine.

The New Britannia Mine

In the New Britannia Mine there are four main zones: the Toots Zone, the Hogg Zone, the Dick Zone and the Ruttan Zone. Of these four zones, two were studied in detail, the Dick and the Ruttan Zones. Here free gold is found in areas of quartz flooding and outside of the quartz flooded areas. In the quartz flooded areas gold has perimeter associations principally with pyrite and arsenopyrite. In the Ruttan Zone, in areas adjacent to these quartz flooded rock types free gold has perimeter associations principally with silicates. This is not the same as in the Dick Zone, where the association of the free gold outside of the quartz flooded areas remains with arsenopyrite. The exception is sample DB21b, which was taken from the edge of a small quartz vein in proximity to the Ruttan Zone, the gold association is principally with silicates.

These results suggest that there was not as much permeation of the quartz plus gold fluids into rocks of the Dick Zone as there was in the Ruttan Zone. In the Dick Zone, the dominant permeating fluid carrying gold was deposited with the preexisting sulphide phases. The dominant mineralizing fluid in the Ruttan Zone carried quartz plus gold, gold which was deposited with the silicate minerals. This further suggests that there was more than one phase of free gold deposition. This supposition is reinforced as free gold shows

average perimeter associations primarily with silicates, secondarily with pyrite, and lastly with arsenopyrite in the Ruttan Zone. In the Dick Zone, however, the average perimeter association is primarily with arsenopyrite, secondarily with silicates, thirdly with quartz and lastly with pyrite.

SIMS results for invisible gold in sulphide minerals of the Dick Zone indicate that in areas of quartz flooding and in the adjacent wall rock, sulphide minerals show very low concentrations of gold in either arsenopyrite (ca.3 ppmw) or pyrite(ca.0 ppmw). This would indicate that there was no gold in the fluids carrying the pyrite, and little in the arsenopyrite phase of deposition. This further suggests that either this deposit was within a different mineralizing system than the Birch Zone, Boundary Zone and the No. 3 Zone or that these sulphide minerals were produced during an episode containing little or no gold. Another possibility is that the conditions in the Dick Zone were not right for gold deposition during the sulphide phase of deposition. Regardless, the gold mineralization in the Dick zone is principally as free gold.

Metamorphism and Timing of the Gold Mineralization

Typically greenschist facies gold deposits are characterized by dolomite, chlorite, muscovite, albite and a pyrite dominated sulphide assemblage. Amphibolite facies gold deposits contain diopside, tremolite, biotite, cordierite, grossular rich garnet, and zoisite, and the dominant sulphides are pyrrhotite and pyrite. At amphibolite to low granulite facies the assemblage is characterized by garnet-diopside - biotite, K-feldspar, and the dominant sulphide minerals are pyrrhotite and arsenopyrite (+/- loellingite)(cp. Barnicoat,

1990; Galley et al., 1990). In Snow Lake, the mineral assemblage is characterized by biotite, +/- chlorite, +/- tremolite/actinolite, +/- muscovite, +/- garnet, +/- diopside, +/- garnet and the sulphide minerals pyrrhotite, pyrite and arsenopyrite. This would suggest that the deposits of Snow Lake are amphibolite to lower granulite facies, or that localized fluids causing the arsenopyrite mineralization are from areas of higher metamorphic grade. It should be noted that the temperature was not sufficient to produce lollingite, and that the actual grade of the Snow Lake area is upper greenschist to lower amphibolite facies. Higher grade alteration assemblage occurs in proximity to the gold bearing faults where there has been the greatest fluid infiltration and fluid movement (Fig. 20).

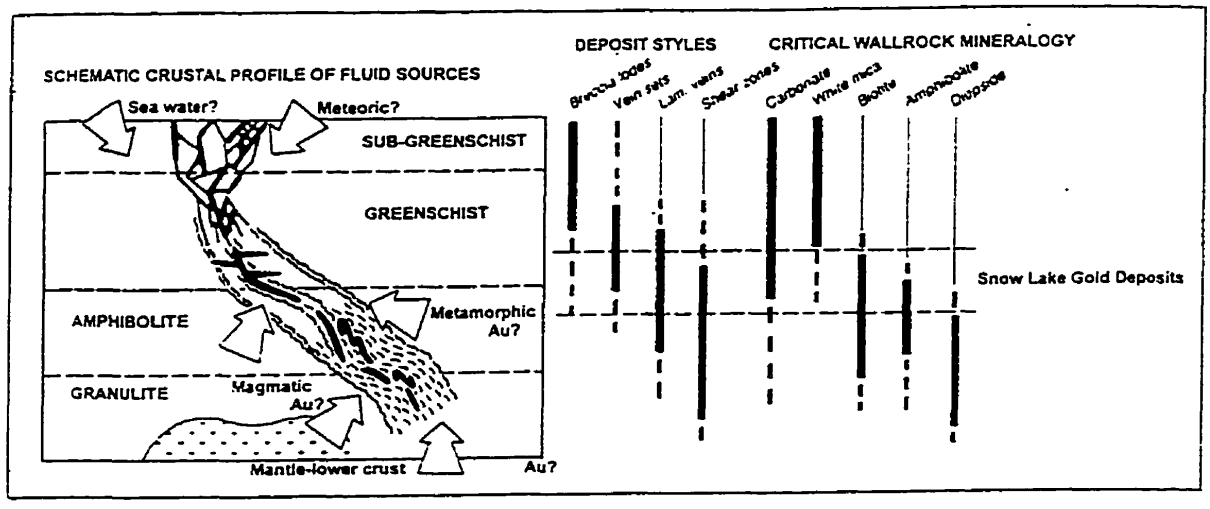

Figure 20 - Diagram showing the location of the Snow Lake Gold deposits, in relation to structure, metamorphism, fluids, possible styles of mineralization and critical wall rock mineralogy (modified from Groves et al., 1991). The gold mineralization, which is associated with higher temperatures, is unlikely to be a consequence of meteoric water or sea water, but it is still unclear whether or not the gold is metamorphic, magmatic or from the mantle / lower crust (Lam. Veins - laminated quartz veins).

According to Menard & Gordon (1996) sulphide striping from schists near massive sulphide lenses in the Snow Lake area and the sulphide minerals consequent deposition

occurred during F2. This sulphide stripping at the New Britannia Mine and associated deposits may have taken place as a consequence of higher temperature fluids, rich in gold, redistributing the sulphide minerals into fault zones, or higher stratigraphic levels within the fault zones. The sulphide minerals deposited would be rich in invisible gold. Arsenopyrite, being a higher temperature sulphide mineral than pyrite or pyrrhotite, would therefore contain the most invisible gold.

Observations by Menard and Gordon (1995) of VMS deposits in the Snow Lake area suggest three stages of alteration:

1. During F2 shearing, quartz was depleted from the rock part way through plagioclase growth and the mineral assemblage changed, suggesting loss of SiO_2, K_2O, Na_2O, and addition of Fe_2O_3 (or oxidation) and REE's.

2. During F3 crenulation, biotite and amphibole were added, plagioclase was partially replaced by chlorite, and quartz coarsened, indicating addition of K_2O, CaO, H_2O and possibly other components.

3. Subsequently, amphibole and magnetite were partially replaced by chlorite, ilmenite, calcite, allanite, and parisite, indicating another episode of fluid infiltration with addition of H_2O, CO_2, F, CaO, FeO, MgO, and REE's, and removal of K_2O, Na_2O, and Fe_2O_3. This event may correlate with bleaching and alteration around quartz veins that crosscut S2 and S3.

Petrographic observations indicate there have been up to 3 stages of biotite growth. This suggests multiple phases of fluid and rock interaction during metamorphism. A sequence of sulphide deposition within the ore zones can be observed; chalcopyrite

(earliest), pyrrhotite , Fe Ti sulphide, arsenopyrite, Fe Ti sulphide, pyrite, pyrrhotite, euhedral chalocopyrite, to pyrrhotite (latest).This sequence would also suggest changes in the fluid chemistry that at times involved Cu, As and various amounts of Fe. This again suggests multiple phases of fluid and rock interaction.

Pyrite and arsenopyrite show elevated gold concentrations. Gold occurs in irregular/patchy distributions in pyrite, and as concentric zoning within some arsenopyrite grains. Disturbance of the zoning present within the arsenopyrite indicates that the invisible gold may have been redistributed, possibly during metamorphism.

Free gold is found overgrowing pyrite and arsenopyrite, this would suggest that free gold deposition occurred after arsenopyrite and pyrite crystallization. Therefor this late gold could be due to late or retrograde metamorphic carrier fluids, magmatic fluids, due to mantle / lower crustal fluids or due to redistribution of the invisible gold in the sulphide minerals to free gold.

Structural constraints on gold mineralization

Geological mapping of Level 2210 and assay data indicate that gold mineralization was a late feature which cross cuts lithology. Gold mineralization is related to faulting in an approximately NE to SW direction, which is terminated against later mineralized faults in an east - west orientation. Other levels in the New Britannia Mine such as 2260 and 2030 in the Dick Zone where the mineralization follows faults orientated in a NE to SW direction or Levels 2006 and 2186 in the Ruttan Zone where the faults are orientated in a NW to SE direction, also show an association of faults with gold mineralization.

In Snow Lake, the structural discussion centers around the relationship the McLeod Road Thrust has to gold mineralization. The mineralization could be related to splays from the McLeod Road Thrust (Galley et al., 1990), or the mineralized Howe Sound Fault (the New Britannia Mine fault system) may be an early feature terminated to the south by the McLeod Road Thrust (Gale, 1997). Mapping of Level 2210 in the Dick Zone (Fig. 16)of the New Britannia Mine shows a late shallow angle fault which dips towards the north and strikes east west. This fault offsets the gold mineralization and is interpreted to be coeval with the McLeod Road Thrust Fault. This feature and mapping by Fieldhouse (1999) would suggest that the gold mineralization does not cross the McLeod Road Thrust (personal communication, 1998), and that gold mineralization came before and/or during movement on the McLeod Road Thrust.

Menard & Gordon (1995)suggest the possibility that gold may be associated with VMS deposits in the area and that the gold found at the New Britannia Mine may have been leached from the Photo Lake VMS Deposit along splays and faults such as the McLeod Road Thrust. These fault/shear zones may correspond to the base of the seismogenic zone which represents a time dependent interface between the near surface hydrostatic fluid pressure regimes and the approximate lithostatic fluid pressures which characterize the deeper portions of deforming, thickening crust (Barnicoat, 1990). Where specific fluid pressure conditions are met, reactivated reverse fault systems have the ability to act as fluid-pressure-activated valves, causing fluid pressure to cycle between pre-failure lithostatic and post-failure hydrostatic values in extreme cases. Pressure fluctuations arising from such fault valve behavior allow the phase separation of CO_2 from

mixed $H_2O - CO_2$ fluids at depth and gold to be precipitated (Sibson, 1990). Pressure seals are transient features related to regional deformation. This leads to complex pressure histories and fluid circulation patterns in rocks where faulting can disrupt fluid migration and efficient gold scavenging from gold source regions. Fluid flow is normally focused into the more permeable, active shear and fault zones, and dilitant structures (Cox et al., 1990) such as those found in the Snow Lake area. Fluid un-mixing fault valve behavior will also control fluid rock interactions and the fluid mixing necessary to promote gold deposition in fault zones and associated hydrofracture networks. Where fault zone failure and valve breaching cause an abrupt drop in fluid pressure within the fault zone, fluids in the wall rocks are drawn back into the transiently lower pressure fault zone where they mix with primary hydrothermal fluids. These processes can be very important in promoting efficient gold deposition (Cox, Etheridge & Wall, 1990). Gold mineralization is found in the shallow angle thrust fault that terminates the Howe Sound Fault, this suggests that the McLeod Road Thrust is mineralized. However, the gold mineralized zone found here is not as thick or as laterally extensive as in the Howe Sound Fault. It is therefore unlikely that the McLeod Road Thrust and parallel faults were major fluid conduits responsible for gold precipitation.

Early fault valve behavior is still a plausible explanation for the gold deposits around Snow Lake, in faults such as the Howe Sound, before closure of the McLeod Road Thrust. Evidence for fault valve behavior during the invisible phase of gold deposition is the gold zoning seen in SIMS ion images of arsenopyrite and the invisible gold concentration within the rock remaining the same regardless of percent sulphide

(indicating that gold precipitation was not reliant on elements Fe, S, or As).

Gold transport and Deposition

Sulphide minerals in the Birch Pit contain gold concentrations of up to 2000 ppmw gold. SIMS analysis of these sulphide minerals indicate higher concentrations of gold within arsenopyrite than pyrite, with ion imaging supplying pictures of the gold zoning present within some euhedral arsenopyrite crystals (Plate 7). Gold is found to be zoned within some arsenopyrites, but with no corresponding zoning of Se, As, Fe, O or S. In pyrite, however, zones within the pyrite mineral enriched in As were found to contain greater concentrations of inclusions, but there was no direct association of As with these gold inclusions. This is different to findings from the Hercynian Belt in Europe, where arsenopyrite was imaged and gold was found associated with zones enriched in arsenic (Cathelineau et al., 1988).

Gold from Snow Lake does not always display zoning within arsenopyrite, and more commonly, due to fluids redistributing the gold and disturbing the zoning, it has a random distribution. Gold present in pyrite was only found to have a random distribution (Plate 8) and again no associations with other elements were found. This random distribution of gold within the pyrite would suggest nucleation of the pyrite around discrete gold particles, which were already in the rock or after introduction of the gold to the rock. If however, the gold was already in the rock before the crystallization of pyrite, it would indicate that the pyrrhotite and chalcopyrite, which came before pyrite, may be incapable of accommodating gold in their structures. If, however, the gold came in during

pyrite formation, the gold may be distributed into pyrite, from the fluid, via the reaction;

$Au(HS)_2^- + FeO \rightarrow Au + FeS_2$ (1) (cf. Barnicoat, 1990).

In all mineralized Zones pyrite is found overgrowing arsenopyrite, indicating that arsenopyrite is older than pyrite. This would not only indicate a change in the fluids from high to low arsenic with time, possibly due to decreasing temperature, but also suggest that the fluid was periodically enriched in gold during the arsenopyrite phase of crystallization, to produce the zones rich in gold.

Mineralizing fluids & chemical controls on gold precipitation

Gold complexes include chloride complexes, bisulphide complexes and thioarsenite complexes (Romberger, 1986; Greenwood & Earnshaw, 1984).

Chloride complexes – the solubility of gold in chloride complexes increases with increasing temperature and oxygen activity. As pH increases the solubility of gold as a chloride complex decreases, resulting in a net deposition of metals transported as chloride complexes (Romberger, 1990).

Bisulphide complexes – the maximum solubility of gold as a bisulphide complex will occur along the equilibria-controlling redox boundary where the activities of sulphate and H_2S are equal. The solubility of gold as a bisulphide complex decreases with decreasing temperature, and with decreasing temperature coupled with increasing oxygen activity. With an increase in pH the solubility of gold as a bisulphide complex increases, however, there may be precipitation of sulphide resulting in a decrease in sulphur activity and leading to the co-precipitation of gold (Romberger, 1990).

Where gold is transported as a chloride complex in a solution above 400 °C, cooling might result in deposition if the solution is close to saturation with gold. If bisulphide complexes predominate, further cooling will result in an increase in gold solubility so that gold deposited during an earlier cooling episode may be re-dissolved. Such a process could account for the remobilization of gold. Finally, when the temperature reaches the sulphate – H_2S boundary, further cooling results in a rapid precipitation of gold as a result of oxidation.

Thioarsenite complexes - sulphides of arsenic are insoluble in water, but dissolve readily in aqueous alkali or alkali-metal solutions to give thioarsenites:

$As_2S_3 + Na_2S$ ----> $2Na\ As^{III}S_2$ (2) (cf. Greenwood & Earnshaw, 1984)

In general, in the deposits of Snow Lake, there is a sequence of sulphide mineralization from chalcopyrite (earliest), pyrrhotite (at 67-68% iron and 35% sulphur) , Fe Ti sulphide, arsenopyrite (at 40% iron and 17% sulphur), Fe Ti sulphide, pyrite (49-54% iron and 42-47% sulphur), pyrrhotite, euhedral chalocopyrite, to pyrrhotite (latest). The fluid composition fluctuated from Cu rich to high Fe & S and low As, to low Fe & S and high As, back to high Fe & S and low As. The Fe Ti sulphide minerals were deposited during times of fluid compositional change, before and after arsenopyrite deposition.

Fluids generated in equilibrium with mafic or granitoid source rocks will be relatively close to equilibrium with mafic or felsic rocks, but will be strongly out of equilibrium with compositions such as banded iron formations and ultramafic rocks. In such relationships, alteration (and mineralization if causally related) will be important near

the lower contacts of rock layers. This could correspond to contrasts between compositionaly distinct lithologies like the felsic and mafic volcanic rocks at Snow Lake. These alteration reactions could drive the precipitation of gold where fluid interacts with Fe rich rocks and cause decreases in sulphur activity and pH, with a concurrent lowering of gold solubility in the form of $Au(HS)^{-2}$ (cf. Barnicoat, 1990). One such wall rock alteration reaction is ;

$$Au(HS)_2^- + FeO \rightarrow Au + FeS_2 \quad (1).$$

H_2S from the fluid is consumed by the formation of iron sulphide minerals in the wall rocks to the fluid conduits. The loss of sulphur from the fluid destabilizes the Au-sulphur complexes, causing gold to precipitate (McCuaig & Kerrich, 1994; Phillip et al., 1984).

In Snow Lake, the New Britannia Mine, the Birch and the Boundary Zones are found at the boundary between felsic and mafic volcaniclastics, and No. 3 Zone is found at the boundary between basalts and mafic volcaniclastic rocks. This association of the gold deposits with compositional changes would suggest that changes in country rock chemistry may be a significant factor in the deposition of gold. Biotite is found surrounding veins of quartz and calcite, this biotite can be found with or without pyrite minerals, making the consumption of ferromagnesian minerals in reaction (1) a likely mechanism for gold precipitation during the pyrite phase of gold deposition.

For comparison, the gold alteration in the Hunt Gold Mine in western Australia, involved addition of Au, S, CO_2 and Large Ion Lithophile (LIL) elements (Cs, Rb, K, Ba) to the metabasalts and addition of Si (+Co, Ta) in veins, but virtually no mobility of first

transition series metals, REE's or high field strength elements (HFSE). The absence of extensive element mobility is consistent with alteration by reduced, near neutral, low salinity, H_2O-CO_2 dominated fluid. Iron is essentially immobile, consistent with a sulphidation model for gold precipitation (Lesher et al., 1991). A similar scenario might explain the addition of Au, S, CO_2 and Si, at the New Britannia Mine.

There is evidence in the form of mass balance studies to support the idea that volatile components such as CO_2, S and H_2O are added to wall rocks in ore deposits and alkali metals are leached out. The effect of this exchange is an increase in pH in the transporting solutions, which will result in a net deposition of metals transported as chloride complexes (Romberger, 1990).

Gold mineralization

In Snow Lake gold is found in two associations; as invisible and inclusion gold in sulphide minerals, and as free gold overgrowing pyrite and arsenopyrite. This implies that there have been two separate mineralizing events, the first to deposit <16 μm sized gold particles in the pyrite and arsenopyrite, and the second to deposit the larger, 15 - 190 μm, free gold. The first gold mineralizing event, because of its association with sulphide minerals, would appear to have carried gold in the sulphide mineralizing fluid as bisulphide or thioarsenide complexes. Due to the lack of association (as shown by SIMS) of this type of gold with either sulphur, iron or arsenic in either pyrite or arsenopyrite this seems unlikely, unless sulphur and arsenic concentrations within the sulphide minerals are forced to remain constant despite fluctuations in gold concentration and degree of gold

complexing with sulphur and / or arsenic. In this case the gold, because of its differing concentrations within pyrite and arsenopyrite, would not be present as a chemically bonded complex to S, Fe or As, but be due to a varying degree of chemical or physical attraction to either S, Fe or As. The chemical attraction in arsenopyrite may be the substitution of Au^{3+} into As sites, which may explain the elevated gold concentrations in arsenopyrite, but not the lack of variation in the As ion images. It may also be that gold is complexing with another element not analyzed for during SIMS analysis. Other elements analyzed for were Se, Si and O, none of which were found to have an association with the invisible gold. Gold in pyrite has a different morphology from gold in arsenopyrite. The gold in pyrite occurs as small inclusions, which is in contrast to the gold zonation seen in arsenopyrite. This suggests that there may have been two different mechanisms for this gold deposition into the sulphide minerals, pyrite and arsenopyrite.

Cathelineau et al., (1988) found that co-precipitation of gold and arsenopyrite occurs when the activity of As and Au complexes is high and the activity of Sb complexes is low. For arsenopyrite of the Marche-Cambrailes deposits, Hercynian belt in Europe, this process was at a maximum at the end of the arsenopyrite depositional period, yielding strong heterogeneities in the gold distribution , especially characterized by strong enrichment at the periphery of crystals and within micro-fracture networks (cf. Harris, 1990). Arsenopyrite with zones of gold enrichment within the crystal and between adjoining arsenopyrite crystals is seen in the Birch Pit and more specifically in sample BE1.

Gold is not an essential constituent of arsenopyrite and hence its concentration is

not controlled by phase relationships. The amount of the trace element gold entering the arsenopyrite is controlled by the amount of gold in the mineralizing solutions. If the concentration of gold in the liquid is increased or decreased, then the amount of gold which partitions into arsenopyrite will change correspondingly. Consequently, arsenopyrite with identified S-Fe-As ratios can have widely differing concentrations of gold, depending on the gold content of the liquid from which these sulphide minerals were precipitated.

CO_2 and gold mineralization

High CO_2 content is an important and universal characteristic of mineralizing fluids along major structures. Phase equilibria studies of mineralized faults at different erosional levels by Albino (1990) have shown that fluid CO_2 content varies with depth. The highest CO_2 contents occur in deposits formed at greatest depth and highest temperature. Upper amphibolite facies rocks formed at middle crustal depths have fluid XCO_2 levels of 0.25 to 0.3, and greenschist facies rocks have fluid XCO_2 levels of 0.1 to 0.15. This would indicate evolution of the fluid while traveling up mineralized shear zones due to fluid wall rock interaction, specifically carbonization reactions. These would result in both the loss of carbon dioxide and the gain of water, which would change the fluid isotopic ratios and the ability to solvate gold.

Fyfe (1991) proposes that gold transport processes start near the Moho with magma underplating. When a 1300 °C dense mafic magma body is injected beneath light continental crust a thermal event occurs. At temperatures of 800-1000 °C the late gas phase will be CO_2 and CO rich. This gas as it cools with decreasing depth in the crust, will

separate into CO_2 and graphite and will precipitate gold. The deposition of graphite onto grain boundaries will cause that grain to become electrically conductive, this grain may then have the ability to attract gold, perhaps further trapping gold (ca. as gold growth bands in arsenopyrite). Zoning of gold in arsenopyrite was observed through SIMS Ion Images (Appendix 5) in Snow Lake, but no relationship with arsenic, sulphur, iron or selenium was observed. Carbon could not be analyzed with the Cs beam used for SIMS analysis of gold. However, small veins of graphite have been observed in the Birch Pit and underground at the New Britannia Mine, along with numerous veins of carbonate. Also, the interaction of fluids rich in gold with carbon rich shear bands may cause a decrease in oxygen fugacity (fO_2) and an increase in CO_2. This is accompanied by the removal of reduced aqueous sulphur species by sulphide precipitation of near neutral, low-salinity fluids causing gold to be precipitated (Xavier & Foster, 1991). In the deposits of Snow Lake there are numerous phases of carbonate veins, making Fyfe's model another possible mechanism for the precipitation of gold in the New Britannia Mine and surrounding deposits. More specifically in the No. 3 Zone, the free gold is found surrounded by veins of carbonate.

Gold Processing

In the Snow Lake gold deposits there are two stages of gold deposition. The first occurs as <2 μm sized invisible gold and 2-16 μm sized inclusion gold found within the sulphide minerals, pyrite and arsenopyrite. This invisible and inclusion gold is interpreted as being deposited contemporaneously with these sulphide minerals. The second stage is

15 - 190 μm sized free gold found occupying small fissures between silicate and sulphide minerals. This type of gold is later than the associated minerals, silicates, pyrite and arsenopyrite.

For effective cyanidation of invisible and inclusion gold, finer grinding is required than for free gold, which results in higher treatment costs. Consequently, ore containing the higher proportions of invisible gold will produce gold that will be more labor intensive and less cost efficient to recover than ores containing higher proportions of the late, free gold.

Free gold, because it occurs on the boundaries between grains where the rock will naturally spilt during crushing, will be recovered during milling. Invisible and inclusion gold, because it is locked within grains, will not be liberated during crushing and cyanide leach. Without roasting this ore, the invisible gold is lost. For example, the Dick Zone in the New Britannia Mine, has approximately 0.5 % of it's gold as invisible gold. If this is compared to the Birch Pit, sample BE1, which contains 92.5 % of the gold as invisible gold, gold recoveries from the Birch Pit will be 7.5% in comparison to 99.5% in the Dick Zone. This may make the difference between an economic and uneconomic gold deposit.

Exploration Implications

Mapping has shown that gold's structural associations are with faults and their associated shear zones. Image Analysis has shown that gold mineralogical associations are primarily with silicate minerals, arsenopyrite and, in the No. 3 Zone, with calcite. These results, coupled with results from SIMS, would suggest that gold amenable to conventional

milling techniques, free gold, is to be found in proximity to areas with arsenopyrite. This arsenopyrite will contain high proportions of invisible gold. This invisible gold can be remobilized along faults by a number of different fluids to produce free gold.

Comparison to other deposits

The New Britannia Mine and surrounding deposits share many of the characteristics of Archean Lode Gold Deposits. In Archean gold-quartz vein ore systems, gold was derived by partition between silicate (+/- sulphide) melts of certain compositions and H_2O - CO_2 - NaCl magmatic fluids transported in solution with or without fluid mixing and deposition (Spooner, 1991).

In Archean Lode Gold Deposits the gold is structurally controlled, hosted in reactivated brittle / ductile, fault / shear zones. The free and invisible gold in general contains up to 6% silver (Ag), with higher percentage Ag in certain localities, arsenic (As) is found as arsenopyrite, tungsten (W) is found as free grains and in scheelite, and boron (B) is found as tourmaline in certain areas not necessarily directly associated with the gold mineralization. Lead (Pb), copper (Cu) and zinc (Zn) are found as the early sulphide minerals galena, chalcopyrite and sphalerite respectively. The alteration assemblage is enriched in CO_2 as calcite veins, in sulphur (S) in the form of the sulphide minerals, pyrite and arsenopyrite, and in potassium (K) as feldspar. There is no consistent lateral zonation around the quartz veins, however there was substantial wall rock alteration to biotite and actinolite around the faults, on the scale of ~10 meters horizontally, but 100's of meters vertically. There is a change from ore containing mainly pyrite to ore containing mainly arsenopyrite with increasing

metamorphic grade. This requires the invisible gold in the pyrite and arsenopyrite to be prograde, not retrograde as required for Mesothermal Archean Lode Gold deposits.

According to Groves et al. (1991), Archean Lode Gold Deposits of the Yilgarn Block in western Australia are characterized by: Being epigenetic (near surface) and structurally controlled in late or reworked earlier brittle / ductile, fault/shear zones;
Being gold only deposits, with significant enrichments of Ag, As, Sb and W, variable enrichments of Te, B and Bi, and low enrichments in Cu, Zn and Pb; An alteration assemblage characteristically enriched in CO_2, S and K (+Rb, Ba) plus the ore related metals, and an overall increase or conservation of volume; Lateral zoning around quartz veins or shear zones is characteristic on the 10's of centimeters to 10's of meters scale, whereas vertical zonation, if present, in the scale of 100's of meters, which implies infiltration of hot fluids into heated wall rocks; "Telescoped" alteration and / or metal zoning characteristic of many other classes of hydrothermal gold deposits is absent; Alteration mineralogy varies in harmony with metamorphic grade of the wall rocks.

In comparison to Archean Lode Gold Deposits in Ontario, the deposits of Snow Lake are hypogene, from depths of greater than 18 km depth in the crust, but reside in fault and shear zones. They are gold only deposits, with significant enrichments of Ag, As and W, variable enrichments of B and low enrichments in Cu, Zn and Pb. The alteration assemblage is characteristically enriched in CO_2, S and K. The lateral zoning around the quartz veins or shear zones is characteristic on the 10's of centimeters scale, whereas vertical zonation is in the scale of 100's of meters, this implies infiltration of hot fluids into heated wall rocks. There

is a zoning of the sulphide minerals and there is evidence of metamorphic overprinting of the deposits of Snow Lake. The alteration mineralogy does not vary in harmony with the metamorphic grade of the wall rocks.

The mesothermal (200-300°C) variety of Archean Lode Gold Deposits occurring at greenschist to amphibolite facies form a distinctive group in which(Groves et al., 1991): Mineralization is typically sited in brittle-ductile structures; Wall rock alteration is typified by an inner zone of ankerite/dolomite-white mica and /or biotite +/- albite +/- pyrite +/- arsenopyrite +/- pyrrhotite; Wall rock alteration is characteristically retrograde with respect to peak metamorphism; Gold is normally deposited from reduced sulphur-gold complexes in low to moderate salinity, near neutral H_2O-CO_2 (CH_4) fluids at 250-400 °C and 1.3 Kb.

In the deposits of Snow lake mineralization is typically sited in brittle-ductile structures. The wall rock alteration is typified by an inner zone of calcite, biotite, albite, pyrite, arsenopyrite and pyrrhotite. The wall rock alteration is prograde with respect to peak metamorphism and the nature of the gold depositing fluids is unknown.

The mesothermal to epithermal Polgera gold deposit in Papua New Guinea is spatially and temporally associated with shallow level (< 2 km emplacement depth) mafic and alkali stocks and dykes of the Polgera Intrusive Complex (PIC). The PIC was emplaced near the northern edge of the Australasian Craton during a period of late to tertiary accretion, and gold mineralization immediately followed emplacement of the PIC: magmatism may have been related to deep subduction beneath the continental margin (Richards et al., 1991). This mineralization is cross cutting and follows late as well as early faults. The deposits of Snow

lake are situated in island arc volcanic rocks, but gold mineralization rather than occurring early in the history of these rocks, during subduction, occurred during metamorphism. The gold mineralization is associated with fault and shear zones, but mineralization occurred at greater depth than seen in the P.I.C..

Foster et al. (1991) is of the opinion that lode gold mineralization was commonly generated by fluid flow into extensional zones, usually Reidel structures. These Reidel structures were developed as a second order response to dominantly strike-slip shearing in and close to supracrustal greenstone sequences in the Midlands greenstone belt, Zimbabwe. Deformation in the southern part of the craton was a response to the movement of crustal blocks, cored by granite, induced by intense crustal shortening and consequent shearing between blocks where most of the strain is taken up by the greenstones. In the Midlands greenstone belt the strain was particularly focused along lithological discontinuities, ranging in scale from the western margin of the major batholith down to the stratigraphic contacts between individual beds. Geologically this is similar to the Snow Lake area, to the north east and north west are large granite plutons surrounded by greenstones. The presence of these plutons may have focused strain into the Snow Lake greenstones, particularly along stratigraphic contacts such as the boundaries between the felsic and mafic volcaniclastics and the mafic volcaniclastics and the basalts. This may have caused the development of shear zones, responsible for the gold deposits seen here.

Conclusions

There are two types of gold mineralization in the gold deposits of the Snow Lake area. An early syn-metamorphic phase of gold deposition contained within the sulphide minerals, pyrite and arsenopyrite, as invisible and inclusion gold. The second type of gold mineralization is a free gold phase which occurs overgrowing pyrite and arsenopyrite, and is interpreted as a syn- to post-metamorphic phase of gold deposition. Inclusion and free gold grains both contain approximately the same concentration of gold and silver, which suggests that the mineralizing fluids which deposited both these types of gold were similar, or that the free gold is remobilized invisible and inclusion gold from the earlier sulphide minerals.

Both types of gold mineralization are found in proximity to faults in the Dick, Ruttan and the Birch Zone and are associated with quartz filled tension gashes and veins at the No. 3 Zone. It is plausible that transient fluid pressure seals and fault valve behavior may have been responsible for the original gold deposition and subsequent remobilization. All the gold deposits occur at or near lithological boundaries, such as from mafic to felsic, which are therefore chemical boundaries. Such chemical boundaries may also cause the precipitation of gold by the reaction;

$$Au(HS)_2^- + FeO \rightarrow Au + FeS_2$$

This is a very likely mechanism for invisible and inclusion gold precipitation during the pyrite and arsenopyrite phase of deposition.

Invisible gold in sulphide minerals has been imaged through SIMS. No association with the elements As, Se, O, Si, Fe or S, has been found. Oxygen has been noted to disturb the gold zoning within arsenopyrite, causing the gold to be removed from areas containing elevated concentrations of oxygen. This suggests that there has been late stage oxygenated

fluid movement. Gold in pyrite cannot be described in this way as there is no zoning of gold to be disturbed.

The constant invisible gold content of the gold bearing rocks regardless of sulphide percentage (low percent sulphide means high concentration gold in those sulphide minerals) and the lack of association of gold zoning with the elements As, Se, O, Si, Fe or S makes gold deposition due to reaction between Fe, S or As unlikely for the deposits of Snow Lake. Therefor transient fluid pressure seals and fault valve behavior are the favored mechanisms for gold deposition.

CHAPTER 6 - SUMMARY

In all the zones studied gold has been found in association with;

1. Arsenopyrite - free along grain boundaries, as inclusions and as invisible gold.

2. Pyrite - free along grain boundaries, as inclusions and as invisible gold.

3. Silicates - free along grain boundaries.

4. Calcite - surrounding gold grains in the secondary quartz vein at the No. 3 Zone outcrop.

Gold associations

Free gold has an association principally with silicates and quartz (65%), secondarily with arsenopyrite (21%) and lastly with pyrite and pyrrhotite (12%). Free gold is mainly found in the quartz dominated units of the New Britannia Mine and in one out of three analyzes in the banded biotite schists. In the Birch Zone, free gold is found mainly in the heavily quartz veined areas corresponding to the location of the Birch Fault or in the banded biotite schists surrounding the Birch Fault. In the No. 3 Zone, free gold is found in the primary or secondary quartz veins and not in the country rock. In the Boundary and Thorne Zones no free gold was found in the samples taken.

Sulphide analysis by EMPA has shown that in zones containing low ppmw gold in the sulphide minerals as shown by SIMS, such as the No. 3 Zone and the New Britannia Mine, the arsenopyrite has a composition of between 43 -54 wt% As. In zones containing high ppmw gold in the sulphide minerals, such as the Birch Zone, the arsenopyrite has a composition of between

44 - 49 Wt% As. This indicates that sulphide minerals with compositions between 50 - 55 Wt% As are associated with a high percentage free gold in the rock and low ppmw gold in the sulphide minerals.

Relationship of high gold assays with size and shape of the sulphide minerals

Visual analysis, using BSE images, of gold in association with arsenopyrite show that 11 out of 30 gold grains are associated with euhedral arsenopyrite, 9 in association with subeuhedral arsenopyrite and 10 with anhedral arsenopyrite. These results indicate that there is no association of free gold with arsenopyrite mineral shape.

SIMS results indicate that there is no association between sulphide shape or size and invisible gold concentration within the sulphide minerals pyrite and arsenopyrite. Gold concentration was only found to vary with sulphide mineralogy and location. The highest gold concentrations were found in arsenopyrite, with lower concentrations being found in pyrite.

Gold processing

The Birch Zone

The Birch Zone contains high percentages of unrecoverable invisible and inclusion gold. The Birch Pit and B96001-H4 contain approximately equal proportions of free to invisible gold. B96001-H1 contains greater proportions of invisible gold than free gold. These results indicate that recoveries in this zone would be approximately 50% of the assayed gold values.

The Boundary Zone

In the Boundary Zone, no free gold was found to analyze. SIMS results indicate low ppmw gold in pyrite from Horizons 1, 3, 4, 5 and 6, but higher concentrations in pyrite from H2. The proportions of invisible gold within the sulphide minerals do not correlate with assays, this indicates that there may be high proportions of gold in discrete areas, not sampled, in a distribution known as the "nugget effect" rather than as disseminated gold.

The Thorne Zone

In the Thorne Zone, no free gold was found using Image Analysis. This Zone contains smaller concentrations of invisible gold within the sulphide minerals than does the Boundary Zone.

No. 3 Zone

In the No. 3 Zone there are relatively high proportions of free gold and low concentrations of invisible gold in the sulphide minerals. The low concentrations of invisible gold coupled with low percent sulphide minerals in the rock mean that good recoveries may be attained with ore of this type.

Dick Zone

In the Dick Zone there are high proportions of free gold and low concentrations of gold in the sulphide minerals. The low concentrations of invisible gold coupled with low percent sulphide minerals in the rock mean that good recoveries may be attained with ore of this type.

Exploration implications

Gold structural associations are with faults and their associated shear zones. Gold mineralogical associations are primarily with silicate minerals, arsenopyrite and, in the No. 3 Zone, with calcite. Results would suggest that gold amenable to conventional milling techniques is to be found in proximity to areas with arsenopyrite, as arsenopyrite has been found to contain high proportions of invisible gold.

Origin of the gold

Answering the question of where the gold originally came from is beyond the scope of this thesis. What I can say is that the gold mineralization found at Snow Lake was not intruded but was deposited by fluid movement. The gold bearing faults have been terminated by shallow angle, northerly dipping faults in a similar orientation to that of the McLeod Road Thrust. Gold mineralization therefore came before closure of the McLeod Road Thrust, unless the McLeod Road Thrust has moved more than once. There is also mineralization in faults in a similar orientation to that of the McLeod Road Thrust, but this mineralization is not as extensive as the original gold mineralization, and it is not known if gold in these faults is contained within sulphide minerals or is free. In the Birch Zone inclusion and free gold both have the same ratio of Au:Ag; There has been more than one phase of gold mineralization, a primary phase to deposit gold within pyrite and arsenopyrite, and a secondary phase to remobilize this invisible and inclusion gold and deposit it as free gold.

These observations lead us to two general theories. Either fluids mobilized gold from an unknown source and the mineralized fluid was focused along faults. This could have happened only

once to deposit gold as sulphide minerals, and then these sulphide were reworked to deposit free gold. Or, this could have happened twice, the same gold rich fluids deposited both the gold in the sulphide minerals and the later free gold. Alternatively, the gold was originally in the rocks in which they were deposited but redistributed and concentrated, firstly in sulphide minerals and then later as free gold, by fault and fluid movement.

REFERENCES

Albino, G., 1990. Fluid sources for "break-type" gold deposits - what do we really know? Greenstone Gold and Crustal Evolution, Geological Association of Canada, NUNA Conference Volume edited by Robert, F., Sheahan, P.A., Green, S.B., pp.127-128.

Bailes, A. H., 1980. Geology of the File Lake area. Manitoba Department of Energy and Mines, Mineral Resources Division, Winnipeg, MB, Canada. Geological report 78-1.

Bailes, A.H., Syme, E.C., Galley, A., Price, D.P., Skirrow, R. & Ziehlke, 1987. Early Proterozoic volcanism, hydrothermal activity and associated ore deposits at Flin Flon and Snow Lake, Manitoba. Geological Association of Canada Field Trip Guide Book #1.

Bailes, A. H. & Schledewitz, D. C. P., 1998. Geology and geochemistry of Paleoproterozoic volcanic rocks between the McLeod Road and Birch Lake Faults, Snow Lake area, Flin Flon Belt (Parts of NTS 63K/16 and 63J/13). Manitoba Energy and Mines Report on Activities 1998, pp. 4-13.

Barnicoat, A.C., 1990. Alteration zones around Mesothermal Gold Deposits: Implications for patterns of deposition and fluid sources. Greenstone Gold and Crustal Evolution, Geological Association of Canada, NUNA Conference Volume edited by Robert, F., Sheahan, P.A., Green, S.B., pp.132-133.

Byers, A.R. & Dahlstrom, C.D., 1954. Structure of the Amisk-Wildnest Lakes area, Saskatchewan. Proceedings of the Geological Association of Canada, 6, Part 2, pp.27-36.

Cabri, L.J., Chryssoulis, S.L., Campbell, J.L., & Teesdale, W.J., 1991. Comparison of *in-situ* analyzes in arsenian pyrite. Applied Geochemistry, Vol. 6, pp. 225-230.

Cathelineau, M., Boiron, M.C., Holliger, Ph., & Marion, Ph., 1988. Gold rich arsenopyrites: Crystal chemistry, gold location and state, physical and chemical conditions of crystallization. Bicentenial Gold 88, Melbourne, Geol. Soc. Aust., Abst. 22, pp.235 - 240.

Colvine, A.C., Fyon, J.A., Heather, K.B., Soussan Marmont, Smith, P.M., & Troop, D.G., 1988. Archean Lode Gold Deposits in Ontario. Mines and Minerals Division, Ontario Geological Survey, Miscellaneous paper 139. Reprinted by the Ministry of Northern Development and Mines.

Cox, S.F., 1990. Fluid generation, fluid circulation and deformation. Greenstone Gold and Crustal Evolution, Geological Association of Canada, NUNA Conference Volume edited by Robert, F., Sheahan, P.A., Green, S.B., pp.95-97.

Cox, S.F., Etheridge, M.A., Wall, V.J., 1990. Fluid pressure regimes and fluid dynamics during

deformation of low-grade metamorphic terranes implications for the genesis of Mesothermal Gold Deposits. Greenstone Gold and Crustal Evolution, Geological Association of Canada, NUNA Conference Volume edited by Robert, F., Sheahan, P.A., Green, S.B., pp. 46-53.

Czamanske, G.K., Kunilov, V.E., Zienter, M.L., Cabri, L.J., Likhachev, A.P., Calk, L.C. &Oscarson, R.L., 1992. A proton-microprobe study of magmatic sulfide ores from the Noril'sk-Talnakh district, Siberia. The Canadian Mineralogist, 30, pp. 249-287.

Fieldhouse, I., 1999. The structural constraints on the occurrence of gold mineralization in the vicinity of the New Britannia Mine, Snow lake, Manitoba. University of Manitoba Masters Thesis.

Fleet, M. E. , Chryssoulis, S. L. , MacLean, P. J. , Davidson, R. , Weisener, C., 1993. Arsenian pyrite from gold deposits; Au and As distribution investigated by SIMS and EMP, and color staining and surface oxidation by XPS and LIMS, The Canadian Mineralogist 31, Part 1, pp. 1-17.

Foster, R.P., Fabiani, W.M.B., Carter, A.H.C., Fisher, N.J. & Porter, C.W., 1991. The tectonic and magmatic framework of Archean Lode Gold mineralization in the Midlands greenstone belt, Zimbabwe. Brazil Gold '91, The Economics, Geology, Geochemistry and Genesis of Gold deposits, edited by Ladeira, E.A., pp. 359-367.

Fox, 1976. Some comments on the volcanic stratigraphy and economic potential of the West Amisk Lake area, Saskatchewan. Geological Association of Canada, Mineralogical Association of Canada, Annual Meeting, Edmonton, Program with abstracts.

Froese, E., & Gasparrini, E., 1975. Metamorphic zones in the Snow Lake area, Manitoba. Canadian Mineralogist, Vol. 13, pp. 162-167.

Froese, E. and Moore, J. M., 1980. Metamorphism in the Snow Lake area, Manitoba. Geological Survey of Canada, Paper 78-27.

Fyfe, W.S., 1991. Gold transport and deposition: Rules of the game. Brazil Gold '91, The Economics, Geology, Geochemistry and Genesis of Gold deposits, edited by Ladeira, E.A., pp. 7-10.

Gale, 1997. Geological setting and genesis of gold mineralization in the Snow Lake area (NTS 63K/16). Manitoba Energy and Mines, Minerals Division, Report of Activities, pp. 73-78.

Galley, A.G., Ziehlke, D.V., Franklin, J.M., 1986. Gold mineralization in the Snow Lake - Wekusko Lake region, Manitoba. In Gold in the Western Shield, (L.A. Clark, ed.).

Canadian Institute of Mining and Metallurgy, Special Volume 38, pp. 379-398.

Galley, A.G., Ames, D.E., & Franklin, J.M., 1988. Geological setting of the gold mineralization, Snow Lake, Manitoba. Geological Survey of Canada, Open file 1700.

Galley, A. G., Bailes, A. H., Syme, E. C., Bleeker, W., Macek, J. J. & Gordon, T. M., 1990. Geology and mineral deposits of the Fin Flon and Thompson Belts, Manitoba. Geological Survey of Canada, Open file 2165.

Greenwood, N.N. & Earnshaw, A., 1984. Chemistry of the elements. Pergamon Press Ltd. pp. 677.

Griffin, W. L., Ashley, P. M., Ryan, C. G., Sie, S. H. & Suter, G. F., 1991 Pyrite geochemistry in the North Arm epithermal Ag-Au deposit, Queensland, Australia; a Proton-Microprobe study. The Canadian Mineralogist, 29, Part 2, pp. 185-198, 1991.

Groves, D.I., 1990. Structural setting and control of greenstone gold deposits. Greenstone Gold and Crustal Evolution, Geological Association of Canada, NUNA Conference Volume edited by Robert, F., Sheahan, P.A., Green, S.B., pp.79-85.

Groves, D.I., Barley, M.E., Cassidy, K.C., Hagemann, S.G., Ho, S.E., Hronsky, J.M.A., Mikucki, E. J., Mueller, A.G., McNaughton, N.J., Perring, C.S., & Ridley, J.R., 1991. Archaean Lode Gold Deposits: The products of crustal scale hydrothermal systems. Brazil Gold '91, The Economics, Geology, Geochemistry and Genesis of Gold deposits, edited by Ladeira, E.A., pp. 299-306.

Halden, N.M., Campbell, J.L., Teesdale, W.J., 1995. PIXE analysis in mineralogy and geochemistry. The Canadian Mineralogist, 33, pp. 293-302.

Harris, D.C., 1990. The Mineralogy of gold and its relevance to gold recoveries. Mineralium Deposita 25 [Suppl] S3 - S7.

Harrison, 1949. Geology and mineral deposits of the File-Tramping Lakes area, Manitoba. Geological Survey of Canada, Memoir 250.

Kerrich, R., 1990. Mesothermal Gold Deposits: A critique of genetic hypotheses. Greenstone Gold and Crustal Evolution, Geological Association of Canada, NUNA Conference Volume edited by Robert, F., Sheahan, P.A., Green, S.B., pp.13-31.

Kerrich, R., Wyman, D., 1990. Late evolution of greenstone belts and gold deposits. Greenstone Gold and Crustal Evolution, Geological Association of Canada, NUNA Conference Volume edited by Robert, F., Sheahan, P.A., Green, S.B., pp.91-94.

Kesler, S.E., 1990. Nature and composition of mineralizing solutions. Greenstone Gold and Crustal Evolution, Geological Association of Canada, NUNA Conference Volume edited by Robert, F., Sheahan, P.A., Green, S.B., pp. 86-90.

Kraus, J., Menard, T., 1997. A thermal gradient at constant pressure: implications for low- to medium-pressure metamorphism in a compressional tectonic setting, Flin Flon and Kisseynew domains, Trans-Hudson Orogen, central Canada. The Canadian Mineralogist, 35, pp.1117-1136.

Kraus, J. & Williams, P. F., 1993. Structural studies along the northern margin of the Fin Flon - Snow Lake greenstone belt, Snow Lake, Manitoba. Manitoba Energy and Mines, Minerals Division, Report of Activities 1993, pp. 117-118.

Kraus, J. & Williams, P.F., 1998. The structural development of the Snow Lake Allochthon and its role in the evolution of the southeastern Trans-Hudson Orogen in Manitoba, central Canada. Department of Geology, The University of New Brunswick, P.O. Box 4400, Fredericton, NB, E3B 5A3 Canada. Submitted to the Canadian Journal of Earth Science, 29th June 1998.

Larocque, A. C. L., Hodgson, C. J., Cabri, L. J. & Jackman, J. A., 1995. Ion Microprobe analysis of pyrite, chalcopyrite and pyrrhotite from the Mobrun VMS deposit in northwestern Quebec: Evidence for metamorphic remobilization of gold. The Canadian Mineralogist, Vol. 33, pp. 373-388.

Lesher, C.M., Phillips, G.N., Groves, D.I. & Campbell, I.H., 1991. Immobility of REE and most high field-strength elements and first transition series metals during Archean gold-related hydrothermal alteration of metabasalts at the Hunt mine, Western Australia. Brazil Gold '91, The Economics, Geology, Geochemistry and Genesis of Gold deposits, edited by Ladeira, E.A, pp. 327-334.

Manitoba Energy and Mines, spring 1998. Manitoba Exploration and Development Highlights 1997. Manitoba Exploration News, pp. 1-2.

McCaig, T.C. & Kerrich, R., 1994. Hydrothermal alteration in active continental hydrothermal systems.Alteration and alteration processes associated with ore-forming systems, Short course notes volume 11, Geological Association of Canada, pp. 339-381.

Melo, G., 1991. Statistical assessment of the large-scale geochemical alteration surrounding the green-stone hosted Fazenda Brasileiro gold deposit, Bahia, Brazil. Brazil Gold '91, The Economics, Geology, Geochemistry and Genesis of Gold deposits, edited by Ladeira, E.A., pp 287-298.

Menard, T. & Gordon, T.M., 1995. GS-35 Syntectonic alteration of VMS deposits, Snow

Lake, Manitoba. In Manitoba Energy and Mines, Minerals Division, Report on Activities 1995, pp. 164-167.

Menard, T. & Gordon, T.M., 1996. Heat and fluid flow during deformation of VMS deposits, Snow Lake, Manitoba. Hajnal, Z. (editor), Lewry, J. (editor), Lithoprobe; Trans-Hudson Orogen transect; report of Sixth transect meeting, Lithoprobe Report, 55, pp.106-112, 1996. Meeting: Lithoprobe sixth transect meeting, Saskatoon, SK, Canada, 1996.

Mumin, A.H., Fleet, M.E., & Chryssoulis, S.L., 1994. Gold mineralization in As-rich mesothermal gold ores of the Bogosu-Prestea mining district of the Ashanti Gold Belt, Ghana: Remobilization of "invisible" gold. Mineralium Deposita, pp.445-460.

Olivio, G.R., Marini, O.J., & Giuliani, G., 1991. Hydrothermal gold occurrences hosted by middle to upper Proterozoic carbonate sequence: The example of the Santa Rita prospect, Goias, Brazil. Brazil Gold '91, The Economics, Geology, Geochemistry and Genesis of Gold deposits, edited by Ladeira, E.A., pp. 339-341.

Petruk, W., 1989. Short Course on Image Analysis Applied to Mineral and Earth Sciences. Mineralogical Association of Canada, Ottawa May 1989. Edited by W. Petruk.

Phillips, G.N., 1990. Wallrock alteration and P-T environments of gold deposition. Greenstone Gold and Crustal Evolution, Geological Association of Canada, NUNA Conference Volume edited by Robert, F., Sheahan, P.A., Green, S.B., pp.98-99.

Phillips, G.N., Groves, D.I., & Martyn, J.E., 1984. An epigenetic origin for archean banded iron-formation-hosted gold deposits. Economic Geology, Vol. 79, pp. 162-171.

Pouchou, J. L. & Pichoir, F., 1985. "PAP" (phi-rho-z) procedure for improved quantitative microanalysis. *In* "Microbeam Analysis", J. T. Armstrong, (ed.), San Francisco Press, pp. 104 - 106.

Pratt, A.R, Huctwith, C.M., van der Heide, P.A.W. & McIntyre, N.S., 1997. Quantitative SIMS analysis of trace Au in pyrite using the Infinite Velocity (IV) method. Unpublished paper, Surface Science Western, The University of Western Ontario, London, Ontario, Canada, N6A 5B7. E-mail; apratt@surf.ssw.uwo.ca

Richards, J.P., Chappell, B.W., McCulloch, M.T. & McDougall, I., 1991. The Porgera gold deposit, Papua New Guinea, 1: Association with alkalic magmatism in a continental-island-arc collision zone. Brazil Gold '91, The Economics, Geology, Geochemistry and Genesis of Gold deposits, edited by Ladeira, E.A., pp. 307-312.

Richardson, D.J. & Ostry, G., 1996. Gold deposits of Manitoba(Revised by W. Weber and D.

fogwill). Economic Geology Report ER86-1 (2nd edition) Manitoba Energy and Mines.

Robertson, D., 1989. What old mines threw out may now be economic. The Northern miner, 74; no. 49.

Romberger, S.B., 1986. The solution chemistry of gold applied to the origin of hydrothermal deposits. In Clark, L.A.,ed., Gold in the western shield: Canadian Inst. Mining Metallurgy Spec. Vol., pp. 68-186.

Romberger, S.B., 1990. Transport and deposition of gold in hydrothermal systems. Greenstone Gold and Crustal Evolution, Geological Association of Canada, NUNA Conference Volume edited by Robert, F., Sheahan, P.A., Green, S.B., pp.61-66.

Schwartz, G.M., 1944. The host minerals of native gold. Economic Geology 39, pp.371 - 411.

Sibson, R.H., 1990. Fault structure and mechanics in relation to greenstone gold deposits. Greenstone Gold and Crustal Evolution, Geological Association of Canada, NUNA Conference Volume edited by Robert, F., Sheahan, P.A., Green, S.B., pp.54-60.

Spooner, E.T.C., 1991. The magmatic model for the origin of Archean Au-quartz vein ore systems: An assessment of the evidence. Brazil Gold '91, The Economics, Geology, Geochemistry and Genesis of Gold deposits, edited by Ladeira, E.A., pp.313-318.

Stauffer, M.R., Mukherjee, A.C. & Koo, J., 1975. The Amisk Group: An Aphebian island arc deposit. Canadian Journal of Earth Sciences, Vol. 12, pp.2021-2035.

Syme, E.C., Bailes, A.H., Price, D.P., & Ziehlke, D.V., 1982. Flin Flon Volcanic belt: Geology and ore deposits of Flin Flon and Snow Lake, Manitoba. Geol. Assoc. Can. And Min. Assoc. Can. Joint Annual Meeting, University of Manitoba, Winnipeg, Manitoba 1982, Field Trip Guide Book No. 6.

Syme, E.C., Lucas, S.B., Zwanzig, H.V., Bailes, A.H., Ashton, K.E. & Haidl, F.M., 1998. Geology, NATMAP shield margin project area Flin Flon Belt, Manitoba/Saskatchewan accompanying notes. NATMAP Shield Margin Project Working Group.

Walford and Franklin, 1982. The Anderson Lake Mine, Snow Lake, Manitoba. Precambrian Sulphide Deposits. (R.W. Hutchinson, C.D. Spence and J.M. Franklin eds.) Geological Association of Canada, Special Paper 25, pp. 481-523.

Xavier, R. P., Foster, R. P., 1991. The role of carbonaceous shear bands in fluid-flow and gold-precipitation in the Fazenda Maria Preta mine, Bahia, north-east Brazil. Brazil Gold '91, The Economics, Geology, Geochemistry and Genesis of Gold deposits, edited by Ladeira, E.A., pp. 269-278.

APPENDIX 1 - SAMPLE STATUS SHEET

Chart showing all the samples that have been analyzed, and which analyses have been performed on each.
M.A. - Modal analysis; P.A. - Perimeter association; SIMS - Secondary Ion Mass Spectrometry;
× - Not found / not analyzed; ✓ - Gold found / analysis completed

Zone	Level / Borehole	Depth (ft)	Sample No.	Gold search	Gold found	Gold M.A.	Gold P.A.	Slide M.A	Sulphide analysis	SIMS
Birch	Pit	0	BA01	✓	×	×	×	✓	✓	×
Birch	Pit	0	BA02	✓	×	×	×	✓	✓	×
Birch	Pit	0	BA03	✓	×	×	×	×	✓	×
Birch	Pit	0	BA04	✓	×	×	×	×	✓	×
Birch	Pit	0	BA05	✓	✓	✓	✓	✓	✓	✓
Birch	Pit	0	BA06a	✓	×	×	×	✓	✓	✓
Birch	Pit	0	BA06b	✓	×	×	×	✓	×	×
Birch	Pit	0	BA06c	✓	×	×	×	✓	×	×
Birch	Pit	0	BA06d	✓	×	×	×	✓	×	×
Birch	Pit	0	BA06e	✓	×	×	×	✓	×	×
Birch	Pit	0	BB01	✓	×	×	×	✓	✓	×
Birch	Pit	0	BB02	✓	×	×	×	✓	✓	×
Birch	Pit	0	BB03	✓	×	×	×	×	✓	×
Birch	Pit	0	BB04	✓	×	×	×	×	✓	×
Birch	Pit	0	BC03	✓	×	×	×	×	✓	×
Birch	Pit	0	BD01	✓	✓	✓	✓	✓	✓	✓

M.A. - Modal analysis; P.A. - Perimeter association; SIMS - Secondary Ion Mass Spectrometry;
× - Not found / not analyzed; ✓ - Gold found / analysis completed; H - Horizon number.

Zone	Level / Borehole	Depth (ft)	Sample No.	Au search	Gold found	Gold M.A.	Gold P.A.	Slide M.A	Sulphide analysis	SIMS
Birch	Pit	0	BE01	✓	✓	✓	✓	✓	✓	✓
Birch-H1	B96001	389.0-389.8	B9601-35b	✓	✓	✓	✓	✓	✓	×
Birch-H1	B96001	390.5-391.2	B9601-37a	×	×	×	×	×	×	✓
Birch-H2	B96001	587-592.7	B9601-45b	✓	×	×	×	✓	×	×
Birch-H3	B96001	626.0-626.3	B9601-39	✓	×	×	×	✓	✓	✓
Birch-H3	B96001	629.8-633.0	B9601-41a	✓	×	×	×	✓	✓	✓
Birch-H4	B96001	660.3-660.6	B9601-4b	✓	✓	✓	✓	✓	✓	✓
Birch-H4	B96001	662.2-662.5	B9601-6	✓	✓	✓	✓	✓	✓	✓
Birch-H4	B96001	664.3-665.3	B9601-7	✓	×	×	×	✓	✓	✓
Birch-H5	B96001	680.1-687.2	B9601-16a	✓	×	×	×	✓	✓	✓
Birch-H5	B96001	680.1-687.2	B9601-16b	✓	×	×	×	✓	✓	×
Birch-H6	B96001	760.8-707.0	B9601-24	✓	×	×	×	✓	✓	✓
Birch-H6	B96001	707.2-708.0	B9601-25	✓	×	×	×	✓	✓	×
Birch	B96013	314.4-314.5	B9613-1	✓	✓	✓	✓	✓	×	×
Birch	B96013	373.0-373.5	B9613-2	✓	×	×	×	✓	×	×
Birch	B96013	429.5-429.7	B9613-3	✓	✓	✓	✓	✓	×	×
Birch	B96013	518.3-518.6	B9613-4	✓	×	×	×	✓	×	×

M.A. - Modal analysis; P.A. - Perimeter association; SIMS - Secondary Ion Mass Spectrometry;
✗ - Not found / not analyzed; ✓ - Gold found / analysis completed; H - Horizon number.

Zone	Level / Borehole	Depth (ft)	Sample No.	Au search	Gold found	Gold M.A.	Gold P.A.	Slide M.A	Sulphide analysis	SIMS
Ruttan	Level 2006	2006	RA1	✓	✓	✓	✓	✓	✓	✗
Ruttan	Level 2006	2006	RA3	✓	✗	✗	✗	✓	✓	✗
Ruttan	Level 2006	2006	RA4	✓	✓	✓	✓	✓	✓	✗
Ruttan	Level 2006	2006	RA5	✓	✗	✗	✗	✓	✓	✗
Ruttan	Level 2006	2006	RC1	✓	✗	✗	✗	✓	✓	✗
Ruttan	Level 2006	2006	RC2	✓	✓	✓	✓	✓	✓	✗
Ruttan	Level 2006	2006	RD1	✓	✗	✗	✗	✓	✗	✗
Dick	Level 2210	2210	DB2ai	✓	✗	✗	✗	✓	✗	✗
Dick	Level 2210	2210	DB6	✓	✗	✗	✗	✓	✗	✗
Dick	Level 2210	2210	DB7	✓	✓	✓	✓	✓	✓	✗
Dick	Level 2210	2210	DB8	✓	✗	✗	✗	✓	✓	✗
Dick	Level 2210	2210	DB9	✓	✗	✗	✗	✓	✗	✗
Dick	Level 2210	2210	DB13i	✗	✗	✗	✗	✗	✗	✗
Dick	Level 2210	2210	DB13ii	✓	✗	✗	✗	✓	✓	✗
Dick	Level 2210	2210	DB16b	✓	✓	✓	✓	✓	✓	✗
Dick	Level 2210	2210	DB17b	✓	✗	✗	✗	✓	✓	✗
Dick	Level 2210	2210	DB18b	✓	✗	✗	✗	✓	✓	✗

M.A. - Modal analysis; P.A. - Perimeter association; SIMS - Secondary Ion Mass Spectrometry;
× - Not found / not analyzed; ✓ - Gold found / analysis completed; H - Horizon number.

Dick	Level / Borehole	Depth (ft)	Sample No.	Au search	Gold found	Gold M.A.	Gold P.A.	Slide M.A	Sulphide analysis	SIMS
Dick	Level 2210	2210	DB19b	✓	×	×	×	×	✓	×
Dick	Level 2210	2210	DB20a	✓	×	×	×	✓	✓	×
Dick	Level 2210	2210	DB21B	✓	✓	✓	✓	✓	✓	×
Dick	Level 2210	2210	DB28	✓	✓	✓	✓	✓	✓	×
Dick	Level 2210	2210	DB29	✓	×	×	×	✓	✓	✓
Dick	Level 2210	2210	DB30	✓	✓	✓	✓	✓	✓	✓
Dick	Level 2210	2210	DB31	✓	×	×	×	✓	✓	✓
Dick	Level 2210	2210	DB36	✓	×	×	×	✓	✓	×
Dick	Level 2210	2210	DB37	✓	✓	✓	✓	✓	✓	×
Dick	Level 2210	2210	DB39	✓	×	×	×	✓	✓	×
Dick	Level 2210	2210	DB66	✓	×	×	×	✓	✓	×
Dick	Level 2260	2260	DC9	✓	×	×	×	✓	✓	✓
No. 3	Outcrop	0	N3-1	✓	✓	✓	✓	✓	✓	✓
No. 3	Outcrop	0	N3-2	✓	×	×	×	✓	✓	×
No. 3	Outcrop	0	N3-3	✓	✓	✓	✓	✓	✓	✓
No. 3	Outcrop	0	N3-4	✓	✓	✓	✓	✓	✓	✓
No. 3	Outcrop	0	N3-9	✓	×	×	×	✓	✓	✓

M.A. - Modal analysis; P.A. - Perimeter association; SIMS - Secondary Ion Mass Spectrometry;
✕ - Not found / not analyzed; ✓ - Gold found / analysis completed; H - Horizon number.

Zone	Level / Borehole	Depth (ft)	Sample No.	Au search	Gold found	Gold M.A.	Gold P.A.	Slide M.A	Sulphide analysis	SIMS
Boundary	BNDY-83-02	185.2-185.4	Bdy-1	✓	✕	✕	✕	✓	✓	✓
Boundary	BNDY-83-02	186.1-186.2	Bdy-2	✓	✕	✕	✕	✓	✓	✓
Boundary	BNDY-83-02	185.9-186	Bdy-3	✓	✕	✕	✕	✓	✓	✓
Boundary	BNDY-83-02	202.3-202.4	Bdy-4	✓	✕	✕	✕	✓	✓	✓
Boundary	BNDY-83-02	203.5-203.7	Bdy-5	✓	✕	✕	✕	✕	✓	✓
Boundary	BNDY-83-02	204.6-204.8	Bdy-6	✓	✕	✕	✕	✕	✓	✓
Boundary	BNDY-83-02	230.9-231.0	Bdy-7	✓	✕	✕	✕	✓	✓	✕
Boundary	BNDY-83-02	231.4-231.6	Bdy-8	✓	✕	✕	✕	✓	✓	✕
Boundary	BNDY-83-02	262.8-263.0	Bdy-9	✓	✕	✕	✕	✓	✓	✕
Boundary	BNDY-83-02	260.0-261.3	Bdy-10	✓	✕	✕	✕	✓	✓	✕
Boundary	BNDY-83-02	264.8-265.0	Bdy-11	✓	✕	✕	✕	✓	✓	✕
Thorne	TZ-83-1	50.2-50.3	TZ1	✓	✕	✕	✕	✓	✓	✓
Thorne	TZ-83-1	50.5-50.6	TZ2	✓	✕	✕	✕	✓	✓	✕
Thorne	TZ-83-1	50.7-50.9	TZ3	✓	✕	✕	✕	✓	✓	✓
Thorne	TZ-83-1	51.2-51.4	TZ4	✓	✕	✕	✕	✓	✓	✕

APPENDIX 2 - IMAGE ANALYSIS RESULTS

Whole slide modal analyzes - Results of whole slide modal analysis on each sample (the modal proportions of each mineral category within the given sample).

Gold modal analyzes & perimeter associations - For each gold grain found the area surrounding each grain has been analyzed for modal proportions of minerals, as has the % perimeter each mineral category has with gold grain measured.

Average gold compositions - The results of measuring the counts for the elements Au, Ag, Si and Hg. This gives an estimate of the proportions of these elements in free gold grains in each of the samples.

WHOLE SLIDE MODAL ANALYSIS RESULTS

Sample No.	% Quartz +Silicates	% Quartz	% Silicates	% Pyrite	% Chalcopyrite	% Arsenopyrite
BA01	99.47	81.55	17.92	0.19	0.02	0.31
BA02	98.66	31.45	67.21	1.07	0.20	0.07
BA05	95.97	-	-	0.32	-	3.71
BA6a	94.18	-	-	5.80	-	0.02
BA6b	90.68	-	-	9.31	-	0.00
BA6c	97.83	-	-	2.09	-	0.09
BA6d	96.40	-	-	3.59	-	0.01
BA6e	96.02	-	-	3.93	-	0.05
BB01	99.65	-	-	0.32	-	0.03
BB02	99.36	-	-	0.61	-	0.03
BD01	98.38	16.84	81.55	0.17	0.00	1.43
BE01	88.64	41.87	46.77	0.51	0.01	10.85
B9601-4b	89.24	19.44	71.47	4.35	0.00	4.75
B9601-6a	92.99	11.79	81.20	2.54	0.00	4.47
B9601-6b	97.83	41.84	55.99	0.30	0.00	1.87
B9601-07	95.90	0.70	95.20	2.84	1.01	0.24

Sample No.	% Quartz +Silicates	% Quartz	% Silicates	% Pyrite	% Chalco -pyrite	% Arsen -opyrite
B9601-16a	98.98	78.90	20.08	0.32	0.00	0.70
B9601-16b	97.39	16.19	81.20	0.46	0.06	2.10
B9601-24	88.67	20.12	74.62	5.11	0.00	0.16
B9601-25	97.84	35.94	61.90	0.67	0.00	1.50
B9601-35	80.56	41.62	57.57	0.06	0.00	0.75
B9601-39	8.49	1.35	7.14	44.37	0.00	47.14
B9601-41	80.75	49.85	30.90	10.57	0.00	8.67
B9601-45	0.03	0.00	0.03	1.21	0.00	98.75
B9613-01	99.68	42.07	57.61	0.32	0.00	0.00
B9613-02	99.47	1.11	98.36	0.05	0.48	0.00
B9613-03	99.45	0.23	99.22	0.55	0.00	0.00
B9613-04	88.30	27.27	61.03	11.38	0.02	0.30
RA1	98.54	0.18	98.36	0.19	0.00	1.27
RA3	99.80	0.03	99.77	0.00	0.00	0.20
RA4	98.50	0.17	98.33	0.03	0.00	1.47
RC2	97.77	0.17	97.60	0.02	0.00	2.21

Sample No.	% Quartz +Silicates	% Quartz	% Silicates	% Pyrite	% Chalco -pyrite	% Arsen -opyrite
DB2ai	99.99	49.80	50.19	0.01	0.00	0.00
DB7	82.15	41.53	40.62	0.38	0.01	2.06
DB8	98.61	42.62	55.99	0.04	0.00	0.15
DB9	97.91	66.85	31.06	0.16	0.08	1.85
DB13ii	98.40	45.93	52.47	0.55	0.02	1.03
DB16b	98.34	76.19	22.15	0.40	0.00	1.26
DB17b	99.15	41.27	57.88	0.09	0.00	0.76
DB18b	99.82	90.45	9.37	0.10	0.00	0.08
DB20a	95.10	76.07	19.03	0.14	0.00	0.23
DB21b	98.32	90.51	7.81	0.24	0.00	1.44
DB28	99.44	89.70	9.74	0.09	0.00	0.47
DB29	99.24	98.99	0.25	0.03	0.00	0.73
DB30	99.60	99.37	0.23	0.02	0.00	0.38
DB31	98.00	58.18	39.82	0.46	0.00	1.54
DB36	99.73	28.28	71.45	0.17	0.04	0.07
DB37	99.00	53.08	45.92	0.18	0.00	0.82
DB39	98.95	55.34	43.61	0.20	0.19	0.66

Sample No.	% Quartz +Silicates	% Quartz	% Silicates	% Pyrite	% Chalcopyrite	% Arsenopyrite
DB66	99.10	68.68	30.42	0.06	0.00	0.84
N3-1	96.75	64.26	32.49	0.47	0.00	2.77
N3-2	99.98	0.60	99.38	0.01	0.00	0.01
N3-3	99.16	60.83	38.33	0.24	0.08	0.53
N3-4	99.97	48.43	51.54	0.02	0.00	0.01
N3-9	99.99	58.52	41.47	0.00	0.00	0.01
BY01	98.97	88.47	10.50	1.03	0.00	0.00
BY02	99.74	85.36	14.37	0.26	0.00	0.00
BY03	97.30	62.38	34.92	0.75	0.02	1.93
BY04	97.83	95.05	2.78	2.12	0.00	0.05
BY07	99.79	54.27	45.52	0.07	0.06	0.07
BY08	95.11	87.87	7.24	0.06	0.00	4.83
BY09	99.46	91.83	7.64	0.51	0.00	0.03
BY10	98.48	55.60	42.88	0.17	0.46	0.89
BY11	99.11	69.51	29.60	0.03	0.00	0.86
TZ1	98.31	9.76	88.55	0.61	0.00	1.08
TZ2	89.41	53.15	36.26	2.80	0.03	7.77

Sample No.	% Quartz +Silicates	% Quartz	% Silicates	% Pyrite	% Chalcopyrite	% Arsenopyrite
TZ3	93.04	67.42	25.62	0.84	0.01	6.12
TZ4	85.75	61.60	24.15	1.34	0.00	12.91

FIELDS CONTAINING GOLD - MODAL ANALYSIS & PERIMETER ASSOCIATIONS

M.A. - Modal Analysis, P.A. - Perimeter Association.

Sample No.	Type	% Quartz +Silicates	% Quartz	% Silicates	% Pyrite	% Arsen -opyrite	% Gold
BA05	M.A.	83.69	-	-	0.38	13.97	0.13
	P.A.	40.65	-	-	7.48	51.87	-
BD01	M.A.	92.00	-	-	0.04	7.20	0.11
	P.A.	58.08	-	-	0.69	34.34	-
BE01	M.A.	77.10	-	-	1.10	20.30	0.40
	P.A.	57.96	-	-	2.72	38.37	-
B9601-4b	M.A.	91.28	-	-	7.43	0.54	0.436
	P.A.	85.07	-	-	1.9	13.04	-
B9601-6a	M.A.	95.3	-	-	1.4	3.15	0.10
	P.A.	47.92	-	-	10.42	41.67	-
B9601-35b	M.A.	96.3	-	-	>0.01	1.10	0.04
	P.A.	31.58	-	-	0.00	68.42	-
B9613-01	M.A.	51.4	-	-	47.9	0.29	0.07
	P.A.	37.43	-	-	51.26		-
B9613-03	M.A.	91.80	-	-	3.40	0.05	4.72
	P.A.	77.94	-	-	17.31	4.75	-
B9613-04	M.A.	53.30	-	-	21.10	10.70	0.14
	P.A.	0.00	-	-	26.56	65.63	-
DB07	M.A.	74.56	-	-	0.63	5.07	0.23
	P.A.	25.06	-	-	0.69	34.36	-
DB16b	M.A.	91.05	-	-	0.91	4.41	0.63
	P.A.	15.94	-	-	0.00	81.88	-
DB21b	M.A.	91.61	78.79	12.82	0.04	7.97	0.30
	P.A.	100	12.50	87.50	0.00	0.00	-
DB28	M.A.	99.70	98.50	1.20	0.00	0.25	0.05
	P.A.	0.00	0.00	0.00	0.00	100	-
DB30	M.A.	68.89	67.63	1.26	0.00	0.96	0.11

Sample No.	Type	% Quartz +Silicates	% Quartz	% Silicates	% Pyrite	% Arsen -opyrite	% Gold
	P.A.	27.21	17.72	9.49	0.00	30.38	-
DB37	M.A.	0.59	0.01	0.58	0.43	98.00	0.88
	P.A.	0.00	0.00	0.00	1.97	98.03	-
RA1	M.A.	100	0	100	0	0	-
	P.A.	98.16	0.07	98.09	0.11	1.65	0.08
RA4	M.A.	53.33	0	53.33	0	46.67	-
	P.A.	77.21	0	77.21	0.03	22.70	0.07
RC2	M.A.	0.27	0.27	0	88.59	11.14	-
	P.A.	0.152	0.033	0.12	98.88	0.19	0.78
N3-1	M.A.	84.60	-	-	0.50	12.50	0.30
	P.A.	49.00	-	-	0.20	50.80	-
N3-3	M.A.	93.70	-	-	0.01	3.10	0.05
	P.A.	100	-	-	0.00	0.00	-
N3-4	M.A.	94.30	-	-	0.60	0.60	4.06
	P.A.	83.44	-	-	13.23	3.01	-

M.A. - Modal Analysis, P.A. - Perimeter Association.

IMAGE ANALYSIS - AVERAGE GOLD COMPOSITIONS

Sample No.	% Au (from Au+Ag=100 %)	Au/Ag Ratio	Au Counts	Ag Counts	Si Counts	Hg Counts
B9601-4b	86.74	6.54	6.34	0.969	-	-
B9601-6a		-	1.213	-	0.157	0.000
B9601-35b	93.67	14.80	1.470	0.0993	0.052	0.000
BA05	91.86	11.28	1.546	0.137	0.055	0.000
BE01	94.69	17.83	1.480	0.083	0.154	0.000
B96013-01	45.51	0.84	0.152	0.182	0.240	0.000
B96013-03	67.29	2.06	1.358	0.660	1.070	0.405
B96013-04	39.64	0.66	0.044	0.067	0.102	0.000
DB07	84.10	5.29	1.650	0.312	0.111	0.000
DB16b	86.67	6.50	1.509	0.232	0.167	0.001
DB21b	90.16	9.16	5.802	0.633	-	-
DB28	85.05	5.69	2.560	0.450	-	-
DB30	95.11	19.46	5.021	0.258	-	-
DB37	88.65	7.81	5.426	0.695	-	-
RA4	80.03	4.01	5.17	1.290	-	-
RC2	87.15	6.78	5.880	0.867	-	-
N3-1	82.77	4.80	1.532	0.319	0.225	0.00
N3-3	84.48	5.44	1.524	0.280	0.161	0.00
N3-4	81.66	4.45	1.621	0.364	0.384	0.242

APPENDIX 3

GOLD BACK SCATTERED ELECTRON IMAGES

The Back Scattered Electron images seen here are of each gold grain found in all the gold searches completed on the ore found at the New Britannia Mine and surrounding deposits. Each image is a visual means of determining atomic number, the brighter areas denoting higher atomic number and the darker areas denoting low atomic number. The diagram below is a guide to determining which type of mineral is present within the field of view.

GRAY LEVEL DISCRIMINATION DIAGRAM

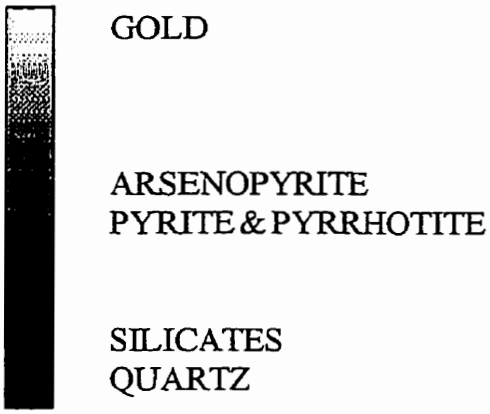

Figure 21 - Diagram showing correlation between dark levels and mineralogy.

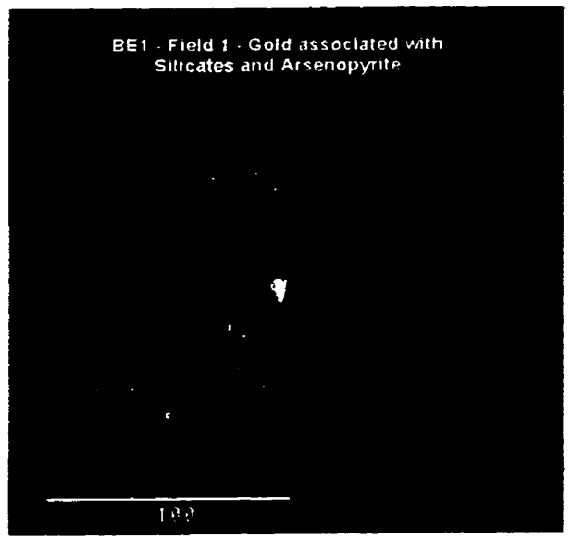
BE1 - Field 1 - Gold associated with
Silicates and Arsenopyrite
100

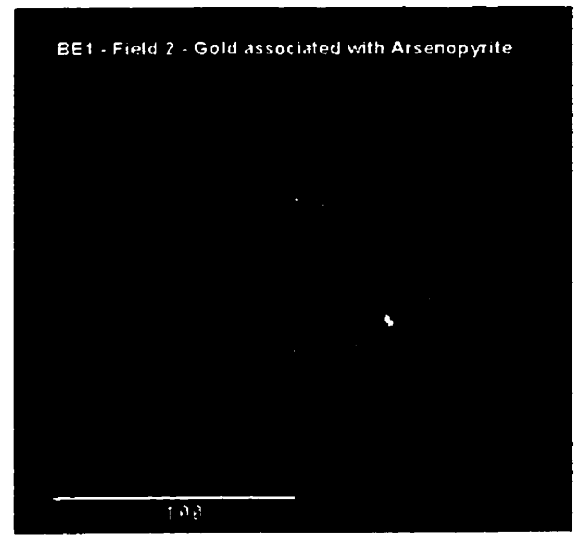
BE1 - Field 2 - Gold associated with Arsenopyrite
100

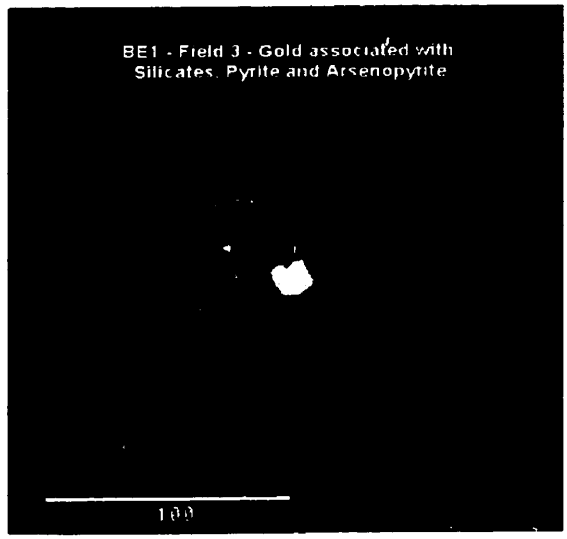
BE1 - Field 3 - Gold associated with
Silicates, Pyrite and Arsenopyrite
100

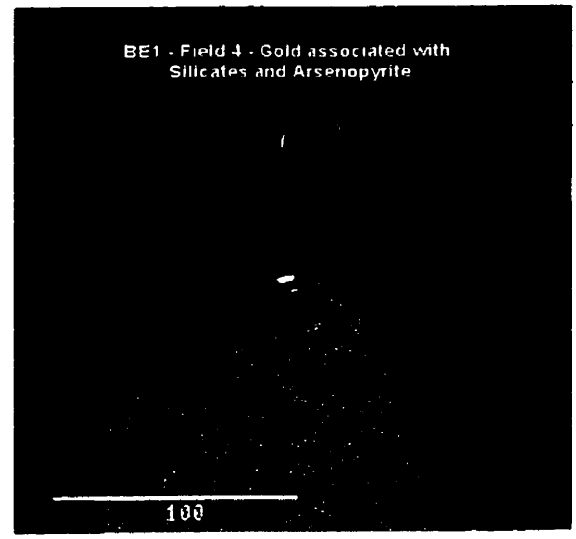
BE1 - Field 4 - Gold associated with
Silicates and Arsenopyrite
100

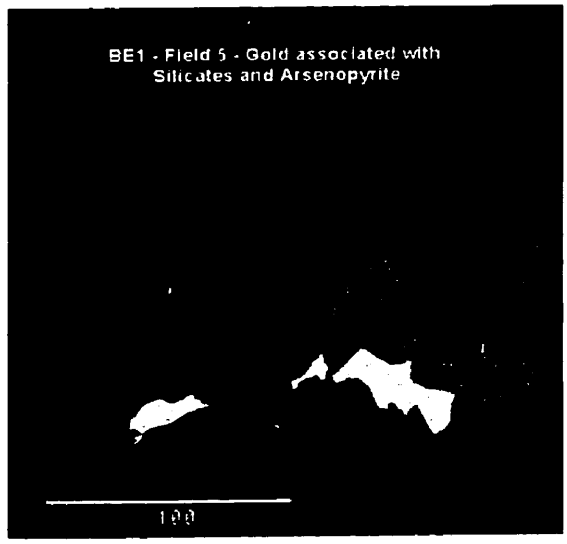
BE1 - Field 5 - Gold associated with
Silicates and Arsenopyrite
100

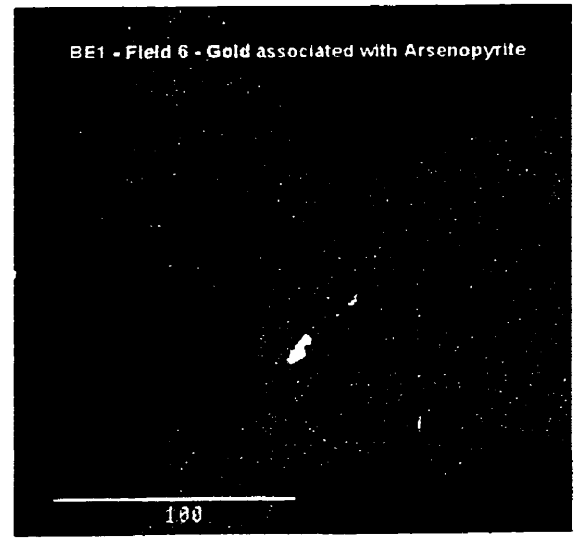
BE1 - Field 6 - Gold associated with Arsenopyrite
100

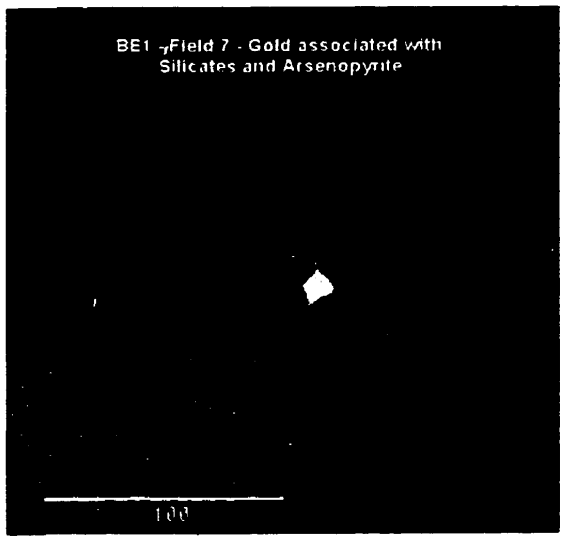
BE1 - Field 7 - Gold associated with
Silicates and Arsenopyrite
100

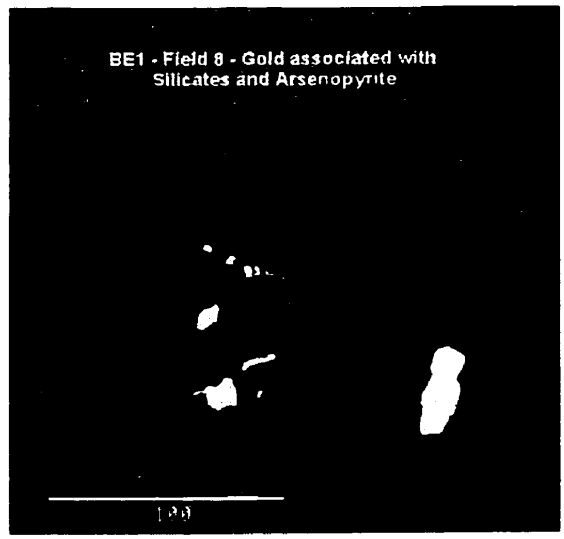
BE1 - Field 8 - Gold associated with
Silicates and Arsenopyrite

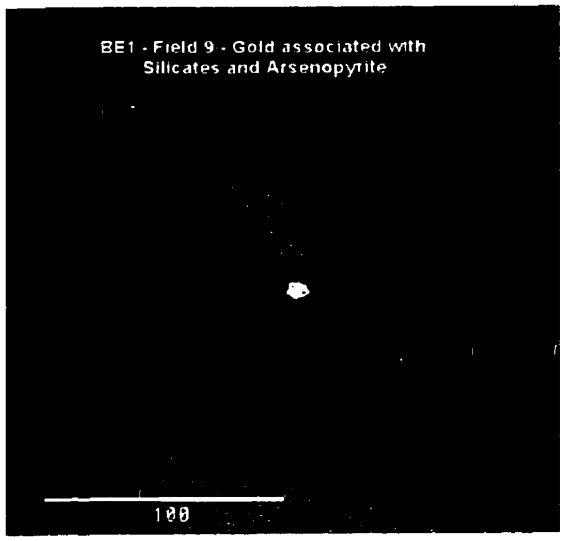
BE1 - Field 9 - Gold associated with
Silicates and Arsenopyrite
100

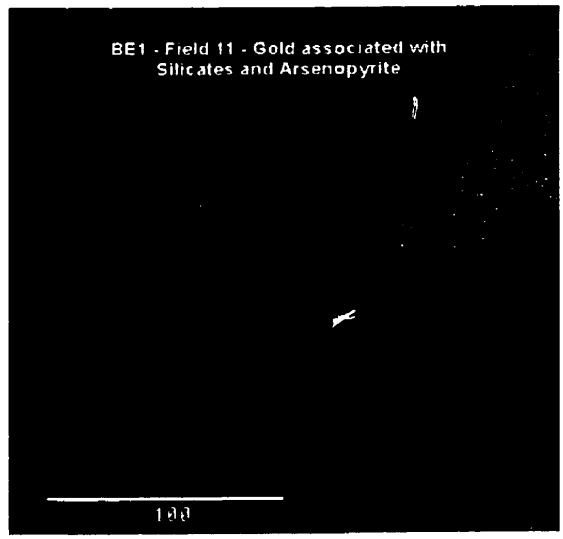
BE1 - Field 11 - Gold associated with
Silicates and Arsenopyrite

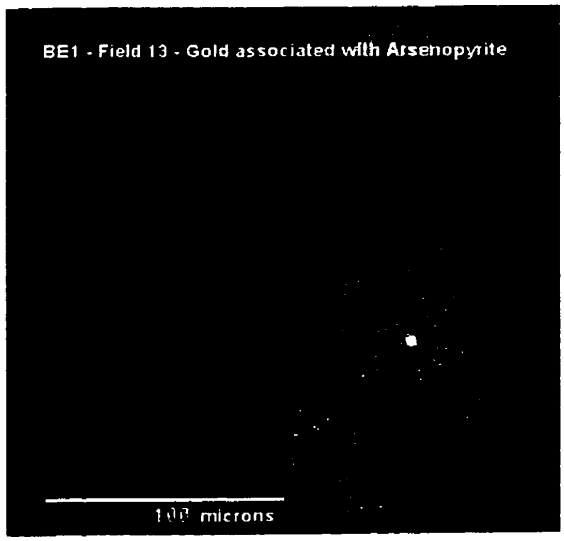
BE1 - Field 13 - Gold associated with Arsenopyrite
100 microns

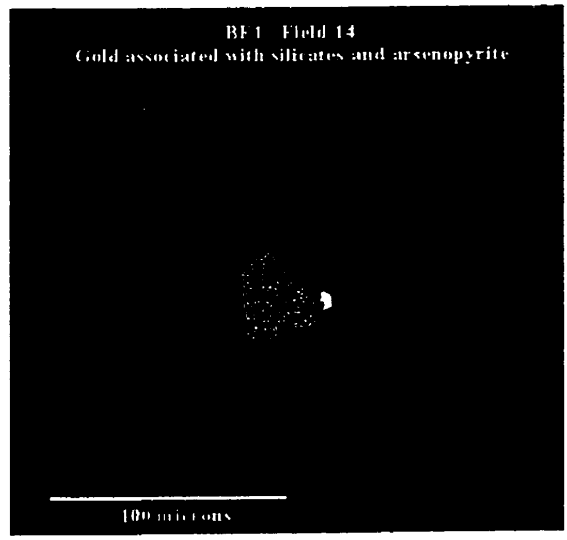
BE1 Field 14
Gold associated with silicates and arsenopyrite

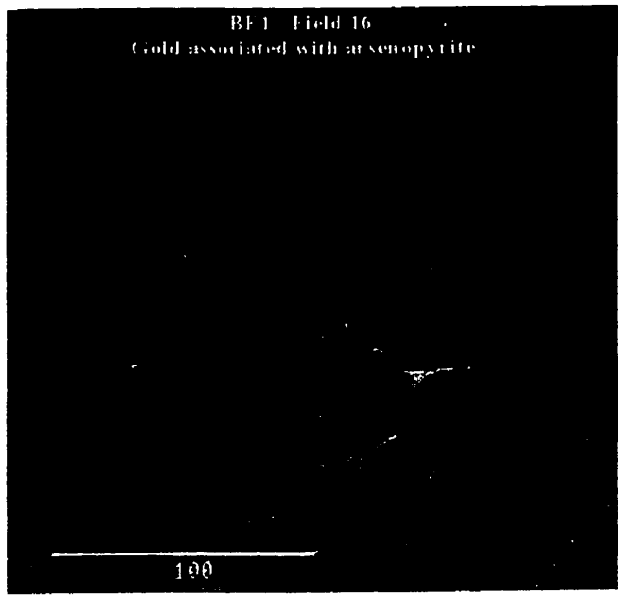
BF1 Field 16
Gold associated with arsenopyrite
100

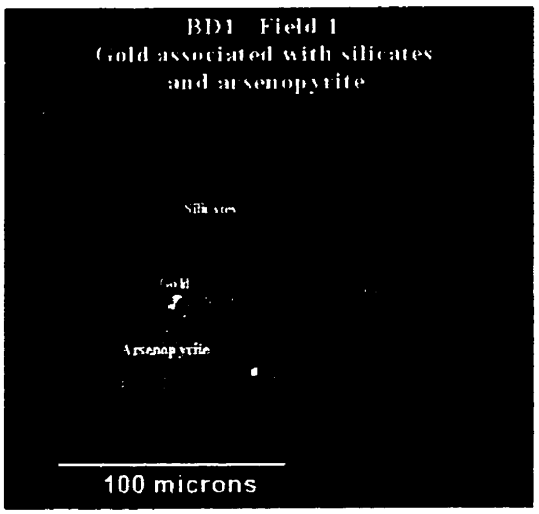
BD1 Field 1
Gold associated with silicates
and arsenopyrite
Silicates
Gold
Arsenopyrite
100 microns

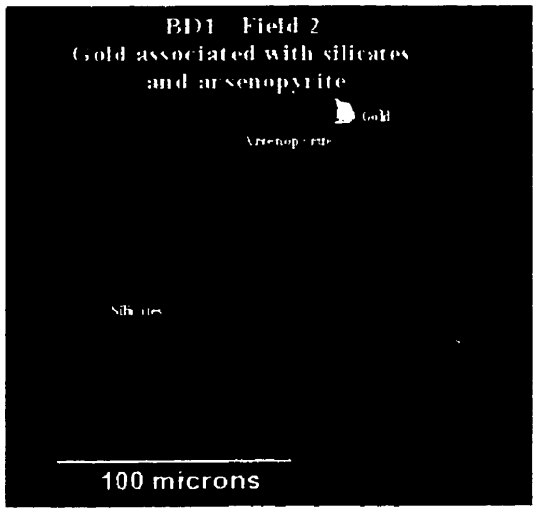
BD1 Field 2
Gold associated with silicates
and arsenopyrite
Gold
Arsenopyrite
Silicates
100 microns

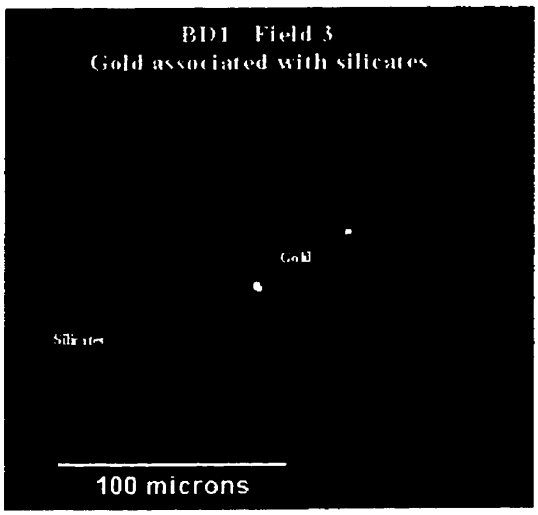
BD1 Field 3
Gold associated with silicates
Gold
Silicates
100 microns

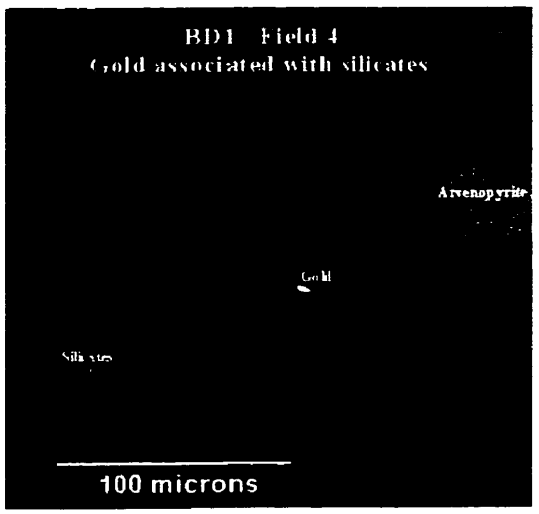
BD1 Field 4
Gold associated with silicates
Arsenopyrite
Gold
Silicates
100 microns

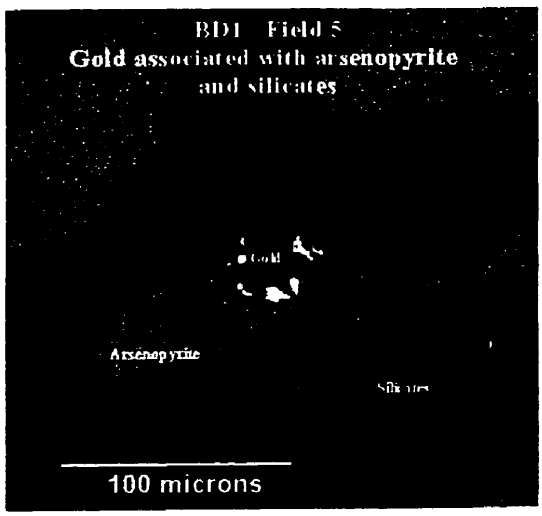
BD1 Field 5
Gold associated with arsenopyrite
and silicates
Gold
Arsenopyrite
Silicates
100 microns

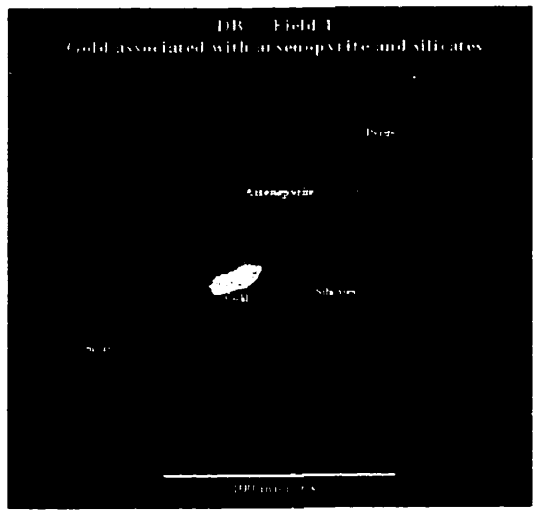

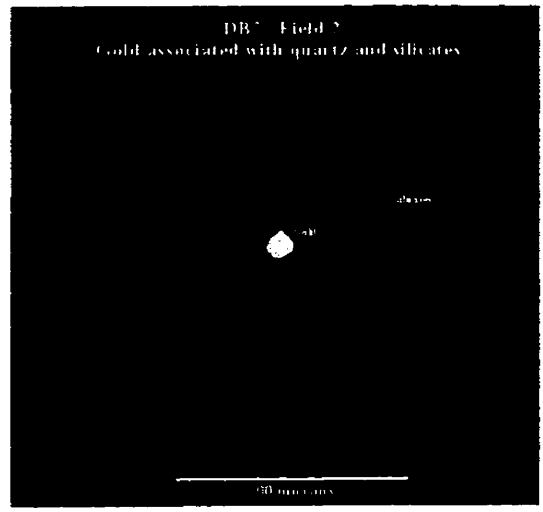

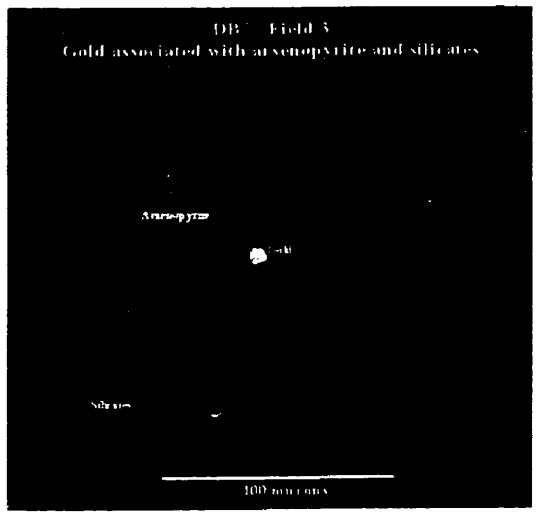

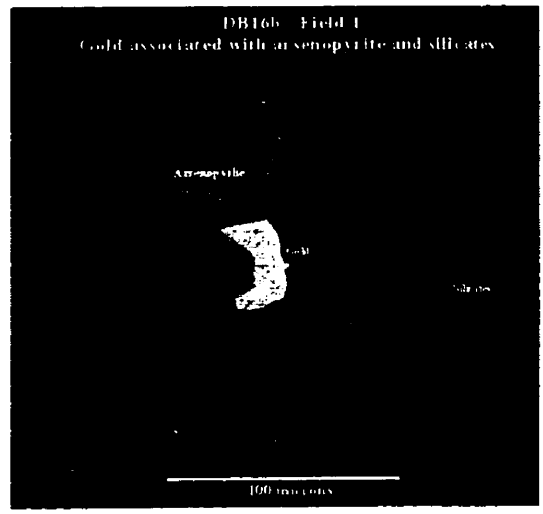

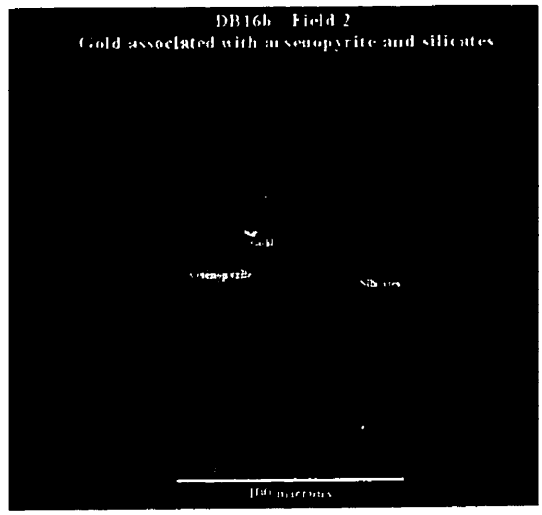

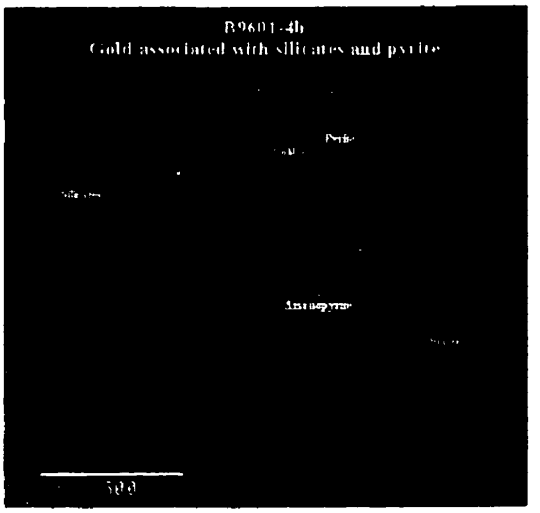
B9601-4b
Gold associated with silicates and pyrite
Pyrite
Arsenopyrite

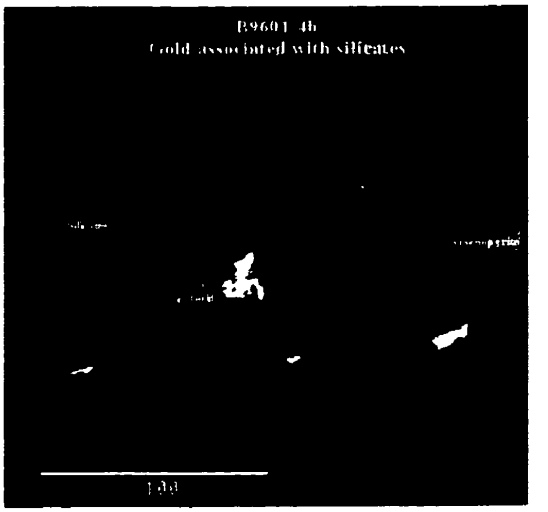
B9601 4b
Gold associated with silicates

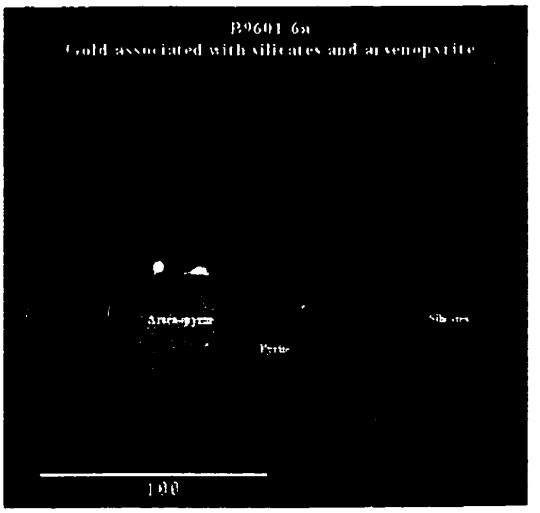
B9601 6a
Gold associated with silicates and arsenopyrite
Arsenopyrite
Pyrite

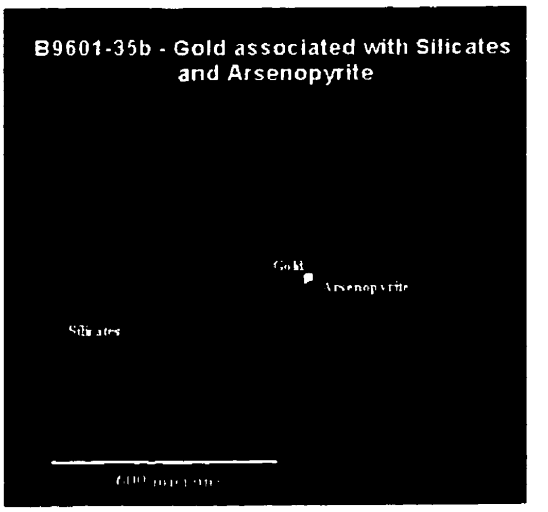
B9601-35b - Gold associated with Silicates and Arsenopyrite
Gold
Arsenopyrite
Silicates

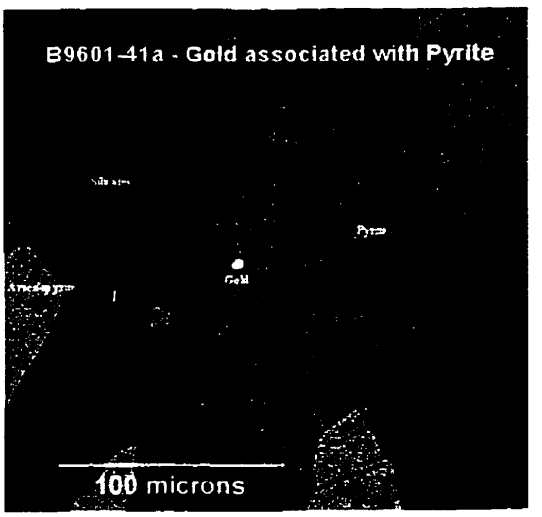
B9601-41a - Gold associated with Pyrite
Silicates
Pyrite
Gold
100 microns

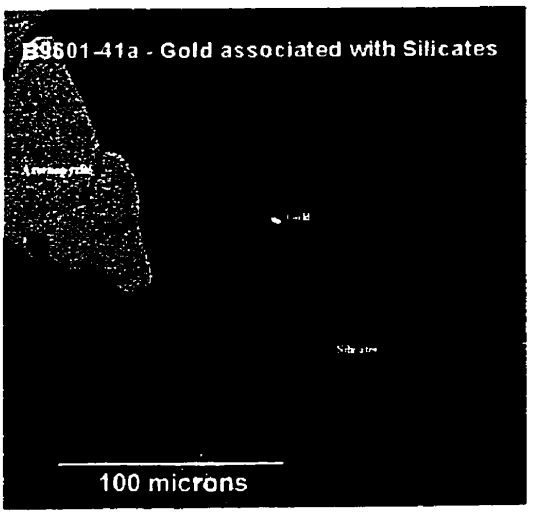
B9601-41a - Gold associated with Silicates
Gold
Silicates
100 microns

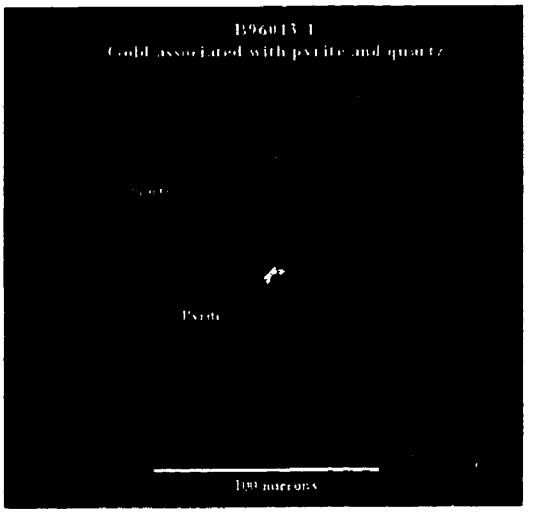
B96013 1
Gold associated with pyrite and quartz
Pyrite
100 microns

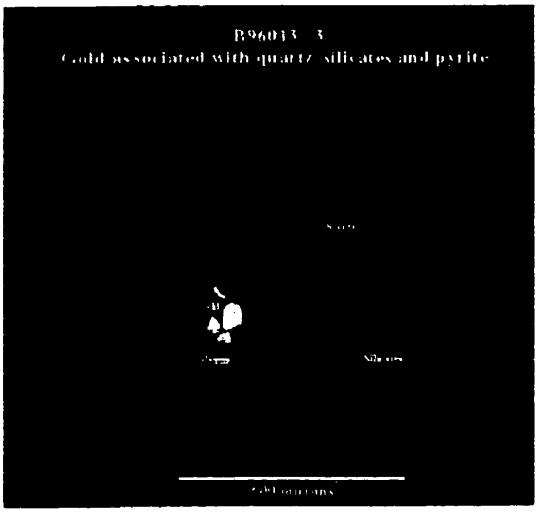
B96013 3
Gold associated with quartz, silicates and pyrite

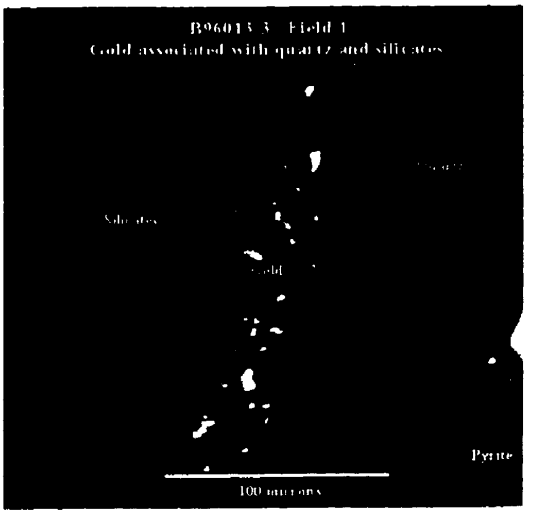
B96013 3 Field 1
Gold associated with quartz and silicates
Pyrite
100 microns

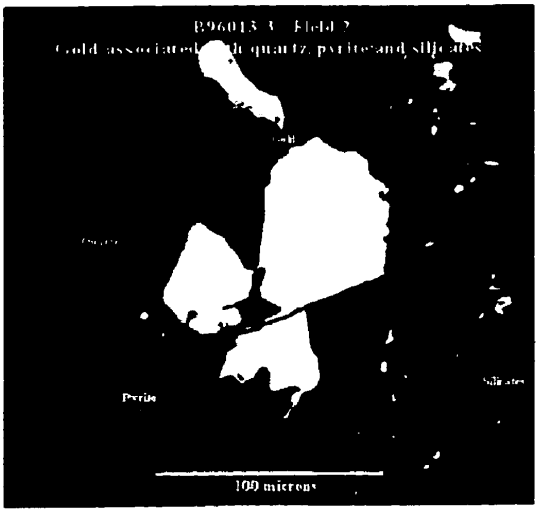
B96013 3 Field 2
Pyrite
100 microns

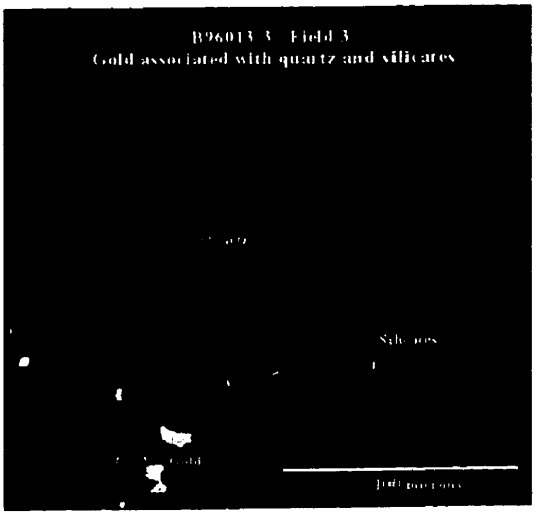
B96013 3 Field 3
Gold associated with quartz and silicates

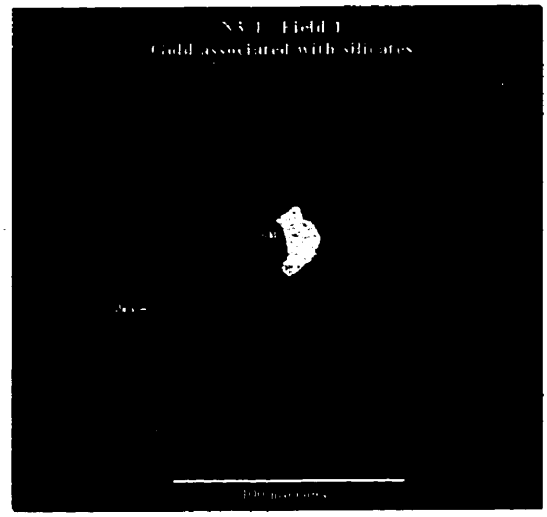
N3-1 Field 1
Gold associated with silicates

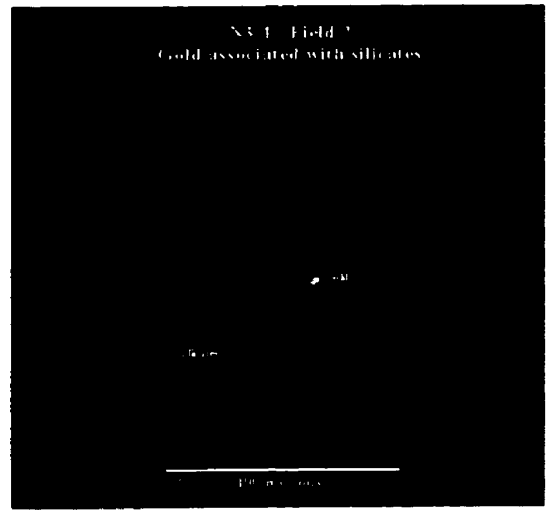
N3-1 Field 2
Gold associated with silicates

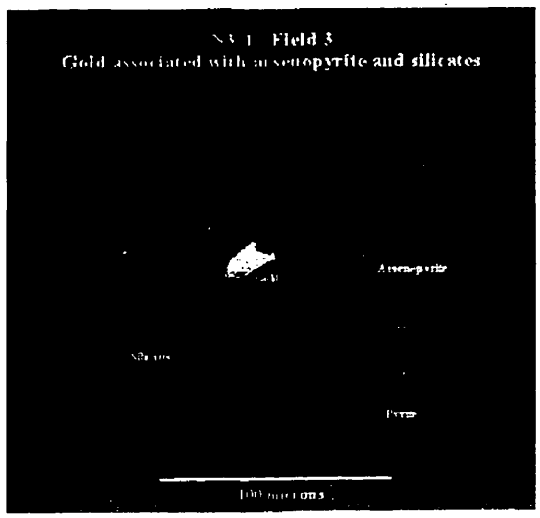
N3-1 Field 3
Gold associated with arsenopyrite and silicates
Arsenopyrite
Pyrite

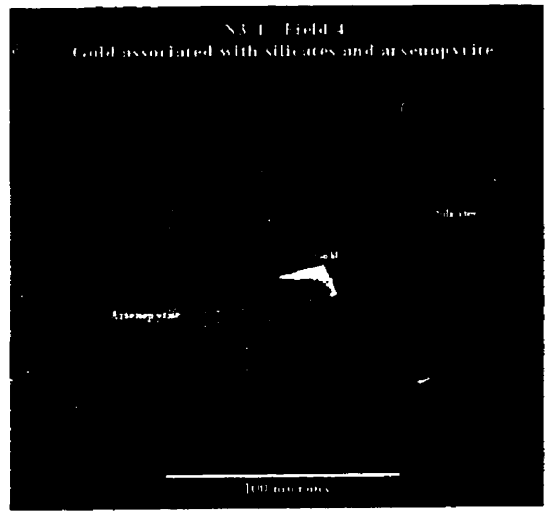
N3-1 Field 4
Gold associated with silicates and arsenopyrite
Arsenopyrite

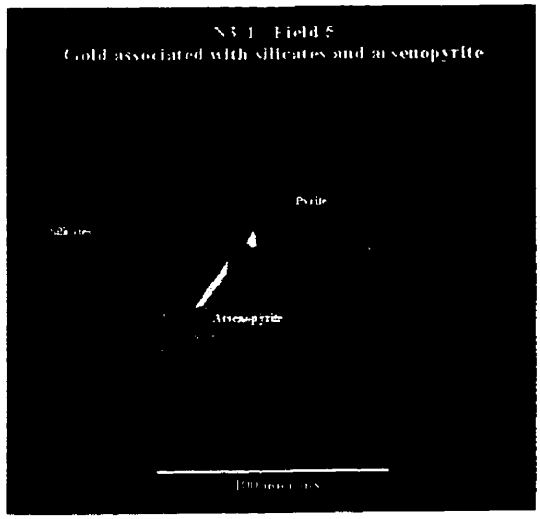
N3-1 Field 5
Gold associated with silicates and arsenopyrite
Pyrite
Arsenopyrite

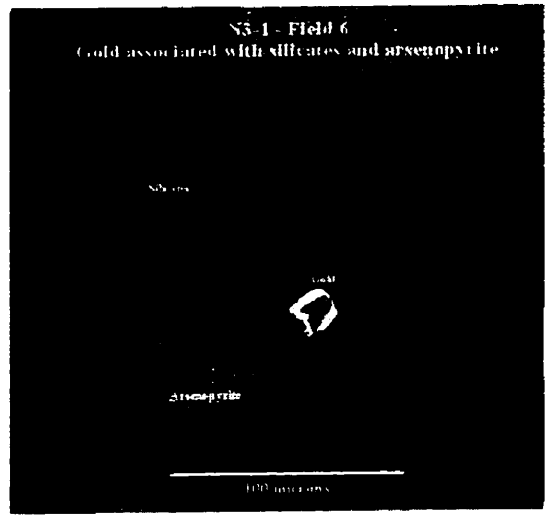
N3-1 - Field 6
Gold associated with silicates and arsenopyrite
Arsenopyrite

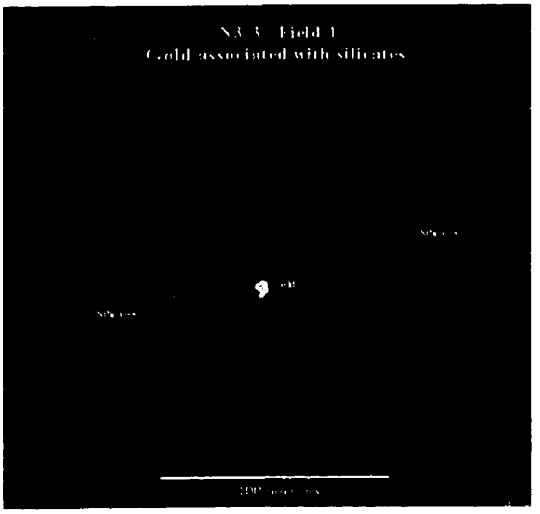
N3-3 Field 1
Gold associated with silicates

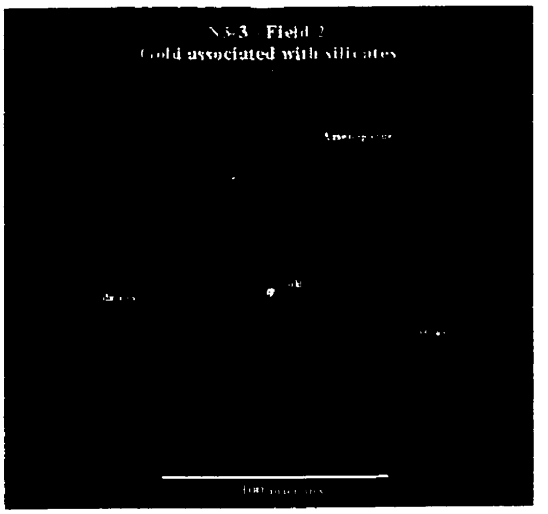
N3-3 Field 2
Gold associated with silicates

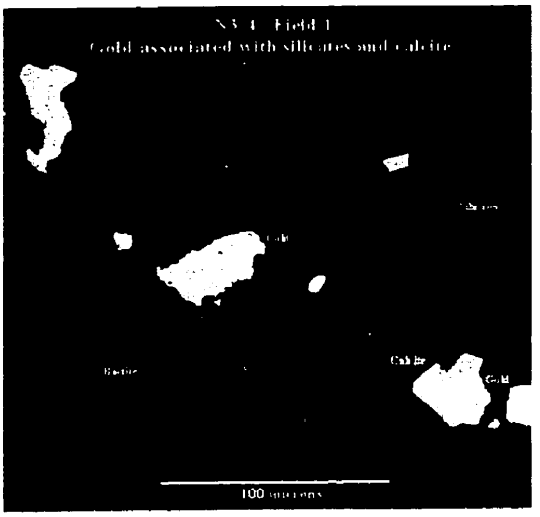
N3-4 Field 1
Gold associated with silicates and calcite
100 microns

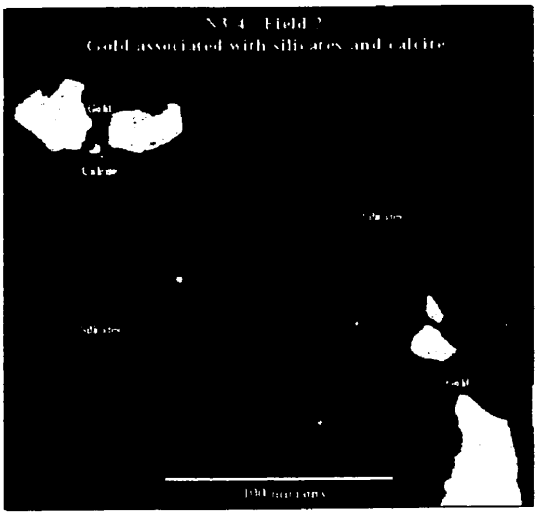
N3-4 Field 2
Gold associated with silicates and calcite

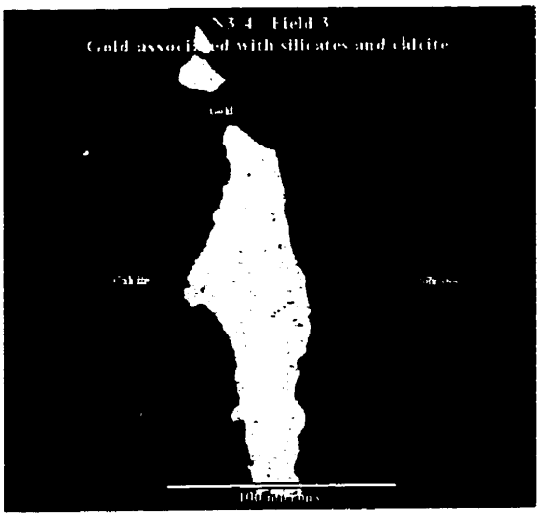
N3-4 Field 3
Gold associated with silicates and calcite

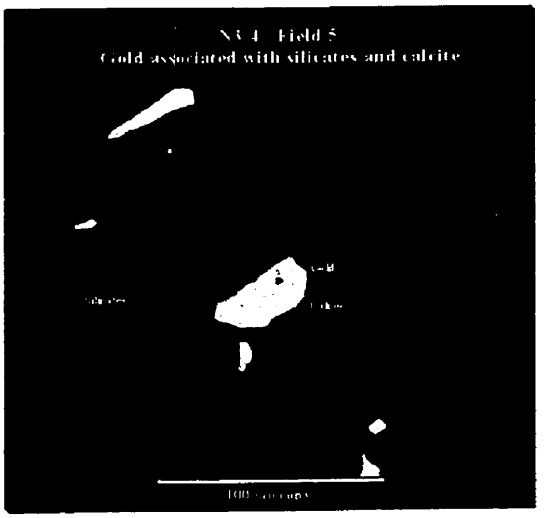
N3-4 Field 5
Gold associated with silicates and calcite

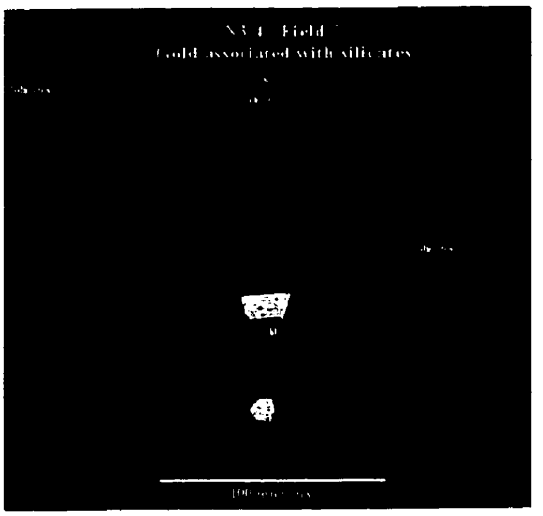

APPENDIX 4

APPENDIX - ELECRON MICROPROBE ANALYSIS RESULTS

The following section is the data collected using the Electron Microprobe, on sulphide minerals in the Birch Zone, the Ruttan Zone (New Britannia Mine), the Dick Zone (New Britannia Mine), the No.3 Zone and the Boundary Zone. All results are given in weight percent (Wt%). The list of abbreviations has been provided to allow interpretation of the labels provided for each analysis.

PROBE ANALYSIS TABLE OF ABBREVIATIONS

Abbreviation	Meaning
An.	Anhedral grain shape
Subeu.	Subeuhedral grain shape
Eu.	Euhedral grain shape
Sp.	Spongy texture to grain
Agg.	Aggregated grains(many grains with touching grain boundaries)
O.G.	Overgrown / Overgrowing
Incl.	Contains inclusions
Ass.	Associated
Fg.	Fine grain size (<50 x 50 microns)
Mg.	Medium grain size (50 x 50 - 150 x 150 microns)
Cg.	Coarse grain size (>150 x 150 microns)
Arseno.	Arsenopyrite
Py.	Pyrite
Chalco.	Chalcopyrite
Pyrr.	Pyrrhotite

Each label is set out in the following format; sample location i.e.B9601-24 means Birch borehole B96001 Sample no. 24.(BA,BB,Bd,BE=Birch Pit; B9613=borehole B96013; RA & RC=Ruttan Zone Level 2006; DB=Dick Zone Level 2210; DC=Dick Zone Level 2260; N3=No. 3 Zone; BY= Boundary Zone).

Sulphide size is given by, i.e.; 75x100, and analysis number on each grain is given by i.e.; a1 at end of the label.

Birch Zone Probe Analysis Results

Arsenopyrite Analyses	No	Wt%S	Wt%Ti	Wt%Fe	Wt%Ni	Wt%Cu	Wt%Zn	Wt%As	Total
BA4-mgeu.arseno-c3	54	13.11	0	34.66	0.01	0.02	0.01	54.42	102.24
BA2-fgeu.arseno-a1	10	15.43	0	38.03	0.58	0.04	0.01	48.78	102.88
BA2-cgsubeu.arsenoOG.ingan.pyrite-c3	36	15.44	0	37	0.55	0	0.02	48.66	101.68
ba5-fgan.arseno-a1	58	15.65	0	37.77	0.25	0.01	0.03	48.42	102.14
ba5-fgan.arseno-a3	60	15.61	0	37.49	0.22	0	0.03	48.39	101.74
BA2-fgeu.arseno-a3	12	15.51	0	37.54	0.57	0.04	0.02	48.38	102.06
ba5-fgan.arseno-a2	59	15.52	0.03	37.09	0.22	0.04	0	48.25	101.16
B9601-16-Anhedralarseno-a3	142	16.23	0	37.31	0.04	0.05	0.02	48.02	101.67
BB1-mgsubeuarseno-a1	37	15.92	0	39.13	0.29	0	0	47.63	102.97
B9601-35b-MGAnhedralarseno-c1	10	16.02	0	38.26	0.16	0.02	0	47.59	102.05
BB1-fganarseno-c2	23	15.88	0	37.1	0.41	0.03	0.03	47.57	101.01
BB1-fganarseno-c1	22	16.06	0	37.65	0.32	0	0.05	47.34	101.42
B9601-16-subeuhedralarseno-d3	161	16.58	0	38.95	0.05	0.01	0.04	47.33	102.96
BA2-cgsubeu.arseno-a3	15	16.38	0	36.43	0.23	0.05	0	47.31	100.39
BA2-f-mgsubeu.arseno-b2	26	15.85	0	36.21	0.22	0.04	0.04	47.14	99.51
B9601-25-Euhedralarseno-c1	89	16.36	0	36.76	0.15	0	0.01	47.05	100.34
BA2-cgsubeu.arseno-a1	13	16.21	0.02	35.94	0.15	0	0.03	47.05	99.41
B9601-25-Euhedralarseno-b2	81	16.33	0	38.59	0.14	0.04	0	46.97	102.06
BA2-cgsubeu.arseno-a2	14	16.58	0	38.45	0.11	0	0.02	46.89	102.05
B9601-4bAggregatedeuarsenoovergrownbyanpyritea/b-a7	86	16.65	0	38.01	0.03	0	0	46.83	101.51
BA2-mgeu.arseno-b1	49	16.64	0	39.42	0.07	0	0	46.79	102.92
B9601-16-euhedralarsenoowergrowinganhedralpyrite(m)-e2	184	16.58	0	38.57	0	0	0.04	46.77	101.95
B9601-16-Subeuhedralarseno-c2	150	17.21	0	38.83	0.02	0	0	46.76	102.82
BB1-mgsubeuarseno-a3	39	16.59	0	39.38	0.09	0.02	0.01	46.74	102.84
ba1-fgsubeu.arseno-a2	14	16.71	0	38.46	0.02	0.04	0.06	46.73	102.01
B9601-4bSubeuhedralarsenoass.withanspongypyritea1a3	44	16.7	0	37.28	0.05	0	0.01	46.72	100.77
BB1-mgsubeuarseno-a2	38	16.73	0	39.12	0.1	0.01	0.02	46.71	102.71
BA4-mgan.arseno-a1	4	16.59	0	38.6	0.15	0	0.02	46.7	102.07
B9601-35b-CGSbeuhedralarseno-b2	31	16.69	0.01	38.74	0.07	0.04	0.02	46.65	102.21
BA2-cgsubeu.arsenoOG.ingan.pyrite-c1	34	16.9	0	39.07	0	0	0	46.61	102.59
B9601-16-aggregatedeuarsenoovergrowingan.pyrite(l)-d1	175	16.9	0.03	39.09	0.05	0	0.01	46.58	102.66
BB1-mgsubeuarseno-b2	41	16.7	0	39.39	0.12	0	0.03	46.57	102.82
B9601-16-Anhedralarseno-a1	140	16.91	0	39.38	0.02	0.04	0.04	46.55	102.94

Birch Zone Probe Analysis Results

Arsenopyrite Analyses	No	Wt%S	Wt%Ti	Wt%Fe	Wt%Ni	Wt%Cu	Wt%Zn	Wt%As	Total
B9601-16-Euhedralarsenoass.withTi/Vmineral(a)-b3	133	17	0	38.44	0.01	0	0	46.54	101.99
B9601-16-Euhedralarsenoass.withTi/Vmineral(a)-b1	131	16.98	0	38.4	0.02	0	0.01	46.54	101.95
ba1-mgeu.arseno-c3	42	16.84	0.03	38.6	0.06	0.01	0	46.53	102.07
BA4-fgan.arseno-b3	18	16.83	0	39.11	0.14	0.01	0.01	46.52	102.62
ba1-fgan.arseno-c1	43	17.08	0	38.94	0.07	0.02	0.01	46.5	102.62
B9601-35b-Subeuhedralarseno-a3	6	16.63	0.02	38.47	0.02	0.01	0.01	46.5	101.65
ba1-mgeu.arseno-c1	40	16.66	0	38.84	0.11	0.01	0.02	46.49	102.13
B9601-35b-MGEuhedralarseno-a1	16	16.95	0	38.51	0.03	0	0	46.48	101.97
BA4-mgan.arseno-a2	5	16.59	0	37.17	0.15	0.01	0.02	46.48	100.42
BB1-mgsubeuarseno-b3	42	16.65	0	38.56	0.14	0.04	0.01	46.47	101.87
ba5-mgeu.arseno-c3	86	16.77	0	38.76	0.03	0.04	0.02	46.41	102.04
B9601-35b-MGEuhedralarseno-c1	21	16.73	0.02	37.52	0.06	0	0	46.41	100.74
BA2-f-mgsubeu.arseno-b1	25	16.17	0	36.12	0.1	0	0	46.41	98.81
B9601-25-Euhedralarseno-b3	82	16.61	0	38.95	0.1	0	0	46.4	102.05
BA2-fgeu.arseno-a2	11	16.45	0.03	37.83	0.11	0.05	0.02	46.39	100.88
B9601-16-euhedralarsenoowergrowinganhedralpyrite(m)-e3	185	16.88	0	39.18	0	0	0	46.37	102.43
ba1-cgeu.arsenocleanovergrowth-b6	36	16.8	0	39.09	0.1	0.01	0	46.37	102.37
BB1-mgsubeuarseno-b1	40	16.74	0.01	38.5	0.12	0	0.01	46.35	101.73
B9601-35b-Anhedralarseno-a1	1	17.09	0	39.27	0.03	0	0	46.33	102.72
B9601-16-subeuhedralarseno-b1	119	16.86	0.18	39.03	0.01	0	0.03	46.31	102.43
ba1-fgsubeu.arseno-a1	13	17.04	0	38.15	0.02	0.03	0	46.3	101.55
ba1-cgeu.arsenoincl.richcore-b2	32	17	0	38.96	0.1	0.03	0.01	46.26	102.36
B9601-24-Subeuhedralarsenowithinspongyan.pyrr.-a2	35	17.03	0	39.13	0.03	0	0.02	46.24	102.47
B9601-16-euhedralarsenoowergrowinganhedralpyrite(m)-e1	183	17.33	0	39.26	0	0	0.04	46.21	102.83
ba1-cgsubeu.arseno-c1	25	17.16	0	39.33	0.01	0.03	0	46.2	102.73
ba5-mgeu.arseno-c1	84	16.92	0	39.35	0.03	0.02	0.05	46.2	102.56
B9601-16-aggregatedeuarsenoovergrowingan.pyrite(l)-d3	177	17.31	0	39.39	0.01	0	0.02	46.19	102.92
B9601-16-euhedralarsenoovergrownbyanhedralpyrite(k)-c1	167	17.21	0	39.34	0.02	0.05	0.04	46.16	102.82
B9601-35b-CGSbeuhedralarseno-b1	30	16.86	0	38.98	0.03	0	0.02	46.12	102
BA2-f-mgsubeu.arseno-b3	27	16.6	0	36.06	0.08	0.03	0	46.12	98.89
B9601-35b-Anhedralarseno-b3	9	16.98	0	39.68	0.05	0	0	46.11	102.82
B9601-4bAggregatedeuarsenoovergrownbyanpyritea/b-a2	81	17.08	0	39.37	0.01	0.03	0	46.09	102.59
B9601-35b-CGEuhedralaggregatedarseno-d2	25	16.92	0	37.73	0.02	0.02	0	46.09	100.78

Birch Zone Probe Analysis Results

Arsenopyrite Analyses	No	Wt%S	Wt%Ti	Wt%Fe	Wt%Ni	Wt%Cu	Wt%Zn	Wt%As	Total
B9601-24-Anhedralarsenowithinspongyanhedralpyrite-a3	42	16.8	0	39.14	0	0	0	46.08	102.04
B9601-16-subeuhedralarseno-d1	159	17.56	0	39.34	0	0	0.02	46.07	102.99
B9601-25-Anhedralarsenoinvein-a3	88	17.07	0	39.72	0.05	0	0	46.06	102.9
ba5-mgeu.arseno-c2	85	16.87	0	39.79	0.02	0.06	0	46.06	102.81
BA4-mgsubeu.arseno-a2	8	17.16	0	38.8	0.04	0.04	0.04	46.04	102.11
BB1-fganarseno-c3	24	15.31	0	36.2	0.2	0	0.02	46.03	97.76
B9601-4bEuhedralarsenoisolatedc2	17	17.5	0	39.09	0.02	0	0.01	46.02	102.64
ba5-mgsubeu.arseno-b2	68	16.54	0	39.95	0.06	0.04	0	46.01	102.61
B9601-35b-CGSbeuhedralarseno-b3	32	16.89	0	39.08	0.05	0.02	0	45.99	102.03
B9601-24-Subeuhedralarsenowithinspongyan.pyrr-b3	39	16.99	0	38.14	0.01	0.01	0.02	45.98	101.15
B9601-35b-CGEuhedralaggregatedarseno-d3	26	16.89	0	38.18	0	0.01	0	45.98	101.06
ba1-cgeu.arsenocleanovergrowth-b4	34	17.22	0	39.18	0.05	0.03	0.06	45.97	102.51
B9601-35b-MGAnhedralarseno-c3	12	17.32	0	39.18	0	0	0.06	45.96	102.53
B9601-4bEuhedralarsenoisolatede2	21	17.27	0	37.9	0.03	0	0.02	45.96	101.18
ba1-mgeu.arseno-c2	41	16.41	0	38.4	0.28	0.05	0.04	45.96	101.13
B9601-4bEuhedralarsenoisolateda1	12	17.6	0.01	38.65	0	0	0	45.93	102.18
B9601-24-Anhedral arseno isolated-b2	51	17.03	0	39.96	0.02	0.01	0.02	45.92	102.95
B9601-24-Euhedralarsenoisolated-a3	49	16.82	0	38.58	0.06	0.02	0.04	45.92	101.44
B9601-24-Euhedralarsenoisolated-a2	48	17.03	0	39.09	0.03	0.01	0	45.91	102.07
B9601-25-Subeuhedralarseno-c2	78	17.03	0	39.09	0.02	0.01	0.03	45.91	102.09
B9601-35b-MGEuhedralarseno-c3	23	16.93	0	36.98	0.01	0	0.07	45.89	99.88
ba1-fgsubeu.arseno-a3	15	16.71	0	37.84	0.05	0.04	0.05	45.89	100.59
B9601-4bSubeuhedralarsenoovergrownbyanpyritec-a5	93	17.39	0	39.47	0.01	0.02	0.02	45.88	102.79
ba1-mgan.arseno-a3	30	17.26	0	39.21	0	0	0.03	45.88	102.37
B9601-25-Euhedralarseno-b1	80	17.05	0	38.81	0.03	0.03	0	45.85	101.78
B9601-35b-MGEuhedralarseno-a3	18	17.01	0.08	36.84	0	0.02	0	45.85	99.8
B9601-41a-Fgeuhedralarsenoisolated-d2	35	16.81	0.03	37.98	0.03	0	0	45.85	100.71
BA4-fgan.arseno-b2	17	17.11	0	38.44	0.07	0.02	0.01	45.83	101.48
ba1-fgan.arseno-b3	39	17.22	0.02	38.98	0	0	0.04	45.82	102.09
B9601-35b-CGEuhedralaggregatedarseno-d1	24	16.99	0	36.94	0.04	0.05	0	45.82	99.84
B9601-24-Subeuhedralarsenowithinspongyan.pyrr.-b1	37	17.32	0	39.18	0.01	0.03	0	45.81	102.35
B9601-24-Anhedralarsenowithinspongyanhedralpyrite-a2	41	17	0.01	39.27	0.01	0.01	0	45.81	102.11
BA4-mgsubeu.arseno-c2	23	17.43	0.02	39.62	0.04	0.02	0.04	45.77	102.93

Birch Zone Probe Analysis Results

Arsenopyrite Analyses	No	Wt%S	Wt%Ti	Wt%Fe	Wt%Ni	Wt%Cu	Wt%Zn	Wt%As	Total
BA4-f-mgsubeu.arseno-b2	14	17.3	0.02	39.34	0.02	0.02	0.05	45.77	102.51
B9601-25-Subeuhedralarseno-a1	71	17.16	0	39.17	0.01	0	0.01	45.76	102.12
BA4-fgeu.arseno-b2	20	17.46	0	39.65	0.04	0.02	0	45.75	102.92
BA2-fgan.arseno-a3	18	16.1	0.04	35.8	0.13	0.04	0.02	45.75	97.89
B9601-24-Anhedral arseno isolated-b3	52	17.33	0	39.76	0.03	0.03	0.06	45.74	102.95
ba1-fgeu.arseno-a3	3	17.18	0	39.29	0.01	0.02	0.02	45.74	102.26
BA4-mgeu.arseno-c1	52	17.24	0.01	38.24	0.02	0.01	0.02	45.73	101.27
B9601-35b-Anhedralarseno-b2	8	17.15	0.01	37.86	0.05	0	0.03	45.73	100.84
ba1-fgan.arseno-c2	44	17.22	0	38.99	0.05	0	0.02	45.72	102.01
BA4-fgeu.arseno-b3	21	17.4	0	39.36	0.03	0	0	45.71	102.5
B9601-24-Anhedralarsenoisolated-c2	54	16.99	0	38.45	0.02	0.01	0.01	45.7	101.18
B9601-35b-MGAnhedralarseno-c2	11	17.47	0	39.72	0.04	0.01	0.03	45.68	102.96
B9601-41a-Euhedralarseno-b1	7	17.22	0	39.78	0.04	0.01	0	45.68	102.73
B9601-41a-Fgeuhedralarsenoisolated-d1	34	17.09	0.03	38.85	0.03	0.01	0	45.67	101.68
ba1-mgan.arseno-a1	28	17.67	0	39.14	0.01	0.01	0	45.66	102.5
BA4-mgeu.arseno-c2	53	17.24	0	38.56	0.04	0	0.05	45.65	101.54
B9601-25-Subeuhedralarseno-a2	72	17.12	0	39.41	0	0	0	45.65	102.19
B9601-4bSubeuhedralarsenoovergrownbyanpyritec-a4	92	17.27	0	38	0	0.01	0.04	45.62	100.95
B9601-35b-CgAnhedralarseno-d2	37	17.22	0	38.43	0.07	0	0.01	45.61	101.35
B9601-35b-Subeuhedralarseno-a2	5	17.16	0	38.71	0.01	0.04	0	45.6	101.53
ba1-fgan.arseno-b2	38	17.02	0	39.65	0.04	0.02	0.02	45.58	102.34
B9601-25-Subeuhedralarseno-a3	73	17.54	0	39.32	0.03	0.02	0	45.57	102.48
B9601-35b-FGEuhedralarseno-b2	20	16.89	0	37.06	0.06	0.05	0	45.56	99.63
B9601-24-Anhedral arseno isolated-b1	50	17.56	0	39.57	0	0.03	0	45.55	102.71
BA4-mgsubeu.arseno-a3	9	17.29	0.01	36.95	0.03	0.03	0	45.53	99.84
B9601-24-Anhedral arseno isolated-c1	53	17.29	0	38.42	0.03	0	0.01	45.52	101.28
ba1-fgeu.arseno-a1	1	17.06	0	38.79	0.03	0	0.01	45.5	101.41
B9601-25-Subeuhedralarseno-c1	77	17.34	0	38.79	0.02	0.01	0	45.45	101.62
ba1-cgeu.arsenoincl.richcore-b3	33	16.55	0	39.86	0.02	0.04	0	45.45	101.93
B9601-35b-MGEuhedralarseno-c2	22	17.23	0	36.99	0.03	0.01	0	45.44	99.7
B9601-4bAnhedralarsenoass.withpyritec4a1	10	17.47	0	39.58	0.02	0.03	0	45.43	102.54
BA2-mgeu.arseno-b2	50	16.18	0.06	38.44	0.12	0.01	0	45.41	100.23
B9601-4bSubeuhedralarsenoovergrownbyanpyritec-a2	90	17.7	0	39.27	0.03	0	0.03	45.4	102.43

Birch Zone Probe Analysis Results

Arsenopyrite Analyses	No	Wt%S	Wt%Ti	Wt%Fe	Wt%Ni	Wt%Cu	Wt%Zn	Wt%As	Total
ba1-fgeu.arseno-a2	2	17.37	0	38.91	0.05	0.03	0	45.38	101.74
BA4-f-mgsubeu.arseno-b3	15	17.42	0	39.14	0.03	0	0.02	45.37	101.98
ba1-fgan.arseno-b1	37	16.88	0	39.6	0.08	0.01	0.03	45.37	101.98
B9601-4bSubeuhedralarsenoisolateda2	25	17.67	0.02	39.57	0.02	0	0.06	45.34	102.67
B9601-4bEuhedralarsenoisolatedj2	40	17.7	0	39.66	0.04	0	0	45.32	102.73
B9601-41a-Largeeuhedralarseno-c2	20	16.38	0	40.23	0.03	0.01	0.01	45.31	101.98
B9601-24-Anhedralarsenoisolated-c3	55	17.29	0.04	39.03	0.05	0	0	45.27	101.68
BA4-mgeu.arseno-a3	3	17.26	0	36.5	0.04	0.04	0	45.27	99.11
B9601-4bSubeuhedralarsenoovergrownbyanpyritec-a3	91	17.06	0.18	38.65	0.02	0.02	0	45.23	101.17
B9601-24-Euhedralarsenoisolated-a1	47	17.28	0	38.08	0.01	0.04	0	45.21	100.61
B9601-4bEuhedralarsenoisolatedb2	15	17.38	0	38.47	0.01	0	0	45.17	101.04
B9601-4bAggregatedeuarsenoovergrownbyanpyritea/b-a6	85	17.7	0	39.91	0	0.02	0.01	45.1	102.75
BA4-fgeu.arseno-b1	19	15.63	0	37.48	0.13	0.02	0	44.78	98.04
B9601-4bEuhedralarsenoisolatedi2	37	17.95	0	39.05	0.01	0	0	44.76	101.77
B9601-25-Anhedralarsenoinvein-a2	87	17.28	0	37.87	0.02	0.01	0.03	44.48	99.7
BA4-f-mgsubeu.arseno-b1	13	17.34	0	38.01	0.01	0.02	0	43.52	98.89
Pyrite Analyses	**No**	**Wt%S**	**Wt%Ti**	**Wt%Fe**	**Wt%Ni**	**Wt%Cu**	**Wt%Zn**	**Wt%As**	**Total**
BA4-mgsubeu.pyrite-a3	27	46.89	0	51.07	0.03	0	0.02	0.51	98.53
BA4-fgeu.pyrite-b2	42	46.88	0	52.29	0.02	0.04	0.02	0.1	99.35
BA4-fgeu.pyrite-b1	41	46.76	0	51.23	0.03	0.04	0.01	0	98.07
ba5-fgeu.pyrite-b1	101	46.74	0	53.69	0.27	0.03	0.03	0.14	100.9
B9601-4banhedralspongypyrited2	66	46.74	0	54.58	0.02	0	0.05	0.04	101.43
BA6A-mgan.pyrite-d2	96	46.72	0.01	52.84	0.06	0.03	0	0.03	99.68
BA3-mgsubeu.pyrite-b1	82	46.71	0.01	54.23	0.04	0	0	0	100.99
BB1-mgspongyanpyrite-a3	3	46.7	0	53.52	0.18	0.15	0.02	0.06	100.64
BA3-mgan.pyrite-a2	62	46.68	0	54.03	0.03	0.01	0.03	0.01	100.79
ba5-fgeu.pyrite-b3	103	46.63	0	54.5	0.03	0.03	0.02	0.07	101.27
BA3-mgeu.pyrite-a2	59	46.63	0	53.03	0.03	0	0	0.03	99.72
BA2-mgan.pyrite-b3	45	46.63	0.06	52.68	0.02	0.01	0	0.02	99.43
B9601-4banhedralspongypyrited3	67	46.62	0	55.15	0	0	0	0.01	101.79
ba5-mgean.pyrite-c1	87	46.61	0	54.03	0	0.03	0.07	0.2	100.93
B9601-4banhedralspongypyriteb1	59	46.61	0	55.74	0.03	0	0	0	102.38
B9601-41a-Spongyanhedralpyrite-a3	3	46.58	0.04	53	0.23	0	0.03	0.06	99.94

Birch Zone Probe Analysis Results

Pyrite Analyses	No	Wt%S	Wt%Ti	Wt%Fe	Wt%Ni	Wt%Cu	Wt%Zn	Wt%As	Total
BA4-fgeu.pyrite-a1	38	46.58	0	51.42	0.08	0	0.03	0	98.12
ba5-mgean.pyrite-d3	92	46.56	0	54.12	0.38	0.02	0.06	0.11	101.24
BA4-fgan.pyrite-b2	29	46.56	0	52.04	0	0.01	0	0.09	98.7
BA6A-mgan.pyrite-c1	81	46.56	0	52.13	0.02	0.05	0	0	98.77
B9601-41a-Mgspongypy.ass.withLargeeuarseno(a,b,c)-c1	22	46.55	0	54.12	0.03	0	0.02	0	100.73
BA6A-mgan.pyrite-d1	95	46.54	0	52.34	0.8	0.04	0.04	0	99.77
ba5-mgean.pyrite-c2	88	46.53	0	53.41	0.01	0	0	0.17	100.12
BA6A-subeu.pyrite-b1	60	46.53	0	53.16	0.09	0.02	0.02	0.02	99.84
BA6A-mgan.pyrite-b3	80	46.51	0	53.82	0	0	0	0	100.34
BA3-mgsubeu.pyrite-b3	84	46.49	0	54.39	0.15	0	0.01	0.04	101.08
BB1-mganpyrite-b3	27	46.49	0	53.74	0.58	0	0.04	0	100.86
B9601-24-Spongyanhedralpyrite-b2	32	46.49	0	54.13	0.02	0	0.02	0	100.67
ba5-fgfgeu.pyrite-a3	100	46.48	0	53.78	0.01	0.05	0.01	0.08	100.41
BB4-f-mganpyrite-a3	60	46.47	0.01	55.08	0.28	0.06	0.06	0.03	101.97
BB1-cganpyrite-d2	32	46.46	0	52.29	0.25	0.04	0	0.06	99.1
BA4-fgan.pyrite-b3	30	46.46	0	52.58	0.02	0.19	0	0	99.26
BA3-mgeu.pyrite-a1	58	46.44	0.01	53.67	0.07	0	0.02	0.15	100.35
BA6A-mgan.pyrite-a2	76	46.44	0	53.4	0	0.06	0	0.02	99.92
BA6A-subeu.pyrite-b2	61	46.44	0	53.25	0.01	0.04	0.03	0	99.78
BA6A-cgsubeu.pyrite-c3	74	46.43	0	53.21	0.03	0	0	0	99.68
BB4-f-mgsubeupyrite-a1	67	46.42	0	54.29	0.03	0.03	0	0.03	100.8
BA6A-fgeu.pyrite-b2	70	46.42	0	53.34	0.04	0.02	0	0.02	99.83
B9601-41a-CgaggregatedEuhedralpy.-a2	40	46.42	0	53.6	0.12	0	0.02	0.01	100.16
B9601-24-Anhedralpyriteinvein-e2	20	46.42	0	53.57	0.06	0	0.02	0	100.08
B9601-24-Euhedralpyrite-c3	24	46.42	0	54.81	0.21	0.03	0.01	0	101.47
B9601-41a-Cgspongypy.enclosingan.arseno(d)-e1	31	46.42	0	53.56	0.02	0.01	0.01	0	100.02
BA3-mgeu.pyrite-a3	60	46.41	0	52.71	0.01	0.03	0	0.07	99.24
BB4-f-mganpyrite-a1	58	46.41	0	54.74	0.21	0.1	0	0.03	101.5
B9601-41a-CgaggregatedEuhedralpy-a1	39	46.41	0	53.44	0.11	0.01	0.03	0.01	100.02
BB4-f-mganpyrite-b1	61	46.41	0	53.52	1.16	0	0.02	0	101.12
B9601-41a-Mgspongypy.ass.withLargeeuarseno(a,b,c)-c3	24	46.4	0	53.28	0.47	0	0	0.03	100.18
B9601-41a-Spongyanhedralpyrite-a2	2	46.4	0	53.63	0.01	0	0.03	0.02	100.1
BB1-cganpyrite-c1	28	46.39	0	54.01	0.16	0	0	0.03	100.58

Birch Zone Probe Analysis Results

Pyrite Analyses	No	Wt%S	Wt%Ti	Wt%Fe	Wt%Ni	Wt%Cu	Wt%Zn	Wt%As	Total
BB1-mganpyrite-a3	6	46.39	0	54.24	0.09	0.03	0	0.02	100.77
BB1-mganpyrite-a2	5	46.39	0	55.17	0.04	0	0	0	101.61
B9601-24-Anhedralpyriteinvein-d3	18	46.38	0	52.62	0.18	0.03	0.02	0	99.23
BA2-mgan.pyrite-b2	44	46.37	0	52.13	0	0.06	0.03	0.01	98.6
BA6A-mgeu.pyrite-a2	99	46.37	0	52.9	0.07	0	0.01	0	99.35
BA6A-subeu.pyrite-b3	62	46.37	0.03	53.74	0	0.04	0	0	100.17
B9601-4banhedralspongypyritec2	63	46.37	0	53.68	0.01	0.02	0	0	100.09
B9601-35b-CgAnhedralpyrite-c1	33	46.36	0	51.32	0.08	0	0.03	0.01	97.81
B9601-35b-CgAnhedralpyrite-c2	34	46.36	0	52.31	0.05	0	0	0	98.73
BA4-cgsubeu.pyrite-b1	34	46.34	0	51.66	0.03	0.02	0	0	98.06
B9601-4banhedralspongypyritec1	62	46.34	0.01	53.29	0.01	0	0	0	99.67
BA6A-mgan.pyrite-c3	83	46.33	0	51.67	0.02	0	0.04	0.04	98.12
BA2-mgan.pyrite-b1	43	46.33	0	52.79	0	0.07	0	0.03	99.23
BB4-f-mgsubeupyrite-b2	71	46.33	0	53.8	0	0	0.07	0.01	100.21
B9601-24-Euhedralpyrite-c2	23	46.33	0.02	53.32	0.09	0.08	0.02	0.01	99.88
B9601-24-Anhedralpyrite-a2	2	46.33	0	53.18	0.02	0	0	0	99.54
B9601-4banhedralspongypyritec3	64	46.33	0	54.53	0.02	0.06	0	0	100.94
BA3-cgan.pyrite-c2	74	46.32	0	54.49	0	0	0	0.21	101.02
ba5-mgean.pyrite-c3	89	46.32	0	54.83	0	0.05	0.04	0.13	101.37
BB4-f-mganspongypyrite-b2	56	46.32	0.12	53.6	0.03	0	0	0.1	100.17
BA6A-mgan.pyrite-b2	79	46.32	0	53.42	0	0	0	0.01	99.76
B9601-24-Anhedralpyrite-c3	15	46.32	0	51.48	0.01	0.01	0	0.01	97.83
BA3-mgan.pyrite-a1	61	46.32	0	52.16	0.11	0	0.02	0	98.61
BB4-f-mganpyrite-b2	62	46.32	0	54.46	0.07	0.04	0	0	100.9
BA6A-cgsubeu.pyrite-c2	73	46.31	0	52.94	0	0.03	0	0.03	99.31
BB1-cganpyrite-d3	33	46.31	0	54.65	0.63	0.05	0.02	0.01	101.68
B9601-35b-MGAnhedralpyrite.-b1	27	46.31	0	51.49	0.03	0	0.06	0.01	97.9
B9601-41a-Mgspongypy.ass.withLargeeuarseno(a,b,c)-c2	23	46.3	0	53.63	0.01	0.01	0.03	0.02	100
BA4-fgeu.pyrite-a3	40	46.3	0	51.59	0.09	0.04	0.06	0	98.08
BB1-cganpyrite-c2	29	46.3	0	54.32	0.67	0.02	0	0	101.3
BA6A-mgeu.pyrite-a3	100	46.29	0	51.67	0	0.06	0.02	0	98.06
BB1-mganpyrite-a1	4	46.28	0	52.76	0.36	0.03	0.05	0.06	99.55
BA6A-cgsubeu.pyrite-c1	72	46.28	0	53.27	0.04	0	0.01	0	99.61

Birch Zone Probe Analysis Results

Pyrite Analyses	No	Wt%S	Wt%Ti	Wt%Fe	Wt%Ni	Wt%Cu	Wt%Zn	Wt%As	Total
B9601-24-Anhedralpyrite-c2	14	46.28	0	51.6	0.05	0.04	0.07	0	98.03
B9601-41a-CgaggregatedEuhedralpy.-a3	41	46.28	0	53.04	0.06	0.04	0	0	99.42
BB4-f-mgsubeupyrite-b1	70	46.27	0	54.16	0	0.02	0	0.03	100.49
BB4-f-mgeupyrite-a1	91	46.27	0	53.17	0.37	0.09	0.02	0	99.93
B9601-24-Anhedralpyrite-h3	58	46.27	0	52.09	0.04	0	0.05	0	98.46
B9601-24-Euhedralpyrite-c1	22	46.27	0	54.19	0.11	0.03	0.04	0	100.65
B9601-41a-Spongyanhedralpyrite-b1	10	46.26	0	53.24	0.06	0.03	0	0.21	99.8
BA6A-fgeu.pyrite-d1	92	46.26	0	51.77	0.05	0	0.04	0.02	98.14
B9601-41a-CgaggregatedEuhedralpy-b1	42	46.26	0	53.35	0.02	0.01	0.04	0.01	99.68
B9601-41a-CgaggregatedEuhedralpy.-b2	43	46.26	0	53.86	0.04	0.02	0	0.01	100.2
BA4-cgsubeu.pyrite-b2	35	46.26	0	52.49	0.08	0	0.07	0	98.91
BA4-mgan.pyrite-c2	32	46.26	0	52.47	0.06	0.05	0	0	98.84
B9601-41a-Fganhedralpyriteisolated-e3	38	46.26	0.01	53.44	0.03	0.03	0.03	0	99.79
BA3-mgan.pyrite-a3	63	46.25	0	52.67	0.15	0.07	0.01	0.03	99.19
BA6A-mgeu.pyrite-b3	103	46.25	0	52.72	0.03	0.01	0.03	0.02	99.06
B9601-24-Euhedralpyrite-b1	10	46.25	0	53.05	0.28	0	0.03	0.01	99.62
BA2-mgsubeu.pyrite-a2	5	46.25	0	53.77	0.03	0	0.02	0	100.07
BA6A-mgan.pyrite-a3	77	46.25	0	53.22	0.01	0	0	0	99.49
B9601-24-Anhedralpyrite-b2	5	46.25	0.01	52.14	0.29	0.02	0.04	0	98.76
B9601-24-Spongyanhedralpyrite-a2	26	46.25	0	54.18	0.45	0	0	0	100.89
BA6A-subeu.pyrite-a1	57	46.24	0	52.82	0.11	0	0	0.04	99.2
BA4-mgan.pyrite-c3	33	46.24	0	52.53	0.01	0.02	0.04	0.02	98.86
ba5-mgean.pyrite-d1	90	46.24	0	53.59	0.04	0.03	0	0	99.89
B9601-41a-Fganhedralpyriteisolated-e1	36	46.24	0.04	53.09	0.01	0.05	0.05	0	99.47
BB4-f-mganpyrite-c1	76	46.23	0	53.27	0.04	0.02	0	0.03	99.6
ba1-fgsubeu.pyrite-b1	22	46.21	0	53.37	0.01	0.02	0	0.33	99.94
ba5-mgean.pyrite-d2	91	46.21	0	54.92	0.1	0.06	0	0.03	101.33
BB1-mganpyrite-b2	26	46.21	0	53.31	0.4	0	0.01	0.02	99.96
BB4-cganpyrite-e3	84	46.21	0	54.02	0.56	0.47	0	0.01	101.27
B9601-41a-CgaggregatedEuhedralpy.-b3	44	46.21	0.02	53.69	0.05	0	0	0.01	99.99
BA6A-subeu.pyrite-a3	59	46.21	0	52.26	0.02	0	0	0	98.5
B9601-24-Spongypy.surroundingsubeu.arseno(a,b)-c4	46	46.21	0.01	51.89	0.03	0.05	0.04	0	98.25
B9601-41a-Spongyanhedralpyrite-b3	12	46.21	0	53.65	0.01	0	0.05	0	99.92

Birch Zone Probe Analysis Results

Pyrite Analyses	No	Wt%S	Wt%Ti	Wt%Fe	Wt%Ni	Wt%Cu	Wt%Zn	Wt%As	Total
BB1-mgspongyanpyrite-a2	2	46.2	0	52.25	0.17	0.08	0.06	0.11	98.87
B9601-24-Euhedralpyrite-a2	8	46.2	0	53.06	0.28	0.02	0	0	99.57
BB1-mganpyrite-b1	25	46.19	0	53.96	0.04	0.04	0	0.06	100.3
BB4-cganpyrite-e1	82	46.19	0	54.26	0.03	0	0	0.01	100.48
BA4-mgsubeu.pyrite-a1	25	46.18	0	51.9	0	0.05	0.05	0.45	98.63
BB4-f-mgsubeupyrite-a3	69	46.18	0.01	54.87	0.08	0	0.03	0.15	101.32
BA2-mgsubeu.pyrite-a1	4	46.18	0.01	53.47	0.04	0.01	0	0	99.71
BA3-mgsubeu.pyrite-b2	83	46.18	0.01	53.46	0.06	0.01	0	0	99.73
BA6A-mgeu.pyrite-c3	86	46.18	0	52.27	0	0	0	0	98.47
BB1-mgspongyanpyrite-a1	1	46.17	0	54.83	0.18	0.21	0	0.04	101.41
BA4-cgsubeu.pyrite-b3	36	46.17	0	52.45	0.07	0	0	0	98.69
BA6A-mgeu.pyrite-c2	85	46.17	0	51.68	0	0	0.04	0	97.89
B9601-24-Spongypy.surroundingsubeu.arseno(a,b)-c1	43	46.16	0	52.86	0.2	0	0	0.02	99.24
BA6A-fgeu.pyrite-d2	93	46.16	0	52.13	0	0.01	0	0.01	98.31
B9601-24-Spongyanhedralpyrite-b3	33	46.16	0	53.32	0.02	0	0.01	0	99.51
BA6A-mgan.pyrite-a1	75	46.15	0.01	52.67	0	0.01	0	0.03	98.87
BA4-mgsubeu.pyrite-a2	26	46.14	0	52.87	0.07	0	0	0.12	99.21
BA6A-mgeu.pyrite-c1	84	46.13	0.04	52.71	0.05	0.04	0.03	0.02	99.02
ba5-mgan.pyrite-a1	52	46.13	0.04	52.24	0.13	0.04	0	0	98.58
BA6A-mgan.pyrite-c2	82	46.13	0	53.7	0.04	0	0.06	0	99.94
B9601-24-Spongyanhedralpyrite-b1	31	46.13	0	54.03	0.02	0.06	0	0	100.25
B9601-25-Anhedralpyrite-c2	75	46.12	0	53.26	0.25	0	0.03	0.01	99.68
BB1-cganpyrite-c3	30	46.11	0.01	53.3	0.24	0.8	0	0.09	100.54
B9601-41a-Spongyanhedralpyrite-b2	11	46.11	0	53.58	0.01	0	0.02	0.02	99.73
BB4-f-mgeupyrite-b1	94	46.11	0	53.54	0.09	0.07	0.03	0	99.84
B9601-24-Anhedralpyriteinvein-e3	21	46.11	0.01	52.27	0.05	0	0.01	0	98.45
BA3-fgsubeu.pyrite-a1	70	46.1	0.01	53.13	0.02	0.06	0	0.03	99.36
B9601-25-Anhedralpyrite-c1	74	46.1	0	52.93	0.39	0	0.02	0	99.45
B9601-41a-Cgspongypy.enclosingan.arseno(d)-e3	33	46.09	0	52.85	0.04	0	0	0.03	99.01
BA2-cgan.pyriteOG.byeu.arseno-e1	31	46.09	0	52.73	0.08	0	0.06	0.01	98.97
BB4-f-mgeupyrite-a3	93	46.09	0.01	53.49	0.74	0.17	0.02	0.01	100.53
B9601-24-Spongypy.surroundingsubeu.arseno(a,b)-c2	44	46.09	0	52.15	0.15	0.03	0	0.01	98.43
BA6A-mgan.pyrite-d3	97	46.08	0	52.89	0.05	0	0.06	0.16	99.24

Birch Zone Probe Analysis Results

Pyrite Analyses	No	Wt%S	Wt%Ti	Wt%Fe	Wt%Ni	Wt%Cu	Wt%Zn	Wt%As	Total
BB4-f-mgeupyrite-b3	96	46.08	0	53.91	0.06	0.08	0.03	0.02	100.17
ba5-mgan.pyrite-a3	54	46.07	0.02	52.98	0.07	0.05	0	0.05	99.25
BB1-mganpyrite-a1	10	46.07	0	53.67	0.75	0.03	0.04	0.04	100.61
B9601-24-Anhedralpyrite-a1	1	46.07	0	51.24	0.15	0.03	0	0	97.49
BA2-fgan.pyrite-b2	8	46.05	0	53.43	0	0.03	0	0.02	99.54
B9601-24-Anhedralpyrite-b3	6	46.05	0	53.1	0.29	0	0	0	99.44
B9601-24-Spongypy.surroundingsubeu.arseno(a,b)-c3	45	46.02	0	53.06	0.07	0.04	0.01	0	99.21
B9601-25-Anhedralpy.nexttoeuhedralarseno(a)-b1	68	46.02	0	53.41	0.28	0	0	0	99.71
B9601-41a-Cgspongypy.enclosingan.arseno(d)-e2	32	46.01	0	53.8	0.03	0.05	0.02	0.12	100.03
B9601-24-Anhedralpyrite-a3	3	46.01	0	53.53	0.06	0.03	0.01	0	99.65
BA3-mgeu.pyrite-c2	77	45.99	0	51.46	1.57	0.01	0	0.04	99.07
BA2-cgan.pyriteOG.byeu.arseno-e2	32	45.98	0	52.53	0.01	0.02	0	0.16	98.71
BA4-mgan.pyrite-d3	46	45.98	0	51.99	0	0.01	0.01	0.04	98.03
BA3-cgan.pyrite-c1	73	45.97	0	53.04	0.1	0	0	0.73	99.84
BA4-f-mgan.pyrite-a2	11	45.97	0.04	51.73	0	0.01	0.03	0.67	98.44
BA4-mgan.pyrite-d2	45	45.97	0	51.84	0.04	0.01	0.05	0.21	98.13
B9601-35b-M-FGAnhedralpy.-a2	14	45.97	0.01	51.45	0.04	0.13	0	0.05	97.65
BB4-f-mgeupyrite-b2	95	45.97	0.02	54.33	0.06	0.07	0.07	0.02	100.54
BA2-mgsubeu.pyrite-a3	6	45.97	0	52.95	0.03	0	0	0.01	98.96
BA3-cgan.pyrite-c3	75	45.96	0.01	53.31	0	0.07	0	0.51	99.85
BB1-mganpyrite-b2	8	45.96	0	52.97	0.28	0	0.02	0	99.23
BB4-f-mganpyrite-a2	59	45.96	0	55.24	0.09	0.11	0	0	101.39
B9601-24-Anhedralpyrite-b1	4	45.96	0	53.62	0.07	0.04	0.03	0	99.73
BA2-cgan.pyriteOG.byeu.arseno-e3	33	45.95	0	53.06	0.01	0	0	0.05	99.08
B9601-35b-CgAnhedralpyrite-c3	35	45.94	0	50.65	0.04	0.01	0	0.8	97.44
BB1-cganpyrite-d1	31	45.94	0	55.63	0.14	0	0.02	0.02	101.75
BA6A-mgeu.pyrite-b2	102	45.94	0	52.35	0	0	0.01	0.01	98.31
B9601-41a-Cgspongypy.ass.withLargeeuarseno(a,b,c)-d3	27	45.93	0.03	53.71	0	0.04	0	0.26	99.98
B9601-4banhedralspongypyriteb2	60	45.92	0	52.9	0.02	0.03	0.01	0.02	98.91
BB1-mganpyrite-b3	9	45.91	0	54.56	0.28	0.02	0.04	0.02	100.83
BA4-cgsubeu.pyrite-b4	37	45.91	0	51.89	0	0.01	0	0	97.82
BB4-cganpyrite-e2	83	45.9	0	55.55	0	0.01	0.08	0	101.55
B9601-24-Euhedralpyrite-b3	12	45.9	0	52.21	0.37	0	0.03	0	98.5

Birch Zone Probe Analysis Results

Pyrite Analyses	No	Wt%S	Wt%Ti	Wt%Fe	Wt%Ni	Wt%Cu	Wt%Zn	Wt%As	Total
BA6A-fgeu.pyrite-d3	94	45.89	0	51.67	0.02	0.01	0.02	0.03	97.64
ba1-fgsubeu.pyrite-b3	24	45.89	0.02	53.05	0.54	0	0	0.02	99.53
B9601-25-Anhedralpy.invein-d3	85	45.89	0	51.12	1.19	0.01	0.02	0.02	98.25
BA3-mgeu.pyrite-c3	78	45.88	0	53.77	0.24	0.01	0.05	0.02	99.97
BA2-fgan.pyrite-b3	9	45.88	0	51.76	0.22	0	0	0	97.87
B9601-24-Euhedralpyrite-b2	11	45.88	0.02	51.34	0.37	0.01	0.03	0	97.65
BA6A-mgeu.pyrite-b1	101	45.87	0	53	0.02	0.04	0	0.02	98.95
BB4-f-mganspongypyrite-b3	57	45.87	0	54.85	0	0	0	0.01	100.73
ba5-mgan.pyrite-a2	53	45.87	0	53.12	0.23	0.04	0.03	0	99.29
BB4-f-mganspongypyrite-a2	53	45.86	0	54.02	0.01	0.01	0.03	0.07	100
BA3-fgsubeu.pyrite-a3	72	45.86	0	53.75	0.03	0.06	0	0	99.71
B9601-24-Spongyanhedralpyrite-a1	25	45.86	0	52.33	0.15	0	0.03	0	98.38
BB4-f-mganpyrite-c3	78	45.85	0	53.14	0	0	0.05	0.03	99.07
BA3-fgeu.spongypyrite-b2	65	45.85	0	52.25	0.55	0	0.06	0.02	98.72
BA6A-fgeu.pyrite-b3	71	45.85	0	52.7	0.02	0	0.04	0	98.6
B9601-41a-Spongyanhedralpyrite-a1	1	45.83	0	53.9	0.02	0.01	0	0.04	99.8
B9601-4banhedralspongypyritee3	70	45.83	0	52.9	0	0.01	0	0	98.74
B9601-41a-Cgspongypy.ass.withLargeeuarseno(a,b,c)-d2	26	45.82	0	53.57	0.03	0.02	0.01	0	99.45
B9601-25-Anhedralpy.invein-d1	83	45.81	0	52.23	1.26	0	0	0	99.31
BB4-f-mganspongypyrite-a1	52	45.8	0	54.1	0.02	0.01	0.03	0.04	99.99
BA3-cgan.spongypyrite-b1	99	45.79	0	53.91	0.84	0.04	0.05	0.02	100.64
BA3-fgeu.spongypyrite-b3	66	45.79	0	52.1	0.31	0.03	0	0.02	98.26
BB1-mganpyrite-a2	11	45.79	0.02	54.68	0.54	0	0	0.01	101.05
B9601-24-Anhedralpyriteinvein-e1	19	45.78	0	52.61	0.2	0.02	0	0	98.63
B9601-25-Anhedralpy.nexttoeuhedralarseno(a)-b3	70	45.76	0	54.26	0.2	0.03	0	0.05	100.3
B9601-25-Anhedralpy.nexttoeuhedralarseno(a)-b2	69	45.7	0	54.88	0.13	0	0	0.02	100.74
BA2-fgan.pyrite-b1	7	45.7	0.02	52.18	0.06	0.01	0	0	97.97
BA3-m-cgan.spongypyrite-a1	85	45.69	0	53.82	0.15	0.08	0	0.1	99.84
BB4-f-mganpyrite-b3	63	45.68	0	54.37	0.31	0.06	0.05	0	100.48
B9601-24-Anhedralpyrite-h1	56	45.66	0	52.1	0.13	0.05	0	0	97.93
B9601-25-Anhedralpyrite-c3	76	45.65	0	53.1	0.65	0	0	0	99.4
ba1-fgsubeu.pyrite-a1	4	45.62	0	52.08	0.04	0.04	0	0.32	98.11
BA3-cgan.spongypyrite-b3	101	45.61	0.01	55	0.25	0.04	0.03	0.07	101.02

Birch Zone Probe Analysis Results

Pyrite Analyses	No	Wt%S	Wt%Ti	Wt%Fe	Wt%Ni	Wt%Cu	Wt%Zn	Wt%As	Total
ba5-mgan.spongypyrite-b3	57	45.61	0	52.48	0.25	0.12	0	0.04	98.5
BB4-f-mganpyrite-d2	80	45.6	0	53.51	0	0	0.03	1.02	100.16
BA3-m-cgan.spongypyrite-a2	86	45.58	0	53.95	0.24	0.06	0.02	0.02	99.87
ba1-fgsubeu.pyrite-a3	6	45.53	0.02	52.33	0.34	0.02	0.02	0.56	98.82
BB4-f-mgeupyrite-a2	92	45.5	0.02	52.62	0.33	1.54	0	0	100
BB4-f-mganpyrite-d3	81	45.46	0	53.8	0.13	0.06	0.02	0.91	100.38
ba5-fgeu.pyrite-b2	102	45.46	0.01	51.38	0.05	0.04	0	0.06	97
BA3-mgeu.pyrite-c1	76	45.46	0	52.6	1.54	0.04	0	0.01	99.65
BA3-fgeu.spongypyrite-b1	64	45.44	0.03	52.77	0.65	0	0.03	0.1	99
BA3-m-cgan.spongypyrite-a3	87	45.37	0.04	53.92	0.16	0.01	0.05	0.07	99.61
BA3-cgan.spongypyrite-b2	100	45.25	0	53.86	0.26	0.07	0.05	0.11	99.6
BB4-f-mganspongypyrite-a3	54	45.18	0	53.42	0.05	0	0	0	98.67
BA2-fgan.pyrite-c2	53	45.17	0	52.73	0.32	0.17	0	0.44	98.82
B9613-01-50x40subeupyrite	60	45.11	0.00	53.79	0.03	0.05	0.00	0.00	99.00
B9613-01-50x40subeupyrite	59	45.10	0.00	54.21	0.00	0.01	0.00	0.00	99.33
B9613-01-400x300aggregatedgrainof10-100subeupyrite	46	45.06	0.00	54.90	0.05	0.00	0.02	0.00	100.04
B9613-01-400x300aggregatedgrainof10-100subeupyrite	47	44.96	0.00	54.27	0.10	0.03	0.03	0.00	99.40
BA6A-fgeu.pyrite-a1	66	44.89	0.00	52.05	0.08	0.02	0.03	0.04	97.11
B9613-01-50x40subeupyrite	58	44.82	0.00	54.12	0.04	0.01	0.00	0.00	99.00
B9601-25-Anhedralpy.invein-d2	84	44.80	0.00	51.46	1.06	0.01	0.02	0.00	97.35
BB4-f-mgsubeupyrite-a2	68	44.77	0.02	54.46	0.04	0.00	0.00	0.00	99.30
B9613-01-100x200anpyrite	64	44.52	0.00	54.49	0.06	0.04	0.04	0.02	99.17
B9613-01-400x300aggregatedgrainof10-100subeupyrite	48	44.41	0.00	53.51	0.12	0.01	0.00	0.00	98.05
ba1-fgsubeu.pyrite-b2	23	44.40	0.00	51.46	0.63	0.00	0.00	0.75	97.24
BA2-fgan.pyrite-c1	52	44.37	0.00	51.70	0.35	0.19	0.00	0.94	97.55
B9601-41a-Cgspongypy.ass.withLargeeuarseno(a,b,c)-d1	25	44.33	0.02	55.86	0.01	0.02	0.02	0.03	100.29
BA3-fgsubeu.pyrite-a2	71	44.31	0.00	52.10	0.78	0.08	0.03	0.05	97.35
B9613-01-100x200anpyrite	66	44.28	0.00	54.37	0.15	0.08	0.00	0.11	98.99
BB4-f-mganpyrite-d1	79	44.11	0.00	52.87	0.00	0.00	0.02	0.96	97.96
B9613-01-100x200anpyrite	65	44.11	0.00	53.87	0.14	0.03	0.00	0.22	98.37
BB4-f-mganpyrite-c2	77	43.91	0.00	54.31	0.00	0.03	0.00	0.19	98.44
B9601-4banhedralspongypyritee1	68	43.82	0.01	53.97	0.00	0.00	0.01	0.00	97.82
BA4-fgeu.pyrite-a2	39	43.80	0.00	49.66	0.04	4.00	1.48	0.00	98.99

Birch Zone Probe Analysis Results

Pyrite Analyses	**No**	**Wt%S**	**Wt%Ti**	**Wt%Fe**	**Wt%Ni**	**Wt%Cu**	**Wt%Zn**	**Wt%As**	**Total**
ba5-mgan.spongypyrite-b5	80	42.36	0.00	48.66	0.18	5.44	0.00	0.66	97.29
ba5-mgan.spongypyrite-b1	55	41.66	0.00	47.26	0.19	9.33	0.02	0.48	98.94
Pyrrhotite Analyses	**No**	**Wt%S**	**Wt%Ti**	**Wt%Fe**	**Wt%Ni**	**Wt%Cu**	**Wt%Zn**	**Wt%As**	**Total**
BA4-fgeu.pyrrhotite-b3	43	36.81	0	61.21	0.06	0.06	0.03	0	98.17
B9601-16a-anhedralpyrr.overgrowingsubeu.arsenoa1-a1	104	34.36	0	67.26	0.06	0.02	0.05	0.01	101.76
B9601-4bAnpyrr.ass.withdiamondshapedTi+Ti/Vmineral-a1	49	34.33	0.27	67.05	0.07	0	0	0.01	101.74
B9601-4bAnpyrr.overgrowingaggregatedeu.arsenoa1-b3	79	34.33	0	66.86	0.06	0.01	0.05	0	101.31
B9601-4bSubeuhedralpyrrhotite-a3	73	34.3	0	68.3	0.04	0.03	0	0.01	102.68
B9601-4bAnhedralpyrrhotite-d2	54	34.22	0	66.92	0.04	0.01	0	0	101.2
B9601-4bAnhedralpyrrhotite-e1	56	34.22	0	67.18	0.04	0	0.02	0	101.46
B9601-24-Anhedralpyrrhotite-f2	29	34.2	0	68.44	0.09	0.05	0.04	0.01	102.83
B9601-16-anhedralpyrr.overgrownbyeuhedralarseno(d)-l1	179	34.2	0	66.97	0	0	0.01	0.01	101.19
B9601-16-Anhedralpyrrhotite-g3	145	34.18	0	68.37	0.05	0	0	0.03	102.63
B9601-4bAnhedralpyrrhoite-e2	57	34.18	0.01	68.77	0.02	0	0	0	102.99
B9601-4bAnhedralpyrrhotite-c2	7	34.16	0	67.02	0.04	0	0.02	0.01	101.25
B9601-4bAnspongypyrr.ass.withsubeuhedralpyritea1a-a4	48	34.15	0	66.32	0.07	0	0	0	100.54
B9601-16-anhedralpyrrhotite-j3	157	34.11	0	66.92	0.03	0	0.03	0.04	101.14
B9601-16-anhedralpyrr.overgrownbyeuhedralarseno(d)-l4	182	34.11	0.01	67.59	0.01	0	0	0.03	101.76
B9601-16-anhedralpyrr.overgrownbyeuhedralarseno(d)-l2	180	34.11	0	68.08	0.03	0.02	0	0.01	102.26
B9601-16-anhedralpyrrhotite-j1	155	34.11	0	68.12	0	0	0	0	102.24
B9601-4bSubeuhedralpyrrhotite-a2	72	34.11	0.04	68.49	0.05	0	0.06	0	102.76
B9601-4bAnhedralpyrrhotite-1	2	34.1	0	66.87	0.06	0.02	0	0.02	101.06
B9601-4bSubeuhedralpyrrhotite-a1	71	34.1	0	67.73	0.04	0	0.02	0	101.89
B9601-16-anhedralpyrrhotite-e2	129	34.09	0	65.43	0.01	0.01	0.02	0.01	99.58
B9601-4bAnhedralpyrrhotite-d3	55	34.09	0	68.24	0.06	0	0	0	102.39
B9601-24-Anhedralpyrrhotite-g3	61	34.07	0.04	67.61	0.36	0.03	0	0	102.12
B9601-16-Anhedralpyrrhotite-g1	143	34.05	0	67.94	0.03	0	0	0	102.04
B9601-4bAnpyrr.overgrowingsubeuhedralarsenoa1-c3	98	34.04	0.03	65.63	0.02	0	0.04	0	99.76
B9601-16-Anhedralpyrrhotite-f2	138	34.03	0	67.89	0.01	0	0	0.02	101.95
B9601-4bAnhedralpyrrhotitec1	6	34.03	0	65.43	0.05	0	0.01	0.02	99.53
B9601-16-Anhedralpyrrhotite-g2	144	34.02	0.02	67.45	0	0.01	0.01	0.04	101.55
B9601-4bAnhedralpyrrhotitec4	9	34.01	0	68.28	0.08	0	0.02	0	102.4
B9601-16-anhedralpyrr.overgrowingeuhedralarseno(c)-k1	171	34	0	67.67	0.02	0	0.05	0.01	101.74

Birch Zone Probe Analysis Results

Pyrrhotite Analyses	No	Wt%S	Wt%Ti	Wt%Fe	Wt%Ni	Wt%Cu	Wt%Zn	Wt%As	Total
B9601-16-anhedralpyrr.overgrownbyeuhedralarseno(d)-l3	181	33.99	0	64.96	0.02	0.01	0	0.24	99.22
B9601-16-anhedralpyrrhotite-e1	128	33.99	0	67.93	0.02	0	0.01	0	101.97
B9601-24-Anhedralpyrrhotite-g2	60	33.97	0.02	66.89	0.31	0.01	0.07	0.02	101.29
B9601-25-Spongyanhedralpyrrhotite-d3	106	33.96	0	68.06	0.2	0.01	0.05	0	102.28
B9601-24-Anhedralpyrrhotite-f1	28	33.95	0	68.56	0.06	0.01	0	0	102.6
B9601-4bAnhedralpyrrhotite-2	3	33.94	0	68.95	0.05	0	0	0.01	102.96
B9601-4bAnpyrr.overgrowingsubeuhedralarsenob-d2	102	33.94	0	67.92	0.03	0	0.03	0	101.92
B9601-4bAnhedralpyrrhotite-c3	8	33.93	0	65.75	0.06	0	0	0.01	99.76
B9601-4bAnspongypyrr.ass.withsubeuhedralpyritea1-a3	47	33.91	0	66.47	0.05	0.01	0	0.02	100.46
B9601-4bAnpyrr.overgrowingsubeuhedralarsenoa1-c2	97	33.9	0.04	68.69	0.05	0	0	0.02	102.7
B9601-24-Anhedralpyrrhotite-f3	30	33.9	0	67.95	0.1	0	0.02	0.01	101.98
B9601-16-Anhedralpyrrhotite-h1	146	33.9	0	67.67	0.02	0.03	0	0	101.64
B9601-25-Anhedralpyrrhotite-a2	63	33.89	0	67.66	0.18	0.01	0	0	101.75
B9601-4bAnhedralpyrrhotite-e3	58	33.89	0	66.41	0.03	0.03	0	0	100.37
B9601-4bAnpyrr.overgrowingsubeuhedralarsenoa1-c5	100	33.88	0	67.39	0.04	0	0	0.04	101.35
B9601-16-anhedralpyrr.overgrowingeuhedralarseno(c)-k4	174	33.88	0	67.61	0.04	0.02	0.03	0	101.58
B9601-25-Spongysubeuhedralpyrrhotite-b1	98	33.87	0.01	68.65	0.19	0	0	0.02	102.75
B9601-25-Spongysubeuhedralpyrrhotite-a1	95	33.85	0.01	66.72	0.25	0	0	0.03	100.86
B9601-16-anhedralpyrrhotite-e3	130	33.85	0	67.71	0.01	0.04	0.09	0	101.7
B9601-25-Spongysubeuhedralpyrrhotite-a2	96	33.83	0.01	68.35	0.31	0.03	0.02	0.02	102.56
B9601-25-Spongysubeuhedralpyrrhotite-a3	97	33.82	0.06	68.05	0.27	0	0.06	0.02	102.29
B9601-25-Anhedralpyrrhotite-a1	62	33.81	0	66.95	0.24	0	0.04	0.04	101.08
B9601-4b-Anhedralpyrrhotite	1	33.81	0	67.83	0.05	0	0	0	101.7
B9601-4bAnhedralpyrrhotite-b1	4	33.8	0	66.12	0.06	0	0.04	0.01	100.03
B9601-24-Anhedralpyrrhotite-g1	59	33.79	0	68.04	0.27	0	0.03	0.05	102.18
B9601-25-Spongyanhedralpyrrhotite-d1	104	33.79	0.02	68.55	0.23	0.02	0.04	0.01	102.65
B9601-4bAnpyrr.overgrowingsubeuhedralarsenoa1-c1	96	33.74	0	68.3	0.05	0	0	0	102.1
B9601-16a--anhedralpyrr.overgrowingsubeu.arsenoa1-a3	106	33.72	0.01	67.07	0.01	0.03	0.01	0.01	100.85
B9601-16-anhedralpyrr.overgrowingeuhedralarseno(c)-k3	173	33.72	0	67.63	0.05	0	0	0.01	101.42
ba1-cgsubeu.pyrrhotite-b3	18	33.69	0	66.83	0.08	0.02	0.09	0	100.71
B9601-25-Anhedralpyrrhotite-a3	64	33.68	0	67.19	0.26	0.03	0	0.01	101.16
ba1-cgsubeu.pyrrhotite-b2	17	33.68	0	66.86	0.05	0.02	0.24	0	100.85
ba1-cgsubeu.pyrrhotite-b1	16	33.67	0	67.39	0.1	0	0.23	0	101.39

Birch Zone Probe Analysis Results

Pyrrhotite Analyses	No	Wt%S	Wt%Ti	Wt%Fe	Wt%Ni	Wt%Cu	Wt%Zn	Wt%As	Total
B9601-16-Anhedralpyrrhotite-h2	147	33.67	0	68.19	0.02	0.02	0	0	101.9
B9601-4bAnpyrr.overgrowingsubeuhedralarsenob-d1	101	33.67	0	68.24	0.09	0	0	0	102.01
B9601-16-anhedralpyrr.overgrownbyeuhedralarseno(e)-m2	187	33.62	0	68.67	0.03	0.02	0	0	102.35
B9601-4bAnspongypyrr.ass.withsubeuhedralpyritea1a-a2	46	33.53	0	65.93	0.05	0	0.04	0	99.56
B9613-02-250x150anpyrrhotite	8	33.20	0.00	69.30	0.15	0.06	0.00	0.00	102.71
B9613-02-50x50anpyrrhotite	22	33.20	0.00	68.85	0.19	0.08	0.02	0.00	102.34
B9613-02-75x150subeupyrrhotite	14	33.16	0.00	69.05	0.13	0.00	0.00	0.01	102.36
B9613-02-75x100anpyrrhotite	18	33.15	0.00	68.99	0.22	0.00	0.00	0.00	102.36
B9613-01-100x50subeupyrrhotite	43	33.12	0.00	67.99	0.24	0.00	0.01	0.02	101.38
B9613-01-300x200anpyrrhotite	68	33.11	0.00	69.30	0.02	0.00	0.05	0.00	102.49
B9613-01-100x50anpyrrhotite	41	33.10	0.00	68.84	0.07	0.01	0.04	0.02	102.09
B9613-02-250x150anpyrrhotite	9	33.09	0.00	69.16	0.12	0.02	0.01	0.01	102.42
B9613-01-100x50subeupyrrhotite	45	33.09	0.04	68.63	0.27	0.00	0.00	0.00	102.03
B9613-02-250x150anpyrrhotite	7	33.06	0.00	69.09	0.18	0.05	0.02	0.00	102.40
B9613-02-200x150subeupyrrhotite	5	33.05	0.00	69.50	0.13	0.05	0.01	0.01	102.75
B9613-01-100x50anpyrrhotite	40	33.04	0.01	69.20	0.05	0.00	0.01	0.00	102.32
B9613-02-75x150subeupyrrhotite	11	33.04	0.00	69.42	0.19	0.04	0.00	0.00	102.70
B9613-02-50x50subeupyrrhotite	33	33.04	0.00	69.07	0.25	0.10	0.00	0.00	102.46
B9613-02-75x150subeupyrrhotite	13	33.01	0.00	69.42	0.14	0.02	0.01	0.00	102.60
B9613-02-50x50subeupyrrhotite	32	33.01	0.00	69.01	0.23	0.11	0.00	0.00	102.36
B9613-02-75x150subeupyrrhotite	12	33.00	0.00	69.06	0.17	0.02	0.04	0.00	102.30
B9613-02-250x150anpyrrhotite	2	33.00	0.00	68.99	0.15	0.01	0.02	0.01	102.17
B9613-02-200x150subeupyrrhotite	4	32.98	0.01	69.22	0.20	0.03	0.05	0.00	102.49
B9613-01-300x500anpyrrhotite	72	32.98	0.00	69.45	0.00	0.02	0.00	0.00	102.47
B9613-02-50x100anpyrrhotite	19	32.98	0.00	68.69	0.18	0.04	0.03	0.01	101.93
B9613-01-300x250anpyrrhotite	61	32.97	0.00	69.30	0.11	0.00	0.02	0.00	102.41
B9613-02-75x75eupyrrhotite	39	32.96	0.00	69.09	0.21	0.03	0.00	0.00	102.29
B9613-02-250x150anpyrrhotite	3	32.96	0.00	68.84	0.20	0.02	0.03	0.00	102.05
B9613-02-75x150subeupyrrhotite	10	32.95	0.01	69.16	0.23	0.06	0.03	0.00	102.44
B9613-02-75x100subeupyrrhotite	28	32.95	0.00	69.21	0.14	0.04	0.00	0.00	102.34
B9613-02-200x150subeupyrrhotite	6	32.94	0.00	69.33	0.18	0.00	0.05	0.00	102.51
B9613-01-200x150anpyrrhotite	57	32.94	0.00	68.95	0.06	0.02	0.00	0.00	101.97
B9613-01-300x200anpyrrhotite	67	32.92	0.00	69.29	0.04	0.02	0.00	0.00	102.27

Birch Zone Probe Analysis Results

Pyrrhotite Analyses	No	Wt%S	Wt%Ti	Wt%Fe	Wt%Ni	Wt%Cu	Wt%Zn	Wt%As	Total
B9613-02-50x50subeupyrrhotite	31	32.92	0.00	68.72	0.19	0.11	0.01	0.02	101.98
B9613-02-250x150anpyrrhotite	1	32.92	0.00	69.04	0.19	0.02	0.02	0.00	102.18
B9613-02-30x50anpyrrhotite	27	32.91	0.00	68.83	0.17	0.05	0.00	0.00	101.96
B9613-01-300x250anpyrrhotite	63	32.91	0.00	69.53	0.01	0.01	0.00	0.00	102.46
B9613-01-300x300anpyrrhotite	74	32.91	0.00	69.44	0.02	0.00	0.02	0.00	102.39
B9613-02-50x100anpyrrhotite	20	32.90	0.00	68.91	0.19	0.02	0.00	0.01	102.03
B9613-02-75x100anpyrrhotite	16	32.89	0.01	69.25	0.20	0.02	0.02	0.02	102.42
B9613-01-300x250anpyrrhotite	62	32.89	0.00	69.66	0.05	0.03	0.00	0.01	102.64
B9613-02-75x100subeupyrrhotite	30	32.88	0.00	69.16	0.17	0.04	0.02	0.00	102.28
B9613-02-50x100anpyrrhotite	21	32.87	0.00	68.81	0.19	0.02	0.01	0.00	101.90
B9613-02-75x75eupyrrhotite	37	32.87	0.00	68.93	0.24	0.05	0.00	0.00	102.09
B9613-02-75x40subeupyrrhotite	36	32.87	0.00	69.04	0.24	0.04	0.00	0.01	102.20
B9613-02-30x50anpyrrhotite	26	32.87	0.00	68.45	0.19	0.08	0.02	0.00	101.61
B9613-02-75x150subeupyrrhotite	15	32.86	0.00	68.76	0.13	0.03	0.00	0.01	101.79
B9613-01-300x200anpyrrhotite	69	32.86	0.00	69.08	0.03	0.04	0.00	0.01	102.02
B9613-02-75x100anpyrrhotite	17	32.86	0.00	69.31	0.21	0.00	0.00	0.00	102.38
B9613-02-30x50anpyrrhotite	25	32.85	0.00	68.50	0.18	0.26	0.00	0.01	101.81
B9613-02-75x100subeupyrrhotite	29	32.85	0.00	68.65	0.16	0.05	0.01	0.00	101.71
B9613-02-50x50anpyrrhotite	24	32.84	0.00	68.68	0.19	0.02	0.02	0.00	101.76
B9613-02-75x40subeupyrrhotite	34	32.84	0.00	69.01	0.26	0.05	0.00	0.00	102.17
B9613-02-50x50anpyrrhotite	23	32.84	0.03	68.64	0.19	0.06	0.02	0.00	101.77
B9613-01-200x150anpyrrhotite	55	32.80	0.00	69.19	0.01	0.05	0.00	0.00	102.06
B9613-02-75x75eupyrrhotite	38	32.78	0.00	69.03	0.24	0.00	0.01	0.00	102.07
B9613-01-300x500anpyrrhotite	70	32.72	0.00	69.61	0.01	0.01	0.02	0.00	102.38
B9601-7-pyrrhotiteinarseno	54	32.71	0.02	64.63	0.07	0.00	0.00	0.02	97.46
B9613-01-300x500anpyrrhotite	71	32.64	0.00	70.09	0.04	0.00	0.00	0.00	102.78
B9601-7-pyrrhotiteinarseno3	57	32.63	0.00	64.74	0.08	0.01	0.01	0.00	97.47
B9613-02-75x40subeupyrrhotite	35	32.62	0.00	69.10	0.26	0.07	0.00	0.00	102.05
B9601-7-pyrrhotiteinarseno1	55	32.59	0.00	65.01	0.07	0.00	0.01	0.00	97.68
B9613-01-300x300anpyrrhotite	75	32.59	0.00	68.45	0.07	0.09	0.03	0.00	101.23
B9613-01-100x50subeupyrrhotite	44	32.53	0.02	67.85	0.24	0.00	0.04	0.00	100.68
B9601-7-pyrrhotiteinarseno2	56	32.47	0.02	65.10	0.08	0.00	0.03	0.00	97.70
B9613-01-100x50anpyrrhotite	42	32.41	0.00	64.52	0.07	4.61	0.00	0.00	101.61

Birch Zone Probe Analysis Results

Pyrrhotite Analyses	No	Wt%S	Wt%Ti	Wt%Fe	Wt%Ni	Wt%Cu	Wt%Zn	Wt%As	Total
B9613-01-100x40anpyrrhotite	76	31.87	0.00	67.54	0.13	0.18	0.02	0.00	99.75
B9613-01-300x300anpyrrhotite	73	31.82	0.00	67.62	0.08	0.00	0.00	0.00	99.54
B9613-01-100x40anpyrrhotite	77	31.64	0.00	67.13	0.13	0.11	0.01	0.00	99.03
Chalocpyrite Analyses	**No**	**Wt%S**	**Wt%Ti**	**Wt%Fe**	**Wt%Ni**	**Wt%Cu**	**Wt%Zn**	**Wt%As**	**Total**
BA3-mgan.chalco-b2	97	30.4	0	35.13	0.03	34.68	0.06	0	100.32
BB1-mganchalco-a2	14	30.01	0	34.04	0.02	33.73	0.05	0	97.84
BA2-mgan.chalco-b2	41	29.86	0	34.29	0.02	33.98	0	0.02	98.17
BB1-mganchalco-a1	13	29.85	0	34.91	0	33.9	0	0.02	98.69
BB1-mganchalco-b3	18	29.83	0.06	35.08	0	33.9	0.03	0	98.92
BB4-f-mganchalco-a3	87	29.82	0	34.26	0.81	32.74	0.04	0	97.67
ba5-fgan.chalco-a1	81	29.75	0	34.35	0.02	34.28	0.01	0.01	98.42
ba5-fgan.chalco-a2	82	29.62	0	34.45	0	33.54	0	0	97.61
BB1-mganchalco-a3	15	29.62	0	34.66	0	33.52	0.02	0	97.84
BA3-mgan.chalco-b3	98	29.57	0	34.02	0	34.35	0.03	0.7	98.68
BA3-fgan.chalco-a1	88	29.54	0	33.22	0.02	34.27	0	0.85	97.89
BA6A-fgan.chalco-c1	89	29.54	0	33.33	0.03	34.17	0.04	0.03	97.14
B9613-01-40x40anchalco-b1	52	29.28	0.00	34.71	0.00	33.45	0.00	0.02	97.47
B9613-01-40x40anchalco-b2	53	29.19	0.00	35.08	0.02	33.22	0.06	0.02	97.59
B9613-01-40x40anchalcoingrainpyb1-a2	50	29.15	0.00	35.16	0.03	33.41	0.03	0.00	97.77
B9613-01-40x40anchalco-b3	54	29.15	0.00	35.30	0.00	33.60	0.00	0.00	98.06
B9613-01-40x40anchalcoingrainpyb1-a3	51	28.99	0.00	35.35	0.02	33.50	0.02	0.00	97.88
B9613-01-200x150anchalcopyrite	56	28.93	0.00	35.55	0.02	33.67	0.05	0.00	98.21

Boundary Zone - Probe Analysis Results

Arsenopyrite Analyses	No	Wt%S	Wt%Ti	Wt%Fe	Wt%Ni	Wt%Cu	Wt%Zn	Wt%As	Wt%Se	Wt%Te	Total
BY7-500x300an.arsenopyrite-a2	67	15.79	0	38.8	0	0.01	0	47.27	0.2	0	102.07
BY7-500x300an.arsenopyrite-a3	68	15.9	0	38.88	0	0.01	0.01	47.14	0.3	0	102.25
BY7-200x200an.arsenopyrite-c4	89	16.31	0	39.76	0	0.02	0.04	46.5	0.23	0	102.87
BY7-75x150an.arsenopyrite-b2	73	16.56	0	39.52	0.05	0.04	0.01	46.3	0.18	0	102.66
BY10-150x100subeuarsenopyrite-c3	81	15.99	0	40.6	0.01	0.02	0.02	46.04	0.23	0	102.91
BY7-200x200an.arsenopyrite-c2	87	16.4	0	39.58	0.01	0.05	0.01	46.03	0.26	0	102.33
BY7-75x150an.arsenopyrite-b3	74	16.7	0	39.52	0.02	0.04	0	45.98	0.18	0	102.45
BY3-200X300subeu.arseno.withincl.'s-d4	124	16.06	0	39.88	0	0.08	0.01	45.83	0.26	0	102.13
BY6-200x100eu.arsenopyrite-a4	33	16.62	0	40.01	0	0.05	0	45.81	0.21	0	102.7
BY7-75x150an.arsenopyrite-b4	75	16.69	0.04	39.16	0.04	0.04	0	45.71	0.24	0	101.93
BY6-200x100eu.arsenopyrite-a2	31	14.7	0.04	39.75	0.08	0.13	0.05	45.66	0.19	0	100.6
BY8a-200x100subeu.arseno-a2	114	16.68	0	40.05	0.01	0.04	0	45.5	0.25	0	102.53
By11-100x75subeuarseno-a4	88	16.81	0	40.16	0.01	0.07	0.04	45.42	0.21	0	102.73
BY4-150X100subeu.arsenonexttoan.py.-c4	142	16.92	0	40.08	0	0.08	0.01	45.39	0.27	0	102.76
BY8a-75x75eu.arseno-a4	122	16.76	0.07	40.09	0	0.04	0	45.3	0.22	0	102.48
BY10-50x200euarsenopyrite-c2	65	16.81	0	40.72	0	0.02	0.01	45.06	0.2	0	102.82
BY5-400x300eu.arsenopyrite-c2	28	17.16	0.03	40.49	0	0	0	45.05	0.24	0	102.97
BY4-40X40SUBEUARSENO-A4	130	17.04	0.02	40.52	0.02	0.04	0.05	44.94	0.12	0	102.76
BY9-75x50subeuarsenopyrite-b3	19	17.05	0.02	40.56	0	0.02	0.02	44.86	0.21	0	102.75
BY8a-300x300subeu.arseno-b4	125	17.09	0	40.47	0	0.06	0.05	44.84	0.18	0	102.7
By11-200x250anarsenopyrite-a4	112	16.69	0	40.69	0	0.03	0.04	44.83	0.21	0	102.49
BY10-200x50euarsenopyrite-a4	58	17.17	0	40.32	0	0.03	0.02	44.7	0.18	0	102.43
BY10-200x50euarsenopyrite-a3	57	17.08	0	40.37	0.01	0.05	0.04	44.67	0.16	0	102.39
BY9-75x75euarsenopyrite-c3	42	16.96	0	40.98	0	0.03	0.02	44.63	0.18	0	102.8
By11-200x250anarsenopyrite-a3	111	17.01	0	40.98	0.02	0.04	0	44.6	0.18	0	102.84
BY9-75x75euarsenopyrite-c4	43	16.93	0	40.63	0.02	0.03	0.01	44.55	0.19	0	102.36
BY10-150x100subeuarsenopyrite-c4	82	16.85	0	41.13	0.01	0.03	0.02	44.55	0.23	0	102.82
By11-50x150euarseno-b4	97	17.44	0	40.79	0	0.04	0.01	44.46	0.16	0	102.92
BY10-200x50euarsenopyrite-a2	56	17.11	0	40.58	0.02	0.05	0.01	44.39	0.2	0	102.36
By11-200x250anarsenopyrite-a2	110	16.95	0	41.02	0.02	0.05	0.02	44.36	0.2	0	102.62
BY9-75x50subeuarsenopyrite-b4	20	17.39	0	40.81	0.02	0.03	0.03	44.34	0.18	0	102.8
BY10-50x200euarsenopyrite-c3	66	17.11	0	41.04	0	0.05	0.01	44.34	0.21	0	102.76
BY9-75x35euarsenopyrite-a3	25	17.15	0	39.96	0	0.06	0	44.32	0.21	0	101.7

Boundary Zone - Probe Analysis Results

Arsenopyrite Analyses	No	Wt%S	Wt%Ti	Wt%Fe	Wt%Ni	Wt%Cu	Wt%Zn	Wt%As	Wt%Se	Wt%Te	Total
By11-50x150euarseno-c4	100	17.4	0	40.77	0.01	0.01	0.01	44.31	0.21	0	102.71
BY9-75x50subeuarsenopyrite-c3	33	17.1	0	40.86	0.01	0.02	0	44.3	0.23	0	102.54
BY10-400x600subeuarsenopyrite-a2	68	17.09	0	40.86	0	0.06	0.05	44.3	0.24	0	102.6
By11-50x150euarseno-c3	99	17.54	0	40.79	0	0.02	0.03	44.24	0.21	0	102.84
BY10-50x200euarsenopyrite-c4	67	17.13	0	40.98	0.01	0.02	0.03	44.18	0.24	0	102.61
BY9-75x50subeuarsenopyrite-c4	34	17.28	0	40.9	0.01	0.04	0.02	44.1	0.23	0	102.58
By11-50x75euarseno-a2	89	17.67	0	40.5	0	0.08	0.05	44.08	0.17	0	102.56
By11-50x150euarseno-b3	96	17.37	0	41.05	0.03	0.05	0	44.05	0.23	0	102.79
By11-50x75euarseno-a3	90	17.62	0	40.87	0	0.06	0	43.97	0.23	0	102.76
BY9-75x50subeuarsenopyrite-c2	32	17.31	0	41.13	0.02	0.05	0	43.9	0.23	0	102.64
By11-100x75subeuarseno-a2	86	17.44	0	40.8	0.02	0.05	0.02	43.87	0.18	0	102.4
By11-50x150euarseno-b2	95	17.65	0	41.1	0.03	0.09	0.03	43.63	0.22	0	102.74
BY9-75x30euarsenopyrite-b3	36	17.59	0	40.56	0	0.04	0.03	43.58	0.26	0	102.06
BY9-75x30euarsenopyrite-b2	35	17.67	0	40.61	0.01	0.01	0.01	43.42	0.23	0.01	101.99
By11-50x75euarseno-a4	91	17.89	0	40.9	0	0.01	0.02	43.42	0.19	0	102.43
BY9-75x30euarsenopyrite-b4	37	17.23	0	40.15	0	0.05	0.01	43.03	0.22	0	100.69
Pyrite Analyses	**No**	**Wt%S**	**Wt%Ti**	**Wt%Fe**	**Wt%Ni**	**Wt%Cu**	**Wt%Zn**	**Wt%As**	**Wt%Se**	**Wt%Te**	**Total**
BY9-150x200anpyrite-c2	26	45.47	0	54.8	0	0.02	0.02	0	0	0	100.32
BY10-400x600anpyrite-c2	71	45.45	0	54.99	0	0.08	0.01	0.02	0	0	100.56
BY9-75x75anpyrite-b3	22	45.45	0	54.4	0.02	0.02	0	0	0	0.02	99.93
BY9-150x50anpyrite-a4	11	45.4	0	54.13	0.01	0.03	0.01	0.01	0	0	99.59
BY10-400x600anpyrite-c4	73	45.39	0.02	54.45	0.01	0.04	0	0.38	0	0	100.29
BY10-150x200subeupyrite-b3	75	45.38	0	54.44	0.04	0.02	0.07	0	0	0	99.95
BY9-150x200anpyrite-c3	27	45.33	0	54.99	0.02	0.04	0	0	0.02	0	100.41
BY9-75x75anpyrite-b4	23	45.31	0	54.51	0.01	0.05	0.04	0.01	0	0	99.94
BY9-75x75subeupyrite-b2	44	45.31	0	54.68	0.01	0.03	0.02	0	0	0	100.06
BY10-150x150subeupyrite-b3	78	45.3	0	54.66	0.01	0.06	0	0.13	0	0	100.16
BY9-75x75anpyrite-b2	21	45.3	0.01	54.67	0.03	0.05	0	0.01	0	0	100.07
BY9-150x50anpyrite-a3	10	45.3	0	54.19	0.02	0.04	0.01	0	0.01	0	99.57
BY9-100x75eupyrite-d3	48	45.29	0.01	54.35	0.01	0.03	0	0	0	0	99.69
BY9-100x75eupyrite-d2	47	45.28	0	54.5	0.01	0.01	0	0	0	0	99.82
BY9-75x75subeupyrite-b3	45	45.27	0	54.6	0.01	0.04	0	0	0	0	99.93
BY10-150x150subeupyrite-b4	79	45.26	0	54.83	0.03	0.08	0.03	0.06	0	0	100.29

Boundary Zone - Probe Analysis Results

Pyrite Analyses	No	Wt%S	Wt%Ti	Wt%Fe	Wt%Ni	Wt%Cu	Wt%Zn	Wt%As	Wt%Se	Wt%Te	Total
BY10-150x200subeupyrite-b4	76	45.24	0	54.72	0.01	0.02	0.04	0.51	0.02	0	100.56
BY10-100x75anpyrite-b3	54	45.22	0	54.42	0.01	0.04	0.03	0.28	0	0	100
BY10-600x00subeupyrite-c2	83	45.22	0	54.64	0.02	0.1	0	0.24	0	0	100.22
BY10-600x00subeupyrite-c4	85	45.22	0	54.62	0	0.05	0.03	0.06	0	0	99.99
BY10-150x200subeupyrite-b2	74	45.2	0	54.2	0.01	0.03	0.01	0.42	0.01	0	99.89
BY10-100x75anpyrite-b2	53	45.16	0	54.44	0.02	0.05	0	0.44	0	0	100.13
BY9-75x75subeupyrite-b4	46	45.16	0	54.59	0.03	0.02	0.03	0	0	0	99.85
BY10-400x600anpyrite-c3	72	45.12	0	54.64	0.03	0.05	0	0.38	0	0	100.23
BY9-150x50anpyrite-a2	9	45.06	0	53.93	0.05	0.04	0	0	0	0	99.09
BY9-100x75eupyrite-d4	49	45.06	0	54.21	0.03	0.09	0.04	0	0.01	0	99.45
BY9-500x300anpyrite-d3	30	45.05	0	54.46	0.02	0.04	0.05	0	0.01	0	99.64
BY10-100x75anpyrite-b4	55	44.94	0	54.18	0.02	0.04	0.01	0.53	0	0	99.74
BY10-600x00subeupyrite-c3	84	44.9	0	54.47	0.05	0.04	0	0.52	0.01	0	99.99
BY2-50X50AN.PYRITE-C4	48	44.83	0	54.14	0.03	0.1	0.05	0.03	0.02	0	99.2
BY2-50X50AN.PYRITE-C3	47	44.79	0	54.03	0.03	0.04	0	0.06	0.01	0	98.96
BY10-150x150subeupyrite-b2	77	44.72	0	54.49	0.01	0.07	0	0.61	0.06	0	99.95
BY9-500x300anpyrite-d2	29	44.71	0	54.74	0.02	0.01	0.03	0	0	0	99.52
BY2-50X50AN.PYRITE-C2	46	44.68	0	54.16	0.03	0.09	0.02	0.02	0.03	0	99.04
BY2-20X20AN.PY.SURR.AN.CHALCO(A)-D2	59	44.68	0	53.25	0.02	0.09	0.05	0.02	0	0	98.09
BY2-200X100AN.PYRITE-B4	45	44.65	0.01	54.07	0	0.09	0.02	0	0	0	98.85
BY2-75X50AN.PYRITE-A2	40	44.61	0	53.29	0	0.51	0	0.22	0	0.02	98.67
BY2-40X40HEX.PYRITE-E3	63	44.58	0	54.31	0.01	0.05	0.02	0.06	0	0	99.03
BY2-40X40HEX.PYRITE-E4	64	44.56	0.01	54.4	0.03	0	0.05	0.02	0	0	99.07
BY2-100X100HEX.PYRITE-F2	65	44.47	0	53.51	0	0.08	0	0.07	0	0	98.14
BY2-75X50AN.PYRITE-A4	42	44.4	0	53.98	0.04	0.2	0.02	0.07	0	0	98.71
BY2-100X100HEX.PYRITE-F3	66	44.29	0	54.32	0	0.09	0.06	0.03	0.02	0	98.82
BY4-250X50AN.PYRITE(WHITE)-A3	153	44.28	0	54.51	0	0.07	0	0.01	0	0	98.86
BY2-75X50AN.PYRITE-A3	41	44.21	0	54.34	0.05	0.08	0.04	0	0	0	98.71
BY4-250X150AN.PYRITE(WHITE)-C2	158	44.09	0.01	54.43	0.01	0	0.03	0.02	0	0	98.59
BY4-250X150AN.PYRITE(WHITE)-C3	159	44.07	0	54.11	0	0	0	0	0.01	0	98.2
BY2-200X100AN.PYRITE-B3	44	44.02	0	54.35	0.02	0.26	0	0.11	0	0.01	98.77
BY2-75X50AN.PYRITE-B2	43	43.8	0	54.13	0.05	0.3	0	0.18	0.02	0	98.49
BY2-100X100HEX.PYRITE-F4	67	43.77	0	53.13	0.11	0.15	0	2.23	0.07	0	99.46

Boundary Zone - Probe Analysis Results

Pyrite Analyses	No	Wt%S	Wt%Ti	Wt%Fe	Wt%Ni	Wt%Cu	Wt%Zn	Wt%As	Wt%Se	Wt%Te	Total
BY4-250X150AN.PYRITE(WHITE)-C4	160	43.58	0	53.55	0	0	0	0	0.02	0	97.17
BY2-20X20AN.PY.SURR.AN.CHALCO(A)-D4	61	43.29	0	51.63	0.04	1.46	0	1.04	0	0	97.46
BY4-250X50AN.PYRITE(WHITE)-A2	152	43.15	0	54.38	0.02	0.05	0	0	0	0	97.6
BY3-300X100AN.PYRITE-C4	106	42.84	0	53.27	0.03	0.05	0.01	3.91	0.03	0	100.14
BY4-250X50AN.PYRITE(WHITE)-A4	154	42.8	0	54.15	0.01	0.04	0.01	0.03	0	0	97.05
BY2-40X40HEX.PYRITE-E2	62	42.66	0	52.91	0.02	0.05	0.01	3.04	0.01	0.02	98.72
BY3-150X100SUBEUSPONGYPYRITE-B4	103	42.56	0	52	0.02	0.15	0.04	4.16	0	0	98.94
BY3-300X200AN.SPONGYPYRITE-D3	108	42.16	0	52.3	0.13	0.13	0.01	4.32	0.03	0	99.07
BY3-400X200AN.PYRITE-F3	114	41.94	0.02	52.21	0.2	0.22	0.02	4.12	0	0	98.74
BY3-400X400AN.SPONGYPYRITE-E2	110	41.78	0	52.03	0.03	0.2	0.02	5.05	0.05	0	99.16
BY3-150X100AN.SPONGYPYRITE-A3	96	41.71	0	51.54	0.19	0.22	0.02	4.69	0	0	98.38
BY3-400X200AN.PYRITE-F2	113	41.62	0	52.24	0.13	0.15	0	4.79	0	0	98.95
BY3-300X200AN.SPONGYPYRITE-D4	109	41.53	0	51.65	0.1	0.23	0.03	5.96	0.03	0	99.54
BY3-400X200AN.PYRITE-F4	115	41.48	0	52.09	0.23	0.16	0.06	4.95	0.01	0	98.97
BY3-150X100SUBEUSPONGYPYRITE-B3	102	41.37	0.05	51.48	0.1	0.29	0.04	5.55	0.02	0	98.9
BY3-300X100AN.PYRITE-C3	105	41.34	0	51.81	0.12	0.11	0	5.87	0.03	0	99.29
BY3-400X400AN.SPONGYPYRITE-E3	111	41.24	0	52.42	0.04	0.19	0	5.82	0	0	99.7
BY3-300X200AN.SPONGYPYRITE-D2	107	41.16	0	52.06	0.11	0.08	0	5.74	0.02	0	99.16
BY3-400X400AN.SPONGYPYRITE-E4	112	41.08	0	52.14	0.04	0.17	0.07	4.99	0.06	0	98.55
BY3-150X100SUBEUSPONGYPYRITE-B2	101	40.98	0	51.57	0.06	0.32	0.06	5.37	0.04	0	98.39
BY3-150X100AN.SPONGYPYRITE-A4	97	40.97	0.02	51.42	0.15	0.38	0	5.66	0	0	98.62
BY3-150X100AN.SPONGYPYRITE-A2	95	40.88	0.03	51.76	0.13	0.3	0	5.66	0.03	0	98.79
BY3-300X100AN.PYRITE-C2	104	40.87	0	51.55	0.09	0.13	0	6.42	0.02	0	99.07
Pyrrhotite Analyses	**No**	**Wt%S**	**Wt%Ti**	**Wt%Fe**	**Wt%Ni**	**Wt%Cu**	**Wt%Zn**	**Wt%As**	**Wt%Se**	**Wt%Te**	**Total**
BY9-15x50subeupyrrhotite-a4	14	33.44	0	69.37	0.02	0.03	0	0	0.01	0	102.88
BY9-200x100anpyrrhotite-e4	40	33.36	0.01	69	0.02	0.05	0	0.02	0	0	102.46
BY9-15x50subeupyrrhotite-a2	12	33.34	0	69.18	0.06	0.04	0	0.02	0	0	102.65
By11-100x50anpyrrhotite-b3	108	33.29	0	68.89	0.03	0.08	0	0	0	0	102.3
By11-75x100anpyrrhotite-c4	115	33.28	0	68.98	0.03	0.08	0.01	0	0	0	102.39
BY10-75x40subeupyrrhotite-a2	59	33.26	0	68.73	0.03	0.08	0	0.01	0	0	102.12
BY9-200x100anpyrrhotite-e2	38	33.26	0	69.45	0.01	0.1	0.02	0	0	0	102.86
BY1-75X150AN.PYRRHOTITE-C2	7	33.23	0	67.93	0.01	0.06	0.01	0.01	0	0	101.25
BY6-30x100an.pyrrhotite-c4	42	33.23	0	68.61	0.03	0.19	0	0.01	0	0	102.07

Boundary Zone - Probe Analysis Results

Pyrrhotite Analyses	No	Wt%S	Wt%Ti	Wt%Fe	Wt%Ni	Wt%Cu	Wt%Zn	Wt%As	Wt%Se	Wt%Te	Total
BY6-30x100an.pyrrhotite-c3	41	33.21	0	67.88	0.06	0.14	0.02	0	0	0	101.32
BY9-150x200anpyrrhotite-c4	28	33.21	0	69.44	0.02	0.03	0.02	0	0	0	102.73
BY10-200x75anpyrrhotite-a3	51	33.21	0	69.03	0.01	0.12	0	0	0	0	102.37
BY10-200x75anpyrrhotite-a2	50	33.18	0	69.36	0.04	0.12	0	0.01	0	0	102.71
By11-100x50eupyrrhotite-a4	106	33.18	0	68.7	0	0.03	0	0	0.01	0	101.91
BY1-250X50AN.VEINPYRRHOTITE-G3	26	33.16	0	67.92	0.05	0.03	0.01	0.04	0	0	101.2
By11-100x50anpyrrhotite-b2	107	33.15	0	68.96	0.01	0.07	0	0	0.01	0	102.21
BY10-75x40subeupyrrhotite-a4	61	33.14	0	68.63	0.01	0.08	0	0	0	0	101.87
BY4-600X100AN.PYRRHOTITEVEIN-A4	127	33.13	0.01	69	0.01	0.05	0	0.01	0.01	0	102.21
BY4-100X50AN.PYRRHOTITE-C2	134	33.12	0.02	68.52	0	0.03	0.02	0.02	0	0	101.74
BY7-200x75an.pyrrhotite-a3	65	33.12	0	68.97	0.03	0.1	0.02	0.02	0.03	0	102.29
BY10-75x40subeupyrrhotite-a3	60	33.12	0	68.92	0	0.12	0.03	0	0	0	102.2
BY5-400x75an.pyrrhotite-c2	10	33.11	0.03	68.12	0.02	0.01	0.06	0.02	0	0	101.37
BY1-75X50AN.PYRRHOTITE-A3	2	33.11	0.01	68.8	0.02	0.11	0	0	0	0	102.06
BY9-200x100anpyrrhotite-e3	39	33.11	0	69.66	0.01	0.03	0.01	0	0	0	102.82
BY7-200x100subeu.pyrrhotite-d3	85	33.1	0	68.79	0.05	0.12	0.01	0	0	0	102.08
BY9-15x50subeupyrrhotite-a3	13	33.1	0	69.13	0.03	0.13	0.02	0	0.01	0	102.42
BY10-200x75anpyrrhotite-a4	52	33.1	0	69.14	0.03	0.12	0	0	0	0	102.4
By11-75x100anpyrrhotite-c2	113	33.1	0	69.13	0.02	0.06	0.03	0	0	0	102.34
BY5-50x50an.pyrrhotite-b4	9	33.09	0	68.67	0	0.04	0.01	0.01	0	0	101.83
By11-75x50subeupyrrhotite-c4	124	33.08	0.02	69.06	0.02	0.02	0.01	0.01	0	0	102.22
BY1-75X150ANPYRRHOTITE-C3	8	33.08	0.03	69.28	0.01	0.07	0.02	0	0	0	102.49
BY1-200X350AN.VEINPYRRHOTITE-I3	32	33.08	0	68.97	0.02	0.09	0	0	0.02	0.04	102.23
BY6-75x300an.pyrrhotite-a4	36	33.08	0	68.72	0.03	0.21	0	0	0	0	102.06
By11-75x50anpyrrhotite-a2	101	33.08	0	69.18	0.02	0.05	0	0	0	0	102.33
By11-75x50anpyrrhotite-a4	103	33.08	0	68.76	0	0.05	0	0	0	0.02	101.92
By11-100x50eupyrrhotite-a2	104	33.08	0	68.72	0	0.05	0.03	0	0.01	0	101.91
BY4-600X100AN.PYRRHOTITEVEIN-A2	125	33.07	0	68.9	0.03	0	0	0	0.01	0	102.02
BY1-100X75SUBEU.PYRRHOTITE-J2	34	33.06	0	69.34	0	0.06	0.07	0.02	0.02	0	102.57
BY1-100X75SUBEU.PYRRHOTITE-J4	36	33.06	0.03	69.02	0.07	0.06	0.03	0	0	0	102.27
By11-50x35anpyrrhotite-d2	128	33.06	0	68.98	0.03	0.01	0	0	0.02	0	102.1
By11-50x50subeupyrrhotite-b2	119	33.05	0	68.81	0.02	0.06	0.06	0.03	0	0	102.03
BY5-400x300an.pyrrhotite-d2	13	33.05	0.05	69.18	0	0	0.02	0	0	0	102.31

Boundary Zone - Probe Analysis Results

Pyrrhotite Analyses	No	Wt%S	Wt%Ti	Wt%Fe	Wt%Ni	Wt%Cu	Wt%Zn	Wt%As	Wt%Se	Wt%Te	Total
By8-100x200an.pyrrhotite-a4	107	33.05	0	68.36	0.02	0.27	0.05	0	0	0.01	101.77
BY7-75x150an.pyrr.surr.an.arsenoinvein-b4	72	33.04	0	68.91	0.04	0.04	0.04	0	0	0	102.07
BY6-30x100an.pyrrhotite-c2	40	33.03	0	68.43	0.03	0.16	0	0.02	0	0	101.68
BY1-75X150AN.PYRRHOTITE-C4	9	33.03	0	68.03	0.02	0.08	0	0	0.01	0	101.18
BY7-200x75an.pyrrhotite-a4	66	33.03	0	68.82	0.03	0.11	0	0	0.03	0	102.02
BY4-100X50AN.PYRRHOTITE-B4	133	33.01	0	68.7	0.02	0.07	0	0.04	0	0	101.83
BY9-500x300anpyrrhotite-d4	31	33.01	0	69.31	0	0.04	0	0.03	0	0	102.39
BY5-200x50an.pyrrhotite-a3	2	33.01	0	68.81	0.01	0.04	0.01	0	0	0	101.88
BY7-200x100subeu.pyrrhotite-d4	86	33.01	0	68.95	0.04	0.1	0.01	0	0	0	102.11
By11-75x50anpyrrhotite-a3	102	33.01	0	69.19	0.03	0.04	0	0	0	0	102.29
BY1-75X75AN.PYRRHOTITE-B4	6	33	0	68.96	0.02	0.05	0.06	0.01	0	0	102.11
By11-100x50eupyrrhotite-a3	105	32.99	0	68.89	0.03	0.04	0	0	0	0	101.96
By11-50x35anpyrrhotite-d3	129	32.99	0	69.08	0.03	0.05	0.03	0	0	0	102.19
BY7-200x100subeu.pyrrhotite-d2	84	32.98	0	69.25	0.03	0.09	0	0.02	0	0	102.37
BY1-75X50AN.PYRRHOTITE-A2	1	32.98	0.02	68.83	0.05	0.08	0	0	0	0	101.97
BY1-400X200AN.PYRR.(SIMS-ANA)-D2	10	32.98	0	68.45	0	0	0	0	0	0	101.45
BY7-700x150an.pyrrhotite-c3	82	32.98	0	68.25	0.01	0.1	0.01	0	0.03	0	101.38
By11-50x50subeupyrrhotite-b3	120	32.98	0	69.14	0.01	0.02	0.04	0	0.01	0	102.2
By11-50x35anpyrrhotite-d4	130	32.97	0.01	68.98	0.04	0.05	0.04	0	0	0	102.1
BY7-700x300an.pyrrhotite-b4	80	32.96	0	69.28	0.06	0.12	0.01	0.03	0.02	0	102.48
BY5-200x50an.pyrrhotite-a4	3	32.96	0.02	68.27	0.01	0.04	0.01	0.02	0	0.01	101.34
BY4-250X150ANPYRRHOTITE-D4	145	32.96	0	69.44	0	0.05	0.03	0	0.06	0	102.54
BY1-75X75AN.PYRRHOTITE-B3	5	32.95	0.01	68.14	0.01	0.09	0.01	0.03	0.01	0	101.25
BY7-200x400an.pyrrhotite-a2	76	32.95	0.05	68.69	0.04	0.08	0.04	0.01	0	0	101.86
BY1-200X50SUBEU.PYRRHOTITE-F2	19	32.95	0	67.71	0	0.17	0.08	0	0.04	0	100.96
BY5-50x50an.pyrrhotite-b2	7	32.95	0.18	68.57	0.02	0	0.01	0	0	0.01	101.74
BY4-100X50AN.PYRRHOTITE-C4	136	32.94	0	68.82	0.02	0.02	0.03	0.01	0	0	101.84
BY6-300x100subeu.pyrrhotite-b2	49	32.94	0	69.01	0.04	0.16	0	0.01	0.02	0	102.18
BY7-700x150an.pyrrhotite-c4	83	32.94	0	67.47	0.04	0.12	0	0.01	0.02	0	100.6
BY1-200X350AN.VEINPYRRHOTITE-I4	33	32.93	0	69.25	0	0.07	0.02	0.01	0.02	0	102.31
BY1-75X50AN.PYRRHOTITE-A4	3	32.93	0.04	68.97	0.02	0.08	0	0	0.01	0	102.06
BY1-200X50SUBEU.PYRRHOTITE-F3	20	32.93	0	68.32	0.03	0.18	0	0	0.01	0	101.46
BY1-250X50AN.VEINPYRRHOTITE-G2	25	32.93	0	68.05	0.01	0.08	0	0	0	0	101.09

Boundary Zone - Probe Analysis Results

Pyrrhotite Analyses	No	Wt%S	Wt%Ti	Wt%Fe	Wt%Ni	Wt%Cu	Wt%Zn	Wt%As	Wt%Se	Wt%Te	Total
BY1-250X400AN.VEINPYRR.(SIMS.ANA)-H3	29	32.93	0	69.25	0.05	0	0.05	0	0.01	0	102.29
By8-75x200an.pyrrhotite-a2	111	32.93	0	69.27	0.05	0.09	0	0	0	0	102.34
BY4-250X150EU.PYRR.(WHITE)-B4	157	32.92	0	69.81	0.02	0	0	0	0.02	0	102.78
By8-75x200an.pyrrhotite-b4	110	32.92	0	68.45	0.03	0.32	0.03	0	0.01	0	101.77
By8-75x200an.pyrrhotite-a3	112	32.92	0	68.96	0.03	0.17	0	0	0	0	102.09
By11-50x50subeupyrrhotite-b4	121	32.92	0	68.91	0.01	0.06	0	0	0	0	101.91
BY1-100X75SUBEU.PYRRHOTITE-J3	35	32.91	0	69.25	0.01	0.08	0.02	0	0	0	102.29
BY7-200x400an.pyrrhotite-a3	77	32.9	0	69.02	0	0.07	0.02	0.03	0.02	0	102.05
BY6-300x100subeu.pyrrhotite-b4	51	32.9	0	68.65	0.04	0.26	0	0.01	0	0	101.87
BY6-75x300an.pyrrhotite-a2	34	32.9	0	69.1	0.02	0.14	0.09	0	0	0.01	102.27
BY6-75x300an.pyrrhotite-a3	35	32.9	0	67.76	0.03	0.14	0.04	0	0	0	100.88
BY5-200x50an.pyrrhotite-a2	1	32.89	0	68.73	0.03	0.03	0.07	0	0	0	101.75
BY1-75X75AN.PYRRHOTITE-B2	4	32.87	0.06	68.96	0.02	0.09	0.02	0.01	0	0	102.04
BY7-75x150an.pyrr.surr.an.arseno(a)invein-b2	70	32.87	0.03	68.82	0.06	0.07	0.03	0.01	0.02	0	101.92
BY6-75x150an.pyrrhotite-b3	38	32.87	0	68.33	0	0.17	0.01	0	0	0	101.38
BY6-75x150an.pyrrhotite-b2	37	32.86	0.02	68.48	0.02	0.15	0.06	0.03	0	0	101.62
BY1-250X50AN.VEINPYRRHOTITE-G4	27	32.86	0.05	68.21	0.01	0.15	0	0	0	0	101.29
BY6-75x150an.pyrrhotite-b4	39	32.86	0	68.32	0.01	0.11	0.05	0	0	0	101.36
BY7-700x150an.pyrrhotite-c2	81	32.85	0	68.05	0	0.13	0.01	0	0	0	101.04
BY7-1500x300an.pyrrhotite-d2	90	32.85	0	69.28	0.04	0.13	0.01	0	0.02	0	102.34
BY1-200X350AN.VEINPYRRHOTITE-I2	31	32.84	0.02	69.22	0.04	0.02	0	0.02	0	0	102.18
BY4-75X50an.pyrr.nexttosubeu.arseno-d3	138	32.83	0	68.82	0.04	0.08	0	0	0	0	101.77
BY4-600X100AN.PYRRHOTITEVEIN-A3	126	32.82	0.01	68.92	0.02	0.07	0	0.01	0	0	101.85
By11-75x50subeupyrrhotite-c2	122	32.82	0	68.3	0.04	0.05	0.04	0	0	0	101.25
BY4-250X150ANPYRRHOTITE-D3	144	32.81	0.04	69.3	0.03	0.04	0.02	0	0	0.02	102.26
BY7-75x150an.pyrr.surr.an.arseno(a)invein-b3	71	32.81	0	68.39	0.03	0.08	0	0	0	0	101.32
By11-75x50subeupyrrhotite-c3	123	32.81	0	68.89	0.02	0.05	0	0	0	0	101.77
BY1-75X100subeu.pyrr.nexttosubeu.sph.-E3	17	32.79	0	67.75	0.03	0	0.14	0	0	0	100.71
BY5-400x75an.pyrrhotite-c3	11	32.79	0	68.79	0	0	0.06	0	0.02	0	101.66
By8-100x200an.pyrrhotite-a2	105	32.79	0	68.58	0	0.2	0.07	0	0.01	0	101.65
BY4-75X50an.pyrr.nexttosubeu.arseno-D4	139	32.78	0	68.3	0	0.03	0	0.03	0	0	101.16
BY4-100X50AN.PYRRHOTITE-B2	131	32.77	0	68.8	0.03	0.01	0	0.03	0	0	101.66
BY1-250X400AN.VEINPYRR(SIMS.ANA)-H4	30	32.77	0	69.28	0.04	0.01	0	0.02	0	0	102.12

Boundary Zone - Probe Analysis Results

Pyrrhotite Analyses	No	Wt%S	Wt%Ti	Wt%Fe	Wt%Ni	Wt%Cu	Wt%Zn	Wt%As	Wt%Se	Wt%Te	Total
BY4-100X50AN.PYRRHOTITE-C3	135	32.76	0.01	68.8	0.02	0.04	0.01	0	0	0	101.65
BY4-250X150EU.PYRR.(WHITE)-B2	155	32.75	0.01	69.18	0.02	0	0.02	0	0.01	0	102
BY1-400X200AN.PYRR.(SIMS-ANA)-D4	12	32.74	0	68.38	0.03	0	0.08	0	0.01	0	101.25
BY1-400X250AN.PYRR.(SIMS.ANA)-K4	39	32.73	0	69.44	0	0.02	0	0	0.01	0	102.2
BY1-75X100subeu.pyrr.nexttosubeu.sph.-E2	16	32.72	0	67.97	0.01	0	0.04	0.01	0	0	100.75
BY4-100X50AN.PYRRHOTITE-B3	132	32.72	0	69.16	0.04	0.08	0.01	0	0	0	102.02
BY4-250X150ANPYRRHOTITE-D2	143	32.72	0	68.42	0	0.1	0	0	0	0	101.24
BY1-400X200AN.PYRR.(SIMS-ANA)-D3	11	32.71	0	68.68	0	0.03	0	0.02	0	0.01	101.46
BY5-400x75an.pyrrhotite-c4	12	32.71	0	67.42	0.03	0.02	0.03	0.01	0.02	0.01	100.24
By8-75x200an.pyrrhotite-b2	108	32.71	0	68.46	0.02	0.2	0.05	0.01	0	0	101.45
By8-75x200an.pyrrhotite-b3	109	32.71	0	68.49	0.01	0.26	0.04	0	0.02	0	101.52
BY5-50x50an.pyrrhotite-b3	8	32.69	0	68.67	0.06	0.03	0.05	0	0.01	0.03	101.53
BY1-400X250AN.PYRRHOTITE-K2	37	32.67	0	69.12	0	0.01	0	0	0	0	101.82
BY7-700x300an.pyrrhotite-b2	78	32.66	0	68.35	0.04	0.06	0.06	0	0.02	0	101.19
By8-100x200an.pyrrhotite-a3	106	32.63	0	69.51	0	0.13	0.03	0.01	0	0	102.31
BY1-250X400AN.VEINPYRR(SIMS.ANA)-H2	28	32.63	0	69.15	0	0	0	0	0	0	101.8
BY1-400X250AN.PYRR.(SIMS.ANA)-K3	38	32.63	0	69.03	0.04	0.01	0.05	0	0	0	101.77
BY1-200X50SUBEU.PYRRHOTITE-F4	21	32.62	0.01	67.95	0	0.16	0.04	0	0.03	0	100.82
BY4-75X50an.pyrr.nexttosubeu.arseno-D2	137	32.6	0	68.89	0.03	0.05	0.02	0.01	0	0.01	101.61
BY7-700x300an.pyrrhotite-b3	79	32.6	0	69.17	0.03	0.36	0.05	0	0.02	0	102.23
BY7-1500x300an.pyrrhotite-d3	91	32.6	0.03	69.29	0	0.07	0.06	0	0	0.03	102.08
BY5-400x300an.pyrrhotite-d4	15	32.58	0	70.02	0.03	0.01	0	0.02	0	0	102.66
BY7-200x75an.pyrrhotite-a2	64	32.5	0	68.73	0	0.08	0	0	0	0	101.31
BY4-250X150EU.PYRRHOTITE(WHITE)-B3	156	32.49	0	69.18	0	0.01	0	0	0	0	101.69
BY6-300x200subeu.pyrrhotite-a4	48	32.46	0	69.88	0.03	0.12	0	0	0	0	102.5
BY6-300x100subeu.pyrrhotite-b3	50	32.45	0	68.83	0.01	0.07	0	0	0	0	101.37
BY1-75X100subeu.pyrr.nexttosubeu.sph.-E4	18	32.43	0	68.32	0.02	0.04	0.51	0.01	0	0	101.33
BY6-300x200subeu.pyrrhotite-a2	46	32.4	0	69.55	0.03	0.11	0	0.02	0.02	0	102.13
BY7-1500x300an.pyrrhotite-d4	92	32.36	0.03	69.67	0.06	0.11	0	0.01	0	0	102.25
BY5-400x300an.pyrrhotite-d3	14	32.32	0	69.46	0.04	0.01	0	0	0	0	101.83
Chalcopyrite Analyses	**No**	**Wt%S**	**Wt%Ti**	**Wt%Fe**	**Wt%Ni**	**Wt%Cu**	**Wt%Zn**	**Wt%As**	**Wt%Se**	**Wt%Te**	**Total**
BY2-100X200AN.CHALCOSURR.BYANPY-B2	52	29.18	0	34.79	0.01	33.9	0	0	0.08	0	97.95
BY2-100X200AN.CHALCOSURR.BYANPY-B3	53	29.1	0	35.46	0.01	33.92	0.02	0.01	0	0	98.53

Boundary Zone - Probe Analysis Results

Chalcopyrite Analyses	**No**	**Wt%S**	**Wt%Ti**	**Wt%Fe**	**Wt%Ni**	**Wt%Cu**	**Wt%Zn**	**Wt%As**	**Wt%Se**	**Wt%Te**	**Total**
BY2-400X250AN.CHALCOSURR.BYANPY-C3	56	29.06	0	35.07	0.01	33.55	0.02	0	0	0	97.71
BY2-400X250AN.CHALCOSURR.BYANPY-C4	57	28.95	0	34.51	0.02	34.24	0	0.03	0	0	97.75
BY2-400X250AN.CHALCOSURR.BYANPY-C5	58	28.9	0	35.29	0.02	33.41	0.05	0.01	0.02	0	97.71
BY2-100X200AN.CHALCOSURR.BYANPY-B4	54	28.84	0	35.32	0	33.62	0.03	0.01	0.03	0	97.84
BY2-400X250AN.CHALCOSURR.BYANPY-C2	55	28.82	0	34.66	0	33.89	0.03	0	0	0	97.4
BY2-50X200an.chalco.surr.byan.py.(d)-a4	51	28.81	0.01	34.91	0.03	33.59	0.03	0	0	0	97.38
BY2-50X75ANCHALCOSURR.BYPYINVEIN-D	69	28.8	0	34.81	0.01	33.46	0	0.11	0	0	97.2
BY2-50X200AN.CHALCOSURR.BYANPY(D)-	49	28.69	0.01	35.08	0.07	33.63	0	0	0.01	0	97.49
Sphalerite Analyses	**No**	**Wt%S**	**Wt%Ti**	**Wt%Fe**	**Wt%Ni**	**Wt%Cu**	**Wt%Zn**	**Wt%As**	**Wt%Se**	**Wt%Te**	**Total**
BY6-75x50an.sph.withinsubeu.arseno(b)-d2	61	27.76	0.03	11.69	0.01	0.19	57.87	0.1	0	0	97.65
BY1-75X100subeu.sph.nexttosubeu.Py(e)-A3	14	27.73	0.03	9.19	0	0.06	60.55	0	0.03	0	97.6
BY6-75x50an.sph.withinsubeu.arsneo(b)-d3	62	27.71	0	11.75	0.01	0.2	57.88	0.1	0	0	97.66
BY1-75X50AN.SPHALERITE-B3	23	27.52	0	6.72	0	0.15	63.61	0	0.01	0	98.01
BY1-75X50AN.SPHALERITE-B4	24	27.5	0.01	6.11	0.01	0.2	63.78	0.02	0	0	97.64

No. 3 Zone - Sulphide Analysis Results from Electron Microprobe

Arsenopyrite Analyses	No	Wt% S	Wt% Ti	Wt% Fe	Wt% Ni	Wt% Cu	Wt% Zn	Wt% As	Total
N3-9-mganhedralarseno-d1	28	14.37	0	33.07	0.26	0.05	0.04	49.88	97.68
N3-9-mgsubeuhedralarseno-a1	20	14.49	0	34.42	0.31	0.03	0.03	49.67	98.95
N3-9-fganhedralarseno-a3	16	14.98	0.02	34.26	0.26	0	0	49.25	98.79
N3-9-mgsubeuhedralarseno-a3	22	15.02	0	36	0.23	0	0.04	49.19	100.48
N3-9-mgsubeuhedralarseno-a2	21	14.86	0	35.41	0.23	0.05	0	49.17	99.72
N3-9-mganhedralarseno-d2	29	14.7	0	34.35	0.26	0.07	0	49.15	98.54
N3-9-fganhedralarseno-a1	14	15.32	0	35.71	0.15	0	0.04	49.08	100.31
N3-9-mganhedralarseno-b1	23	15.16	0	35.9	0.18	0.01	0	48.99	100.23
N3-9-mganhedralarseno-b2	24	15.24	0	35.51	0.23	0	0	48.68	99.65
N3-9-mganhedralarseno-b3	25	15.32	0	36.04	0.2	0	0.06	48.54	100.16
N3-9-mganhedralarseno-c2	26	15.48	0	36.6	0.2	0	0	48.49	100.77
N3-9-fganhedralarseno-a2	15	14.96	0	34.9	0.24	0.06	0	48.44	98.6
N3-4-F-Mgsubeuhedralarseno-a1	60	16.08	0.03	38.32	0.04	0.03	0	47.93	102.42
N3-4-Mgsubeuhedralarseno-b1	66	16.21	0	38.07	0.08	0	0	47.9	102.26
N3-9-mganhedralarseno-c3	27	16.06	0	36.96	0.06	0	0.05	47.6	100.73
N3-3-Fgeuhedralarsenoaggregated-c3	13	16.95	0	38.52	0	0.01	0.02	46.96	102.46
N3-3-Fgeuhedralarseno-b2	4	17.12	0	38.61	0.02	0.03	0.01	46.6	102.38
N3-2-fgsubeuhedralarsenoinsilicates-c2	74	17.07	0	38.52	0.01	0	0	46.47	102.07
N3-3-Fganhedralarseno-a3	7	17.36	0	38.79	0.04	0	0.04	46.31	102.54
N3-2-fgeuhedralarsenoinvein-b1	54	16.9	0	39.3	0.02	0	0.02	46.29	102.52
N3-2-fganhedralarsenoinvein-a1	57	16.73	0.18	39.82	0.01	0	0.05	46.09	102.86
N3-3-Fgeuhedralarseno-b1	3	17.32	0	39.32	0.02	0.01	0	46.05	102.73
N3-3-Fganhedralarseno-a2	6	17.28	0	39.32	0	0.04	0.05	46.03	102.72
N3-3-Fganhedralarseno-a1	5	17.31	0	39.47	0.01	0	0.01	46.01	102.81
N3-3-Fganhedralarseno-b2	21	17.34	0.01	39.16	0.02	0.01	0.01	46.01	102.56
N3-3-Fganhedralarseno-b1	20	17.23	0	39.46	0	0.03	0.03	45.87	102.63
N3-1-Mgeuhedralarseno-a2	12	17.19	0	39.86	0	0.04	0.01	45.83	102.93
N3-2-euhedralarsenoinvein-a3	53	17.29	0	39.77	0.07	0	0.01	45.82	102.95
N3-3-Mgsubeuhedralarseno-b1	17	17.18	0	38.98	0	0.01	0.03	45.81	102.01
N3-1-Mgeuhedralarseno-a3	13	16.9	0.02	39.68	0.01	0.01	0.04	45.8	102.47
N3-3-Mgsubeuhedralarseno-a1	14	17.49	0	39.71	0	0	0	45.78	102.98
N3-1-Mgeuhedralarseno-a1	11	17.34	0	39.76	0	0	0	45.6	102.71
N3-2-euhedralarsenoinvein-a1	51	17.2	0.03	40.04	0	0	0	45.6	102.88

No. 3 Zone - Sulphide Analysis Results from Electron Microprobe

Arsenopyrite Analyses	**No**	**Wt% S**	**Wt% Ti**	**Wt% Fe**	**Wt% Ni**	**Wt% Cu**	**Wt% Zn**	**Wt% As**	**Total**
N3-3-Fgeuhedralarsenoaggregated-c1	11	17.71	0	39.34	0.03	0.01	0.02	45.59	102.71
N3-2-fganhedralarsenoinvein-a2	58	17.3	0.01	39.87	0.03	0	0	45.53	102.74
N3-3-F-Mganhedralarseno-c2	23	17.78	0	38.62	0.01	0	0.01	45.49	101.91
N3-2-euhedralarsenoinvein-a2	52	17.45	0	39.49	0.08	0.02	0.02	45.42	102.42
N3-1-mganhedralarseno-a1	45	17.38	0.02	40.04	0	0	0.02	45.32	102.78
N3-2-fganhedralarsenoinvein-b3	62	17.47	0	40.03	0.02	0.06	0.02	45.1	102.71
N3-3-F-Mganhedralarseno-c1	22	17.73	0	39.19	0	0	0.04	45.05	102.01
N3-2-fgeuhedralarsenoinvein-b3	56	17.13	0	39.95	0.01	0	0.04	45.03	102.16
N3-1-subeuhedralarseno-b3	50	17.66	0	39.81	0.03	0.01	0.01	45.02	102.53
N3-2-fgeuhedralarsenoinvein-b2	55	17.46	0.01	40.36	0	0.02	0	44.93	102.77
N3-9-mganhedralarseno-d3	30	16.79	0	35.85	0.08	2.83	0	44.74	100.28
N3-1-Euhedralarseno,isolated-b2	18	17.76	0	40.06	0.05	0.01	0	44.54	102.42
N3-1-Euhedralarseno,isolated-b3	19	18.13	0.02	40.35	0.02	0.04	0.02	44.4	102.97
N3-1-mgsuban.arsenoinsidean.pyrite-a3	7	18.27	0	40.5	0.04	0	0	44.03	102.84
Pyrite Analyses	**No**	**Wt% S**	**Wt% Ti**	**Wt% Fe**	**Wt% Ni**	**Wt% Cu**	**Wt% Zn**	**Wt% As**	**Total**
N3-1-Cganpyriteenclosingchalco+an.-eu.arseno-a2	2	46.94	0.01	53.89	0.07	0.04	0.02	0.03	100.99
N3-3-F-Mganpyriteass.withsubeu.arseno-a2	28	46.75	0	53.6	0.08	0.15	0.02	0.08	100.69
N3-9-mgspongyanpyritewithchalcoinclusions-c1	11	46.61	0.02	53.03	0.07	0.03	0	0	99.76
N3-9-fgsubeuhedralpyrite-a2	18	46.57	0	53.3	0.12	0	0	0	99.99
N3-3-F-Mganpyriteass.withsubeu.arseno-a1	27	46.56	0	52.94	0.05	0.06	0	0.03	99.64
N3-1-spongyanhedralpyrite-mg-d1	39	46.54	0	54.19	0.01	0.01	0.03	0.04	100.81
N3-9-fgsubeuhedralpyrite-a1	17	46.53	0.05	52.55	0.03	0	0.05	0	99.21
N3-9-F-mganhedralpyrite-b3	5	46.47	0	52.27	0.05	0.34	0	0.01	99.14
N3-3-Fganhedralpyriteinvein-c3	47	46.43	0	53.04	0	0.01	0	0.03	99.52
N3-4-Mganhedalpyritespongyatedges-c1	78	46.41	0	54.02	0.03	0.02	0	0	100.49
N3-4-Mganhedalpyritespongyatedges-c2	79	46.39	0.05	53.64	0.05	0.01	0	0.05	100.19
N3-1-spongyanhedralpyrite-mg-d3	41	46.39	0	53.56	0.03	0.02	0.02	0.02	100.04
N3-1-Cganpyriteenclosingchalco+an.-eu.arseno-a3	3	46.39	0	54.31	0.03	0.03	0.05	0	100.81
N3-3-F-Mganpyriteass.withsubeu.arseno-a3	29	46.37	0	53.38	0	0.05	0.01	0.23	100.03
N3-1-Cganpyriteenclosingchalco+an.-eu.arseno-a1	1	46.35	0	54.01	0.06	0.07	0.04	0.01	100.54
N3-9-mgspongyanpyritewithchalcoinclusions-c2	12	46.35	0	52.94	0.24	0.21	0	0	99.74
N3-1-spongyanhedralpyrite-mg-d2	40	46.34	0.04	53.86	0.03	0.08	0.01	0.1	100.45
N3-1-Cgspongyanhedralpyrite-a2	21	46.32	0	53.82	0.03	0.04	0.02	0.11	100.34

No. 3 Zone - Sulphide Analysis Results from Electron Microprobe

Pyrite Analyses	No	Wt% S	Wt% Ti	Wt% Fe	Wt% Ni	Wt% Cu	Wt% Zn	Wt% As	Total
N3-3-Mganhedralpyriteinvein-b3	32	46.31	0	53.17	0.04	0.01	0.02	0.05	99.61
N3-9-mgspongyanpyritewithfgchalcoinclusions-a2	7	46.28	0	52.48	0.05	0.17	0	0	98.98
N3-3-Mganhedralspongypyrite-b1	39	46.23	0.01	53.75	0.06	0.04	0.02	0.02	100.13
N3-1-Cgspongyanhedralpyrite-b1	23	46.22	0	53.96	0.07	0.01	0.07	0	100.33
N3-9-mganhedralpyriteinvein-d3	33	46.13	0	52.46	0.13	0	0.08	0.02	98.82
N3-1-mganhedralpyrite-b3	32	46.1	0	53.5	0.02	0.22	0.05	0.01	99.9
N3-3-Fganhedralpyriteinvein-d3	50	46.08	0	52.51	0.02	0.02	0	0.03	98.65
N3-9-F-mganhedralpyrite-b2	4	46.05	0	52.79	0.03	0.27	0	0.22	99.36
N3-4-Mganhedalpyritespongyatedges-c3	80	46.04	0	52.76	0.01	0	0.03	0.04	98.88
N3-1-Cgspongyanhedralpyrite-a3	22	46.04	0	53.86	0.06	0.03	0.03	0	100.03
N3-9-mgspongyanpyritewithfgchalcoinclusions-a1	6	46.04	0	53.5	0.02	0.27	0.05	0	99.87
N3-3-Cganhedralpyrite-e1	51	46.02	0	52.48	0.03	0.08	0	0.07	98.68
N3-1-Cgspongyanhedralpyrite-b2	24	45.99	0.01	54.64	0.07	0.06	0	0	100.77
N3-1-Cganpyriteenclosingchalco+an.-eu.arseno-a4	4	45.97	0	53.88	0.1	0.01	0	0.03	99.99
N3-4-Cgsubeuhedralspongypyrite-a3	56	45.84	0	49.65	0.06	0.05	5.88	0.11	101.59
N3-3-Mganhedralpyrite-a3	10	45.82	0.01	53.18	0.03	0.05	0	0.18	99.27
N3-9-fgsubeuhedralpyrite-a3	19	45.81	0	52.82	0.14	0.38	0.03	0.03	99.2
N3-1-mganhedralpyrite-b2	31	45.76	0	53.11	0.03	0.08	0	0	98.97
N3-2-fganhedralpyriteinveinwithpyrite-a3	71	45.74	0	53.2	0.02	0	0.03	0.49	99.49
N3-3-Fganhedralpyriteinvein-c1	45	45.6	0	52.69	0.01	0.01	0.04	0	98.35
N3-3-Cganhedralpyrite-e2	52	45.59	0.04	52.31	0.06	0.12	0	0.03	98.15
N3-3-Mganhedralpyriteinvein-b2	31	45.58	0	52.25	0.01	0.01	0.03	0	97.88
N3-9-F-mganhedralpyrite-b1	3	45.56	0	52.9	0.05	0.48	0	0.02	99.02
N3-3-Cganhedralpyrite-e3	53	45.53	0	51.85	0.08	0.1	0	0.04	97.6
N3-2-fganhedralpyriteinveinwithpyrite-a1	68	45.51	0	53.3	0.03	0.01	0	0.29	99.14
N3-3-Fganhedralpyriteinvein-d2	49	45.38	0	52.12	0	0	0.05	0	97.55
N3-9-mgspongyanpyritewithfgchalcoinclusions-a3	8	45.35	0	51.8	0.22	0.11	0	0.15	97.63
N3-1-mganhedralpyrite-b1	30	45.24	0	53.92	0.03	0.03	0	0.02	99.25
N3-3-Mganhedralpyrite-a1	8	45.19	0	52.01	0.01	0.03	0	0.72	97.97
N3-2-fganhedralpyriteinveinwitharseno-a1	63	45.18	0	53.1	0.01	0.01	0.02	0.4	98.72
N3-3-Mganhedralpyriteinvein-b1	30	45.1	0	52.5	0.07	0	0.03	0.02	97.72
N3-1-Cgspongyanhedralpyrite-b3	25	45.01	0	53.42	0.05	0.08	0.06	0.01	98.63
N3-3-Mganhedralpyrite-a2	9	44.84	0	51.85	0.04	0.06	0.01	0.6	97.41

No. 3 Zone - Sulphide Analysis Results from Electron Microprobe

Pyrite Analyses	**No**	**Wt% S**	**Wt% Ti**	**Wt% Fe**	**Wt% Ni**	**Wt% Cu**	**Wt% Zn**	**Wt% As**	**Total**
N3-2-fganhedralpyriteinveinwithpyrite-b2	70	44.82	0	53.3	0.07	0	0	0.25	98.44
N3-2-fganhedralpyriteinveinwitharseno-a3	65	44.51	0	52.79	0.12	0	0	0.37	97.79
N3-2-fganhedralpyriteinveinwithpyrite-b3	69	44	0	52.77	0.04	0.02	0	0.53	97.36
N3-9-mgspongyanpyritewithchalcoinclusions-c3	13	43.74	0.08	49.31	0.09	5.12	0	0.12	98.47
N3-4-Cgsubeuhedralspongypyrite-a2	55	42.48	0.01	44.52	0.03	0.09	11.09	0.4	98.62
Pyrrhotite Analyses	**No**	**Wt% S**	**Wt% Ti**	**Wt% Fe**	**Wt% Ni**	**Wt% Cu**	**Wt% Zn**	**Wt% As**	**Total**
N3-4-Mganhedalpyrrhotite-c3	74	35.01	0	67.56	0.03	0.03	0.03	0	102.66
N3-4-Fganhedalpyrrhotite-b3	71	34.6	0	67.64	0.02	0.01	0	0	102.28
N3-4-Fganhedalpyrrhotite-b2	70	34.29	0	67	0.03	0.02	0.01	0.01	101.36
N3-4-Fganhedalpyrrhotite-b1	69	34.26	0	66.91	0.01	0	0.01	0.01	101.2
N3-4-Mganhedalpyrrhotite-b1	75	34.11	0	67.71	0.01	0.04	0.06	0.04	101.97
N3-4-Mganhedalpyrrhotite-b3	77	34.07	0.03	68.19	0.01	0	0	0.01	102.32
N3-4-F-Mganhedralpyrrhotite-a3	59	34.02	0	67.58	0.04	0.04	0.4	0	102.08
N3-4-Mganhedalpyrrhotite-c2	73	34.01	0	67.43	0.05	0	0	0.01	101.5
N3-4-Mganhedalpyrrhotite-c1	72	34	0	66.51	0.03	0.01	0.04	0	100.6
N3-4-Mganhedalpyrrhotite-d2	82	33.99	0	67.38	0.01	0	0.02	0.03	101.43
N3-4-F-Mganhedralpyrrhotite-a1	57	33.93	0	67.26	0	0	0.27	0	101.46
N3-4-F-Mganhedralpyrrhotite-a2	58	33.85	0	66.21	0.05	0.03	0.31	0	100.45
N3-4-Mganhedalpyrrhotite-d1	81	33.8	0	66.75	0.03	0.01	0.01	0	100.6
N3-4-Mganhedalpyrrhotite-d3	83	33.79	0	68.22	0	0	0	0	102.01
Chalcopyrite Analyses	**No**	**Wt% S**	**Wt% Ti**	**Wt% Fe**	**Wt% Ni**	**Wt% Cu**	**Wt% Zn**	**Wt% As**	**Total**
N3-9-fganchalcoinclusionsinspongypyrite(a)-a1	9	31.6	0	36.03	0.01	29.8	0.03	0.03	97.5
N3-1-chalcoalongcrackinan.pyrite-a2	9	31.44	0	35.22	0.04	32.41	0.06	0.25	99.42
N3-1-mganhedralchalcoass.withan.pyrite-c1	33	30.38	0	34.91	0.02	33.24	0.01	0.02	98.57
N3-9-fganchalcoinclusionsincganpyrite-c2	35	30.23	0	35.41	0.01	32.55	0.02	0	98.22
N3-9-fganchalcoinclusionsincganpyrite-c3	36	29.99	0	34.67	0.04	32.71	0.03	0.02	97.45
N3-9-fganchalcoinclusionsincganpyrite-c1	34	29.98	0	34.16	0	33.5	0	0.05	97.7
N3-4-F-mganhedralchalcowithanhedralpyrite-b1	96	29.97	0	34.11	0	34.06	0.02	0.02	98.19
N3-1-mganhedralchalco-b3	28	29.96	0	34.65	0.04	34.47	0.03	0.03	99.18
N3-1-chalcoalongcrackinan.pyrite-a3	10	29.94	0	34.34	0.02	34.85	0	0.05	99.2
N3-1-mganhedralchalcoass.withan.pyrite-c2	34	29.85	0	34.67	0	33.73	0	0	98.26
N3-4-F-mganhedralchalcowithanhedralpyrite-b2	97	29.84	0	34.05	0.03	34.5	0.03	0.02	98.47
N3-4-F-mganhedralchalcowithanhedralpyrite-b3	98	29.84	0	33.87	0.03	33.69	0.08	0.02	97.53

No. 3 Zone - Sulphide Analysis Results from Electron Microprobe

Chalcopyrite Analyses	No	Wt% S	Wt% Ti	Wt% Fe	Wt% Ni	Wt% Cu	Wt% Zn	Wt% As	Total
N3-1-mganhedralchalco-b2	27	29.74	0	34.62	0	34.38	0	0.06	98.8
N3-1-mganhedralchalco-b4	29	29.72	0	34.54	0.01	34.9	0.03	0	99.19
N3-1-mganhedralchalco-b1	26	29.65	0	34.84	0	34.29	0.02	0.02	98.82
N3-1-mganhedralchalcoass.withan.pyrite-c3	35	28.98	0	32.91	0	34.6	0.02	0.62	97.14

Main mine Dick Zone - Probe Analysis Results

Arsenopyrite Analyses	No	Wt%S	Wt%Ti	Wt%Fe	Wt%Ni	Wt%Cu	Wt%Zn	Wt%As	Wt%Se	Total
Db66-100x75subeuarseno	80	14.38	0	36.63	0.61	0.06	0.04	49.42	0.24	101.38
Db66-100x75subeuarseno	77	14.54	0	36.54	0.39	0.03	0.02	48.97	0.23	100.75
Db66-100x75subeuarseno	78	14.28	0	35.98	0.42	0.07	0.06	48.93	0.22	99.97
Db66-100x75subeuarseno	79	14.75	0	36.74	0.5	0.08	0.04	48.88	0.21	101.2
DB8-250X200ANARSENO	91	15.42	0	37.77	0.27	0	0.04	48.49		101.99
Db66-100x75subeuarseno	81	14.98	0	37.43	0.45	0.07	0	48.41	0.19	101.54
Db66-500x600subeuarseno	96	15.21	0	38.7	0.19	0.04	0	48.25	0.21	102.59
DB39-200x250euarseno	51	15.56	0	38.46	0.22	0.02	0.03	48.19	0.23	102.7
DB8-250X200ANARSENO	92	15.51	0	37.71	0.17	0	0	48.13		101.52
DB8-400X200EUARSENO	75	15.08	0.01	35.58	0.32	0.02	0.01	47.98		98.99
DB8-300X300SUBEUARSENO	89	15.21	0	36.89	0.12	0.01	0	47.9		100.13
DB8-400X600EUARSENO	86	15.27	0	37.05	0.19	0	0.01	47.65		100.18
DB8-400X200EUARSENO	74	15.41	0	36.39	0.19	0	0	47.62		99.62
DB8-300X300SUBEUARSENO	90	15.26	0	36.76	0.17	0.03	0.03	47.62		99.86
DB8-400X600EUARSENO	87	15.44	0	36.97	0.15	0	0	47.61		100.18
DB8-600X300SUBEUARSENO	80	15.35	0	37.45	0.2	0.01	0.02	47.59		100.63
DB8-200X100ANARSENO	56	15.57	0	38.24	0.15	0.04	0.01	47.57		101.58
DB8-900X400ANARSENO	77	15.4	0	36.34	0.2	0	0	47.55		99.5
DB8-100X200SUBEUARSENO	67	15.68	0	37.26	0.13	0	0.01	47.54		100.61
DB8-250X250EUARSENO	84	15.43	0	36.63	0.26	0	0	47.48		99.81
DB8-250X250EUARSENO	83	15.47	0.01	36.56	0.27	0	0.01	47.47		99.78
DB8-900X400ANARSENO	78	15.32	0.01	37.91	0.25	0.01	0	47.39		100.89
DB8-100X200SUBEUARSENO	68	15.83	0	37.43	0.05	0.02	0	47.31		100.65
DB8-250X200ANARSENO	93	15.7	0	36.74	0.14	0.02	0.03	47.3		99.93
DB8-600X300SUBEUARSENO	81	15.47	0	36.6	0.21	0.01	0.01	47.21		99.5
DB8-100X200SUBEUARSENO	69	16.02	0	36.9	0.06	0	0.01	47.2		100.2
DB39-euarsenoOGanpyrrhotite	71	16.21	0	38.94	0.09	0.05	0	47.18	0.19	102.67
DB8-900X400ANARSENO	76	16.1	0	38.14	0.13	0.06	0	47.09		101.52
DB8-300X300SUBEUARSENO	88	15.94	0	38.04	0.04	0	0.01	47.09		101.12
DC9-150x75subeuarseno	146	15.25	0	39.39	0.18	0.02	0.02	47.09	0.22	102.17
DB8-250X250EUARSENO	82	15.42	0	37.58	0.26	0	0	47.08		100.34
DB39-euarsenoOGanpyrrhotite	70	16.31	0	39.29	0.06	0.06	0.03	47.07	0.16	102.98
DB7-350X75ANARSENO-A3	15	16	0	38.49	0.18	0	0	47.06		101.73

Main mine Dick Zone - Probe Analysis Results

Arsenopyrite Analyses	No	Wt%S	Wt%Ti	Wt%Fe	Wt%Ni	Wt%Cu	Wt%Zn	Wt%As	Wt%Se	Total
DB39-75x50euarseno	56	16.25	0	39.07	0.06	0.09	0.01	47.03	0.26	102.77
DB39-75x50euarseno	57	15.98	0	39.03	0.1	0.07	0	47	0.2	102.39
DB8-200X100ANARSENO	55	15.72	0	37.09	0.14	0.02	0	46.93		99.91
DB28-75x50anarseno	31	15.98	0	39.31	0.01	0	0	46.79	0.16	102.26
DB8-200X100ANARSENO	57	15.62	0	35.77	0.15	0.03	0	46.78		98.36
DB8-400X200EUARSENO	73	15.8	0.01	36.71	0.18	0	0	46.71		99.41
DB7-100X300ANARSENO	31	15.9	0	38	0.13	0	0	46.67		100.71
DB8-600X300SUBEUARSENO	79	15.63	0	35.9	0.14	0	0.01	46.63		98.3
DB8-400X600EUARSENO	85	15.88	0.01	36.52	0.12	0.03	0	46.57		99.14
DB28-600x200subeuarseno	39	16.16	0	39.37	0	0	0	46.56	0.21	102.31
DB28-150x100subeuarseno	26	16.14	0	39.79	0	0	0.01	46.51	0.19	102.63
DC9-100x175anarseno	135	16.14	0	39.55	0.09	0.03	0	46.48	0.25	102.56
DB28-100x100euarseno	36	16.2	0	39.63	0.01	0.03	0.05	46.34	0.24	102.49
DB28-150x150anarseno	49	16.54	0	39.79	0.03	0.05	0.04	46.31	0.18	102.94
DB30-200x300anarseno	78	15.91	0	39.68	0.06	0	0	46.3	0.25	102.21
DB7-100X30ANARSENO	51	16.35	0	38.66	0.11	0	0.05	46.28		101.44
DB30-200x300anarseno	79	15.92	0	39.22	0.05	0	0.03	46.23	0.21	101.66
DB28-600x600euarseno	48	16.41	0	40.21	0.02	0	0	46.12	0.23	102.99
DB7-100X150FRACTUREDEUARSENO	2	16.34	0	37.43	0.04	0	0.01	46.1		99.92
DB28-600x200subeuarseno	37	16.44	0	39.89	0.01	0	0	46.08	0.19	102.62
DB7-100X50SUBEUARSENO-A1	7	16.66	0	39.39	0	0	0.02	46.07		102.14
DC9-100x75subeuarseno	141	16.26	0.01	40.05	0.04	0	0.01	46.02	0.27	102.65
DB30-200x300anarseno	80	15.83	0	39.75	0.07	0	0	46.01	0.24	101.9
DB28-150x150anarseno	51	16.47	0	39.74	0.01	0	0	45.99	0.19	102.4
DB21b-50x100euarseno	15	16.95	0	39.64	0.02	0.01	0	45.94	0.25	102.81
DC9-75x100subeuarseno	133	16.27	0	39.96	0.03	0.06	0.07	45.93	0.23	102.55
DB28-75x50anarseno	32	16.02	0	39.52	0.04	0.02	0	45.9	0.18	101.68
DB28-150x100subeuarseno	27	16.46	0	39.33	0	0.02	0.02	45.86	0.23	101.92
DB28-100x100euarseno	35	16.59	0	40.2	0	0	0.04	45.86	0.19	102.89
DC9-150x225subeuarseno	149	16.44	0	40.2	0.02	0.04	0.01	45.82	0.23	102.76
DB28-150x100subeuarseno	43	16.76	0	40.14	0.01	0.03	0	45.81	0.18	102.93
DB28-150x100subeuarseno	25	16.47	0	39.28	0	0.01	0	45.8	0.24	101.81
DB7-200X200EUARSENO	40	16.71	0	39.42	0.03	0.02	0	45.79		101.98

Main mine Dick Zone - Probe Analysis Results

Arsenopyrite Analyses	No	Wt%S	Wt%Ti	Wt%Fe	Wt%Ni	Wt%Cu	Wt%Zn	Wt%As	Wt%Se	Total
DB28-150x100subeuarseno	44	16.78	0	40.12	0.02	0.01	0.04	45.79	0.17	102.94
DB28-600x200subeuarseno	38	16.56	0	40.12	0.03	0.02	0	45.78	0.18	102.7
DC9-100x75subeuarseno	138	16.42	0	40.4	0.01	0.04	0	45.76	0.26	102.9
DB21b-75x50subeuarseno	19	17.04	0	39.48	0.03	0.04	0.02	45.75	0.17	102.54
DB28-100x100euarseno	34	16.73	0	40.26	0.01	0.02	0	45.75	0.2	102.98
DC9-100x75anarseno	143	16.45	0	40.52	0.01	0.01	0	45.75	0.2	102.94
DB21b-75x200subeuarseno	30	16.8	0	39.85	0.01	0.05	0.01	45.74	0.18	102.64
DB7-150X200SUBEUARSENO-B2	26	16.81	0	38.14	0.04	0.05	0	45.72		100.76
DB21b-50x100euarseno	13	17.2	0	39.69	0.01	0.04	0.04	45.72	0.17	102.87
DB7-100X150FRACTUREDEUARSENO	3	16.96	0.01	39.14	0	0	0	45.7		101.82
DB7-100X50SUBEUARSENO-A3	9	16.94	0	38.03	0.02	0.01	0	45.7		100.69
DB29-200x100subeuarseno	44	16.02	0	39.24	0.03	0	0	45.69	0.24	101.22
DB28-100x100euarseno	41	16.85	0	40.17	0.03	0.01	0.02	45.68	0.16	102.92
DC9-100x75subeuarseno	140	16.21	0	40.03	0.03	0.03	0	45.68	0.22	102.21
DB28-150x150anarseno	50	16.66	0	40.34	0	0.01	0.03	45.65	0.19	102.88
DB28-75x50anarseno	33	16.49	0	39.87	0.02	0.01	0	45.63	0.19	102.22
DB7-100X30ANARSENO	48	16.43	0	36.62	0.13	0.03	0.01	45.61		98.83
DB7-100X30ANARSENO	50	16.95	0.08	37.85	0.04	0	0	45.61		100.52
DC9-100x75anarseno	142	16.52	0.01	40.37	0.01	0.04	0.04	45.6	0.24	102.84
DC9-150x225subeuarseno	150	16.49	0	40.17	0.02	0.06	0	45.58	0.25	102.58
DB7-200X200EUARSENO	41	16.77	0.02	37.26	0.04	0.01	0.04	45.56		99.7
DB7-150X75EUARSENO-B2	11	16.65	0.01	38.94	0.03	0.02	0.02	45.55		101.21
DC9-100x175anarseno	136	16.49	0.01	40.56	0.02	0.05	0.01	45.55	0.21	102.91
DC9-100x75subeuarseno	139	16.25	0	39.74	0.03	0	0	45.52	0.23	101.76
DB21b-75x50subeuarseno	21	17.06	0	39.9	0.01	0.05	0.04	45.42	0.18	102.67
DB7-150X200SUBEUARSENO-B1	25	16.93	0	39.43	0	0.04	0.03	45.4		101.84
DB7-100X150FRACTUREDEUARSENO	1	17.06	0.03	38.83	0.01	0	0	45.34		101.27
DB29-100x50anarseno	35	16.14	0	39.3	0.02	0	0.01	45.34	0.23	101.05
DB21b-75x200subeuarseno	29	17.01	0	39.94	0	0.05	0.01	45.31	0.21	102.53
DB7-100X50SUBEUARSENO-A2	8	16.71	0	38.94	0	0	0	45.29		100.95
DB7-150X200SUBEUARSENO	27	17.1	0	39.21	0.02	0.01	0.01	45.25		101.6
DB30-50x50subeuarseno	53	16.42	0	38.69	0.01	0.03	0	45.25	0.2	100.61
DB29-100x50anarseno	36	16.32	0	39.42	0	0	0.02	45.24	0.23	101.24

Main mine Dick Zone - Probe Analysis Results

Arsenopyrite Analyses	No	Wt%S	Wt%Ti	Wt%Fe	Wt%Ni	Wt%Cu	Wt%Zn	Wt%As	Wt%Se	Total
DB7-300X200SUBEUARSENO	43	16.85	0	37.5	0.03	0.02	0.01	45.23		99.64
DB7-150X75EUARSENO-B1	10	16.85	0	38.38	0.02	0.03	0	45.2		100.49
DB29-100x125euarseno	11	16.31	0.04	39.53	0.03	0.01	0	45.2	0.22	101.35
DB7-150X75EUARSENO-B3	12	17.17	0.01	38.56	0.02	0.02	0.11	45.18		101.07
DB7-100X300ANARSENO	32	16.59	0	38.46	0.01	0.01	0.01	45.16		100.23
DB21b-75x200subeuarseno	28	17.13	0	39.66	0	0.05	0.01	45.15	0.18	102.19
DB7-150X100EUARSENO-C3	24	17.01	0	37.64	0.02	0	0.06	45.14		99.88
DB29-200x200euarseno	17	16.7	0	40.24	0	0.01	0.02	45.13	0.21	102.31
DB29-100x50anarseno	34	16.25	0.2	39.38	0.01	0.01	0	45.13	0.25	101.22
DB29-200x100subeuarseno	43	16.31	0	39.1	0.03	0	0	45.13	0.21	100.78
DB21b-75x75euarseno	3	17	0	39.87	0.01	0.07	0.02	45.12	0.16	102.25
DB7-250X500SUBEUARSENO	28	16.79	0	37.06	0	0	0.06	45.08		98.99
DB30-50x50subeuarseno	57	16.52	0	39.24	0.01	0	0.01	45.08	0.18	101.05
DB7-200X200EUARSENO	42	16.91	0	38.65	0	0	0	45.07		100.64
DB7-300X200SUBEUARSENO	45	16.97	0	38.1	0.02	0.02	0	45.05		100.16
DB7-100X30ANARSENO	47	16.86	0	37.46	0.02	0	0	45.04		99.38
DB30-50x50subeuarseno	55	16.86	0	40.01	0.01	0	0.03	45.03	0.2	102.15
DB7-100X30ANARSENO	46	16.98	0	36.28	0.01	0.02	0	45.01		98.3
DB30-50x50subeuarseno	60	16.6	0	39.95	0.03	0	0	45.01	0.23	101.82
DB30-50x50subeuarseno	58	16.48	0.23	39.47	0.02	0	0	45	0.26	101.48
DB29-200x200euarseno	18	16.78	0	40.05	0	0	0	44.98	0.24	102.06
DB29-100x200subeuarseno	38	16.29	0	39.72	0.02	0	0.03	44.98	0.3	101.35
DB7-350X75ANARSENO-A1	13	17.3	0	38.89	0.01	0	0	44.97		101.18
DB29-75x100euarseno	1	16.61	0	39.57	0.02	0	0	44.96	0.16	101.32
DB7-150X100EUARSENO-C1	22	17.35	0	38.47	0	0.02	0	44.95		100.79
DB7-150X100EUARSENO-C2	23	17.2	0	39.5	0.04	0.03	0	44.93		101.71
DB7-100X30ANARSENO	49	17.02	0.03	38.65	0.05	0.03	0.03	44.93		100.74
DB29-75x100euarseno	2	16.42	0	38.22	0.04	0.01	0	44.93	0.23	99.85
DB30-50x50subeuarseno	52	16.38	0.08	39.33	0.02	0	0.01	44.91	0.21	100.94
DB7-250X500SUBEUARSENO	29	16.99	0.06	39.22	0	0.06	0.04	44.89		101.25
DB29-200x200euarseno	16	16.98	0	40.22	0	0.01	0.04	44.86	0.2	102.32
DB7-300X200SUBEUARSENO	44	16.97	0	39.85	0.02	0	0	44.81		101.66
DB29-100x125euarseno	12	16.57	0	39.61	0.01	0	0.01	44.8	0.16	101.17

Main mine Dick Zone - Probe Analysis Results

Arsenopyrite Analyses	No	Wt%S	Wt%Ti	Wt%Fe	Wt%Ni	Wt%Cu	Wt%Zn	Wt%As	Wt%Se	Total
DB7-350X75ANARSENO-A2	14	16.32	0	37.3	0.04	0	0.01	44.77		98.45
DB21b-75x100euarseno	4	17.02	0	40.24	0.01	0.09	0.03	44.73	0.21	102.33
DB29-100x200subeuarseno	37	16.4	0.3	39.92	0.02	0	0.02	44.66	0.24	101.55
DB21b-75x100euarseno	5	16.91	0	40.09	0.02	0.07	0.02	44.61	0.24	101.96
DB29-100x125euarseno	10	16.67	0	39.67	0.04	0.01	0.05	44.59	0.21	101.24
DB7-250X500SUBEUARSENO	30	17.11	0	37.45	0	0.03	0	44.57		99.17
DB21b-75x75euarseno	2	17.18	0	39.62	0.02	0.1	0	44.55	0.21	101.68
DB29-100x200subeuarseno	39	16.59	0	39.15	0.01	0.01	0.01	44.55	0.2	100.51
DB30-50x50subeuarseno	59	16.9	0	39.62	0	0.01	0.02	44.48	0.18	101.22
DB29-75x100euarseno	3	16.68	0	37.82	0.01	0	0.02	44.44	0.26	99.23
DB29-200x100subeuarseno	45	16.37	0	39.21	0.03	0	0	44.39	0.21	100.21
DB7-100X300ANARSENO	33	17.24	0	39.04	0	0.04	0.02	44.36		100.71
DB21b-100x150subeuarseno	11	17.2	0	40.38	0	0.09	0	44.31	0.23	102.22
DB21b-100x150subeuarseno	10	17.05	0	40.44	0	0.11	0.05	44.28	0.21	102.15
DB21b-75x100euarseno	6	17.17	0.01	40.33	0.01	0.13	0	44.17	0.19	102.01
DB21b-100x150subeuarseno	12	17.53	0	40.32	0.01	0.08	0.02	44.04	0.24	102.24
DB30-50x50subeuarseno	56	16.05	1.73	38.06	0.01	0.01	0	42.51	0.21	98.58
DB30-50x50subeuarseno	54	17.7	0.01	42.28	0.01	0	0.01	41.81	0.15	101.96
Pyrite Analyses	**No**	**Wt%S**	**Wt%Ti**	**Wt%Fe**	**Wt%Ni**	**Wt%Cu**	**Wt%Zn**	**Wt%As**	**Wt%Se**	**Total**
DB21b-200x150subeupyrite	7	46.59	0	54.01	0.01	0.05	0.02	0.01	0	100.7
DB21b-200x150subeupyrite	8	46.26	0	53.57	0.04	0.04	0	0	0	99.92
DB21b-75x50subeupyrite	23	46.16	0.02	53.4	0.01	0.09	0	0.01	0	99.69
DB21b-200x150subeupyrite	9	46.13	0	53.7	0.01	0.09	0.02	0.03	0	99.99
DB21b-75x100anpyrite	26	46.1	0	53.14	0	0.09	0	0.05	0.01	99.39
DB21b-75x150anpyrite	18	46.06	0	52.98	0.02	0.05	0.03	0	0	99.15
DB21b-75x100anpyrite	27	46.05	0	53.75	0.02	0.06	0.02	0.01	0	99.91
DB21b-200x200subeupyrite	32	45.97	0	53.87	0.01	0.05	0.04	0.04	0	99.98
DB21b-75x100anpyrite	25	45.95	0	53.07	0.04	0.05	0.03	0.02	0.01	99.17
DB21b-200x200subeupyrite	33	45.94	0	53.96	0	0.02	0.01	0.03	0	99.97
DB21b-75x50subeupyrite	24	45.93	0	52.53	0.01	0.14	0	0	0	98.61
DB21b-200x200subeupyrite	31	45.85	0.01	54.03	0.03	0.04	0	0.12	0	100.09
DB21b-75x150anpyrite	16	45.82	0	53.63	0.01	0.17	0.02	0.23	0	99.88
DB21b-75x50subeupyrite	22	45.79	0	53.17	0	0.08	0.01	0.22	0	99.28

Main mine Dick Zone - Probe Analysis Results

Pyrite Analyses	No	Wt%S	Wt%Ti	Wt%Fe	Wt%Ni	Wt%Cu	Wt%Zn	Wt%As	Wt%Se	Total
DB21b-150x50anpyrite	36	45.76	0	52.67	0	0.03	0.03	0.27	0	98.78
DB21b-150x50anpyrite	34	45.73	0.01	53.84	0	0.07	0	0.25	0	99.9
DB21b-75x150anpyrite	17	45.58	0	53.07	0.02	0.98	0	0	0	99.66
DB21b-150x50anpyrite	35	45.53	0	53.4	0.02	0.05	0	0.71	0	99.72
DC9-75x50subeupyrite	154	45.48	0	54.76	0.01	0.04	0.04	0	0.01	100.34
DC9-200x500Anpyrite	168	45.45	0	54.94	0.03	0.03	0	0.01	0	100.47
DC9-100x150subeupyrite	163	45.37	0	54.56	0.01	0.05	0	0.01	0.01	100.01
DC9-100x150subeupyrite	162	45.36	0	54.68	0.01	0.02	0	0	0	100.08
DC9-300x100Anpyrite	164	45.19	0.02	53.85	0.02	0.1	0	0.03	0	99.23
DC9-100x150subeupyrite	161	45.19	0	54.16	0.03	0.01	0.03	0	0.02	99.44
DC9-300x100Anpyrite	165	45.13	0.03	54.6	0.03	0.14	0.02	0.01	0.01	99.97
DC9-50x150anpyrite	160	45.1	0	54.27	0.01	0.39	0.02	0.01	0.03	99.82
DC9-200x500Anpyrite	167	45.1	0	54.38	0.02	0.52	0.03	0.01	0	100.06
DC9-50x150subeupyrite	151	45.06	0	54.66	0.02	0.05	0	0	0	99.8
DC9-300x100Anpyrite	166	45.06	0	54.25	0.01	0	0	0	0.01	99.33
DC9-200x500Anpyrite	169	45.03	0	54.35	0.03	0.27	0.02	0	0.02	99.73
DC9-50x150anpyrite	159	44.98	0.01	54.55	0.02	0.4	0	0	0.02	99.97
DC9-50x150subeupyrite	152	44.88	0	54.08	0	0.02	0.01	0.02	0.02	99.04
DC9-50x150anpyrite	158	44.81	0	53.91	0.22	0.4	0	0.01	0.01	99.36
DC9-75x50subeupyrite	156	44.64	0	54.15	0.03	0.04	0.01	0.03	0	98.9
DC9-50x150subeupyrite	153	44.25	0	53.33	0.04	1.26	0.02	0	0.03	98.94
Pyrrhotite Analyses	**No**	**Wt%S**	**Wt%Ti**	**Wt%Fe**	**Wt%Ni**	**Wt%Cu**	**Wt%Zn**	**Wt%As**	**Wt%Se**	**Total**
DB8-800X300SUBEUPYRHOTITE	97	34.05	0	66.76	0.1	0.04	0.01	0		100.96
DB8-300X300ANPYRHOTITE	72	33.99	0	66.62	0.09	0.03	0	0.02		100.74
DB8-300X300ANPYRHOTITE	70	33.97	0	66.35	0.1	0	0	0		100.42
DB8-250X250SUBEUPYRHOTITE	95	33.97	0	66.56	0.08	0	0.01	0		100.64
DB8-450X50ANPYRHOTITE	58	33.96	0	67.88	0.05	0	0	0.01		101.91
DB8-800X300SUBEUPYRHOTITE	99	33.96	0	66.26	0.1	0.06	0.01	0		100.38
DB8-250X250SUBEUPYRHOTITE	96	33.94	0	67.26	0.09	0.02	0	0.02		101.34
DB8-450X50ANPYRHOTITE	60	33.93	0	67.23	0.04	0	0	0		101.21
DB8-200X150ANPYRHOTITE	52	33.91	0	67.56	0.11	0.01	0.01	0		101.6
DB8-100X300SUBEUPYRHOTITE	64	33.91	0	65.37	0.1	0	0	0		99.39
DB8-100X300SUBEUPYRHOTITE	65	33.91	0.01	65.7	0.13	0	0	0		99.76

Main mine Dick Zone - Probe Analysis Results

Pyrrhotite Analyses	No	Wt%S	Wt%Ti	Wt%Fe	Wt%Ni	Wt%Cu	Wt%Zn	Wt%As	Wt%Se	Total
DB8-600X300ANPYRHOTITE	63	33.9	0	65.76	0.12	0	0	0.01		99.79
DB8-600X300ANPYRHOTITE	61	33.87	0	64.99	0.08	0.01	0	0.03		98.97
DB8-450X50ANPYRHOTITE	59	33.87	0	65.73	0.07	0	0	0		99.67
DB8-200X150ANPYRHOTITE	54	33.84	0	66.64	0.09	0	0.03	0.01		100.62
DB8-600X300ANPYRHOTITE	62	33.84	0	67.15	0.11	0	0.01	0		101.12
DB8-100X300SUBEUPYRHOTITE	66	33.81	0	67.2	0.13	0	0.05	0.04		101.22
DB8-200X150ANPYRHOTITE	53	33.8	0	66.72	0.16	0.03	0.01	0.03		100.74
DB8-300X300ANPYRHOTITE	71	33.76	0.01	65.21	0.11	0	0.04	0.01		99.14
DB8-250X250SUBEUPYRHOTITE	94	33.75	0	67.09	0.06	0.02	0	0		100.93
DB8-800X300SUBEUPYRHOTITE	98	33.63	0.01	67.21	0.03	0.04	0	0.03		100.96
DB21b-150x50anpyrrhotite	38	33.63	0	67.55	0	0.06	0.02	0	0	101.27
DB28-400x150anpyrrhotite	17	33.62	0	66.61	0.03	0	0.03	0	0	100.29
DB21b-150x50anpyrrhotite	39	33.61	0	67.96	0.04	0.05	0	0.01	0	101.68
DB39-200x100anpyrrhotite	45	33.58	0	67.51	0.05	0.05	0.02	0.02	0	101.24
DB39-200x100anpyrrhotite	44	33.56	0	68.6	0.04	0.05	0.02	0	0	102.28
DB39-150x75anpyrrhotite	46	33.55	0	67.96	0.03	0.04	0.01	0	0	101.58
DB39-200x100anpyrrhotite	43	33.53	0	67.47	0.06	0.06	0.03	0	0	101.16
DB39-300x100anpyrrhotite	62	33.5	0	67.62	0.07	0.07	0.01	0.01	0	101.29
DB21b-150x50anpyrrhotite	37	33.49	0	68.44	0	0.07	0 02	0	0.02	102.04
DB39-75x50anpyrrhotiteOgbyarseno	59	33.49	0	67.74	0.03	0.05	0.03	0	0	101.35
DB39-75x50anpyrrhotiteOgbyarseno	60	33.49	0	68.47	0.04	0.07	0	0	0	102.08
DB39-75x50anpyrrhotiteOgbyarseno(56+57)	58	33.48	0	67.7	0.03	0.06	0	0	0	101.28
DB39-150x75anpyrrhotite	47	33.44	0.01	66.99	0.04	0.07	0.01	0	0	100.57
DB39-250x75anpyrrhotite	41	33.43	0	67.75	0.05	0.06	0.02	0	0	101.33
DB39-300x100anpyrrhotite	61	33.41	0	68.35	0.06	0.04	0.03	0.02	0	101.92
DB39-250x75anpyrrhotite	42	33.41	0	68.23	0.04	0.04	0	0.01	0	101.74
DB28-400x150anpyrrhotite	18	33.38	0	67.08	0	0	0.02	0.01	0	100.49
DB39-250x75anpyrrhotite	40	33.37	0.01	67.2	0.06	0.05	0.01	0.03	0.02	100.76
DB39-300x100anpyrrhotite	63	33.33	0.02	68.31	0.06	0.09	0.02	0.01	0	101.83
DB28-100x50anpyrrhotite	13	33.32	0.06	68.18	0	0.01	0.03	0.02	0	101.63
DB30-100x150anpyrrhotite	73	33.26	0	68.41	0.03	0	0.02	0	0.01	101.74
DB7-600X300ANPYRHOTITE	39	33.22	0	65.26	0.01	0	0	0.01		98.5
DB28-100x50anpyrrhotite	14	33.17	0	68.45	0.01	0	0.05	0	0	101.7

Main mine Dick Zone - Probe Analysis Results

Pyrrhotite Analyses	No	Wt%S	Wt%Ti	Wt%Fe	Wt%Ni	Wt%Cu	Wt%Zn	Wt%As	Wt%Se	Total
DB7-300X150ANPYRHOTITE-A1	4	33.14	0	64.89	0.06	0	0.05	0		98.15
DB39-150x75anpyrrhotite	48	33.12	0.03	67.26	0.07	0.07	0.04	0	0.02	100.62
DB28-600x200anpyrrhotite	22	33.11	0	68.7	0.03	0	0.02	0.01	0	101.88
DB28-600x200anpyrrhotite	24	33.1	0	68.47	0	0.02	0.02	0.01	0.01	101.63
DB7-600X300ANPYRHOTITE	38	33.1	0	67.41	0.03	0	0	0		100.55
DB7-450X400ANPYRHOTITE-B2	17	33.03	0	68.2	0.03	0.03	0.01	0		101.3
DB7-150X100ANPYRHOTITE	35	33.02	0	66.19	0.04	0.01	0	0		99.27
DB30-100x150anpyrrhotite	74	32.91	0	68.04	0.05	0	0.02	0	0.02	101.04
DB30-300x200subeupyrrhotite	76	32.87	0	67.85	0.06	0	0.01	0.04	0	100.83
DB30-300x200subeupyrrhotite	75	32.87	0	67.34	0.03	0	0	0	0	100.25
DB7-450X200ANPYRHOTITE-C1	19	32.86	0	68.51	0.01	0.02	0.05	0.03		101.46
DB7-150X100ANPYRHOTITE	36	32.85	0	66.35	0.01	0	0	0		99.21
DB39-anpyrrhotiteOGbyeuarseno	74	32.83	0	67.83	0.08	0.06	0	0	0	100.8
DB39-anpyrrhotiteOGbyeuarseno	73	32.82	0	68.78	0.11	0.01	0	0.02	0	101.75
DB7-450X400ANPYRHOTITE-B3	18	32.82	0	67.84	0.03	0	0	0		100.69
DB29-150x75subeupyrrhotite	13	32.8	0	68.48	0.03	0	0	0	0	101.33
DB7-600X300ANPYRHOTITE	37	32.78	0	66.8	0.09	0	0	0		99.68
DB7-450X200ANPYRHOTITE-C3	21	32.76	0	68.7	0.05	0	0	0.02		101.54
DB30-300x200subeupyrrhotite	77	32.76	0	68.3	0.01	0	0.03	0	0	101.1
DB39-anpyrrhotiteOGbyeuarseno	75	32.76	0	68.79	0.1	0.07	0	0	0.04	101.77
DB7-300X150ANPYRHOTITE-A2	5	32.75	0	67.84	0	0	0.05	0		100.65
DB7-150X100ANPYRHOTITE	34	32.75	0.01	66.72	0.03	0	0.02	0		99.54
DB28-600x200anpyrrhotite	23	32.7	0	67.99	0.01	0	0.01	0	0	100.73
DB39-400x100anpyrrhotite	69	32.7	0	66.49	0.04	0.08	0.01	0	0	99.32
DB29-150x75subeupyrrhotite	14	32.69	0	68	0.01	0	0	0	0	100.71
Db66-200x100anpyrrhotite	86	32.66	0	69.07	0.1	0.05	0.02	0.01	0	101.9
DB7-450X400ANPYRHOTITE-B1	16	32.64	0	66.81	0.04	0.01	0.01	0.03		99.55
DB39-200x75subeupyrrhotite	66	32.64	0	65.06	0.06	0.06	0.01	0.01	0	97.85
DB30-100x50anpyrrhotite	71	32.62	0	68.18	0.01	0.03	0	0	0	100.85
Db66-200x100anpyrrhotite	87	32.6	0	69.04	0.13	0.07	0.02	0	0	101.86
DB30-100x50anpyrrhotite	70	32.57	0	67.74	0.02	0	0.01	0	0	100.34
Db66-200x100anpyrrhotite	85	32.57	0	69.29	0.07	0.1	0.01	0	0.02	102.06
DB30-100x100subeupyrrhotite	63	32.54	0	68.88	0.06	0	0	0	0	101.49

Main mine Dick Zone - Probe Analysis Results

Pyrrhotite Analyses	No	Wt%S	Wt%Ti	Wt%Fe	Wt%Ni	Wt%Cu	Wt%Zn	Wt%As	Wt%Se	Total
DB29-100x35anpyrrhotite	8	32.51	0	67.2	0.03	0	0.01	0	0	99.76
DB39-200x75subeupyrrhotite	65	32.51	0	64.8	0.04	0.05	0	0	0	97.4
Db66-100x150anpyrrhotite	84	32.5	0	68.81	0.09	0.08	0.04	0	0	101.55
DB30-100x100subeupyrrhotite	62	32.47	0	69.08	0.05	0.01	0.02	0.01	0	101.64
DB7-300X150ANPYRHOTITE-A3	6	32.46	0.01	68	0.06	0.03	0.02	0		100.57
DB30-200x150subeupyrrhotite	68	32.41	0	68.65	0	0.01	0.01	0.03	0	101.12
DB30-200x150subeupyrrhotite	67	32.41	0	68.23	0.05	0.02	0	0	0	100.71
DB29-100x400anpyrrhotite	22	32.38	0	68.67	0	0	0.05	0	0	101.11
DB30-200x150subeupyrrhotite	69	32.35	0	68.28	0.03	0	0.03	0	0	100.7
Db66-50x100anpyrrhotite	91	32.35	0	68.76	0.03	0.23	0.01	0	0.04	101.41
DB30-300x150anpyrrhotite	64	32.34	0	68.71	0.05	0	0	0.01	0	101.12
DB29-100x400anpyrrhotite	24	32.33	0	68.75	0	0	0	0.02	0.02	101.12
DB29-125x75subeupyrrhotite	46	32.31	0	68.35	0.04	0.01	0.02	0.02	0	100.76
Db66-100x150anpyrrhotite	82	32.31	0.01	68.37	0.1	0.09	0.04	0	0	100.94
Db66-100x150anpyrrhotite	83	32.31	0	69.45	0.09	0.06	0	0	0	101.92
DB30-100x100subeupyrrhotite	61	32.29	0	68.93	0.06	0	0.02	0	0	101.31
DB39-400x100anpyrrhotite	67	32.26	0	66.12	0.07	0.06	0	0.01	0	98.53
DB29-125x75subeupyrrhotite	48	32.25	0	68.67	0.06	0	0	0	0	100.99
DB29-100x400anpyrrhotite	25	32.23	0.01	67.87	0	0.02	0	0	0	100.14
DB30-300x150anpyrrhotite	66	32.23	0	68.9	0.05	0.01	0	0	0	101.21
DB29-75x75eupyrrhotite	6	32.19	0	68.41	0.06	0	0.02	0.01	0	100.69
DB29-75x75anpyrr.asswitheuarseno(d)	20	32.19	0	68.5	0	0.02	0	0	0.02	100.73
DB39-400x100anpyrrhotite	68	32.19	0	66.59	0.09	0.03	0	0	0	98.92
DB30-100x150anpyrrhotite	72	32.18	0	68.4	0.07	0	0.02	0	0	100.68
DB29-125x75subeupyrrhotite	47	32.11	0	68.03	0.04	0.01	0.02	0	0	100.22
DB29-75x75anpyrr.asswitheuarseno(d)	19	32.08	0	67.35	0	0	0	0.02	0	99.46
DB29-100x35anpyrrhotite	9	32.07	0	68.01	0.05	0	0.02	0	0	100.16
DB29-100x400anpyrrhotite	23	32.05	0	68.95	0	0	0	0	0	101.01
DB29-300x400anpyrrhotite	42	32.05	0	68.53	0.06	0.01	0.03	0	0	100.69
DB29-100x35anpyrrhotite	7	32.03	0	67.73	0.05	0	0.01	0	0	99.84
DB29-300x400anpyrrhotite	40	32.01	0	68.31	0.05	0	0	0.01	0	100.38
DB29-75x75anpyrr.asswitheuarseno(d)	21	31.97	0	67.85	0	0	0.03	0	0	99.85
DB30-300x150anpyrrhotite	65	31.94	0	67.95	0.06	0	0	0	0	99.97

Main mine Dick Zone - Probe Analysis Results

Pyrrhotite Analyses	No	Wt%S	Wt%Ti	Wt%Fe	Wt%Ni	Wt%Cu	Wt%Zn	Wt%As	Wt%Se	Total
DB29-75x75eupyrrhotite	5	31.88	0.03	67.43	0.05	0	0.02	0	0	99.41
DB29-75x75eupyrrhotite	4	31.86	0.01	65.82	0.07	0	0	0.03	0	97.79
DB29-300x400anpyrrhotite	41	31.84	0	68.47	0.02	0	0	0	0	100.33
DB7-450X200ANPYRHOTITE-C2	20	31.77	0	66.9	0.03	0	0.01	0.04		98.75
DB29-150x75subeupyrrhotite	15	31.19	0	66.54	0.04	0	0.01	0	0	97.79
DB29-125x75subeupyrrhotite	49	30.96	0	67.94	0.04	0	0.03	0	0	98.98
Db66-50x100anpyrrhotite	93	30.89	0	71.26	0.01	0.08	0.05	0	0	102.3
Db66-50x100anpyrrhotite	92	30.73	0	71.92	0.03	0.08	0.03	0.03	0	102.85

New Britannia Mine, Ruttan Zone - Sulphide Electron Microprobe Analysis Results

Arsenopyrite Analyses	No	Wt%S	Wt%Ti	Wt%Fe	Wt%Ni	Wt%Cu	Wt%Zn	Wt%As	Wt%Sc	Wt%Te	Wt%Pb	Total
RA5-100x75anarseno-a1	46	13.45	0	32.56	0.73	0	0.04	50.68	0.22	0	0	97.68
RA5-50x200anarseno-c1	52	13.91	0.01	33.37	0.72	0	0.01	50	0.16	0	0	98.2
RA5-350x200anarseno-b3	51	14.6	0	35.17	0.33	0	0	49.22	0.24	0	0	99.58
RD1-fgsubeuhedralarseno-b2	85	15.20	0.00	36.48	0.34	0.06	0.04	48.96				101.07
RA5-100x75anarseno-a3	48	14.86	0	34.79	0.27	0.01	0	48.83	0.22	0.02	0	99.01
RD1-fgsubeuhedralarseno-b3	86	15.43	0.00	38.07	0.24	0.00	0.06	48.57				102.38
RA5-350x200anarseno-b1	49	15.32	0	36.85	0.19	0.01	0	48.55	0.16	0	0	101.09
RA5-350x200anarseno-b2	50	15.32	0	36.86	0.18	0	0.03	48.51	0.2	0	0	101.1
RA5-50x200anarseno-c2	53	15.19	0	36.61	0.25	0	0	48.31	0.27	0	0	100.64
RA5-50x200anarseno-c3	54	15.28	0	36.07	0.3	0.07	0.03	48.27	0.16	0	0	100.2
RA5-100x75anarseno-a2	47	15.29	0	36.26	0.19	0.02	0.04	48.23	0.21	0	0	100.24
RD1-cgsubeuhedralarseno-a2	77	15.84	0.00	37.92	0.11	0.00	0.01	48.20				102.09
RD1-cgsubeuhedralarseno-a1	76	15.80	0.00	38.58	0.08	0.02	0.00	48.14				102.62
RD1-fgsubeuhedralarseno-b1	84	15.63	0.00	37.11	0.25	0.00	0.00	48.12				101.11
RA1-100x50euarseno-b1	54	15.86	0.05	38.43	0.29	0.02	0.01	48.05	0.19	0	0	102.9
RD1-cgsubeuhedralarseno-a3	78	15.78	0.00	38.91	0.07	0.00	0.04	47.93				102.73
RA1-200x150euarseno-a1	51	15.91	0.02	38.44	0.27	0.03	0.04	47.85	0.22	0	0	102.77
RA3-50x75anarseno-a1	7	15.46	0	34.51	0.17	0	0.02	47.67	0.23	0	0	98.06
RA3-50x75anarseno-a3	9	15.6	0.01	34.27	0.16	0	0	47.5	0.19	0	0	97.73
RA3-50x75anarseno-a2	8	15.71	0	34.96	0.16	0	0	47.48	0.21	0	0	98.52
RA4-300x200anarseno-b1	20	15.96	0.03	39.11	0.06	0.05	0.02	47.37	0.18	0	0	102.79
RA1-200x100anarseno-b2	73	16.33	0	39.25	0.05	0	0.05	47.11	0.19	0	0	102.99
RA3-75x100anarseno-b1	16	16.56	0	38.92	0.06	0	0.03	46.55	0.22	0	0	102.35
RA1-150x200subeuarseno-a1	63	16.6	0	39.05	0.05	0.01	0	46.51	0.21	0	0	102.44
RA1-250x100anarseno-c3	77	16.92	0	39.34	0.04	0	0	46.39	0.17	0	0	102.86
RA1-200x150euarseno-a3	53	16.85	0	38.65	0	0.01	0	46.38	0.2	0	0	102.1
RA3-50x100subeuarseno-c1	13	16.82	0	37.97	0.01	0	0.02	46.37	0.22	0	0	101.43
RA1-200x150euarseno-a2	52	16.82	0.01	38.88	0.05	0.02	0	46.29	0.21	0	0	102.28
RA1-200x100anarseno-b3	74	16.89	0	39.77	0	0	0.02	46.19	0.18	0	0	103.06
RA3-100x200eudgrayarseno-c1	40	17.11	0	39.48	0.01	0	0	46.14	0.12	0	0	102.85
RA1-100x50euarseno-b3	56	17.13	0	39.5	0.03	0.03	0	46.1	0.19	0	0	102.98
RA3-100x75euarseno-c4	30	16.88	0	39.63	0.06	0	0	46.1	0.17	0	0	102.84
RA3-50x100subeuarseno-c3	15	16.99	0	39.19	0.03	0.04	0	46.04	0.2	0	0	102.49

New Britannia Mine, Ruttan Zone - Sulphide Electron Microprobe Analysis Results

Arsenopyrite Analyses	No	Wt%S	Wt%Ti	Wt%Fe	Wt%Ni	Wt%Cu	Wt%Zn	Wt%As	Wt%Se	Wt%Te	Wt%Pb	Total
RC2-150X75SUBEUARSENOSURRAU-B3	4	16.67	0	39.92	0.03	0	0.05	46.02	0.21	0	0	102.9
RA4-200x150anarseno-c2	24	16.73	0	39.75	0	0	0	45.99	0.14	0	0	102.61
RA1-200x100anarseno-a3	71	16.86	0	39.49	0	0.04	0.03	45.95	0.22	0	0	102.59
RA3-100x100euarseno-a2	20	17.1	0	39.36	0.02	0	0.05	45.87	0.21	0	0	102.61
RA3-75x75subeuarseno-b3	6	17	0	39.96	0.02	0	0.02	45.85	0.14	0	0	102.99
RA3-200x100subeuarseno-a1	1	17.18	0	39.74	0.03	0.02	0	45.66	0.25	0	0	102.87
RA3-100x100euarseno-b1	22	17.38	0	39.48	0.05	0.02	0.01	45.61	0.14	0	0	102.7
RA3-100x75euarseno-c2	28	17.18	0	39.74	0.05	0	0	45.58	0.14	0	0	102.69
RA3-75x100anarseno-b3	18	17.08	0.02	38.86	0.03	0.02	0.03	45.51	0.18	0	0	101.75
RA4-300x200subeuarseno-a2	16	17.09	0	39.95	0.01	0	0	45.46	0.15	0.01	0	102.66
RC2-150X100EUARSENO-C3	27	17.11	0	39.95	0.04	0.01	0	45.44	0.27	0	0	102.84
RC2-150X75SUBEUARSENOSURRAU-B4	5	16.98	0	39.82	0.03	0.02	0.02	45.27	0.29	0	0	102.44
RA4-200x150anarseno-c3	25	17.36	0	39.42	0	0	0	45.21	0.19	0	0	102.19
RC2-300X75EUARSENO-B3	24	17.01	0	38.62	0.02	0.04	0.02	45.12	0.21	0	0	101.05
RA4-200x150anarseno-c1	23	17.41	0	39.69	0.01	0.01	0	45.1	0.15	0	0	102.37
RA4-200x150euarseno-a1	26	17.32	0	40.04	0.04	0.03	0.02	45.07	0.19	0	0	102.72
RC2-150X100FRACTUREDARSENO-C1	16	16.96	0	40.07	0.01	0.05	0.01	45.04	0.24	0	0	102.37
RA4-300x200anarseno-b2	21	17.69	0	39.69	0	0.02	0	44.97	0.23	0	0	102.6
RC2-75X75EUARSENO-A3	21	17.26	0	40.23	0	0	0.01	44.9	0.21	0	0	102.63
RC2-300X100FRACTUREDARSENO-B3	15	17.21	0	40.32	0.02	0	0.01	44.83	0.29	0	0	102.68
RC2-150X100EUARSENO-C1	25	17.39	0	39.86	0	0.02	0.04	44.65	0.27	0	0	102.23
RC2-150X100EUARSENO-C2	26	17.32	0	40.81	0	0	0.01	44.62	0.17	0	0	102.93
RC2-300X100FRACTUREDARSENO-B1	13	17.22	0	40.03	0.01	0	0.02	44.59	0.16	0	0	102.03
RC2-150X100FRACTUREDARSENO-C2	17	17.4	0.02	39.96	0.01	0	0.03	44.55	0.21	0	0	102.17
RC2-300X100FRACTUREDARSENO-B2	14	17.26	0	39.76	0.02	0	0	44.54	0.22	0	0	101.81
RC2-100X50SUBEUARSENO-C3	9	17.34	0	39.46	0.03	0.02	0.07	44.52	0.23	0	0	101.67
RC2-200X50FRACTUREDARSENO-A1	10	17.5	0	39.75	0.06	0	0	44.51	0.21	0	0	102.03
RC2-200X50FRACTUREDARSENO-A2	11	17.47	0	39.46	0.02	0.02	0.03	44.33	0.27	0	0	101.59
RC2-150X75SUBEUARSENOSURRAU-B5	6	17.74	0	39.39	0.01	0.04	0	44.31	0.17	0	0	101.66
RC2-300X75EUARSENO-B1	22	17.6	0	40.03	0.03	0.01	0.01	44.22	0.13	0	0	102.04
RC2-75X75EUARSENO-A1	19	17.52	0	40.61	0	0	0	44.15	0.25	0	0	102.53
RC2-75X75EUARSENO-A2	20	17.43	0	40.39	0	0	0.08	44.09	0.19	0	0	102.19
RC2-200X50FRACTUREDARSENO-A3	12	17.55	0.03	39.73	0.03	0	0.02	44.04	0.18	0	0	101.59

New Britannia Mine, Ruttan Zone - Sulphide Electron Microprobe Analysis Results

Arsenopyrite Analyses	**No**	**Wt%S**	**Wt%Ti**	**Wt%Fe**	**Wt%Ni**	**Wt%Cu**	**Wt%Zn**	**Wt%As**	**Wt%Se**	**Wt%Te**	**Wt%Pb**	**Total**
RC2-100X50SUBEUARSENO-C2	8	17.74	0.02	39.82	0	0	0	43.65	0.19	0.02	0	101.45
Pyrite Analyses	**No**	**Wt%S**	**Wt%Ti**	**Wt%Fe**	**Wt%Ni**	**Wt%Cu**	**Wt%Zn**	**Wt%As**	**Wt%Se**	**Wt%Te**	**Wt%Pb**	**Total**
RD1-fgsubeuhedralpyrite-a1	61	46.94	0.00	53.21	0.02	0.07	0.01	0.02				100.28
RD1-mganhedralpyrite-d1	67	46.75	0.00	53.95	0.10	0.01	0.00	0.05				100.86
RD1-fgsubeuhedralpyrite-a3	63	46.70	0.00	53.92	0.03	0.03	0.00	0.00				100.69
RD1-fgeuhedralpyrite-b2	53	46.60	0.00	53.38	0.12	0.00	0.00	0.05				100.15
RD1-cganhedralpyritewithchalcoincl.-e2	88	46.59	0.00	52.36	0.36	0.00	0.00	0.03				99.34
RD1-fgsubeuhedralpyrite-a2	62	46.58	0.00	53.98	0.03	0.05	0.00	0.00				100.64
RD1-fgeuhedralpyrite-c2	56	46.56	0.00	53.07	0.10	0.03	0.05	0.00				99.81
RD1-mganhedralpyrite-d3	69	46.55	0.00	53.11	0.11	0.01	0.04	0.00				99.83
RD1-mganhedralpyrite-a1	40	46.55	0.00	53.66	0.10	0.00	0.00	0.01				100.32
RD1-mganhedralpyrite-d2	68	46.54	0.00	53.79	0.07	0.00	0.06	0.01				100.47
RD1-fgeuhedralpyrite-b1	52	46.50	0.00	53.52	0.06	0.00	0.02	0.01				100.11
RD1-fgeuhedralpyrite-a1	49	46.49	0.00	53.67	0.11	0.03	0.00	0.02				100.32
RD1-cganhedralpyritewithchalcoincl.-e1	87	46.46	0.02	53.71	0.06	0.00	0.00	0.00				100.26
RD1-cganhedralpyritewithchalcoincl.-e3	89	46.39	0.01	52.22	0.05	0.01	0.03	0.03				98.74
RD1-fgeuhedralpyrite-c1	55	46.38	0.00	53.94	0.09	0.01	0.00	0.00				100.42
RD1-fgeuhedralpyrite-c3	57	46.38	0.00	53.29	0.16	0.00	0.00	0.03				99.87
RD1-fgeuhedralpyrite-b3	54	46.32	0.01	53.36	0.08	0.03	0.04	0.03				99.87
RD1-fgeuhedralpyrite-a2	50	46.30	0.00	52.95	0.23	0.05	0.04	0.01				99.58
RD1-fgeuhedralpyrite-a3	51	46.07	0.00	53.72	0.05	0.00	0.00	0.05				99.90
RD1-fgeuhedralpyrite-b2	83	46.03	0.00	52.25	0.00	0.01	0.04	0.02				98.35
RC1-400x200anpyrite-c1	67	45.92	0	53.33	0.29	0.02	0.01	0	0.03	0	0	99.6
RC1-700x300anpyrite-a2	53	45.82	0	53.65	0.06	0	0.03	0.04	0.02	0	0	99.61
RC2-200X100ANPYRITE-B3	37	45.8	0	53.32	0.37	0.02	0.02	0.1	0	0	0	99.63
RC1-400x200anpyrite-c2	68	45.8	0.01	54.14	0.17	0.02	0	0	0	0	0	100.14
RC2-200X100ANPYRITE-B2	36	45.71	0	53.34	0.22	0	0.01	0.01	0	0	0	99.29
RC1-600x300anpyrite-b2	56	45.68	0	53.01	0.05	0.03	0.01	0.01	0	0	0	98.79
RC2-200X500SUBEUPYRITE-A3	30	45.65	0	53.29	0.06	0.02	0	0.03	0.01	0	0	99.05
RC2-200X500SUBEUPYRITE-A4	31	45.63	0	53.72	0.04	0	0.02	0.06	0	0	0	99.48
RC2-200X500SUBEUPYRITE-A2	29	45.61	0	53.54	0.09	0	0	0.07	0.01	0	0	99.33
RC2-200X100ANPYRITE-B1	35	45.58	0	52.51	0.17	0	0	0.03	0	0	0	98.29
RC1-700x300anpyrite-a1	52	45.55	0	52.82	0.58	0	0.01	0	0.01	0.01	0	98.99

New Britannia Mine, Ruttan Zone - Sulphide Electron Microprobe Analysis Results

Pyrite Analyses	**No**	**Wt%S**	**Wt%Ti**	**Wt%Fe**	**Wt%Ni**	**Wt%Cu**	**Wt%Zn**	**Wt%As**	**Wt%Se**	**Wt%Te**	**Wt%Pb**	**Total**
RD1-mganhedralpyrite-a3	42	45.54	0.00	52.11	0.17	0.00	0.00	0.00				97.82
RC1-600x300anpyrite-b3	57	45.53	0	53.64	0.03	0.05	0	0	0.01	0	0	99.27
RC1-700x300anpyrite-a3	54	45.52	0	53.87	0	0	0.01	0	0	0	0	99.41
RC1-600x300anpyrite-b1	55	45.46	0	52.74	0	0.26	0.09	0	0	0	0	98.56
RD1-mganhedralpyrite-a2	41	45.43	0.00	52.62	0.02	0.00	0.00	0.00				98.07
RC2-100X400ANPYRITE-A3	34	45.41	0.02	53.32	0.27	0	0.08	0.01	0	0	0	99.12
RC2-100X400ANPYRITE-A1	32	45.37	0	53.72	0.04	0.03	0.02	0.01	0	0	0	99.2
RC1-400x200anpyrite-c3	69	45.31	0	53.34	0.04	0.58	0.06	0	0.02	0	0	99.35
RC2-200X500SUBEUPYRITE-A1	28	45.24	0	53.74	0.09	0.02	0	0.08	0.01	0	0	99.17
RC2-100X400ANPYRITE-A2	33	44.7	0	52.87	0.1	0.03	0.05	0.17	0	0	0	97.92
Pyrrhotite Analyses	**No**	**Wt%S**	**Wt%Ti**	**Wt%Fe**	**Wt%Ni**	**Wt%Cu**	**Wt%Zn**	**Wt%As**	**Wt%Se**	**Wt%Te**	**Wt%Pb**	**Total**
RC2-200X75ANPYRRHOTITE-C1	38	33.83	0	67.3	0.02	0.02	0	0	0.02	0	0	101.19
RD1-fganhedralpyrrhotite-c3	66	34.30	0.00	68.22	0.10	0.00	0.06	0.00				102.69
RD1-fganhedralpyrrhotite-c2	65	34.29	0.00	67.50	0.09	0.00	0.02	0.00				101.92
RD1-fganhedralpyrrhotite-c1	64	34.17	0.00	67.60	0.03	0.01	0.03	0.00				101.85
RD1-mganhedralpyrr.witharseno+chalcoinclus	44	33.96	0.02	68.23	0.10	0.00	0.00	0.00				102.31
RD1-mganhedralpyrr.witharseno+chalcoinclus	45	33.89	0.00	67.83	0.07	0.02	0.00	0.04				101.85
RD1-mganhedralpyrr.witharseno+chalcoinclus	43	33.83	0.00	66.02	0.09	0.02	0.00	0.00				99.96
RA5-200x100anpyrrhotite-c2	41	33.72	0	66.94	0.11	0.02	0	0.01	0.01	0	0	100.82
RC2-200X75ANPYRRHOTITE-C2	39	33.68	0	67.09	0.03	0	0.02	0.01	0	0	0	100.85
RA5-200x200anpyrrhotite-a2	35	33.61	0	67.19	0.07	0.1	0	0.01	0.01	0	0	101
RA5-200x150anpyrrhotite-b1	37	33.56	0	67.93	0.09	0.06	0.01	0	0.02	0	0	101.68
RA1-75x50anpyrrhotite-a2	58	33.55	0	67.67	0.1	0.02	0	0	0	0	0	101.34
RA5-75x100ansppyrrhotite-b1	58	33.55	0.04	67.58	0.06	0	0	0	0	0	0	101.24
RA5-200x150anpyrrhotite-b2	38	33.52	0.01	68.27	0.07	0	0	0.02	0.01	0.02	0	101.93
RA5-200x150anpyrrhotite-b3	39	33.52	0	67	0.07	0.01	0.04	0.01	0.04	0	0	100.7
RC2-200X75ANPYRRHOTITE-C3	40	33.51	0	68.06	0	0.01	0	0	0	0	0	101.59
RA3-150x75anpyrrhotite-c2	32	33.5	0	68.51	0.07	0	0	0	0	0	0	102.09
RA3-150x75anpyrrhotite-c3	33	33.5	0.01	68.3	0.07	0	0.01	0	0.06	0	0	101.96
RA5-200x100anpyrrhotite-c3	42	33.5	0	67.67	0.11	0	0.02	0	0	0.01	0	101.33
RA3-150x75anpyrrhotite-c1	31	33.48	0	68.54	0.07	0.02	0	0	0.04	0	0	102.16
RA5-200x50subeupyrrhotite-a2	44	33.48	0	66.74	0.09	0	0	0	0	0	0	100.32
RA5-200x100anpyrrhotite-c1	40	33.47	0.01	68.2	0.08	0	0.03	0	0.02	0	0	101.82

New Britannia Mine, Ruttan Zone - Sulphide Electron Microprobe Analysis Results

Pyrrhotite Analyses	**No**	**Wt%S**	**Wt%Ti**	**Wt%Fe**	**Wt%Ni**	**Wt%Cu**	**Wt%Zn**	**Wt%As**	**Wt%Se**	**Wt%Te**	**Wt%Pb**	**Total**
RA5-200x200anpyrrhotite-a1	34	33.45	0	67.56	0.11	0	0.03	0	0	0	0	101.15
RA5-100x200ansppyrrhotite-c1	61	33.45	0	67.83	0.06	0.02	0.04	0	0.01	0	0	101.42
RA1-75x50anpyrrhotite-a3	59	33.44	0	68.26	0.11	0	0	0.02	0.02	0	0	101.86
RA1-75x50anpyrrhotite-a1	57	33.42	0	67.22	0.16	0	0.06	0	0	0	0	100.87
RA4-350x250anpyrrhotite-c2	19	33.41	0	68.1	0.07	0.02	0.03	0.01	0	0	0	101.66
RA5-200x200anpyrrhotite-a3	36	33.39	0	67.64	0.1	0	0.03	0.02	0.01	0	0	101.19
RA5-75x100ansppyrrhotite-b3	60	33.39	0	66.95	0.05	0	0.02	0.01	0	0	0	100.42
RA5-200x50subeupyrrhotite-a1	43	33.38	0.03	66.68	0.06	0	0	0.02	0.01	0	0	100.18
RA5-100x200ansppyrrhotite-c3	63	33.37	0.05	67.92	0.06	0	0.02	0.03	0	0.01	0	101.47
RA5-300x100ansppyrrhotite-a3	57	33.37	0.01	67.03	0.06	0.01	0	0	0.01	0	0	100.49
RA4-250x200anpyrrhotite-a2	10	33.36	0	66.19	0.05	0	0	0.01	0.01	0	0	99.62
RA4-350x250anpyrrhotite-c1	18	33.35	0	68.04	0.05	0	0.05	0	0.01	0	0	101.51
RA5-200x50subeupyrrhotite-a3	45	33.33	0	68.49	0.04	0	0.02	0	0.05	0	0	101.93
RA5-75x100ansppyrrhotite-b2	59	33.3	0.02	67.83	0.08	0	0.04	0.02	0	0	0	101.3
RA5-300x100ansppyrrhotite-a1	55	33.28	0	68.26	0.06	0.04	0.06	0.01	0	0	0	101.72
RA5-100x200ansppyrrhotite-c2	62	33.28	0	67.92	0.1	0.04	0.02	0	0.03	0	0	101.41
RA5-300x100ansppyrrhotite-a2	56	33.27	0	66.64	0.06	0.03	0	0	0	0	0	100.02
RA4-250x200anpyrrhotite-a3	11	33.11	0	65.73	0.06	0.01	0	0.03	0	0	0	98.95
RA4-350x300anpyrrhotite-b3	14	33.1	0	66.39	0.06	0	0	0	0	0	0	99.56
RA4-250x200anpyrrhotite-a1	9	33.09	0	67.27	0.08	0	0	0.02	0	0	0	100.47
RA4-350x300anpyrrhotite-b2	13	32.99	0	65.67	0.07	0	0	0.01	0	0	0	98.75
RA4-350x300anpyrrhotite-b1	12	32.94	0	66.58	0.06	0.01	0.02	0.01	0.02	0	0	99.65
Chalocpyrite Analyses	**No**	**Wt%S**	**Wt%Ti**	**Wt%Fe**	**Wt%Ni**	**Wt%Cu**	**Wt%Zn**	**Wt%As**	**Wt%Se**	**Wt%Te**	**Wt%Pb**	**Total**
RD1-mgchalcoass.witharseno-d2	91	30.90	0.00	34.13	0.00	34.15	0.05	0.00				99.25
RD1-fganhedralchalcoincrackinpyrite(b)-a3	48	30.67	0.00	35.11	0.02	33.56	0.08	0.01				99.45
RD1-fganhedralchalco-b1	58	30.08	0.00	33.47	0.02	33.67	0.02	0.03				97.30
RD1-fganhedralchalco-b2	59	30.04	0.00	33.60	0.02	33.86	0.03	0.02				97.57
RD1-fganhedralchalco-b3	60	29.98	0.00	33.71	0.02	33.55	0.00	0.00				97.25
RD1-fganhedralchalcoincrackinpyrite(b)-a2	47	29.95	0.00	35.09	0.00	33.54	0.07	0.00				98.66
RD1-mgchalcoass.witharseno-d3	92	29.75	0.00	34.44	0.01	33.38	0.08	0.00				97.66
RD1-mgchalcoass.witharseno-d1	90	29.68	0.00	34.65	0.01	33.71	0.03	0.00				98.09

APPENDIX 5

SECONDARY ION MASS SPECTROMETRY RESULTS

Analysis parameters - Table of experimental conditions.

Table of results - Results of SIMS analyzes (all values are given in parts per million by weight) on various sulphide minerals, plus comparison with amount of free and inclusion gold.

Ion images - Intensity maps of sulphide grains, displaying the intensities of the different elements analyzed. Bright areas denote high intensities and dark areas low intensities, see diagram below;

SIMS ION IMAGE INTENSITY DIAGRAM

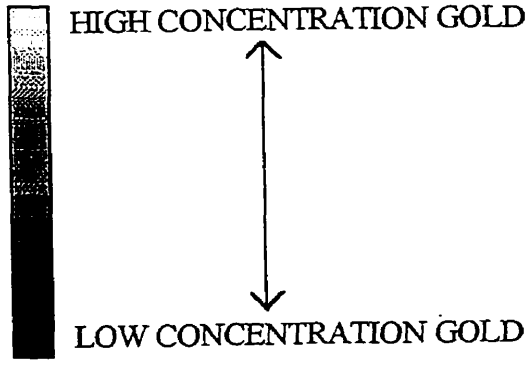

Figure 22- SIMS intensity map.

SIMS - ANALYSIS PARAMETERS

GENERAL PARAMETERS	
Instrument	Cameca IMS-4f ion microprobe
Standardization	external (ion implantation)
ION IMPLANTATION	
Ion Source	Low pressure krypton dc thermal ionization source
Nominal Ion Energies	300-2000 KeV
Operating Ion Energies	1 MeV
Implanted Species	^{197}Au
Implantation dose	2.5 E13 ion/cm^3
Mineral Species	Arsenopyrite, pyrite and chalcopyrite
OPERATING CONDITIONS	
Beam Source	Cs
Primary ion polarity	Positive
Secondary ion polarity	Negative
Impact energy(primary ions)	14.5 KeV
Primary beam diameter	50μm
Analysis diameter	10μm
Energy offset	none

RESULTS OF SIMS ANALYSIS

Details of the amount of gold present within different sulphide phases, numbers in parts per million by weight.

ZONE	HORIZON / LEVEL	SAMPLE NO.	MINERAL ANALYZED	DESCRIPTION	GOLD CONC. (PPMW)	% FREE GOLD IN SLIDE	% FREE GOLD AS INCLUSIONS
Birch	Pit	BA5-01	Arsenopyrite	Fine grained euhedral	325	9.23E-5	-
Birch	Pit	BA5-02	Arsenopyrite	Anhedral next to fine grained anhedral pyrite	420	9.23E-5	-
Birch	Pit	BA5-03	Arsenopyrite	Fine grained isolated, euhedral	75	9.23E-5	-
Birch	Pit	BA5-04	Arsenopyrite	Fine grained euhedral	2.4	9.23E-5	-
Birch	Pit	BA5-05	Pyrite	Fine grained anhedral	5	9.23E-5	-
Birch	Pit	BA5-06	Pyrite	Fine grained anhedral	1.3	9.23E-5	-
Birch	Pit	BA5-07	Pyrite	Fine grained anhedral	2.3	9.23E-5	-
Birch	Pit	BA6A-01	Pyrite	Fine grained anhedral	2.3	-	-
Birch	Pit	BA6A-02	Pyrite	Coarse grained anhedral	3	-	-
Birch	Pit	BA6A-03	Arsenopyrite	Medium grained anhedral	0.2	-	-
Birch	Pit	BA6A-04	Pyrite	Medium grained anhedral	0.6	-	-
Birch	Pit	BA6A-05	Pyrite	Fine grained euhedral	0.3	-	-
Birch	Pit	BD1-01	Arsenopyrite	Isolated anhedral	4	1.32 E-4	9.2
Birch	Pit	BD1-02	Arsenopyrite	Isolated sub-euhedral	3	1.32 E-4	9.2
Birch	Pit	BE1-01	Arsenopyrite	Isolated euhedral	400	1.12 E-3	1.83

Details of the amount of gold present within different sulphide phases, numbers expressed in parts per million by weight.

ZONE	HORIZON / LEVEL	SAMPLE NO.	MINERAL ANALYZED	DESCRIPTION	GOLD CONC. (PPMW)	% FREE GOLD IN SLIDE	% FREE GOLD AS INCLUSIONS
Birch	Pit	BE1-02	Arsenopyrite	Isolated euhedral	1000	1.12 E-3	1.83
Birch	Pit	BE1-03	Arsenopyrite	Anhedral overgrown by euhedral	350	1.12 E-3	1.83
Birch	Pit	BE1-04	Arsenopyrite	Euhedral overgrowing anhedral arsenopyrite	150	1.12 E-3	1.83
Birch	Pit	BE1-05	Pyrite	Anhedral overgrown by euhedral arsenopyrite	7	1.12 E-3	1.83
Birch	Pit	BE1-06	Arsenopyrite	Euhedral overgrowing anhedral arsenopyrite	1000	1.12 E-3	1.83
Birch	Pit	BE1-07	Arsenopyrite	Isolated anhedral	1800	1.12 E-3	1.83
Birch	Pit	BE1-08	Pyrite	Isolated anhedral	4.5	1.12 E-3	1.83
Birch	Pit	BE1-09	Arsenopyrite	Anhedral overgrown by euhedral arsenopyrite	3000	1.12 E-3	1.83
Birch	Pit	BE1-10	Arsenopyrite	Euhedral overgrowing anhedral arsenopyrite	2500	1.12 E-3	1.83
Birch	B96001-H4	B9601-4B-01	Arsenopyrite	Subeuhedral	75	1.6 E-6	-
Birch	B96001-H4	B9601-4B-02	Pyrite	Anhedral	19.3	1.6 E-6	-
Birch	B96001-H4	B9601-4B-03	Arsenopyrite	Anhedral	119.6	1.6 E-6	-
Birch	B96001-H4	B9601-4B-04	Arsenopyrite	Anhedral	269.8	1.6 E-6	-
Birch	B96001-H4	B9601-4B-05	Arsenopyrite	Anhedral	9.1	1.6 E-6	-

Details of the amount of gold present within different sulphide phases, numbers expressed in parts per million by weight.

ZONE	HORIZON / LEVEL	SAMPLE NO.	MINERAL ANALYZED	DESCRIPTION	GOLD CONC. (PPMW)	% FREE GOLD IN SLIDE	% FREE GOLD AS INCLUSIONS
Birch	B96001-H4	B9601-4B-06	Pyrite	Anhedral	0	1.6 E-6	-
Birch	B96001-H4	B9601-4B-07	Arsenopyrite	Euhedral	45.8	1.6 E-6	-
Birch	B96001-H4	B9601-4B-08	Pyrite	Coarse grained Anhedral	0.1	1.6 E-6	-
Birch	B96001-H4	B9601-4B-09	Arsenopyrite	Fine grained (150μm) Subeuhedral	75.2	1.6 E-6	-
Birch	B96001-H4	B9601-4B-10	Arsenopyrite	Euhedral	239	1.6 E-6	-
Birch	B96001-H4	B9601-4B-11	Arsenopyrite	Euhedral	75.5	1.6 E-6	-
Birch	B96001-H4	B9601-4B-12	Arsenopyrite	Anhedral	24.8	1.6 E-6	-
Birch	B96001-H4	B9601-4B-13	Pyrite	Fine grained (150μm) Anhedral	0.1	1.6 E-6	-
Birch	B96001-H4	B9601-4B-14	Pyrite	Fine grained (150μm) anhedral	0	1.6 E-6	-
Birch	B96001-H4	B9601-4B-15	Pyrite	Subeuhedral	1332.7	1.6 E-6	-
Birch	B96001-H4	B9601-4B-16	Arsenopyrite	Subeuhedral	57	1.6 E-6	-
Birch	B96001-H4	B9601-6-01	Arsenopyrite	Coarse grained anhedral	51	5.11 E-4	-
Birch	B96001-H4	B9601-6-02	Arsenopyrite	Fine grained euhedral	306.5	5.11 E-4	-
Birch	B96001-H4	B9601-6-03	Arsenopyrite	Fine grained subeuhedral	96.8	5.11 E-4	-
Birch	B96001-H4	B9601-6-04	Arsenopyrite	Fine grained subeuhedral	351.6	5.11 E-4	-
Birch	B96001-H4	B9601-6-05	Pyrite	Fine grained subeuhedral	570.4	5.11 E-4	-
Birch	B96001-H4	B9601-6-06	Arsenopyrite	Fine grained euhedral	173.2	5.11 E-4	-

Details of the amount of gold present within different sulphide phases, numbers expressed in parts per million by weight.

ZONE	HORIZON / LEVEL	SAMPLE NO.	MINERAL ANALYZED	DESCRIPTION	GOLD CONC. (PPMW)	% FREE GOLD IN SLIDE	% FREE GOLD AS INCLUSIONS
Birch	H4	B9601-6-07	Arsenopyrite	Medium grained subeuhedral	512.6	5.11 E-4	-
Birch	H4	B9601-6-08	Pyrite	Coarse grained anhedral	0.4	5.11 E-4	-
Birch	B96001-H4	B9601-6-09	Arsenopyrite	Coarse grained euhedral	206.5	5.11 E-4	-
Birch	B96001-H4	B9601-6-10	Pyrite	Fine grained anhedral	0.4	5.11 E-4	-
Birch	B96001-H4	B9601-6-11	Pyrite	Medium grained anhedral	8.4	5.11 E-4	-
Birch	B96001-H4	B9601-07-01	Pyrite	Anhedral	1.8	-	-
Birch	B96001-H4	B9601-07-02	Pyrite	Anhedral	0.1	-	-
Birch	B96001-H4	B9601-07-03	Pyrite	Coarse grained anhedral	0.1	-	-
Birch	B96001-H4	B9601-07-04	Pyrite	Medium grained anhedral	0.2	-	-
Birch	B96001-H4	B9601-07-05	Arsenopyrite	Fine grained euhedral	4	-	-
Birch	B96001-H5	B9601-16a-01	Arsenopyrite	Isolated euhedral	10	-	-
Birch	B96001-H5	B9601-16a-02	Arsenopyrite	Isolated euhedral	15	-	-
Birch	B96001-H5	B9601-16a-03	Arsenopyrite	Anhedral next to subeuhedral	1	-	-
Birch	B96001-H5	B9601-16a-04	Arsenopyrite	Subeuhedral next to anhedral	4	-	-
Birch	B96001-H5	B9601-16a-05	Arsenopyrite	Anhedral next to subeuhedral	7	-	-
Birch	B96001-H5	B9601-16a-06	Arsenopyrite	Isolated anhedral	15	-	-
Birch	B96001-H5	B9601-16a-07	Arsenopyrite	Large anhedral fractured	110	-	-

Details of the amount of gold present within different sulphide phases, numbers expressed in parts per million by weight.

ZONE	HORIZON / LEVEL	SAMPLE NO.	MINERAL ANALYZED	DESCRIPTION	GOLD CONC. (PPMW)	% FREE GOLD IN SLIDE	% FREE GOLD AS INCLUSIONS
Birch	B96001-H5	B9601-16a-08	Pyrite	Isolated spongy/anhedral	5	-	-
Birch	B96001-H5	B9601-16a-09	Arsenopyrite	Isolated euhedral	13	-	-
Birch	B96001-H5	B9601-16a-10	Arsenopyrite	isolated anhedral	3	-	-
Birch	B96001-H5	B9601-16a-11	Pyrite	Isolated anhedral	2	-	-
Birch	B96001-H6	B9601-24-02	Arsenopyrite	Isolated anhedral	13	-	-
Birch	B96001-H6	B9601-24-03	Arsenopyrite	Anhedral next to spongy pyrite	110-100	-	-
Birch	B96001-H6	B9601-24-04	Pyrite	Spongy next to anhedral arsenopyrite	300	-	-
Birch	B96001-H1	B9601-37-01	Arsenopyrite	Coarse grained anhedral	1370	-	-
Birch	B96001-H1	B9601-37-02	Arsenopyrite	Coarse grained anhedral	571	-	-
Birch	B96001-H1	B9601-37-03	Arsenopyrite	Medium grained subeuhedral	890	-	-
Birch	B96001-H1	B9601-37-04	Arsenopyrite	Anhedral	33	-	-
Birch	B96001-H1	B9601-37-05	Arsenopyrite	Subeuhedral	1199	-	-
Birch	B96001-H1	B9601-37-06	Arsenopyrite	Euhedral	567	-	-
Birch	B96001-H1	B9601-37-07	Arsenopyrite	Euhedral	672	-	-
Birch	B96001-H1	B9601-37-08	Arsenopyrite	Subeuhedral	547	-	-
No.3	Outcrop	N301-01	Arsenopyrite	Medium grained euhedral	969	3.96 E-4	-
No. 3	Outcrop	N301-02	Arsenopyrite	Medium grained euhedral	162	3.96 E-4	-

Details of the amount of gold present within different sulphide phases, numbers expressed in parts per million by weight.

ZONE	HORIZON / LEVEL	SAMPLE NO.	MINERAL ANALYZED	DESCRIPTION	GOLD CONC. (PPMW)	% FREE GOLD IN SLIDE	% FREE GOLD AS INCLUSIONS
No.3	Outcrop	N301-03	Arsenopyrite	Subeuhedral	136	3.96 E-4	-
No.3	Outcrop	N301-04	Pyrite	Anhedral	0.9	3.96 E-4	-
No.3	Outcrop	N301-05	Pyrite	Anhedral	0.6	3.96 E-4	-
No.3	outcrop	N301-06	Pyrite	Anhedral	2	3.96 E-4	-
No.3	Outcrop	N303-01	Arsenopyrite	Medium grained euhedral	77	2.26 E-5	-
No. 3	Outcrop	N303-02	Arsenopyrite	Fine grained euhedral	322	2.26 E-5	-
No.3	Outcrop	N303-03	Arsenopyrite	Subeuhedral	41.4	2.26 E-5	-
No.3	Outcrop	N303-04	Pyrite	Anhedral	1	2.26 E-5	-
No.3	Outcrop	N303-05	Pyrite	Fine grained anhedral	0.8	2.26 E-5	-
No.3	outcrop	N303-06	Pyrite	Medium grained anhedral	0.8	2.26 E-5	-
No.3	Outcrop	N304-01	Arsenopyrite	Coarse grained anhedral	2.6	8.85 E-4	-
No. 3	Outcrop	N304-02	Arsenopyrite	Fine grained subeuhedral	1.6	8.85 E-4	-
No.3	Outcrop	N304-03	Arsenopyrite	Fine grained euhedral	1.8	8.85 E-4	-
No.3	Outcrop	N304-04	Pyrite	Fine grained anhedral	1.2	8.85 E-4	-
No.3	Outcrop	N304-05	Pyrite	Fine grained anhedral	1.7	8.85 E-4	-
No.3	Outcrop	N304-06	Pyrite	Fine grained anhedral	0.7	8.85 E-4	-
No.3	Outcrop	N309-01	Pyrite	Fine grained anhedral	3.8	-	-

Details of the amount of gold present within different sulphide phases, numbers expressed in parts per million by weight.

ZONE	HORIZON / LEVEL	SAMPLE NO.	MINERAL ANALYZED	DESCRIPTION	GOLD CONC. (PPMW)	% FREE GOLD IN SLIDE	% FREE GOLD AS INCLUSIONS
No. 3	Outcrop	N309-02	Pyrite	Medium grained anhedral	2.4	-	-
No.3	Outcrop	N309-03	Arsenopyrite	Fine grained anhedral	5.5	-	-
No.3	Outcrop	N309-04	Arsenopyrite	Fine to medium grained anhedral	4.9	-	-
No.3	Outcrop	N309-05	Arsenopyrite	Fine grained subeuhedral	5.5	-	-
No.3	Outcrop	N309-06	Pyrite	Fine grained anhedral	2.9	-	-
Dick	2210	DB29-02	Pyrite	-	0	-	-
Dick	2210	DB29-03	Pyrite	-	0	-	-
Dick	2210	DB29-04	Pyrite	-	0	-	-
Dick	2210	DB29-05	Arsenopyrite	-	1	-	-
Dick	2210	DB29-06	Arsenopyrite	-	0.8	-	-
Dick	2210	DB29-07	Arsenopyrite	-	1.1	-	-
Dick	2210	DB29-08	Arsenopyrite	-	4.9	-	-
Dick	2210	DB29-09	Pyrite	-	0.0	-	-
Dick	2210	DB29-11	Arsenopyrite	-	5.9	-	-
Dick	2210	DB30-11	Pyrite	-	0.0	7.18 E-4	-
Dick	2210	DB30-12	Pyrite	-	0.0	7.18 E-4	-
Dick	2210	DB30-13	Pyrite	-	0.0	7.18 E-4	-

Details of the amount of gold present within different sulphide phases, numbers expressed in parts per million by weight.

ZONE	HORIZON / LEVEL	SAMPLE NO.	MINERAL ANALYZED	DESCRIPTION	GOLD CONC. (PPMW)	% FREE GOLD IN SLIDE	% FREE GOLD AS INCLUSIONS
Dick	2210	DB30-14	Pyrite	-	0.0	7.18 E-4	-
Dick	2210	DB30-15	Pyrite	-	0.0	7.18 E-4	-
Dick	2210	DB30-19	Pyrite	-	0.0	7.18 E-4	-
Dick	2210	DB31-31	Pyrite	-	0.0	-	-
Dick	2210	DB31-32	Pyrite	-	0.0	-	-
Dick	2210	DB31-33	Arsenopyrite	-	8.5	-	-
Dick	2210	DB31-34	Arsenopyrite	-	5.5	-	-
Dick	2210	DB31-35	Arsenopyrite	-	1.4	-	-
Dick	2210	DB31-36	Arsenopyrite	-	1.1	-	-
Dick	2210	DB31-37	Pyrite	-	0.0	-	-
Dick	2210	DB31-38	Arsenopyrite	-	1.1	-	-
Dick	2210	DB31-39	Pyrite	-	0.0	-	-
Dick	2260	DC9-01	Arsenopyrite	Anhedral	2.5	-	-
Dick	2260	DC9-02	Arsenopyrite	Medium grained subeuhedral	4.8	-	-
Dick	2260	DC9-03	Pyrite	Coarse grained anhedral	0.3	-	-
Dick	2260	DC9-04	Pyrite	Coarse grained anhedral	0.7	-	-
Dick	2260	DC9-05	Pyrite	Coarse grained anhedral	1.2	-	-

Details of the amount of gold present within different sulphide phases, numbers expressed in parts per million by weight.

ZONE	HORIZON / LEVEL	SAMPLE NO.	MINERAL ANALYZED	DESCRIPTION	GOLD CONC. (PPMW)	% FREE GOLD IN SLIDE	% FREE GOLD AS INCLUSIONS
Dick	2260	DC9-06	Arsenopyrtie	Medium grained subeuhedral	~13	-	-
Dick	2260	DC9-07	Arsenopyrtie	Coarse grained subeuhedral	2	-	-
Thorne	TZ-83-1	TZ1-01	Pyrite	Medium grained anhedral	5.9	-	-
Thorne	TZ-83-1	TZ1-02	Pyrite	Coarse grained anhedral in vein	1.4	-	-
Thorne	TZ-83-1	TZ1-03	Pyrite	Coarse grained subeuhedral	8.5	-	-
Thorne	TZ-83-1	TZ1-04	Pyrite	Fine grained anhedral	6.2	-	-
Thorne	TZ-83-1	TZ1-05	Arsenopyrite	Medium grained euhedral within coarse grained anhedral pyrite	28	-	-
Thorne	TZ-83-1	TZ2-01	Pyrite	Coarse grained subeuhedral	10.6	-	-
Thorne	TZ-83-1	TZ2-02	Spongy pyrite	Medium grained around coarse grained subeuhedral pyrite	60.3	-	-
Thorne	TZ-83-1	TZ2-03	Spongy pyrite	Medium grained	9	-	-
Thorne	TZ-83-1	TZ2-04	Chalcopyrite	Medium grained anhedral next to subeuhedral pyrite	2.2	-	-
Thorne	TZ-83-1	TZ2-05	Arsenopyrite	Coarse grained subeuhedral	9.8	-	-
Thorne	TZ-83-1	TZ2-06	Arsenopyrite	Coarse grained euhedral	4.9	-	-
Thorne	TZ-83-1	TZ2-07	Pyrite	Fine to medium grained anhedral	1.6	-	-
Thorne	TZ-83-1	TZ2-08	Pyrite	Anhedral	1.7	-	-

Details of the amount of gold present within different sulphide phases, numbers expressed in parts per million by weight.

ZONE	HORIZON / LEVEL	SAMPLE NO.	MINERAL ANALYZED	DESCRIPTION	GOLD CONC. (PPMW)	% FREE GOLD IN SLIDE	% FREE GOLD AS INCLUSIONS
Thorne	TZ-83-1	TZ2-09	Arsenopyrite	Medium grained subeuhedral	11.3	-	-
Thorne	TZ-83-1	TZ2-10	Chalcopyrite	Fine grained anhedral	3.3	-	-
Thorne	TZ-83-1	TZ2-11	Chalcopyrite	Fine grained anhedral	1.4	-	-
Thorne	TZ-83-1	TZ3		Sample charging		-	-
Thorne	TZ-83-1	TZ4-01	Arsenopyrite	Medium grained subeuhedral	6.7	-	-
Thorne	TZ-83-1	TZ4-02	Arsenopyrite	Coarse grained subeuhedral	11.4	-	-
Thorne	TZ-83-1	TZ4-03	Chalcopyrite	Fine grained anhedral	1.3	-	-
Thorne	TZ-83-1	TZ4-04	Arsenopyrite	Coarse grained subeuhedral	25.1	-	-
Thorne	TZ-83-1	TZ4-05	Pyrite	Medium grained anhedral	2.7	-	-
Thorne	TZ-83-1	TZ4-06	Pyrite	medium grained anhedral	3.6	-	-
Thorne	TZ-83-1	TZ4-07	Chalcopyrite	Fine grained anhedral	3.3	-	-
Thorne	TZ-83-1	TZ4-08	Pyrite	Fine grained anhedral	3.7	-	-
Thorne	TZ-83-1	TZ4-09	Pyrite	Medium grained anhedral	2.4	-	-
Boundary	BNDY-83-02	BY1-01	Pyrite	Fine grained anhedral	12.2	-	-
Boundary	BNDY-83-02	BY1-02	Pyrite	Fine grained anhedral	1.6	-	-
Boundary	BNDY-83-02	BY1-03	Pyrite	Medium grained anhedral	10.7	-	-
Boundary	BNDY-83-02	BY1-04	Pyrite	Fine grained anhedral	4.6	-	-

Details of the amount of gold present within different sulphide phases, numbers expressed in parts per million by weight.

ZONE	HORIZON / LEVEL	SAMPLE NO.	MINERAL ANALYZED	DESCRIPTION	GOLD CONC. (PPMW)	% FREE GOLD IN SLIDE	% FREE GOLD AS INCLUSIONS
Boundary	BNDY-83-02	BY2-01	Chalcopyrite	Medium grained	0.7	-	-
Boundary	BNDY-83-02	BY2-02	Pyrite	Medium grained anhedral in vein with medium grained anhedral chalcopyrite	29.8	-	-
Boundary	BNDY-83-02	BY2-03	Chalcopyrite	medium grained anhedral	36.7	-	-
Boundary	BNDY-83-02	BY2-04	Chalcopyrite	Medium grained anhedral	92.5	-	-
Boundary	BNDY-83-02	BY2-05	Pyrite	Medium grained anhedral	69.4	-	-
Boundary	BNDY-83-02	BY3-01	Arsenopyrite	Medium grained subeuhedral	517.6	-	-
Boundary	BNDY-83-02	BY3-02	Arsenopyrite	Fine euhedral	118.1	-	-
Boundary	BNDY-83-02	BY3-03	Arsenopyrite	Fine grained euhedral	146.2	-	-
Boundary	BNDY-83-02	BY3-04	Pyrite	Fine grained anhedral	6.8	-	-
Boundary	BNDY-83-02	BY3-05	Pyrite	Fine grained anhedral	17.6	-	-
Boundary	BNDY-83-02	BY3-06	Pyrite	Fine grained anhedral	11.4	-	-
Boundary	BNDY-83-02	BY4-01	Pyrite	Medium grained anhedral	4.5	-	-
Boundary	BNDY-83-02	BY4-02	Pyrite	Medium grained anhedral	2.8	-	-
Boundary	BNDY-83-02	BY4-03	Pyrite	Coarse grained subeuhedral	3	-	-
Boundary	BNDY-83-02	BY4-04	Spongy pyrite	Fine grained anhedral	7.2	-	-
Boundary	BNDY-83-02	BY4-05	Spongy pyrite	Fine grained anhedral	8.2	-	-

Details of the amount of gold present within different sulphide phases, numbers expressed in parts per million by weight.

ZONE	HORIZON / LEVEL	SAMPLE NO.	MINERAL ANALYZED	DESCRIPTION	GOLD CONC. (PPMW)	% FREE GOLD IN SLIDE	% FREE GOLD AS INCLUSIONS
Boundary	BNDY-83-02	BY4-06	Arsenopyrite	Fine grained anhedral	433.7	-	-
Boundary	BNDY-83-02	BY4-07	Spongy pyrite	Fine to medium grained anhedral	12.8	-	-
Boundary	BNDY-83-02	BY5-42	Arsenopyrite	-	11.85	-	-
Boundary	BNDY-83-02	BY5-44	Pyrite	-	0.00	-	-
Boundary	BNDY-83-02	BY5-45	Arsenopyrite	-	5.85	-	-
Boundary	BNDY-83-02	BY5-46	Arsenopyrite	-	18.95	-	-
Boundary	BNDY-83-02	BY5-47	Arsenopyrite	-	0.21	-	-
Boundary	BNDY-83-02	BY5-48	Pyrite	-	0.00	-	-
Boundary	BNDY-83-02	BY6-50	Arsenopyrite	-	1.14	-	-
Boundary	BNDY-83-02	BY6-51	Arsenopyrite	-	13.25	-	-
Boundary	BNDY-83-02	BY6-52	Arsenopyrite	-	11.29	-	-
Boundary	BNDY-83-02	BY6-53	Pyrite	-	.29	-	-
Boundary	BNDY-83-02	BY6-54	Pyrite	-	0.0	-	-
Boundary	BNDY-83-02	BY6-55	Arsenopyrite	-	1.47	-	-

Detection limits;Pyrite = 0.22 ppmw
Arsenopyrite = 0.074 ppmw

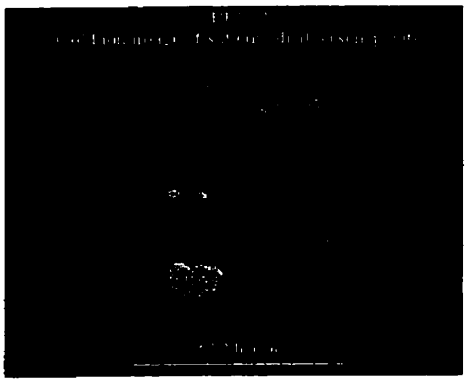

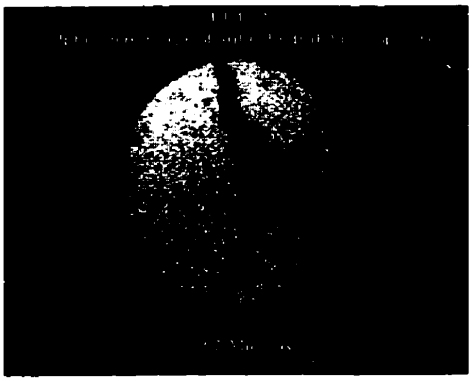

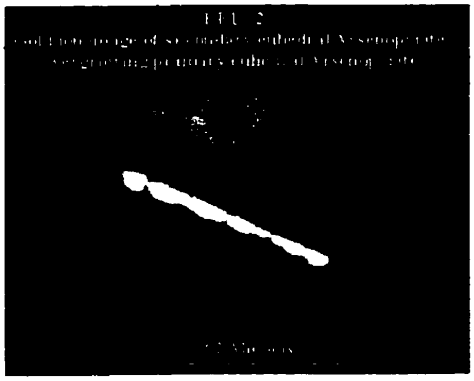

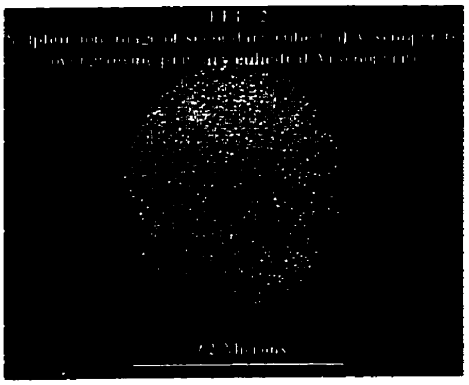

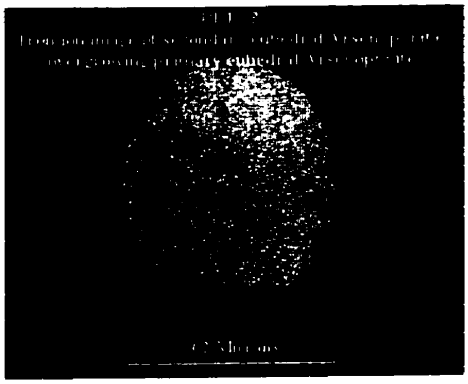

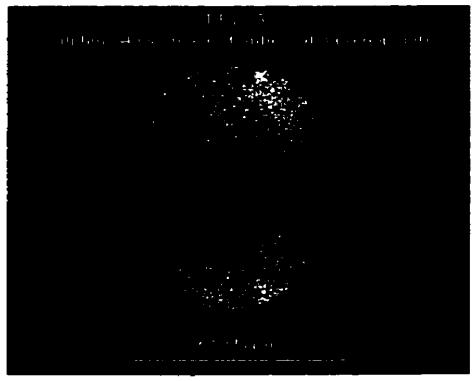

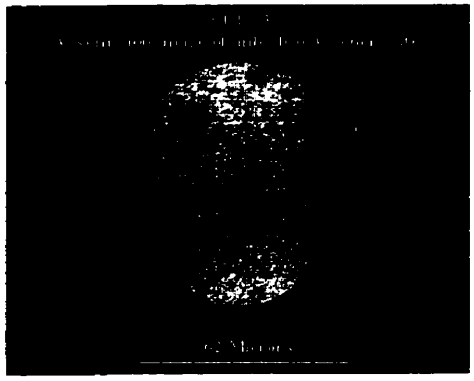

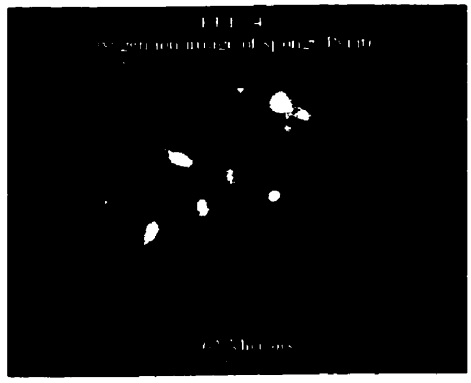

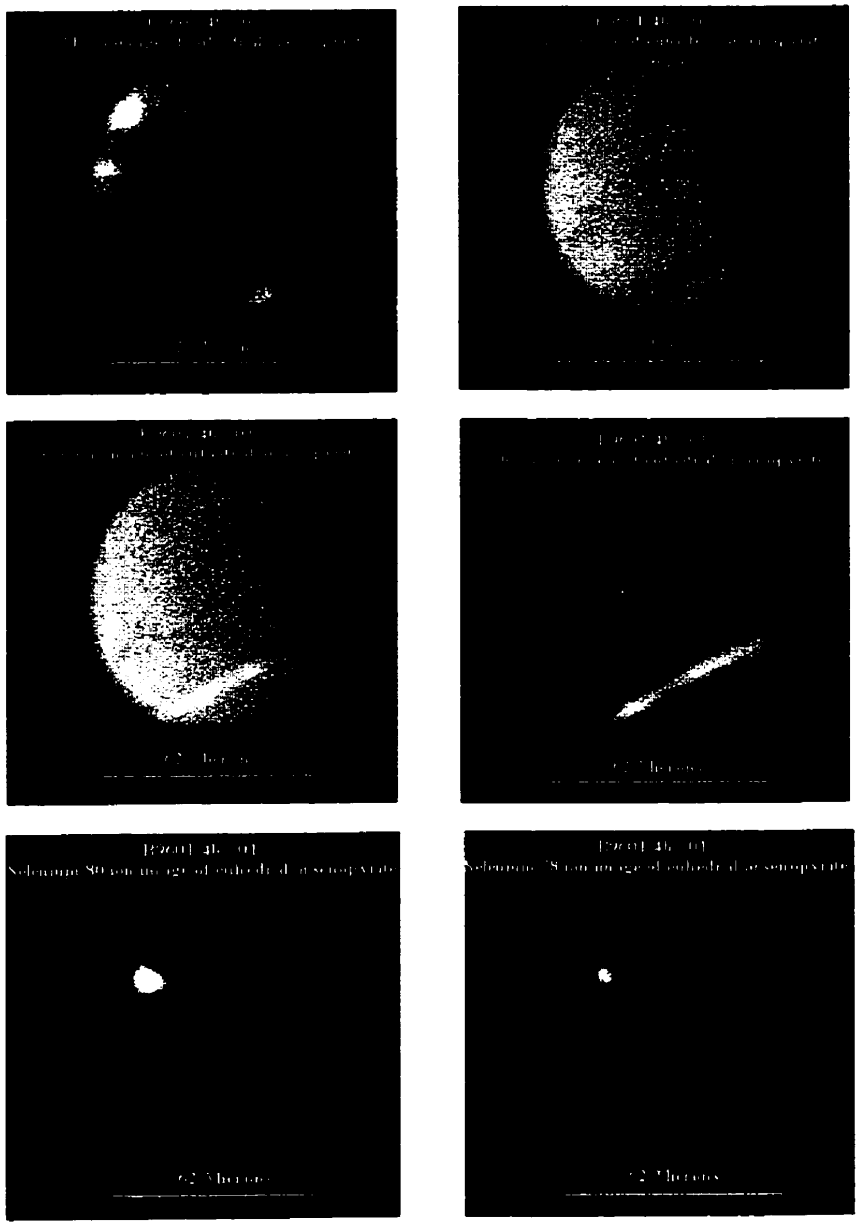

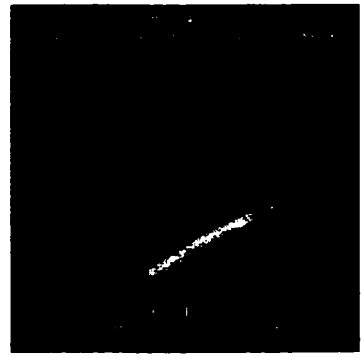

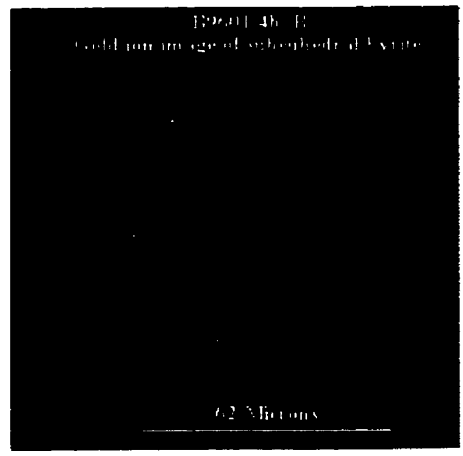

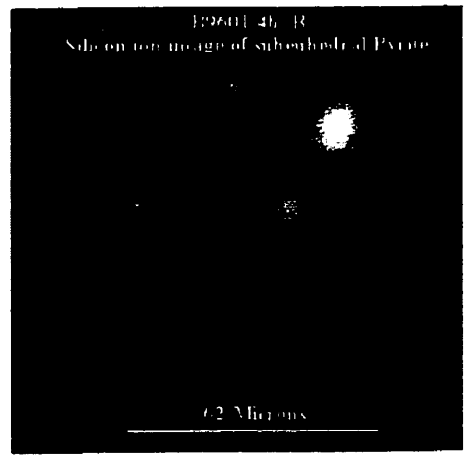

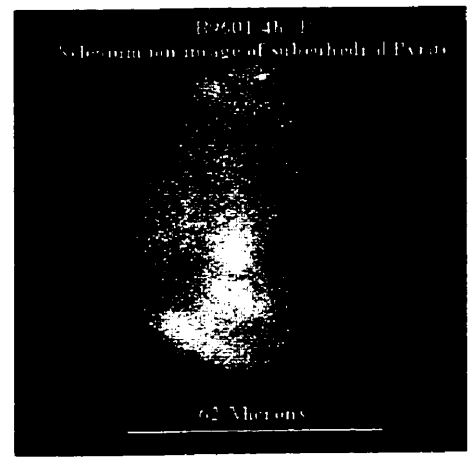


62 Microns

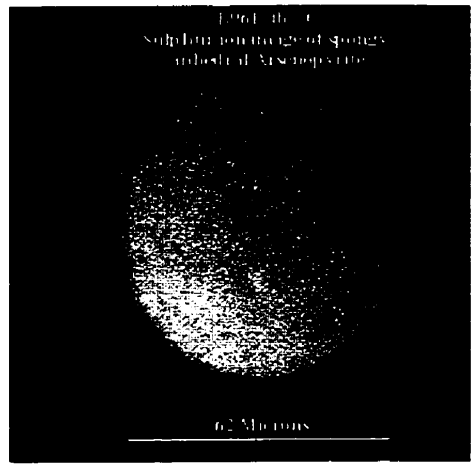
62 Microns

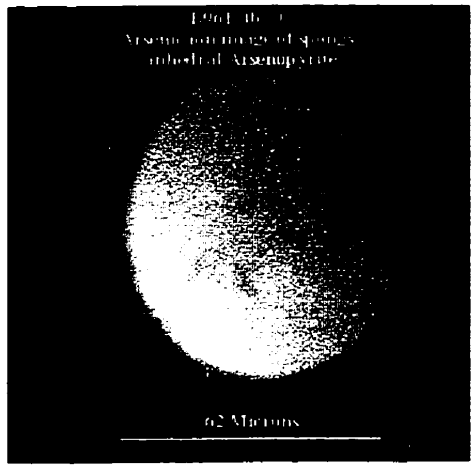
62 Microns

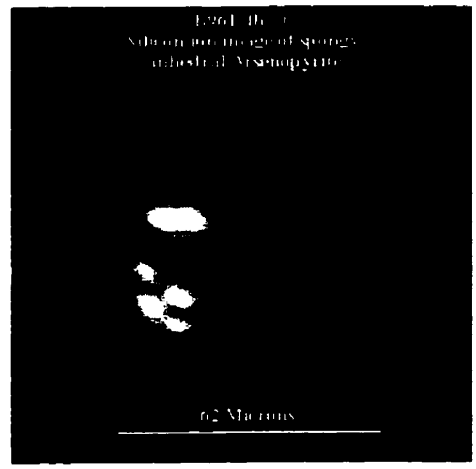
62 Microns

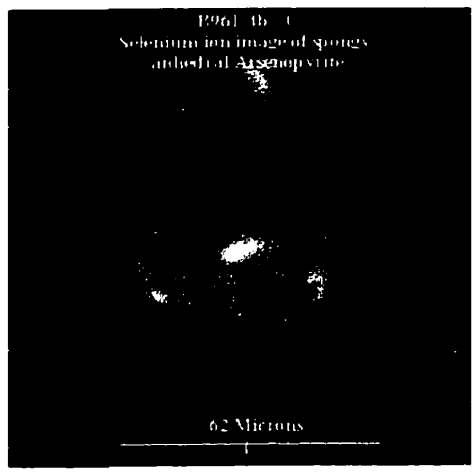
62 Microns

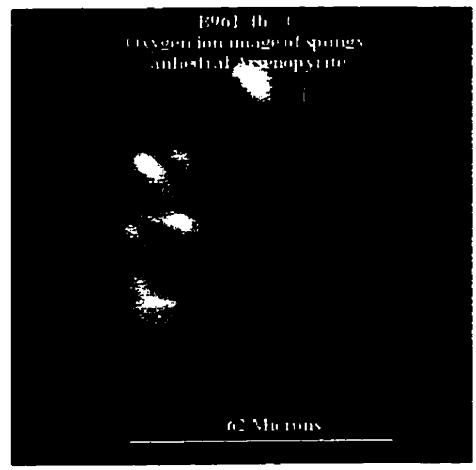
62 Microns

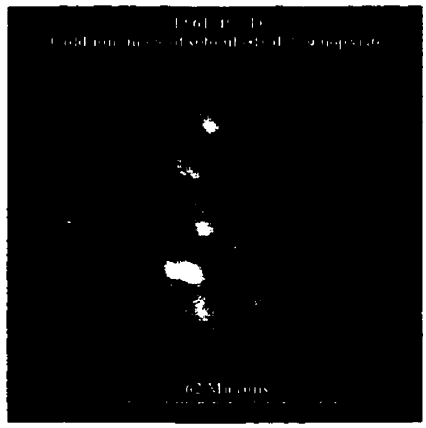

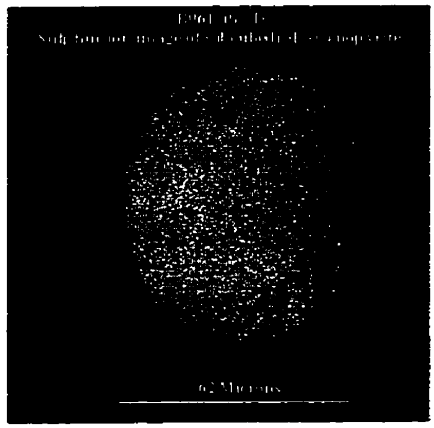

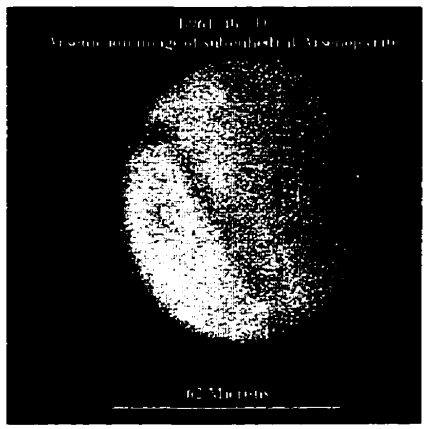

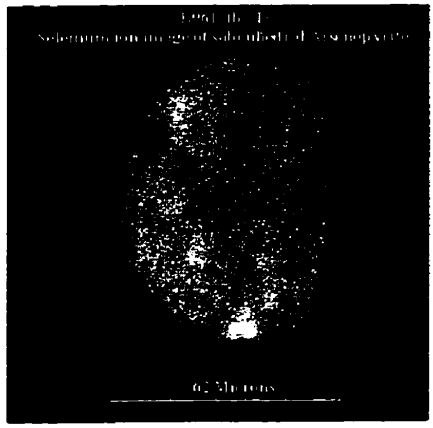

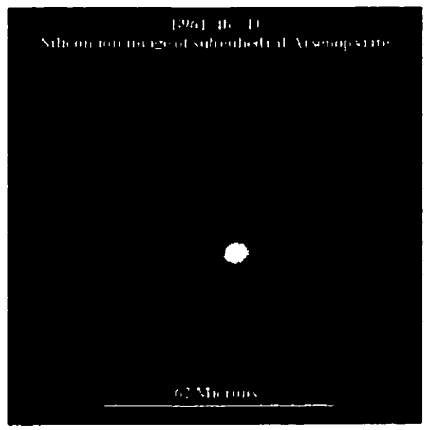

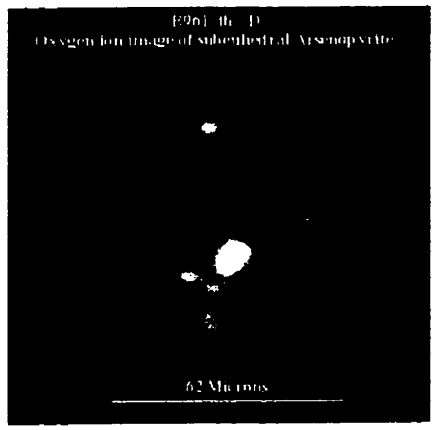


62 Microns


62 Microns

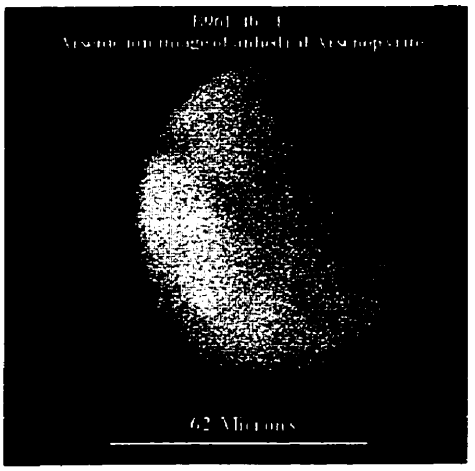
62 Microns

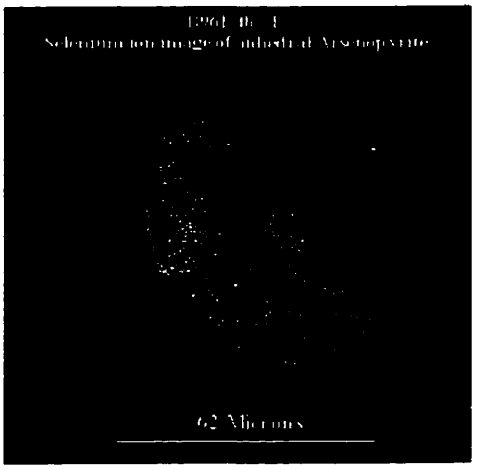
62 Microns

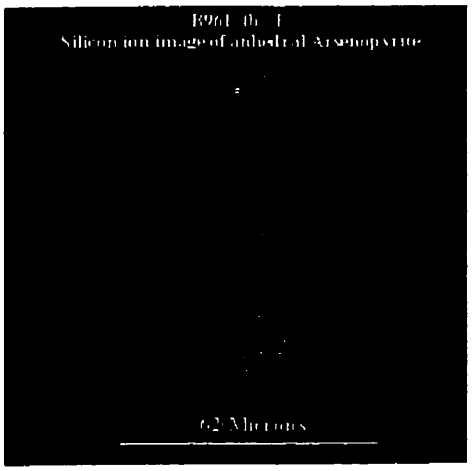
62 Microns


62 Microns

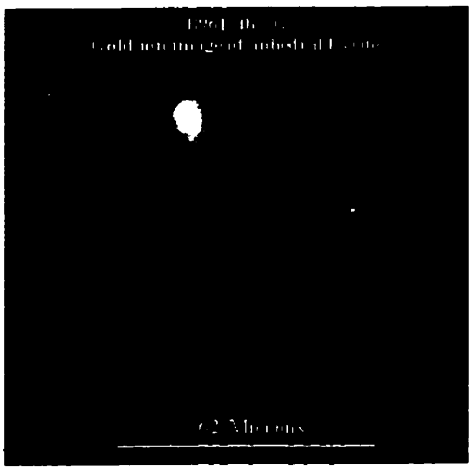

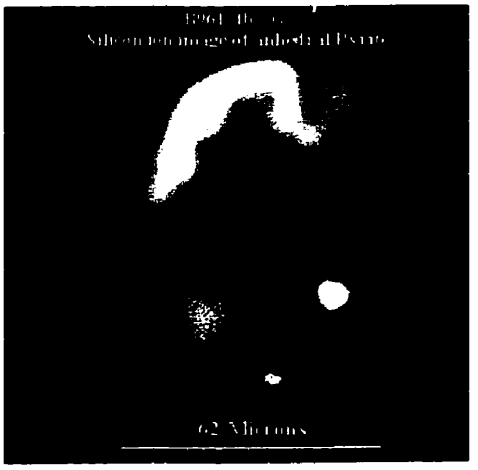

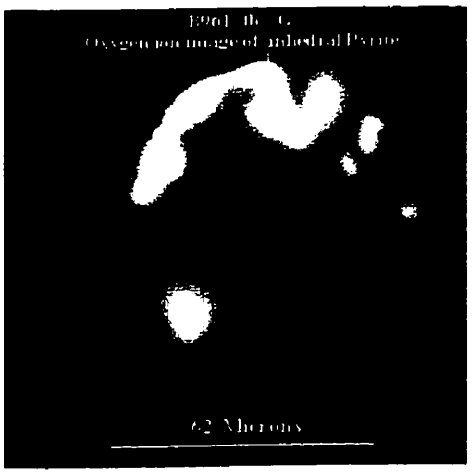

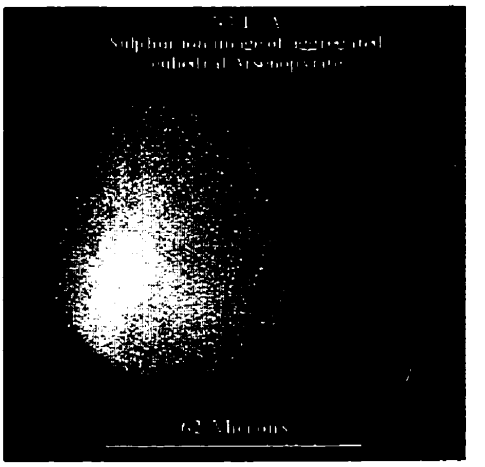

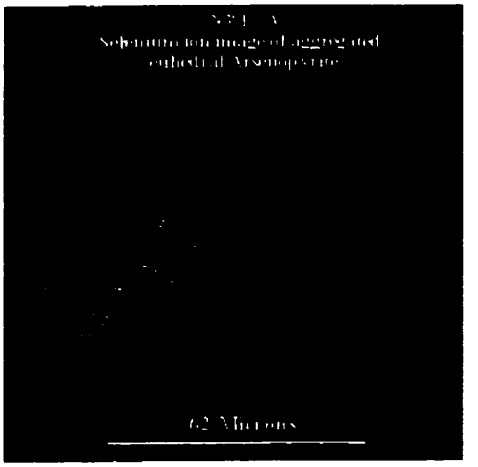

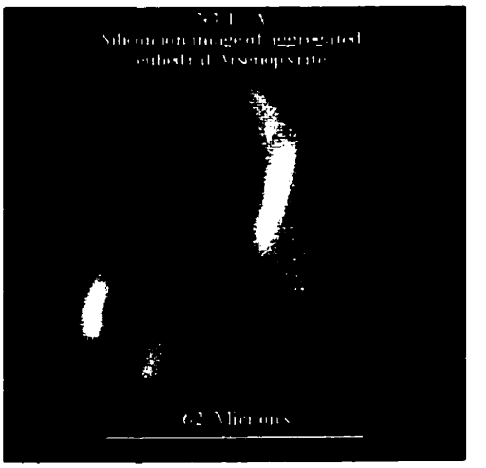

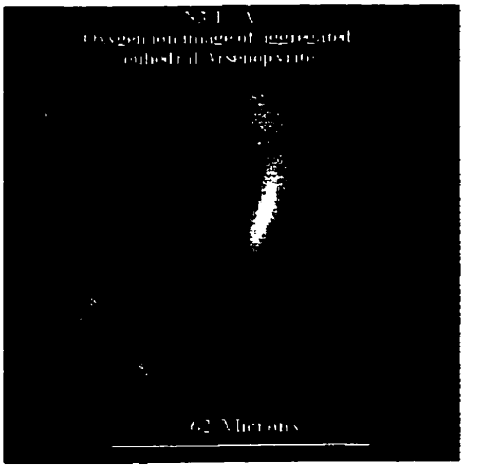

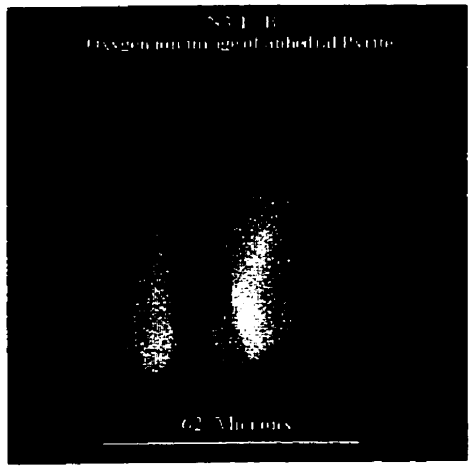

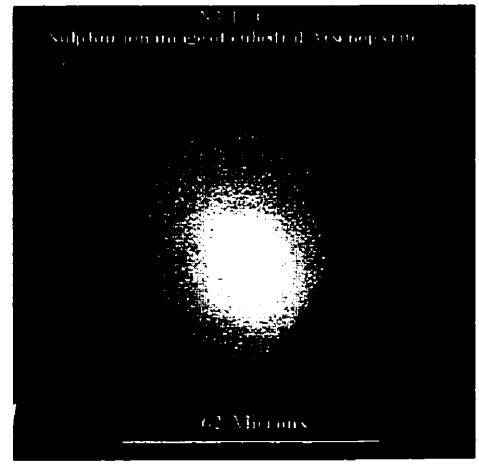

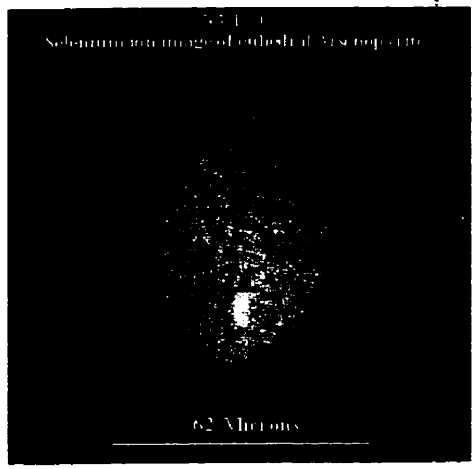

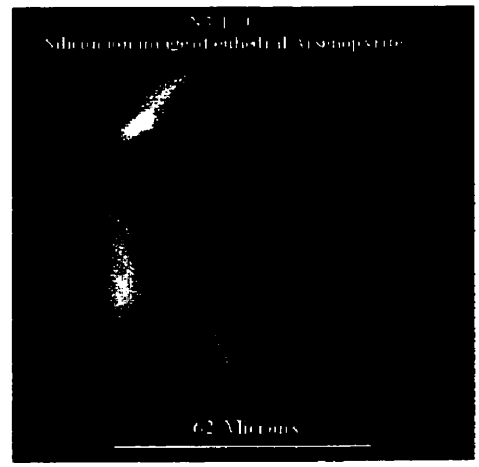

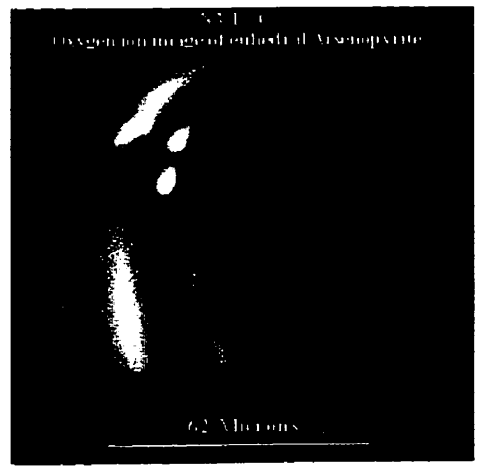

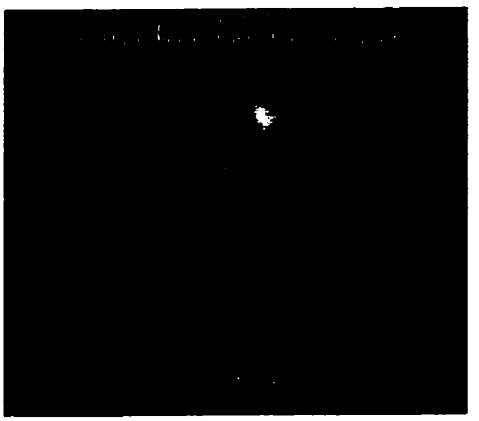

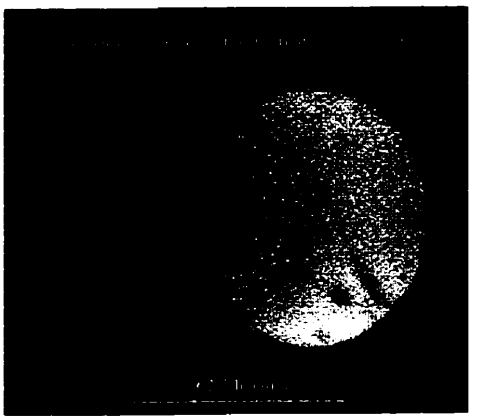

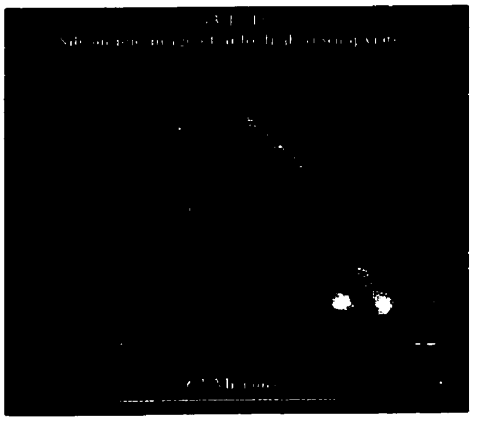
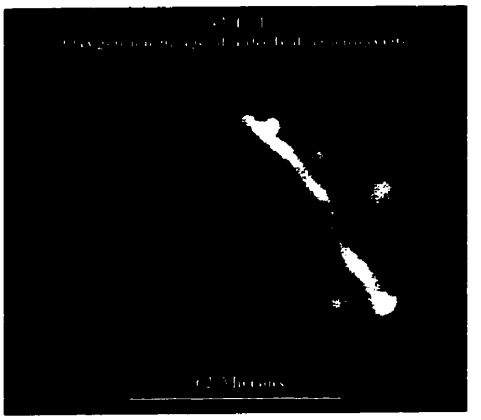

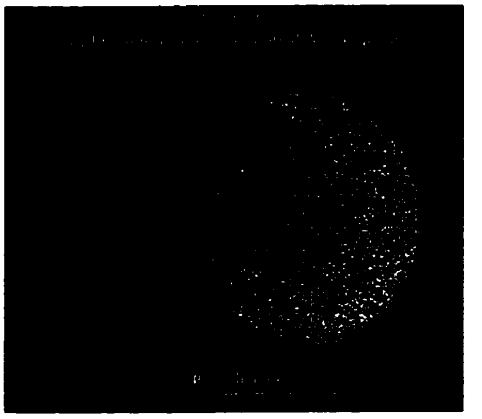

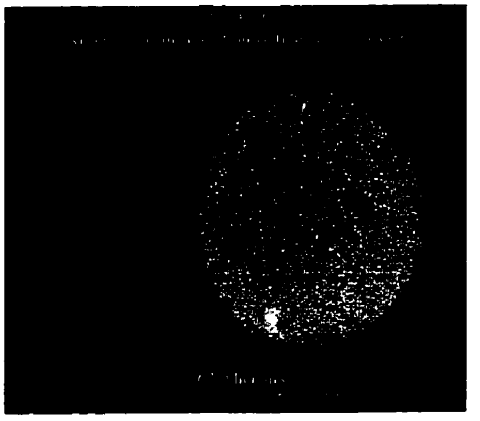

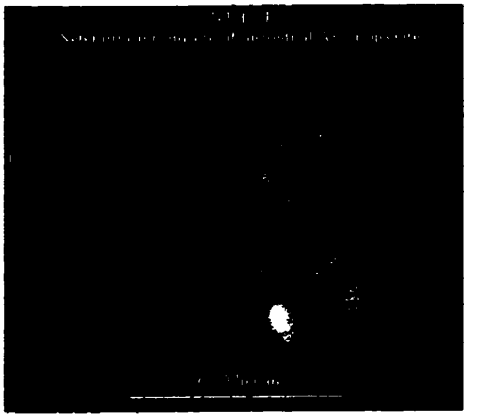

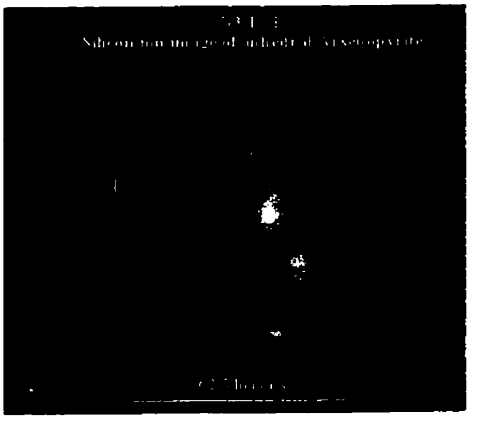

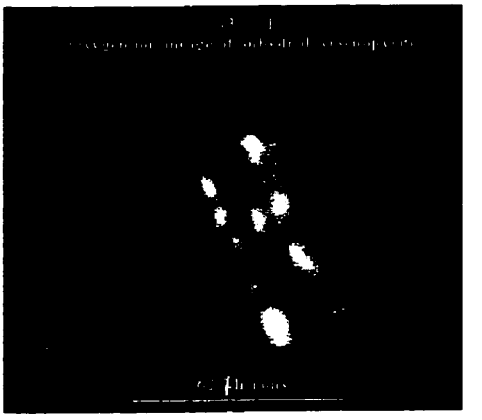

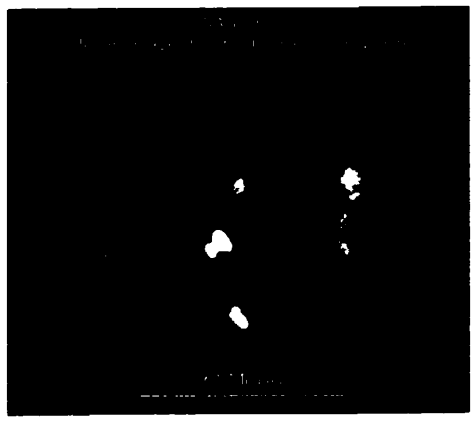

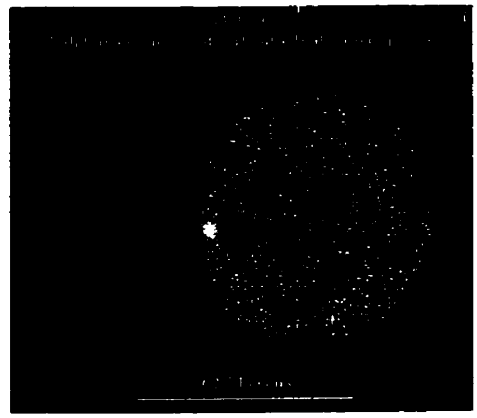

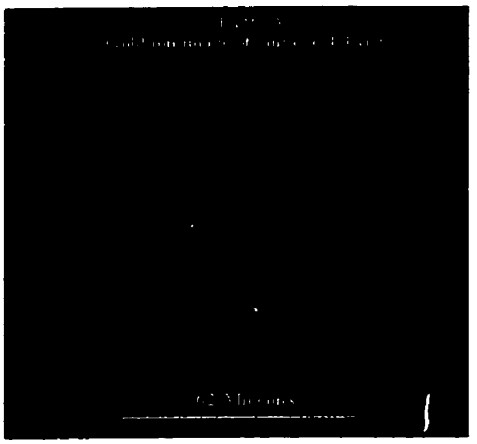

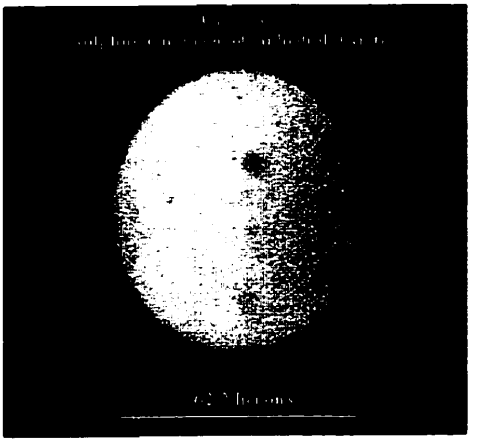

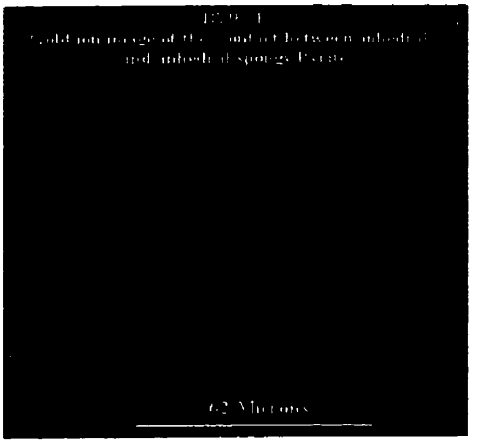

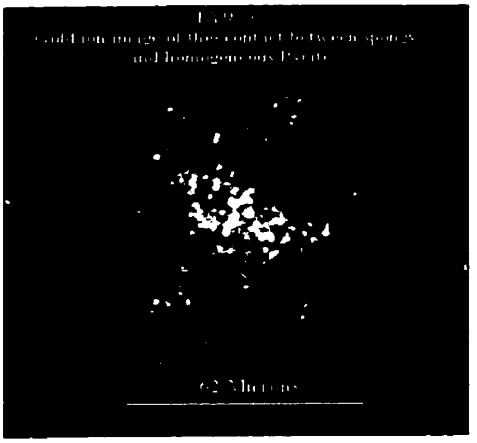

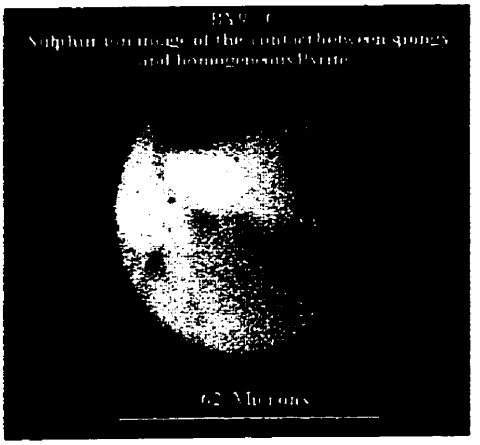

APPENDIX 6 - SAMPLE LOCATIONS

Level 2006 - Map displaying faults and sample locations on Level 2006.

Level 2210 - Map displaying faults and sample location on Level 2210.

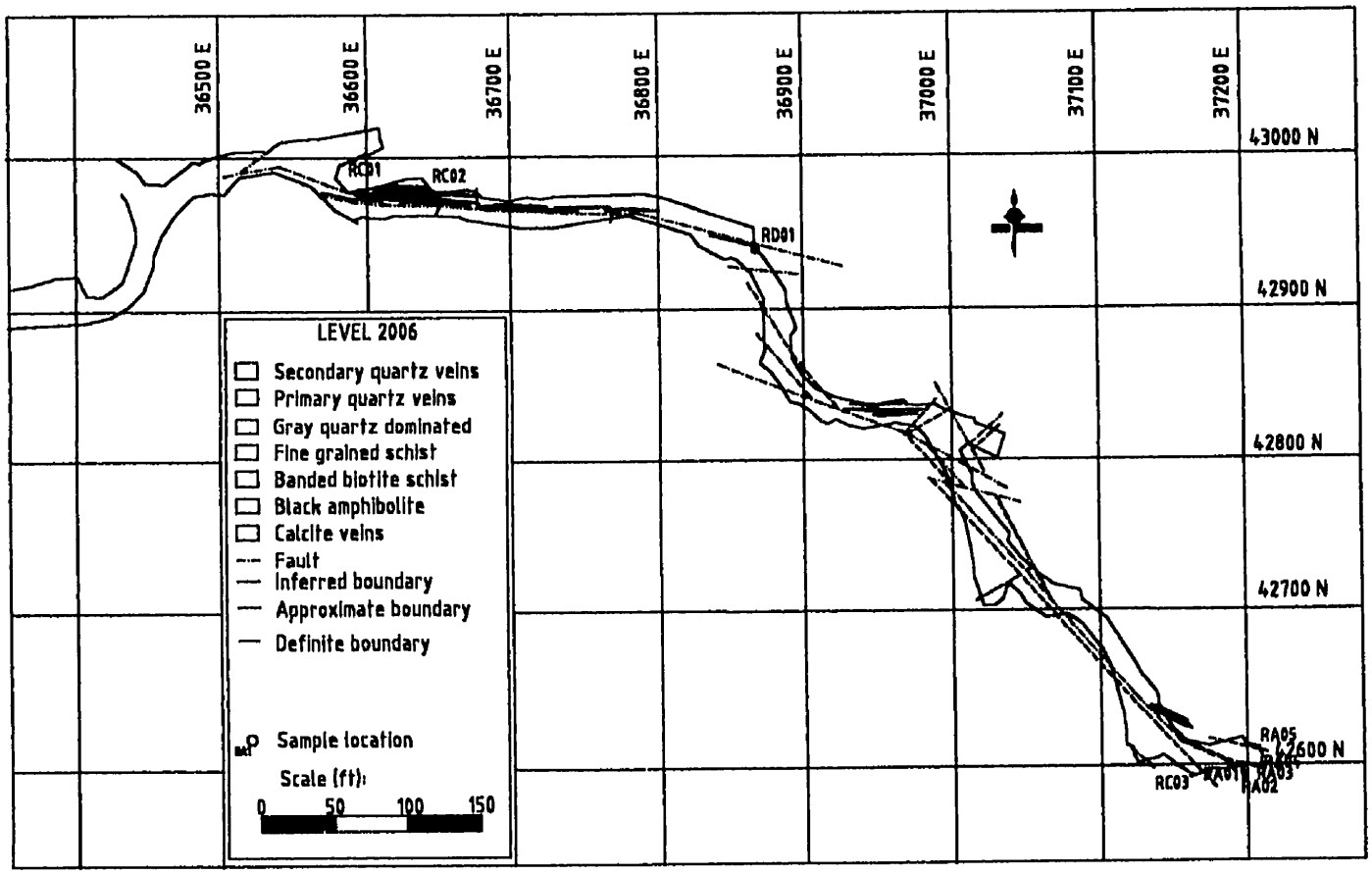

Mapped and drawn by P.J.Fulton (1999).

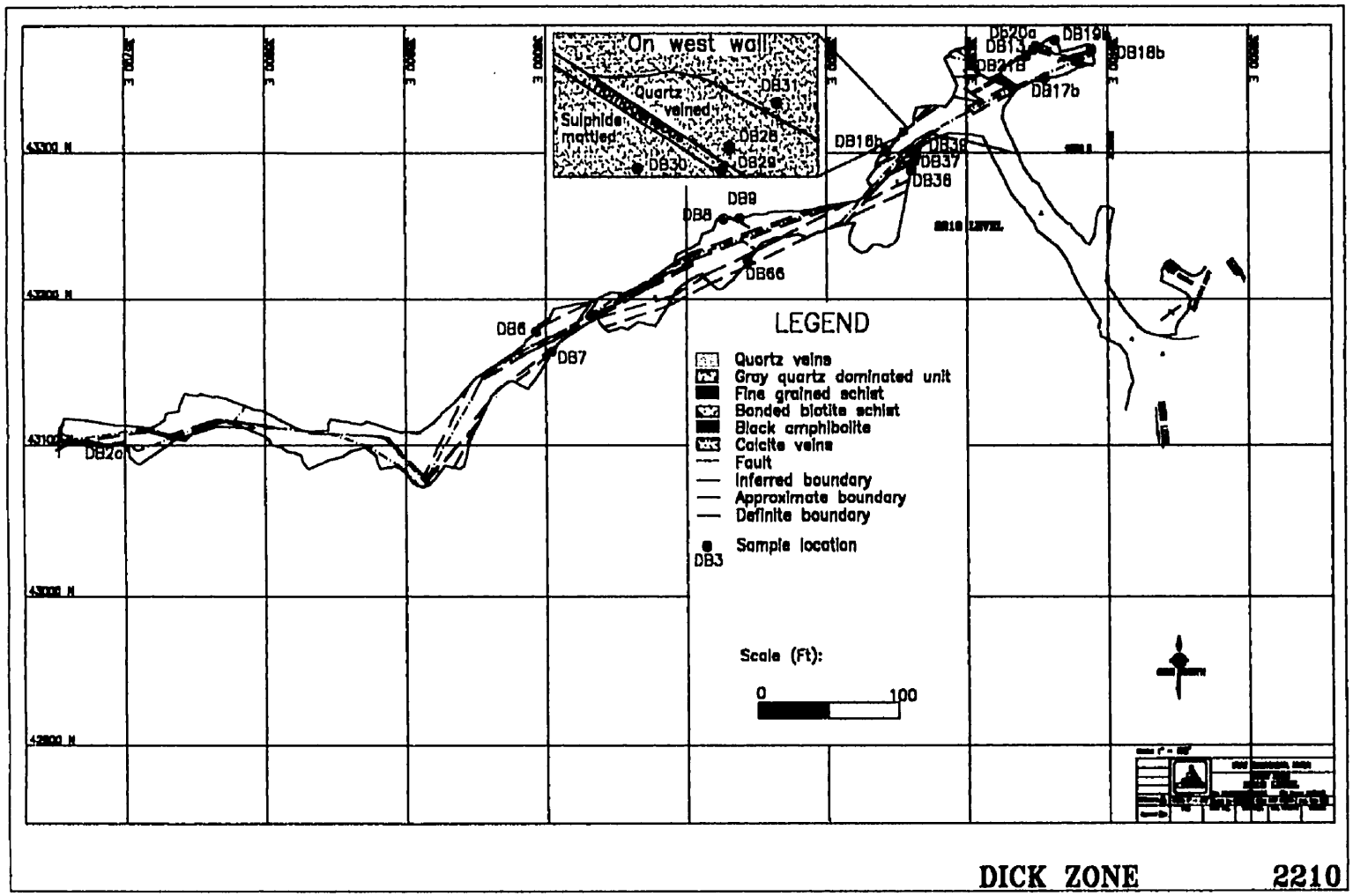
On west wall
Quartz veined
Sulphide mottled
DB31
DB28
DB29
DB30
DB16b
DB20a
DB19b
DB18b
DB17b
DB21B
DB36
DB37
DB38
DB9
DB8
DB66
DB6
DB7
DB2a
LEGEND
Quartz veins
Gray quartz dominated unit
Fine grained schist
Banded biotite schist
Black amphibolite
Calcite veins
Fault
Inferred boundary
Approximate boundary
Definite boundary
Sample location
DB3
Scale (Ft):
0
100
DICK ZONE
2210